Late Quaternary changes in paleoproductivity and hydrography in the Azores region deduced from coccolithophore assemblages

Dissertation

zur Erlangung des Doktorgrades der Mathematisch-Naturwissenschaftlichen Fakultät
der Christian-Albrechts-Universität zu Kiel

Vorgelegt von
Christian Schwab
Kiel, Januar 2013

Erster Gutachter:	Prof. Dr. Ralph Schneider
Zweite Gutachterin:	PD Dr. Mara Weinelt
Tag der Disputation:	26.03.2013
Zum Druck genehmigt:	26.03.2013
Der Dekan:	Prof. Dr. Wolfgang J. Duschel

Erklärung

Hiermit erkläre ich, dass ich die vorgelegte Dissertation „Late Quaternary changes in paleoproductivity and hydrography in the Azores region deduced from coccolithophore assemblages“, abgesehen von der Beratung durch meine akademischen Betreuer, selbstständig und nur mit Hilfe der angegebenen Quellen und Hilfsmittel erstellt habe. Weiterhin versichere ich, dass der Inhalt dieser Dissertation weder in dieser noch in ähnlicher Form zu einem anderen Prüfungsverfahrens eingereicht worden ist. Die Arbeit ist unter Einhaltung der Regeln guter wissenschaftlicher Praxis der Deutschen Forschungsgemeinschaft entstanden.

Kiel, Januar 2013 _____

(Christian Schwab)

Für Hanna

Summary

Marine sediment cores provide the opportunity to study past climatic changes, which is essential to understand the ongoing and future climate change. Within this context, the North Atlantic Ocean is one of the best-studied areas. However, most of these studies focus on the continental margins and shelfs, where thick piles of sediment allow a detailed reconstruction of past environmental changes. In contrast, little is known about the low- to midlatitude open ocean areas, which would be crucial regarding the large area covered. Furthermore, the low latitudes of the North Atlantic are considered to play a key role in modulating the global climate on at least orbital and millennial timescales. This key role is attributed to their ability to retain/release heat to the higher latitudes and therefore to influence the Atlantic Meridional Overturning Circulation (AMOC).

Especially changes in marine primary productivity, which due to their impact on the ocean carbon cycle are an integral part of the climate system, are of interest to the (paleo-) climate community. Therefore, in this PhD thesis, changes in primary productivity and hydrography were reconstructed with high temporal resolution in the temperate/subtropical open ocean North Atlantic, from three sediment cores (GEOFAR KF16, MD08-3179Cq and MD08-3180Cq) taken slightly south of the Azores Islands. These reconstructions are primarily based on quantitative analysis of coccolithophore assemblages, which are supplemented by alkenone analysis, X-ray fluorescence (XRF) core scanning and diatom counts. The results indicate that profound changes in productivity and in hydrographic conditions occurred during the selected time periods of the last 130 kyrs in the Azores region, which can convincingly be deduced from changes in coccolithophore assemblages.

For example, an increased productivity prevailed in the Azores region during the last deglacial and early Holocene, especially during cold Heinrich event 1 (H1) and the cold Younger Dryas that are characterized by a strongly reduced AMOC. This is evidenced by increased coccolith accumulation rates, increased alkenone concentrations/accumulation rates, increased Ba/Ti ratios and increased diatom abundances. The increased productivity was a response to intensified westerly winds and the advection of northern-sourced, nutrient-rich surface waters. Furthermore, a more southern position of the Azores Front (AzF), as indicated by abundance changes of key coccolithophore species (*G. muellerae*, grouped subtropical species), contributed to the observed increased productivity. In conjunction with other studies from the midlatitude North Atlantic, these results indicate that

there was a band of high productivity at the northern rim of the contracted North Atlantic subtropical gyre during times of a reduced Atlantic Meridional Overturning Circulation (AMOC).

A similar pattern of changes can be observed during weak AMOC phases between 130 and 48 kyrs BP. During the penultimate deglacial and cold Marine Isotope (sub-) Stages (MIS) 5.4, 5.2 and 4, an increased productivity and a more southern position of the Azores Front is observed. On the other hand, during warm periods (MIS 5.3, MIS 5.1, MIS 3) a decreased productivity and a more northern position of the Azores Front are found. An exception to this general pattern is the last interglacial period (MIS 5.5), which is characterized by strongly increased coccolithophore productivity. This increased productivity was probably caused by the opportunity for coccolithophores to occupy new habitats after glacial conditions and/or by an increased advection and upwelling of nutrient-rich Subantarctic Mode Water (SAMW).

Because a more comprehensive knowledge of natural interglacial climate variability is important within the context of future climate change, special emphasis is given to the present and last interglacial period in this thesis. Comparing the results for the present (Holocene) and the last (MIS 5.5) interglacial period reveals a similar pattern of changes in the Azores region, and leads to the following hypothesis: Due to an early northern hemisphere insolation maximum, a first amelioration of climate, characterized by a decreased productivity and a more northern position of the Azores Front is found during the early interglacials. Thereafter, a delayed response of the northern hemisphere ice-sheets caused an increased input of freshwater to the North Atlantic, leading to a reversal towards more glacial conditions. This accelerated melting was terminated by a collapse of the ice-sheets, resulting in an outburst of proglacial lakes, an event that is recognized in the Azores region at least during the Holocene (8.2 kyr event). After the freshwater forcing ceased, full interglacial conditions established during the late interglacials.

In general, an increased primary productivity and a more southern position of the Azores Front are found during cold periods, whereas a decreased primary productivity and more northern position of the Azores Front are found during warm periods. As the Azores Front delineates the northern boundary of the North Atlantic subtropical gyre, these results indicate a contracted gyre during cold periods and an expanded gyre during warm periods. Furthermore, within the context of an expected future global warming, these results lead to the assumption that the oligotrophic waters of the North Atlantic subtropical gyre probably

would expand northwards in response to a warming. A resulting decreased marine primary productivity, and hence a decreased atmospheric CO_2 fixation by marine phytoplankton, would provide a positive feedback to the increasing temperatures. However, taking MIS 5.5 as an analogue scenario for the expected future climate change, the presented results indicate that a future decrease in marine primary productivity, due to an expansion of the oligotrophic gyre, could probably be counteracted by increased coccolithophore productivity.

Zusammenfassung

Marine Sedimentkerne bieten die Möglichkeit klimatische Veränderungen in der Vergangenheit zu studieren, und somit den zukünftigen Klimawandel besser zu verstehen. In diesem Zusammenhang ist der Nordatlantik eines der am besten untersuchten Gebiete. Allerdings konzentrieren sich die meisten dieser Studien auf die Bereiche der Kontinentalhänge und Schelfe, wo mächtige Sedimentablagerungen eine detaillierte Rekonstruktion der vergangen Umweltveränderungen erlauben. In Gegensatz dazu ist wenig über die offenen Ozeanbereiche der niedrigen bis mittleren Breiten des Nordatlantik bekannt, welche jedoch entscheidend sind, da sie eine große Fläche abdecken. Weiterhin spielen die niedrigen Breiten des Nordatlantiks eine wichtige Rolle bei Klimaveränderungen, zumindest auf orbitalen und millennium-skaligen Zeitskalen. Diese wichtige Rolle wird den niederen Breiten des Nordatlantiks zugeschrieben, da sie Wärme speichern können, bzw. and die höheren Breiten abgeben können, und somit die atlantische Umwälzzirkulation (AMOC) beeinflussen können.

Besonders Veränderungen in der marinen Primärproduktivität, welche durch ihren Einfluss auf den ozeanischen Kohlenstoffkreislauf ein wichtiger Bestandteil des Klimasystems sind, sind von Interesse für die (Paläo-) Klimatologie. Deshalb wurden in der vorliegenden Dissertation die Veränderungen in der Primärproduktivität und Hydrographie im gemäßigten/subtropischen Bereich des offenen Nordatlantiks mit hoher zeitlicher Auflösung rekonstruiert. Als Grundlage für diese Untersuchungen dienten drei Sedimentkerne (GEOFAR KF16, MD08-3179Cq und MD08-3180Cq), welche südlich der Azoren entnommen wurden. Die Rekonstruktionen basieren hauptsächlich auf der quantitativen Analyse von Coccolithophoridengemeinschaften, welche durch Messungen von Alkenonen, Röntgenfluoreszenz (XRF) Kernanalysen und Diatomeen-Zählungen ergänzt werden. Die Ergebnisse zeigen, dass tiefgreifende Veränderungen in der Primärproduktivität und den hydrographischen Bedingungen während ausgesuchter Zeitabschnitte der letzten 130 kyrs im Bereich der Azoren stattfanden, die überzeugend aus den Veränderungen in der Coccolithophoridengemeinschaft abgeleitet werden können.

Zum Beispiel herrschte im Bereich der Azoren eine erhöhte Primärproduktivität während des letzten Deglazials und frühen Holozäns, vor allem während des kalten Heinrich Ereignisses 1 (H1) und der kalten Jüngeren Dryas, die durch eine stark reduzierte AMOC gekennzeichnet sind. Die erhöhte Primärproduktivität wird durch erhöhte Coccolithen-

Akkumulationsraten, erhöhte Alkenonen-Konzentrationen/Akkumukationsraten, erhöhte Ba/Ti-Verhältnisse und erhöhte Konzentrationen an Diatomeen belegt. Die erhöhte Primärproduktivität wurde durch verstärkte Westwinde sowie durch die Advektion von oberflächennahen, nährstoffreichen Wassermassen aus den höheren Breiten verursacht. Darüber hinaus trug eine südlichere Position der Azorenfront (AzF) zu der erhöhten Primärproduktivität bei. Diese südlichere Position der Azorenfront kann aus den beobachteten Häufigkeitsveränderungen ausgewählter Coccolithophoridenarten (*G. muellerae*, gruppierte subtropische Arten) abgeleitet werden. In Verbindung mit anderen Ergebnissen aus den mittleren Breiten des Nordatlantiks zeigen diese Ergebnisse, dass sich während Zeiten einer reduzierten atlantischen Umwälzzirkulation eine Zone erhöhter Primärproduktivität am Nordrand der zusammengezogenen subtropischen Gyre befand.

Ein ähnliches Muster an Veränderungen lässt sich während Zeiten schwacher AMOC zwischen 130 und 48 kyrs BP beobachten. Während des vorletzten Deglazials sowie während der kalten Marinen Isotopen (sub-) Stadien (MIS) 5.4, 5.2 und 4 herrschte eine erhöhte Primärproduktivität im Bereich der Azoren und die Azorenfront lag weiter südlich. In Gegensatz dazu wird eine erniedrigte Primärproduktivität und eine nördlichere Position der Azorenfront während der warmen Perioden (MIS 5.3, MIS 5.1, MIS 3) beobachtet. Eine Ausnahme zu diesem generellen Muster ist das letzte Interglazial (MIS 5.5), welches durch eine strak erhöhte Coccolithophoridenproduktivität gekennzeichnet ist. Diese erhöhte Produktivität wurde durch die Besetzung neuer Lebensräume nach der vorausgegangenen Eiszeit und/oder durch die verstärkte Advektion und den Auftrieb von nährstoffreichem Subantarktischen Modewassers (SAMW) hervorgerufen.

Im Rahmen des zu erwartenden künftigen Klimawandels ist die Kenntnis der natürlichen interglazialen Klimavariabilität von besonderer Bedeutung. Daher wird in dieser Arbeit besonders auf die Änderungen während des gegenwärtigen und letzten Interglazials eingegangen. Beim Vergleich der Ergebnisse aus dem gegenwärtigen (Holozän) und dem letzten (MIS 5.5) Interglazial, erhält man ein ähnliches Muster an Veränderungen im Bereich der Azoren, was zu folgender Hypothese führt: Aufgrund eines frühen Insolationsmaximums in der nördlichen Hemisphäre, kam es zu einer frühen Besserung des Klimas, das im Bereich der Azoren durch eine geringe Primärproduktivität und eine nördliche Position der Azorenfront gekennzeichnet ist. Danach verursachte die verzögerte Reaktion der nördlichen Eisschilde einen erhöhten Eintrag an Frischwasser in den Nordatlantik, was wiederum zu einer Umkehr hin zu mehr eiszeitlichen Bedingungen führte. Das beschleunigte

Abschmelzen der nördlichen Eisschilde wurde durch deren Zusammenbruch beendet. Dies wiederum führte zu einem Zusammenbruch von proglazialen Seen, ein Ereignis, das zumindest während des Holozäns im Bereich der Azoren festgestellt wurde (8.2 kyr Ereignis). Nachdem sich der Einfluss des Frischwassers abgeschwächt hatte, etablierten sich die vollen interglazialen Bedingungen erst spät während des gegenwärtigen und letzten Interglazials.

Im Allgemeinen wird eine erhöhte Primärproduktivität und eine südlichere Position der Azorenfront während kalter Perioden gefunden. Im Gegensatz dazu wird eine erniedrigte Primärproduktivität und eine nördlichere Position der Azorenfront während warmer Perioden festgestellt. Da die Azorenfront den nördlichen Rand der nordatlantischen subtropischen Gyre markiert, implizieren diese Ergebnisse eine zusammengezogene Gyre während kalter Perioden und eine Ausdehnung der Gyre während warmer Perioden. Im Rahmen der erwarteten künftigen Klimaerwärmung führen diese Ergebnisse weiterhin zu der Annahme, dass sich die oligotrophen Wassermassen der nordatlantische subtropische Gyre als Reaktion auf die Erwärmung weiter nordwärts ausdehnen werden. Eine daraus resultierende Abnahme der marinen Primärproduktivität, und eine damit verbundene Abnahme der atmosphärischen CO_2-Fixierung durch marines Phytoplankton, würden einen positiven Rückkopplungsmechanismus für die zu erwartende Erwärmung darstellen. Zieht man jedoch das letzte Interglazial als ein analoges Szenario für den zu erwartenden Klimawandel heran, zeigen die hier dargestellten Ergebnisse, dass eine erhöhte Coccolithophoridenproduktivität der zu erwartenden Abnahme in der marinen Primärproduktivität möglicherweise entgegenwirkt.

Acknowledgments

Bei Prof. Dr. Ralph Schneider möchte ich mich für die Bereitstellung des Arbeitsplatzes, sowie für die Übernahme des Erstgutachtens dieser Arbeit bedanken.

PD Dr. Mara Weinelt danke ich für die Möglichkeit, dass ich meine Dissertation im Rahmen des AMOCINT Projektes erstellen durfte. Diese Arbeit profitierte durch die stets konstruktive und detaillierte Diskussion mit ihr. Zuletzt möchte ich Mara für die Möglichkeit an diversen Konferenzen teilzunehmen, sowie für die Übernahme des Zweitgutachtens danken.

Ganz spezieller Dank geht an Dr. Hanno Kinkel, für die Einführung in die Welt der Coccolithophoriden, sowie für seine exzellente Betreuung dieser Arbeit. Durch seine Ideen, sowie durch zahlreiche Diskussionen, bestimmte er den Verlauf dieser Arbeit maßgeblich mit. Danke Hanno!

Meiner lieben Kollegin Janne Repschläger danke ich für die angenehme Arbeitsatmosphäre in unserem „Exklaven"-Büro. Weiterhin danke ich ihr für die zahlreichen Diskussionen und manches Korrekturlesen.

Für alle Arten von Diskussionen und Ratschlägen, möchte ich mich auch bei Dr. Sebastian Meier, Dr. Guillaume Leduc und Christine Bauke bedanken.

Herzlicher Dank geht auch an Frau Ute Schuldt, für ihre Unterstützung im REM-Labor.

Weiterer Dank geht an: Dr. Karl-Heinz Baumann für Korrekturlesen; Dr. Thomas Blanz für die Messung der Alkenone; Prof. Dr. Michael Sarnthein für Diskussionen und Bernard Dannielou für die Bereitstellung der GEOFAR KF16 Proben.

Danke auch an meine Eltern, die mir immer mit Rat und Tat zur Seite stehen.

Zuletzt danke ich meiner geliebten Frau Julia, die immer für mich da war und ohne deren Unterstützung diese Dissertation nicht möglich gewesen wäre.

Table of contents

Chapter I.

Introduction

1.1 Late Quaternary changes in paleoceanography and climate

The climate during the Quaternary is strongly modulated by variations in the Earth's orbit, leading to the pronounced succession of glacial and interglacial periods (Imbrie et al., 1984; Berger, 1988; Mudelsee and Stattegger, 1997; Lisiecki and Raymo, 2005). The glacial and interglacial periods, which are well expressed in terrestrial (Figure 1.1a) and marine climate records (Figure 1.1b), are characterized by significantly different environmental conditions. For example, during glacial periods global sea level was lower due to expanded ice-sheets (Lambeck et al., 2002; Bintanja et al., 2005), oceanic fronts shifted to lower latitudes (Ruddiman and McIntyre, 1973; Bard and Rickaby, 2009), the Thermohaline Circulation (THC) was weaker (Sarnthein et al., 1994; Lopes dos Santos et al., 2010) (Figure 1.1c), the global wind field changed and the Inter Tropical Convergence Zone (ITCZ) shifted southward (Lea et al., 2003; Schmidt and Spero, 2011).

During the first 1.8 Ma of the Quaternary, glacials and interglacials had a recurrence rate of 41 kyrs, corresponding to variations in the obliquity of the Earth's axis (cf. Lisiecki and Raymo, 2005). In contrast, during the Late Quaternary (0.8 - 0 Ma), the recurrence rate of glacials and interglacials was approximately 100 kyrs (cf. Lisiecki and Raymo, 2005), corresponding to variations in Earth's axis eccentricity. However, it is discussed controversially how the comparatively small insolation forcing resulting from the variations in eccentricity led to the Late Quaternary glacial/interglacial cycles with a pacing of 100 kyrs (Hays et al., 1976; Muller and MacDonald, 1996; Maslin and Ridgwell, 2005). One possible explanation may be that the solar forcing was amplified by internal feedback mechanisms such as changes in the THC (Walin, 1985; Broecker and Denton, 1989; Peeters et al., 2004; Beal et al., 2011) and/or in atmospheric greenhouse gas concentrations (e.g. CO_2, CH_4) (e.g. Sigman and Boyle, 2000). The changes in atmospheric greenhouse gases are well documented in Antarctic ice-cores and changed in parallel with the succession of the Late Quaternary climate cycles, at which low values prevailed during glacial periods and increased values are found during interglacials (Figure 1.1d).

Although several mechanisms influence the atmospheric CO_2 concentrations (Archer et al., 2000; Falkowski et al., 2000), changes in the oceanic carbon cycle are considered the most prominent factor to explain the glacial to interglacial changes in CO_2 (e.g. Broecker, 1982a; Sarmiento and Toggweiler, 1984; Sigman and Boyle, 2000). Especially

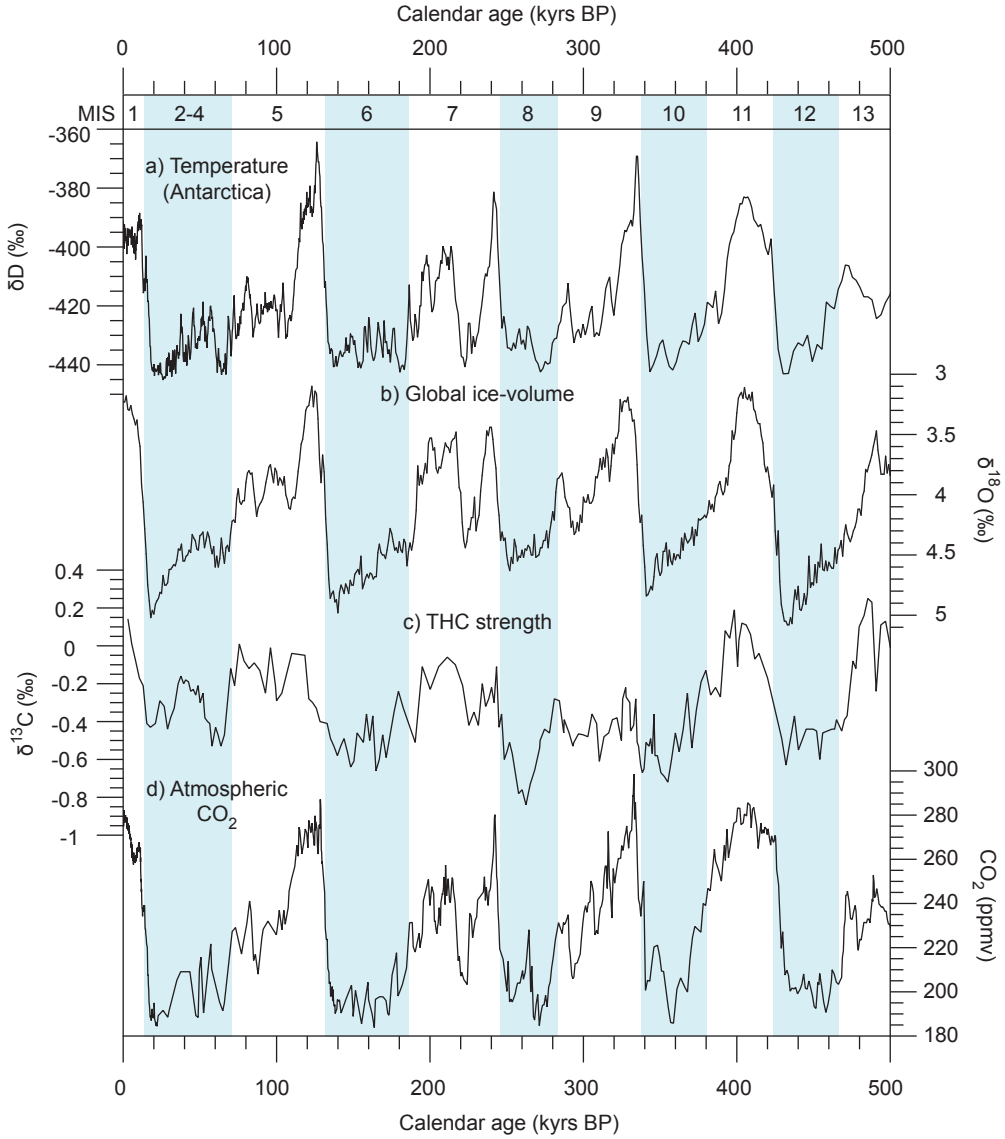

Figure 1.1. a) Deuterium measured in Antarctic ice core (EPICA community members, 2004). b) Stacked benthic foraminiferal stable oxygen isotope record (Lisiecki and Raymo, 2005). c) Benthic foraminifersal carbon isotope record from ODP Site 846 (Mix et al., 1995). d) Atmospheric CO_2 measured in Antarctic ice cores (Lüthi et al., 2008). Abbreviations: Marine Isotope Stage (MIS), Thermohaline Circulation (THC). Glacial MISs are marked with light blue vertical bar.

changes in marine primary productivity (PP) are proposed to explain the observed CO_2 changes (Broecker, 1982b; McElroy, 1983; Ganeshram et al., 1995). This is because marine PP is an integral part of the oceanic carbon pump, and therefore potentially could influence the atmospheric/oceanic CO_2 exchange (Falkowski et al., 2000).

As outlined above, changes in marine PP and the associated changes in atmospheric CO_2 play an important role in climate changes. Therefore, in this thesis, changes in marine PP and their possible implications on atmospheric CO_2 are investigated in the vicinity of the North Atlantic subtropical gyre. Although PP is low within the subtropical gyres, their

large size allows for a significant contribution on a global scale (Polovina et al., 2008). For example, they account for a quarter of global PP (Longhurst et al., 1995) and contribute up to 50% of global ocean carbon export (Emerson et al., 1997). Therefore they are essential for the atmospheric/oceanic CO_2 exchange.

Within the context of the Late Quaternary succession of glacial/interglacial cycles, the last interglacial periods are of special interest to the (paleo-) climate community, as they reflect a mean climatic state that also characterizes the present Holocene period. As past interglacials ran their full course and demise, they can teach us a valuable lesson about natural interglacial climate variability (Cheddadi et al., 1998; Müller and Sánchez Goñi, 2007). Furthermore, as past interglacials mostly occurred under different boundary conditions (e.g. orbital and ice-sheet configuration), the comparison of different interglacials can give insights into the interglacial climate sensitivity to different forcing mechanisms (e.g. Kutzbach et al., 1991). In summary, the investigation of past interglacials can give insights into climate sensitivity and natural climate variability during periods comparable to the present Holocene, and therefore will help to refine future climate predictions (e.g. Howard, 1997; Tzedakis et al., 2009).

Key targets for interglacial climate research are Marine Isotope Stage (MIS) 11 and MIS 5.5 (the last interglacial period). Many studies focus on MIS 11, as this period occurred under a similar orbital configuration as the ongoing Holocene (e.g. McManus et al., 2003; Loutre, 2003; Kandiano and Bauch, 2007). Therefore the long-lasting MIS 11 can give insights into the natural climate variability during a period comparable to the Holocene, and can hint at changes that can be expected for the remainder of the Holocene period. Moreover, it could help to disentangle the natural and human impact on the ongoing climate change. On the other hand, global temperature was 1.5 - 2°C warmer and sea-level was about 6 m higher during the presumably brief last interglacial period (MIS 5.5) compared to the Holocene, which is within the range of the predicted future changes (Clark and Huybers, 2009; Kopp et al., 2009). Therefore the last interglacial period (MIS 5.5) can serve as a possible analogue scenario for the future climate change, and thus could help to evaluate the environmental impact of the predicted future changes. A key question would be, wether productivity in the studied area would decrease due the expansion of the subtropical gyre, or if a changed modewater circulation, as proposed by Romero et al. (2011), would have the opposite effect.

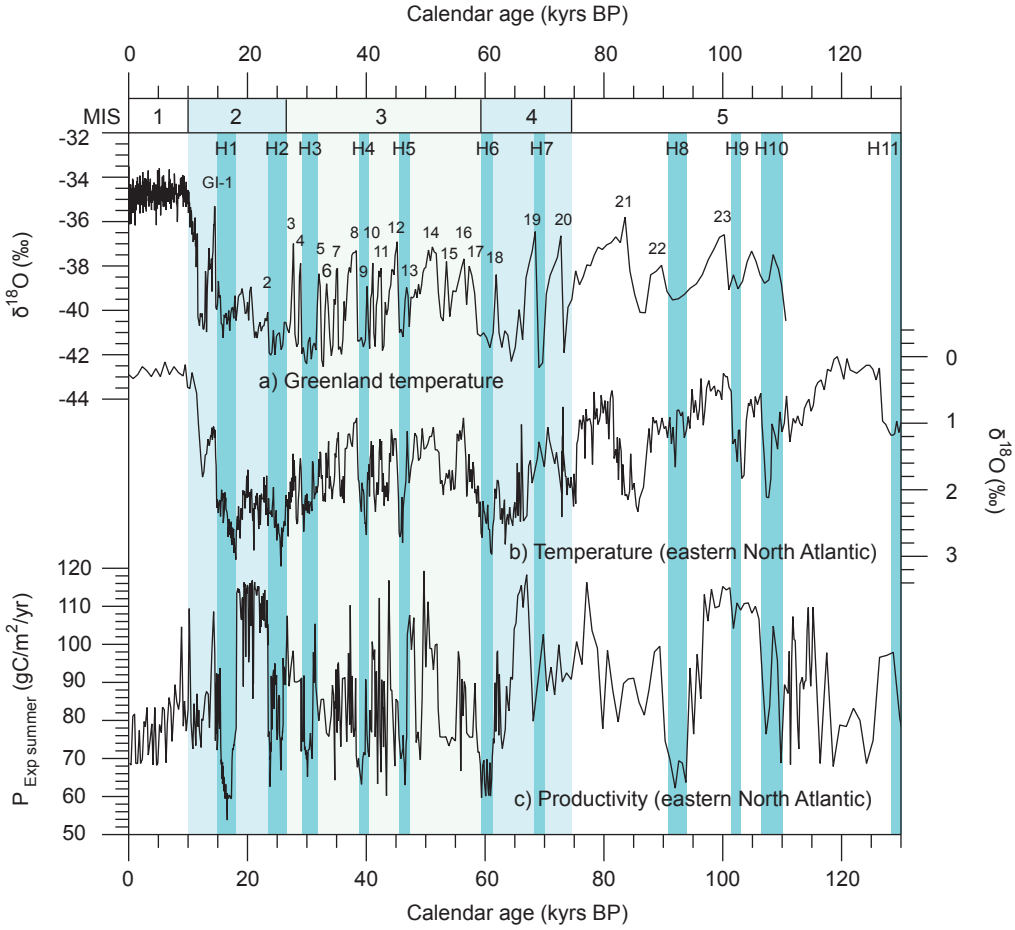

Figure 1.2. a) Stable oxygen isotope record from GISP2 icre core (Grootes and Stuiver, 1997) b) Planktic foraminiferal oxygen isotope record from sediment core MD95-2042 (Shackleton et al., 2000) c) SIMMAX derived changes in marine primary productivity from sediment core MD95-2040 (Salgueiro et al., 2010). Glacial MISs are marked with light blue vertical bars. Heinrich events (Hs) are marked with darker blue vertical bars. Greenland Indterstadials (GIs) are labeled with numbers in uppermost record.

Aside of these orbital-scale changes, considerable climate fluctuations also occurred on millennial timescales during the Late Quaternary. The millennial-scale climate fluctuations were first identified in ice cores drilled in the Greenland ice-sheet (Figure 1.2a) (Dansgaard et al., 1993; Grootes et al., 1993). These climate cycles, termed Dansgaard-Øschger cycles (DO) or Greenland Stadials (GS)/Greenland Interstadials (GI), have a mean recurrence rate of 1470 yrs, at least during MIS 2 - MIS 4 (Grootes and Stuiver, 1997; Schulz, 2002). GS/GI cycles have been found in various global climate archives (e.g. Figure 1.2b) (for a review see Voelker, 2002), indicating that these fluctuations are a fundamental mode of climate variability. Furthermore the cold reversals during deglacials

(e.g. the Younger Dryas) are discussed as a continuation of the DO cycles (e.g. Tzedakis et al., 2012).

Climate fluctuations with a similar recurrence rate have also been reported during the present and last interglacial period (Bond et al., 2001), indicating a generally instable climate during interglacials (see also Fronval and Jansen, 1996; Couchoud et al., 2009). On the other hand, other climate records indicate a rather stable climate during interglacials (e.g. McManus et al., 1994; Rasmussen et al., 2003; Andersen et al., 2004). Therefore the stability of interglacial climates is still a matter of ongoing research and will be addressed in this thesis.

Superimposed on the GS/GI fluctuations are the lower frequency cycles of the Heinrich events, which have a mean recurrence rate of 7200 yrs (Sarnthein et al., 2001), occurring during cold GI (Figure 2). The Heinrich events are associated with a drastic collapse of the Northern Hemisphere ice-sheets, resulting in a massive input of icebergs and hence in a massive discharge of freshwater into the North Atlantic (Heinrich, 1988; Broecker et al., 1992; MacAyeal, 1993; Maslin et al., 1995). As other Greenland Stadials, the Heinrich events are associated with a reduction in the Atlantic Meridional Overturning Circulation (AMOC), which is the Atlantic part of the THC (e.g. Zahn et al., 1997; Dokken and Jansen, 1999; Seidov and Maslin, 1999; Boyle, 2000; Rasmussen and Thomsen, 2004; Schmidt et al., 2006).

Regarding PP, recent freshwater modeling experiments indicate a significant reduction in marine PP during Heinrich events, especially in the North Atlantic (Schmittner, 2005; Menviel et al., 2008; Mariotti et al., 2012). In accordance to these modeling results, a decreased PP is observed in the high to mid latitudes of the North Atlantic based on proxy reconstructions (Figure 1.2c) (e.g. Thomas et al., 1995; Villanueva et al., 1998; Weinelt et al. 2003; Nave et al., 2007). However, mismatches between the modeling and proxy results have also been reported (Gil et al., 2009; Salgueiro et al., 2010). These mismatches can probably be related to local mechanisms, such as the advection of nutrient-rich surface waters or the expansion of the subtropical gyres, which are not considered by the models (Mariotti et al., 2012). Furthermore, in the mid to low latitude open ocean North Atlantic there are no suitable proxy records (with a sufficient temporal resolution) available to test the model results within this region, which would be crucial regarding the large area covered.

1.2 Structure of thesis

1.2.1 Aims and objectives

The presented study is conducted within the framework of the European Science Foundation (ESF) project AMOCINT (Atlantic Meridional Overturning Circulation during Interglacials). The project aims to identify suitable key sites to explore interglacial AMOC variability and to reconstruct changes in interglacial AMOC and their environmental impact with a high temporal resolution, in order to provide marine records comparable to ice-core records, which are one of the most intriguing and detailed climate archives (Dansgaard et al., 1993; Jouzel et al., 2007). The project should allow detailed insights into AMOC variability over past interglacials, which is thought to be a major component in climate changes (see chapter 1.1).

For this purpose, key sites along the warm water routes of the upper AMOC limb (Figure 1.3) were surveyed and drilled onboard the research vessel Marion Dufresne during cruise MD-168 in 2008 (Kissel et al., 2008). As part of the AMOCINT project the presented thesis investigates subtropical AMOC variability and related changes in marine primary productivity. Particularly the thesis investigates changes in paleoproductivity and hydrography in the Azores region, mainly based on changes in coccolithophore assemblages (see chapter 1.4). The objectives of this thesis are to:

- Provide high-resolution reconstructions of paleoproductivity and hydrographic changes from the temperate/subtropical open ocean North Atlantic, an area where existing paleoreconstructions are rare.

- Evaluate the impact of AMOC changes on the primary productivity and hydrographic conditions in the Azores region during the last deglaciation and Holocene period.

- Evaluate the stability of the Holocene period in terms of productivity and hydrography in the Azores Current System at an inner ocean site.

- Investigate the paleoecological changes in the Azores region during MIS 5, with special emphasizes on the last interglacial period (MIS 5.5).

- Draw possible conclusions of the observed productivity changes on the oceanic carbon cycle.

- Detect comparable patterns of short-term (i.e. millennial- to centennial-scale) changes in the paleoecological conditions in the Azores region during the present and last interglacial.

- Compare the present and last interglacial periods in terms of productivity and hydrography, in order to gain insights into climate sensitivity and response of the carbon cycle during interglacial periods.

- Answer the following question: If MIS 5.5 is an analog of expected future climate scenarios, will productivity increase in the subtropical region due to a changed mode water circulation?

1.2.2 Thesis outline

The thesis will address the objectives listed in chapter 1.2.1 in 7 distinct chapters. General background informations are given in chapter 1 and the materials and methods used in this thesis are explained in chapter 2. Chapters 3 to 5 correspond to manuscripts that are either published, submitted or will be submitted shortly to scientific journals. Chapter 6 gives the conclusions of this thesis and chapter 7 gives an outlook on (possible) future work. The single chapters of this thesis contain the following information:

Chapter I gives an introduction to Late Quaternary climate changes, which is followed by a description of the aims and objectives of the presented thesis. Furthermore background information on the geological and present hydrographic conditions in the working area (Azores) are given. At last, an introduction to coccolithophores and their application in paleoceanographic studies is given.

Chapter II deals with the materials and methods used in this study. First, a brief sedimentological description of the used sediment cores is given. Afterwards the applied methods (quantitative coccolithophore analysis, alkenone measurements and X-ray Fluorescence (XRF) core-scanning) are explained in detail.

Chapter III, entitled „Coccolithophore paleoproductivity and ecology response to deglacial and Holocene changes in the Azores Current System“, is a manuscript published in Paleoceanography (Schwab et al., 2012). This chapter deals with last deglacial and Holocene changes in productivity and hydrography in the Azores region. I wrote the manuscript and conducted all the coccolithophore analysis. Furthermore I contributed significantly to the establishment of the age models of the used sediment cores and I did the diatom counts. Stable Isotope analysis and XRF core-scanning were conducted by J. Repschläger. I prepared the samples for alkenone analysis (weighing, grounding), which were measured by T. Blanz. All the data were interpreted by me and the co-authors of the manuscript.

Chapter IV, entitled „Paleoenvironmental changes in the Azores region between 48 and 130 ka BP with special emphasizes on MIS 5.5“, is a manuscript submitted to Quaternary Science Reviews (Schwab et al., submitted). The manuscript investigates paleoecological changes in the Azores region between 130 and 48 ka BP. Furthermore, changes during the last interglacial period (MIS 5.5) are discussed based on high-resolution records of coccolithophore abundances. I wrote the manuscript and conducted all the coccolithophore analysis. I also established the isotope stratigraphy of the used sediment core and conducted the diatom counts. Stable Isotope analysis and XRF core-scanning were conducted by J. Repschläger. All the data were interpreted by me and the co-authors of the manuscript.

Chapter V, entitled „Comparison of the present and last interglacial in the Azores region based on calcareous nannoplankton“, corresponds to a manuscript, which will be submitted to Climate of the Past in March 2013 after a final proofreading of the co-authors (Kinkel, H., Weinelt, M., Repschläger, J.). This manuscript focusses on a qualitative and quantitative comparison of the present and last interglacial period, in order to gain insights

into natural climate variability and climate sensitivity during interglacials. I wrote the manuscript, conducted the coccolithophore analysis and established the refined age model of sediment core MD08-3179Cq. Furthermore, I interpreted the data with contributions of the co-authors of the manuscript.

Chapter VI and **Chapter VII** contain the general conclusions of the thesis and an outlook on ongoing and possible future work.

The **Appendix** contains supplementary data and figures mentioned in the text, as well as a data compilation**.**

1.3 Regional setting

The surface water hydrography in the working area is characterized by the Azores Current System (Figure 1.3). The Azores Current System is an eastward branch of the North Atlantic Current (NAC), the dominant surface water current in the North Atlantic. The North Atlantic Current transports heat and salt to the higher latitudes and thus forms the main upper limb of the AMOC in the North Atlantic (McCartney and Talley, 1984; Rahmstorf, 2003; Thornally et al., 2009). As the Azores Current Sytem is an eastward branch of the main upper limb of AMOC in the North Atlantic, a close coupling between AMOC and the Azores Current System can be assumed.

The Azores Current System mainly consists of the Azores Current (AC) and its associated Azores Front (AzF), which are persistent features of the North Atlantic throughout the year (Kielmann and Käse, 1987; Klein and Siedler, 1989; Maillard and Käse, 1989). Furthermore, there are evidences for the presence of an Azores Counter Current (Onken, 1993; Alves and de Verdière, 1999) and an additional northern flow termed North Azores Flow (Bashmachnikov et al., 2004). The AC travels eastward at a mean latitude of 35°N (Klein and Siedler, 1989), and joins the Canary Current, which flows southward. Due to its connections to the North Atlantic Current and Canary Current, the AC is part of the anticyclonic circulation that characterizes the North Atlantic subtropical gyre, forming its northern boundary (e.g. Bashmachnikov et al., 2004).

Position and strength of the AC varies on seasonal and interannual timescales (Klein and Siedler, 1989; Pingree, 1997; Alves and de Verdière, 1999). The seasonal changes in the strength of the AC are expressed in transport volumes of 9 Sv in winter, 12 SV in summer, to about 19 SV in spring (Alves and de Verdi, 1999). The seasonal changes in the transport volume are accompanied by changes in its latitudinal position, at which seasonal latitudinal migrations of ± 3° around the mean zonal axis at 35°N have been reported (Käse and Siedler, 1982). Thereby a more southern position and less meridian flow of the AC mean axis is found during summer (Klein and Siedler; 1989), coinciding with a smaller north-south extension of the SG in the North East Atlantic (Stramma and Siedler, 1988). Interannual shifts of 2° in latitude of the mean flow axis have been described by Pingree (1997).

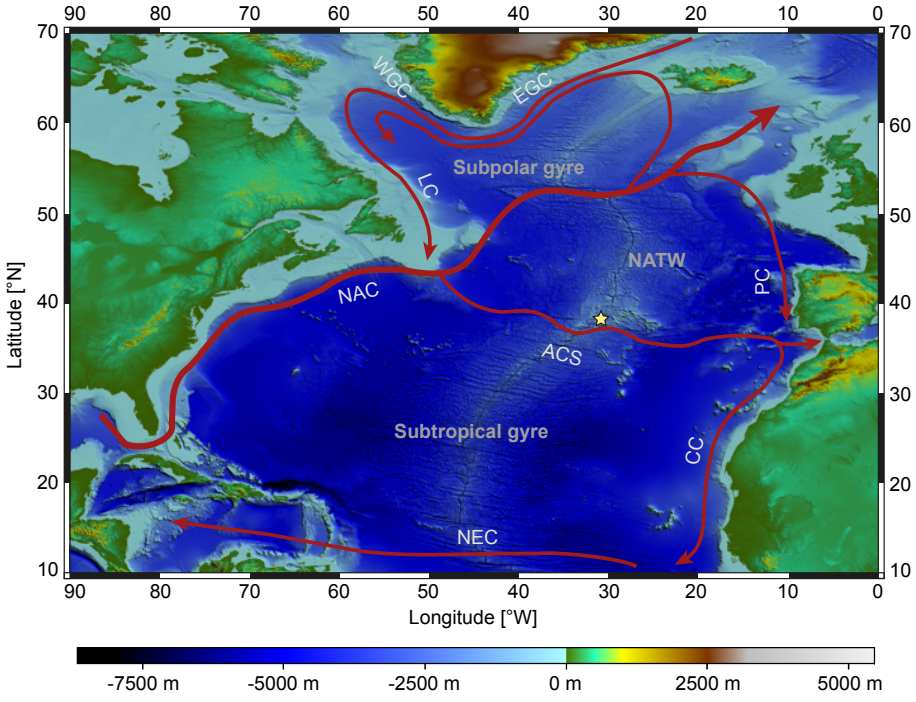

Figure 1.3. Schematic surface circulation (red arrows) of the North Atlantic. Shown are the North Equatorial Current (NEC), Canary Current (CC), North Atlantic Current (NAC), Azores Current System (ACS), Portugal Current (PC), East Greenland Current (EGC), West Greenland Current (WGC) and Labrador Current (LC). Between the subtropical and subpolar gyres there is a transitional surface water mass termed North Atlantic Transitional Water (NATW). Yellow star marks working area.

However, waters transported by the AC partly flow into the Gulf of Cadiz and into the Mediterranean Sea (Figure 1.3). These waters are thought to replace the waters lost from the Mediterranean Sea due to the overflow in the Street of Gibraltar. Therefore a hypothetical connection between the AC and the Mediterranean Overflow Waters (MOW) has been

proposed (Jia, 2000; Özgökmen et al., 2001; Kida et al., 2008; Volkov and Fu, 2010, 2011). Thereby the comparatively small MOW of 1 Sv forces the formation of the AC, which has a mean transport of about 10 - 12 Sv (Sy, 1988; Schmitz and McCartney, 1993).

As already mentioned, another important feature of the Azores Current System is the AzF. At the surface the AzF separates southern regions with a permanent thermohaline mixed layer and a subtropical thermocline from northern regions with a seasonal thermocline formation and winter convective and advective mixing (Käse and Siedler; 1982). I will refer to the surface water masses north of the AzF as North East Atlantic Transitional Water (NATW) (Ottens, 1991; Schiebel et al., 2011) and to the southern water masses as sub-

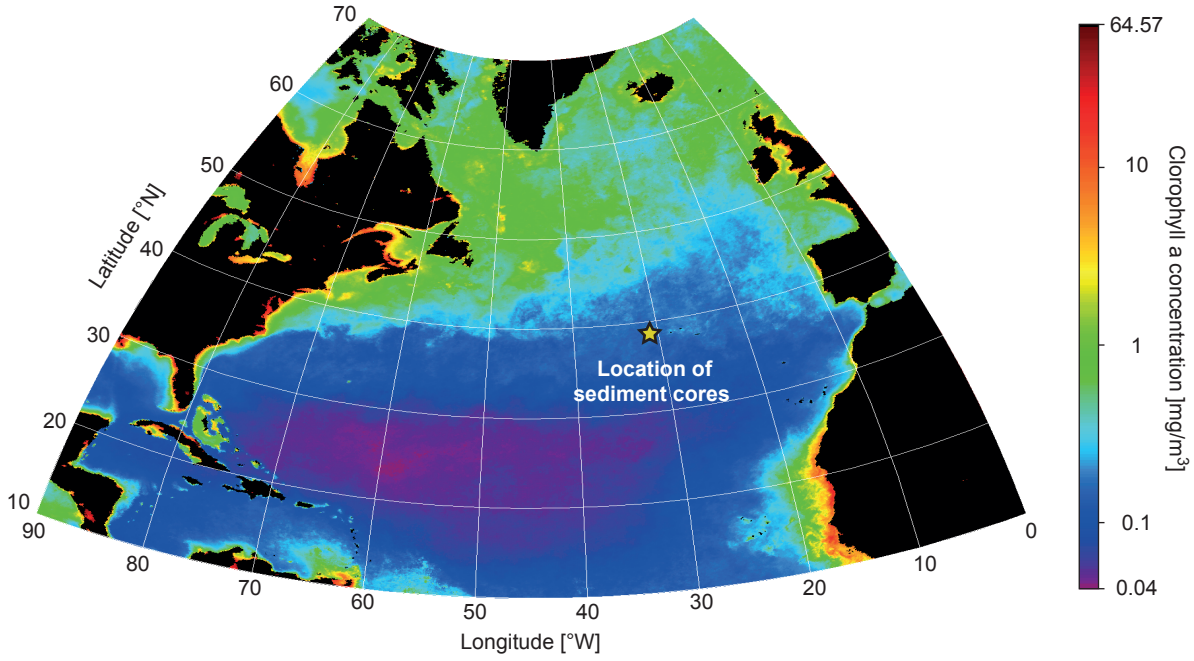

Figure 1.4. Sattelite based mean annual (2006) chlorphyll concentration in the North Atlantic (data available at http://seadas.gsfc.nasa. gov).

tropical water. Southernmost NATW is the dominant surface water mass at the coring sites today. Because the front can be shielded by the development of a seasonal thermocline in the working area, the position of the front is best defined as the location where the 15°C isotherm is between 200 and 300 m waterdepth (Gould, 1985).

The AC is a strongly meandering current, and therefore mesoscale activity is a common feature in the working area. This mesoscale activity is expressed by the formation of eddies. Thereby mature meanders pinch off the AC, forming cyclonic eddies to the south and anticyclonic eddies to the north of the AC (Alves et al., 2002). Only the anticyclonic

eddies, which transport subtropical waters to the north, occasionally reach our coring site (Alves et al., 2002; Pingree et al., 2002). There are different opinions about the seasonal variability of the eddy activity in the working area. For example Mourino et al. (2003) and Martins and Sinah (2002) report maximum eddy activity during winter, whereas Klein and Siedler (1989) report minimum eddy activity during this period. According to Mourino et al. (2003) this may be attributed to interannual variability of the eddy kinetics. Furthermore, there is a debate about the relationship of the eddy activity in the Azores region and the North Atlantic Oscillation (NAO). Pingree (2002) reports a more vigorous subtropical gyre circulation and an intensified eddy activity during phases of positive NAO, whereas Mourino et al. (2003) found a negative relation between the NAO and the eddy activity of the AC. At last, Oeschlies (2001) found no significant dependence of the eddy activity and the NAO in the North Atlantic.

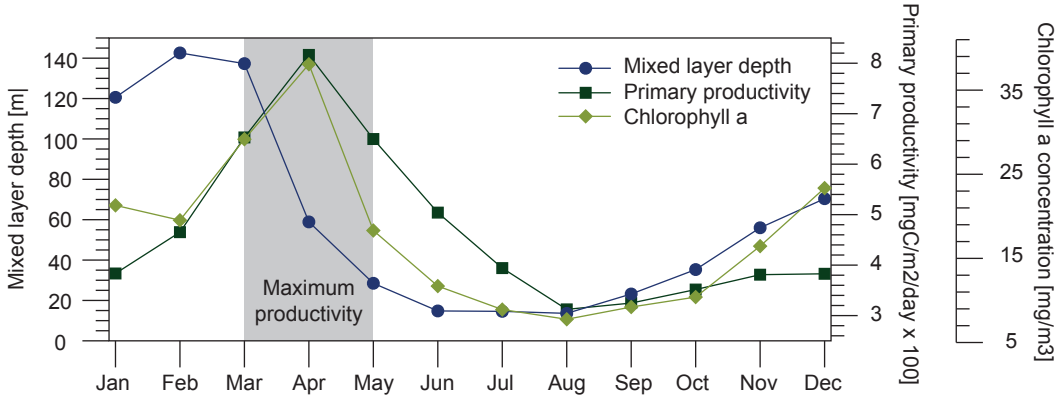

Figure 1.5. Seasonal variations in mixed layer depth (Monterey and Levitus, 1997), primary productivity (http://www.science.oregonstate.edu/ocean.productivity) and chlorophyll a concentration (data from http://seadas.gsfc.nasa. gov) at the location of the studied sediment cores. Season of maximum primary productivity is marked with grey vertical bar.

The different surface hydrographic conditions on each side of the Azores Current System create a high PP gradient in the working area (Figure 1.4). The regions to the south of the Azores Current System are generally characterized by a low PP. The low PP is a result of a strong water-column stratification, which leads to a weak vertical mixing and hence to a diminished replenishment of nutrients (Mouriño-Carballido and Neuer, 2008). In contrast, in the regions to the north of the Azores Current System, a high PP can be found. This high PP is a result of the deep winter mixed layer (200 - 300 m), which causes an effective renewal of consumed surface-nutrients due to upward mixing of deeper-sourced nutrients (Lévy et al., 2005). Furthermore PP in the working area can be influenced by the

eddy activity in the region. The cyclonic eddies to the south of the Azores Current System can cause an episodic nutrient input due to eddy pumping (Mouriño-Carballido and Neuer, 2008). On the other hand, the anticyclonic eddies, which occasionally transport oligotrophic subtropical waters to the coring site, are normally associated with low PP (Hernández-León et al., 2007; Mouriño-Carballido and Neuer, 2008). The mean annual PP at the coring site amounts 460 mgC/m^2/day (Behrenfeld and Falkowski, 1997). Substantial phytoplankton production takes place in the early spring, when winter mixing relaxes and stratification sets in (Figure 1.5). Regarding coccolithophores, the peak production periods starts slightly after the main PP peak (see chapter 3.3). As coccolithophores are one of the main groups of marine primary producers, they account for a substantial part of marine primary productivity (Baumann et al., 2005). This holds true in the working area, where the contribution of coccoliths to the total amount of sinking particles can be estimated to be one third (Broerse et al., 2000a).

1.4 Coccolithophores

1.4.1 Biology, ecology and environmental significance

Coccolithophores are unicellular algae belonging to the division Haptophyta and to the class Prymnesiophyceae (Edvardsen et al., 2000). They posses a haptonema, which is thought to act as an obstacle-sensing device (Billard and Inouye, 2004). Although the class Prymnesiophyceae includes also non-calcified organisms, coccolithophores are characterized by an exoskeleton made up of minute calcified platelets (coccoliths). The function of the coccoliths is discussed controversially (for a review see Young, 1994). Possible functions of coccoliths may be protection against grazing by zooplankton, mechanical damage and/or bacterial infestation. Furthermore, as water can be trapped between the cell membrane and the layer of coccoliths, they can act as a buffer against changes in the environmental conditions and probably can help to assist nutrient uptake. Another function of coccoliths may be their biochemical assistance in photosynthesis, at which the CO_2 produced during the calcification process can be used during photosynthesis. Additionally, coccoliths are probably used in regulating the incident light used for photosynthesis. The regulation of incident light into or away from the cell may allow life in the lower or upper photic zone re-

spectively. The morphology of coccoliths is used for the taxonomy of coccolithophores. Coccoliths can be divided into two major groups, the holo- and heterococcoliths. The most commonly investigated coccoliths are heterococcoliths, which are formed by an array of interlocked crystal units with variable shape (Young et al., 1992; Henriksen et al., 2004), and which are produced intracellularly (Brownlee and Taylor, 2004; Taylor et al., 2007). In contrast, holococcoliths are made up of numerous minute (ca. 0.1μm) euhedral crystallites (Young et al., 2003). They are produced extracellularly (e.g. Rowson et al., 1986). Holococcoliths are very fragile, and therefore are rarely preserved in sediment samples. Both coccolith groups (holo- and heterococcoliths) are not related to different coccolithophore species but represent different stages in the complex life-cycle of coccolithophores (Cros et al., 2000). In general, coccolithophores reproduce asexually by mitotic division, at which

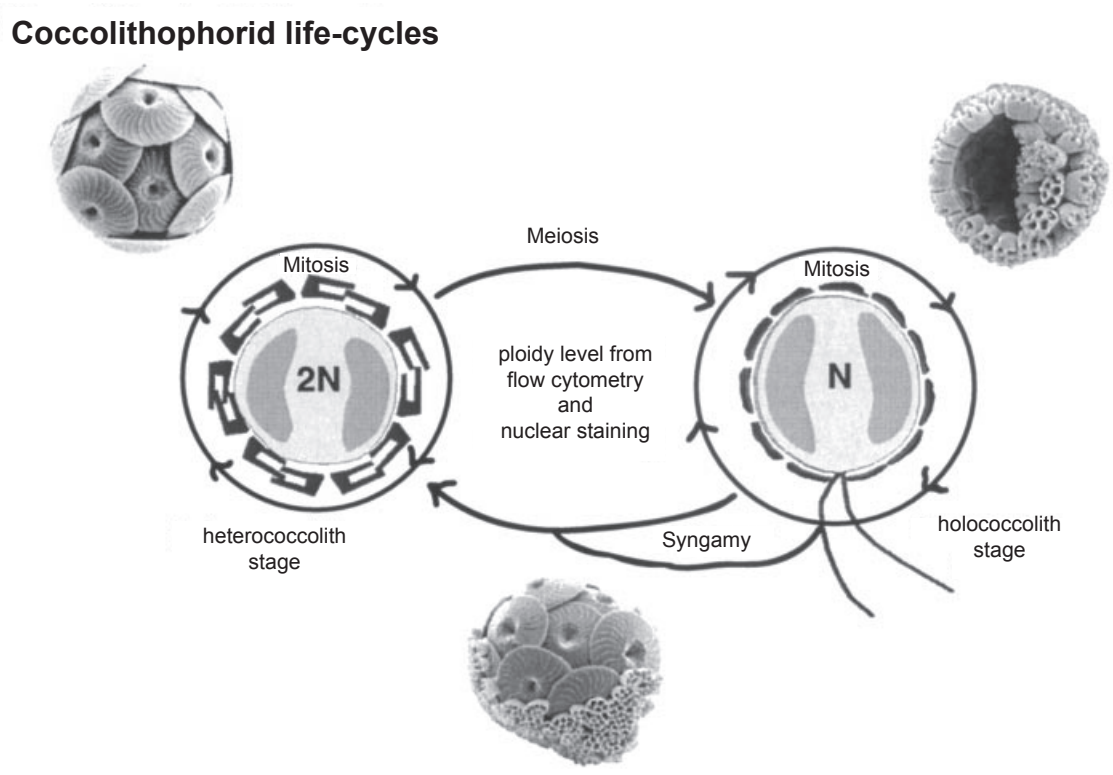

Figure 1.6. Schematic illustration of coccolithophorid life-cycles (from Geisen et al., 2002).

the coccoliths are redistributed on the daughter cells (Baumann et al., 2005). However, in many haptophytes, including coccolithophores, a more complex life-cycle has been reported, which involves the transition from a diploid stage to a motile, haploid stage (Figure 1.6). The transition from the diploid to the haploid stage takes place via the sexual process

of meiosis, whereas the transition from the haploid to the diploid stage takes place via the sexual process of syngamy (Houdan et al., 2004). The cells of the diploid stage are covered by heterococcoliths, whereas the haploid cells are covered by holococcoliths.

Coccolithophores are one of the main primary producers in the oceans today (Cortés et al., 2001). As coccolithophores need light for their photosynthetic activity, they thrive in the photic zone of the oceans. Furthermore, coccolithophores strongly rely on nutrients

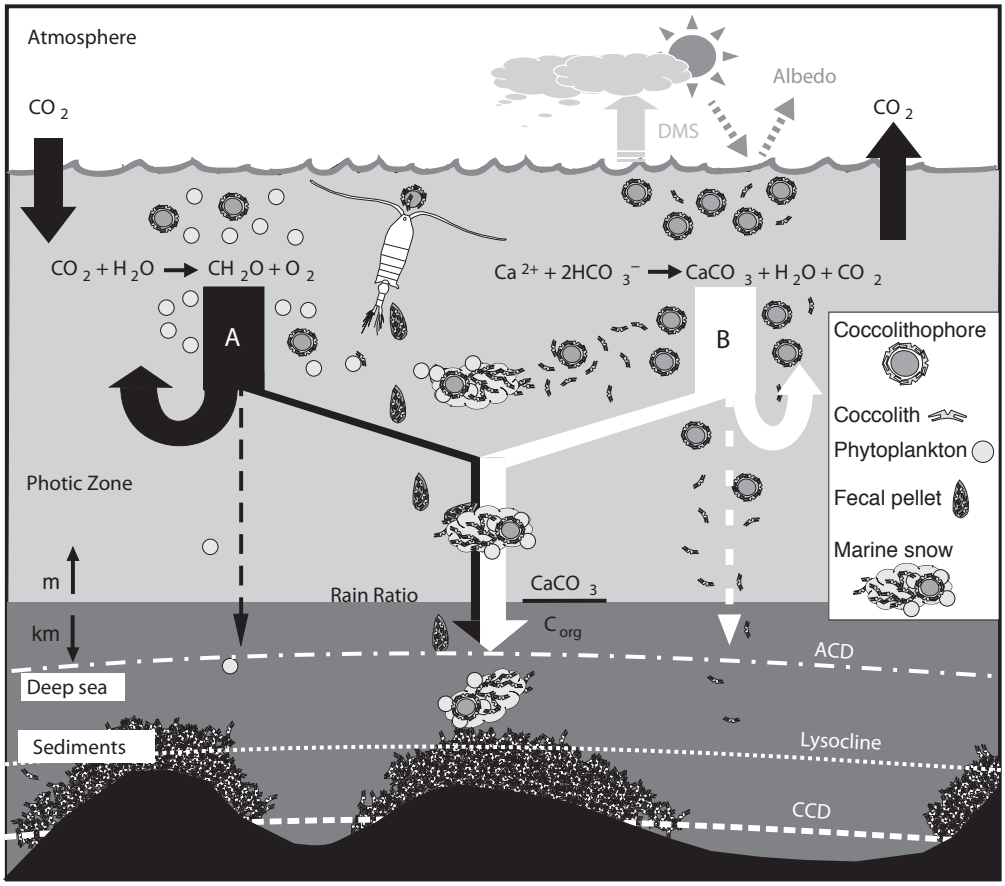

Figure 1.7. Coccolithophores and their role in biogeochemical cycles (slightly modified from De Vargas et al., 2007) . Coccolithophores affect the marine organic carbon pump (A) via their photosynthetic activity, and affect the marine inorganic carbon pump (B) due to the calcification of coccoliths. Furthermore they can affect climate via the production of dimethyl sulfide (DMS) and via an enhanced albedo of the sea surface due to the generation of large blooms. Abbreviations: Aragonite Compensation Depth (ACD), Calcite Comensation Depth (CCD).

and other physico-chemical parameters of the sea-surface (temperature, salinity, turbulence). Nevertheless, coccolithophores are adapted to a wide range of environmental conditions. For example, certain coccolithophore species have been found in the high saline waters of the Gulf of Elat (Winter et al., 1979), and in the low saline waters of Norwegian fjords (Kristiansen et al., 1997). However, in general, coccolithophores are adapted to sa-

linities that prevail in the open ocean (32 - 37 psu) (Baumann et al., 2005). The same wide tolerance is observed in terms of temperature, ranging from 31°C to below 0°C (Okada and McIntyre, 1979; Samtleben et al., 1995). Coccolithophores are furthermore found in eutrophic upwelling regions (Giraudeau et al., 1993; Ziveri et al., 1995; Broerse et al., 2000b; Sprengel et al., 2002), as well as in the oligotrophic subtropical gyres (Cortés et al., 2001; Sprengel et al., 2002; Boeckel and Baumann, 2008). As most coccolithophores are K-selected, highest diversity of coccolithophores are found in the oligotrophic regions of the subtropical gyres (Winter et al., 1994). However, individual coccolithophore species are mainly adapted to a relatively narrow range of environmental conditions (McIntyre and Bé, 1967; Okada and McIntyre, 1979; Brand, 1984; Haidar and Thierstein, 2001; Giraudeau et al., 2010). Therefore certain coccolithophore species only thrive in specific oceanic environments, resulting in a biogeographical distribution of coccolithophore species. Based on water and sediment samples McIntyre and Bé (1967) and Okada and Honjo (1973) divided the Atlantic and Pacific Ocean into distinct coccolithophore biogeographical provinces. They distinguished a subarctic, temperate (transitional), subtropical, tropical and subantarctic province, which each are characterized by a specific assemblage of coccolithophore species. The different ecological preferences of coccolithophore species are furthermore reflected in their morphology. Based on their ecological distribution, Young (1994) distinguished between placolith bearing, umbelliform and floriform coccolithophore species. Placolith bearing species are abundant in eutrophic environments, whereas umbelliform species are abundant in oligotrophic environments. The floriform species occur in the lower photic zones of the low- to midlatitudes. In order to use coccolithophores as a tool for paleoceanographic studies, a deep knowledge about the ecological preferences of coccolithophore species is needed.

Coccolithophores are one of the most productive carbonate producers in the oceans today (Westbroek et al., 1993; Zondervan et al., 2001; Beaufort et al., 2007), contributing about 50% of the global carbonate that reaches the deep oceans (Broecker and Clark, 2009). The carbonate produced by coccolithophores (coccoliths) mainly reaches the deep oceans via their incorporation into fecal pellets or marine snow (Honjo, 1976; Samtleben and Bickert, 1990). Up to 92% of coccolith carbonate reaches the deep oceans (Honjo, 1976). Due to the intracellular calcification of coccoliths, which produces CO_2, coccolithophores are a major component of the oceanic inorganic carbon pump. On the other hand, as coccolithophores build up their organic material via photosynthesis, which consumes

CO_2, they also affect the organic carbon pump of the ocean. The balance between the inorganic and organic carbon pump therefore regulates the CO_2 exchange between the surface ocean and the atmosphere (Sarmiento et al., 1998, Sigman, 2000) (Figure 1.7). Furthermore coccolithophores affect the carbon cycle via their ballasting effect. Like inorganic carbon, organic carbon is preferentially transferred to the deep ocean by fecal pellets and marine snow (Turner, 2002). As coccoliths have a higher density than biogenic opal and as they are more abundant than terrigenous sediments, their incorporation into the sinking particles makes the sinking process and hence the burial of organic carbon more efficient (Ziveri et al., 2007). Aside of their impact on the ocean carbon cycle, coccolithophore probably influence the environment due to their production of dimethyl sulfide (DMS), which they produce as a protection against grazing by zooplankton (Wolfe and Steinke, 1996; Levasseur et al., 1996). The DMS produced by coccolithophores leads to an enhanced reflection of incoming solar radiation, and it could act as condensation-nuclei for clouds (Burkill et al., 2002). At last, coccolithophores can produce large blooms, which are even visible from space (Brown and Yoder, 1994). The large quantities of calcite produced within such a bloom, up to $1x10^9$ kg calcite-C (Holligan et al., 1993), can increase the albedo of the sea-surface, at least on a regional scale (Tyrrell et al., 1999).

1.4.2 Evolution of coccolithophores and their use in paleoceanographic studies

The earliest occurrence of coccolithophores has been reported from Upper Triassic sediments from the Southern Alps in Italy (Bown, 1998). There, coccolithophores are abundant, but with a low diversity. Furthermore, Triassic coccolithophores seem to have been restricted to low-latitude regions (Bown, 1998). After a major extinction event at the Triassic /Jurassic boundary, coccolithophore diversity increased to reach maximum values during the Late Cretaceous. At the Cretaceous/Tertiary boundary 90% of coccolithophore species got extinct (Bown et al., 2004). Although coccolithophores recovered rapidly during the Paleocene/Eocene, a general decline in coccolithophore diversity is observed since the Eocene (Bown et al., 2004). Today, approximately 200 extant coccolithophore species are known (Young et al., 2003). Because coccolithophores evolve rapidly, and because they

Table 1.1. Use of coccolithophores and coccolithophore related proxies in paleoenvironmental studies (modified after Stolz, 2009). Methods used in this thesis are marked in grey.

Coccolithophore component	Analysis	Information	Examples
Coccolithophore assemblage	Assemblage composition	Ecological conditions (e.g. temperature, nutrients, hydrography)	Giraudeau et al. (2000) Flores et al. (2003)
		Biostratigraphy	Bown (1998)
		Coccolithophorid carbonate production	López-Otálvaro et al. (2008)
Single coccolithophore species	Morphometry of coccoliths	Surface-water conditions (temperature, salinity)	Hagino et al. (2005) Bollmann et al. (2002) Colmenero-Hidalgo et al. (2002)
	Calcification (SYRACO)	Indirect pCO_2 of seawater	Beaufort et al. (2011)
Coccolith carbonate	Mg/Ca	Sea-surface temperature	Stoll et al. (2001)
	Sr/Ca	Coccolithophore growth rate and productivity	Stoll and Schrag (2000) Stoll and Bains (2003)
	$\delta^{18}O$	Sea-surface temperature	Beltran et al. (2007)
	$\delta^{13}C$	Productivity	Rickaby et al. (2007)
Coccolithophorid biomarkers (alkenones)	$U^{K'}_{37}$, undersaturation ratio of alkenones	Sea-surface temperature	Schneider et al. (1995) Bard and Rickaby (2009)
	$\delta^{13}C$ of alkenones	pCO_2 of seawater	Pagani (2002)
	Tetra-undersaturated alkenones ($C_{37:4}$)	Position of oceanic fronts	Rosell-Melé et al. (1998)
	Alkenone concentration	Productivity	Villanueva et al. (1998)

are abundant in nearly all marine sediments, these species are successfully used as a biostratigraphic tool (e.g. Martini, 1971).

Because coccolithophores are sensitive to changes in the physicochemical conditions of the sea-surface (see chapter 1.4.1), have a fast reproduction cycle and are abundant in nearly every oceanic realm, they are perfectly suited for paleoceanographic studies. This suitability is furthermore strengthened by the fact that coccoliths have a higher preservation potential than foraminiferal $CaCO_3$ (e.g. Frenz et al., 2005). Based on the different ecological demands of individual coccolithophore species, many paleoceanographic studies deduce ecological changes based on changes within the coccolithophore assemblage (e.g. Flores et al., 1997, Flores et al., 2000; Giraudeau et al., 2000; Giraudeau et al., 2004; Baumann and Freitag, 2004; Stolz and Baumann, 2010; Chiyonobu et al., 2012). An important prerequisite for this approach is that the fossil coccolithophore assemblage has to reflect the assemblage in the sea-surface. There are several factors, such as (differential) dissolution, advection or grazing, which could influence the transformation from the living to the fossil assemblage (Samtleben and Bickert, 1990; Harris, 1994; Ziveri et al., 2000). However, surface sediment-, sediment trap- and water sample-studies indicate that the fossil coccolithophore assemblage works as a reliable representative of the sea-surface conditions (Baumann et al., 1999; Kinkel et al., 2000; Andruleit and Rogalla, 2002). Especially in the eastern North Atlantic, the working area of the presented thesis, changes in coccolithophore assemblages have been successfully used to reconstruct past environmental changes during the Late Quaternary (Lototskaya et al., 1998; Incarbona et al., 2010; Stolz and Baumann, 2010). Aside of this approach, there are numerous other applications of coccolithophores in paleoceanography (see summary in Table 1.1).

1.4.3 Ecology of selected coccolithophore species

As stated in chapter 1.4.1 and 1.4.2, a precise knowledge about the ecology of coccolithophore species is essential, in order to deduce past environmental changes based on abundance variations. Therefore this chapter will describe the ecology of the coccolithophore species used in this study.

Emiliania huxleyi

E. huxleyi is the most abundant extant coccolithophore species in modern oceans and has been dominating coccolithophore assemblages for the last 73 kyr (Thierstein et al., 1977). It has a wide biogeographical distribution and tolerates temperatures between 1 and 30°C (McIntyre et al., 1970; Okada and Honjo, 1973; Okada and McIntyre, 1979). *E. huxleyi* has been reported to grow at low salinities down to 12 psu (Paasche et al., 1996) and to occur in high saline waters (41 psu) of the Gulf of Elat (Winter et al., 1979). In general, it thrives in the upper photic zone with higher abundances in nutrient-rich subpolar waters as well as along the borders of subtropical gyres, in equatorial and coastal upwelling regions and outer shelf areas (Flores et al., 2010). Especially in the subpolar regions of the North Atlantic *E. huxleyi* forms extensive blooms during summer and early autumn, even visible from space (Brown and Yoder, 1994). There are three well-established, genotypical different morphotypes of *E. hux*leyi (Young and Westbroek, 1991). These are termed Type A, B and C and can be distinguished by the size of their distal shield and by the degree of calcification of distal shield elements. Furthermore there are evidences for a morphotype termed Type B/C, which has the same morphology than Type B and C but is intermediate in size, a morphotype Type R, which has heavy calcified distal shield elements, and a morphotype termed *E. huxleyi* var. *corona* (Young et al., 2003). Frequent occurrences of large *E. huxleyi* (≥ 4 µm; corresponding to Type B) have been linked to cold surface water conditions (Colmenero-Hidalgo et al., 2002; Hagino et al., 2005; Flores et al., 2010). An inverse relationship between the coccolith size of *E. huxleyi* and temperature has been found by Sorrosa et al. (2005) based on culturing experiments. Furthermore a positive correlation of distal shield length of *E. huxleyi* and sea surface salinity has been reported (Bollmann and Herrle, 2007; Bollmann et al., 2009). At last, *E. huxleyi* together with *G. oceanica* (and presumably other species of the family *Gephyrocapsa*) are known to synthesize alkenones, which are biomarkers that are successfully used as proxies in paleoceanography (e.g. Müller et al., 1998).

Gephyrocapsa muellerae

G. muellerae is described as a species preferring cool to temperate water conditions (Samtleben, 1980; Samtleben and Bickert, 1990; Samtleben et al., 1995). It is common in the temperate biogeographical zones at mid- to high latitudes of the Atlantic and Pacific

Oceans (Winter et al., 1994). Therefore it is widely used as an indicator for colder water temperatures compared to other gephyrocapsids (e.g. Weaver and Pujol, 1988; Di Stefano and Incarbona, 2004). Regarding the North Atlantic, Giraudeau et al. (2010) recently published a temperature range of 12 - 18°C and an optimum temperature of 14°C for *G. muellerae*. Furthermore the authors concluded on the basis of a comprehensive North Atlantic surface sediment sample set, that the eastern North Atlantic is an ecological niche for this species. Especially in the Azores Current System region, *G. muellerae* exclusively thrives in the transitional water masses to the north of the AzF (Jordan, 1988; Schiebel et al., 2011). However, local occurrences of this species have been reported from the Norwegian-Greenland Sea and from the upwelling regions off northwest Africa. The occurrence in the higher latitudes of the North Atlantic has been related to drifting of this species within transitional water masses transported by the North Atlantic Current (e.g. Samtleben and Schröder, 1992). The local occurrence of *G. muellerae* in the upwelling regions off northwest Africa indicates an affiliation to eutrophic conditions of this species (Sprengel et al., 2002).

Gephyrocapsa ericsonii

G. ericsonii has been described to have ecological preferences similar to those of *E. huxleyi* (Haidar and Thierstein, 2001). This results in a wide biogeographical distribution, ranging from temperate to tropical oceans (e.g. Okada and Honjo, 1973; Ziveri et al., 2004). Nevertheless increased *G. ericsonii* abundances can be found under high nutrient conditions (Baumann et al., 2008, and references therein). Beside this affinity, a weak positive correlation of increased *G. ericsonii* abundances to low salinities, turbulent water conditions and colder temperatures was found by Boeckel et al. (2006).

Coccolithus pelagicus

C. pelagicus preferentially lives in subpolar to polar regions (McIntyre and Bé, 1967), tolerating cold temperatures below 0°C (Okada and McIntyre, 1979; Samtleben et al., 1995). Beside the well-known cold water affinity of *C. pelagicus,* Cachão and Moita (2000) showed an increased abundance of *C. pelagicus* under high nutrient conditions at the Iberian margin. There are two well-established morphotypes of *C. pelagicus*, a small (6–10 *µ*m) morphotype (*C. pelagicus* ssp. *pelagicus*) associated with arctic conditions and a

larger (9–15 μm) morphotype (*C. pelagicus* ssp. *braarudii*) associated with more temperate and nutrient-rich conditions (Ziveri et al., 2004, and references therein). Studies of Parente et al. (2004) confirmed the usefulness of a small-sized morphotype as a subpolar water proxy and the usefulness of an intermediate-sized morphotype as a productivity proxy at the Iberian margin. Furthermore, these authors proposed a new, very large (> 14 μm) morphotype (*C. pelagicus* spp. *azorinus*), which probably could be used as a proxy for the influence of the AC in this region. However, the overall abundance of *C. pelagicus* in North Atlantic surface sediments closely parallels the abundance pattern its small morphotype, with clear abundance maxima in the polar and subpolar North Atlantic (Baumann et al., 2005).

Calcidiscus leptoporus

C. leptoporus is a cosmopolitan species occurring at nearly all latitudes (McIntyre and Bé, 1967). In the equatorial Atlantic and Arabian Sea an affinity of *C. leptoporus* to cold and nutrient-rich conditions has been successfully established (Kinkel et al., 2000; Andruleit and Rogalla, 2002). Fincham and Winter (1989) and Boeckel et al. (2006) concluded that a positive correlation to elevated nutrient levels might be the primary response of *C. leptoporus*. However, the overall distribution pattern of *C. leptoporus* in the North Atlantic is patchy with no clear ecological/hydrological preference (Ziveri et al., 2004). Knappertsbusch et al. (1997) introduced a subdivision of *C. leptoporus* into three morphotypes (small (≤ 5 μm), intermediate (≤ 8 μm) and large (≥ 8 μm)). It has been shown by Renaud et al. (2002) that the abundances of the intermediate and large morphotypes have similar variations with temperature, whereas the large morphotype is more opportunistic and can be associated with productive waters. The increasing relative abundance of the small morphotype seems to be mostly due to the decreasing fitness of the two other types in warm, nutrient-rich, stratified waters (Renaud et al., 2002).

Florisphaera profunda

F. profunda is abundant in tropical to temperate regions with a temperature range of 10 - 28°C (Okada and McIntyre, 1979). It lives in the lower photic zone at about 150 - 200 m water depth (e.g. Andruleit and Rogalla, 2002). Together with *G. flabellatus*, it is the only coccolithophore species known to inhabit the deep photic zone. Abundance variations

of *F. profunda* are associated with variations in nutricline-depth (Molfino and McIntyre, 1990). Therefore *F. profunda* is widely used as an indicator of past productivity changes (e.g. Ahagon et al., 1993; Beaufort, 1997; Flores et al., 2000; Kinkel et al., 2000; Li et al., 2010). The abundance of *F. profunda* also depends on lower photic zone temperatures with higher abundances during warmer periods (Okada and Wells, 1997; Tanaka and Tada, 2000; Baumann and Freitag, 2004).

Subtropical coccolithophore species

Umbellosphaera spp., *Umbilicosphaera* spp. and *Oolithotus* spp. are associated with warm and oligotrophic water masses (Incarbona et al., 2011; and references therein). These species are adapted to low-nutrient conditions, and therefore they are typical coccolithophore species in the warm and oligotrophic gyres of the Atlantic and Pacific Oceans (McIntyre and Bé, 1967; Okada and Honjo, 1973). *Umbellosphaera* spp. represent coccolithophores with umbelliform coccoliths, which thrive in the subtropical gyres of the oceans (see chapter 1.4.1; Young, 1994). Based on their known ecological preferences, these species have been grouped together as „subtropical species“ in this thesis.

Chapter II.

Materials and methods

2.1 Sample material

The sediment cores (GEOFAR KF16, MD08-3179Cq and MD08-3180Cq) used in this study were retrieved slightly south of the Azores Islands (Figure 2.1, Table 2.1). GEOFAR KF16 was retrieved onboard the research vessel Le Noroit, whereas MD08-3179Cq and MD08-3180Cq were retrieved onboard the research vessel Marion Dufresne during cruise MD-168. The major geological feature in the working area is the Mid Atlantic Ridge (MAR), which together with the East Azores Fracture Zone forms a triple junction between the North American, Eurasian and African tectonic plates (Searle, 1980). The MAR interacts

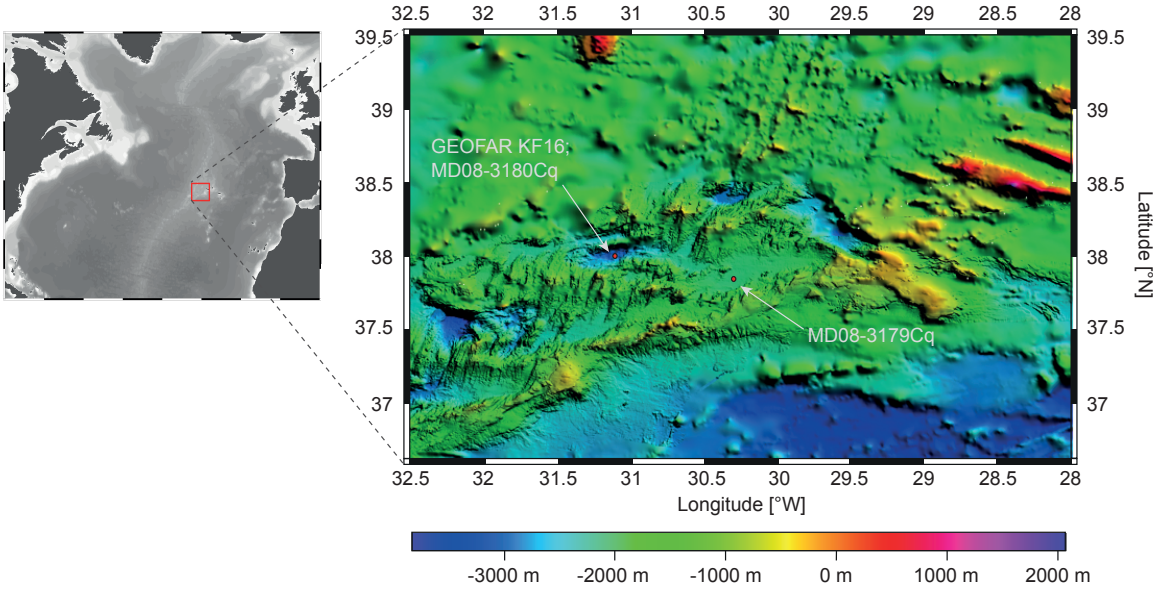

Figure 2.1. Bathymetric map of working area. High resolution bathymetric data (from Escartin et al., 2001), overlain on ETOP01 data. Position of used sediment cores indicated by red dots.

with a magmatic mantle plume. This results in active hydrothermalism in the working area (German et al., 1996). Although the cores GEOFAR KF16 and MD08-3180Cq were taken in the vicinity of the Menez Gwen hydrothermal field, the sediments at the coring site are not geochemically influenced by the venting (Richter, 1998). Furthermore, the topography of the working area is characterized by bathymetric heights (second order ridge segments), which are separated by non-transform discontinuities forming deep basins (Richter, 1998). Sediment cores GEOFAR KF16 and MD08-3180Cq have been retrieved in one of those basins, whereas MD08-3179Cq has been taken on a plateau at the MAR (Figure 2.1). The deep basin at the MAR, where the coring sites of GEOFAR KF16 and MD08-3180Cq are located, acts as a sediment trap, resulting in high accumulation rates and al-

lowing high-resolution sampling (Richter, 1998). The presence of laminations in the cores indicates an undisturbed sedimentation, as it has also been proposed by Richter (1998). Because the coring sites are far offshore, the sediment is primarily of biogenic origin. All studied cores consist of nannofossil ooze with foraminifera. The purely pelagic character of the sediment is also indicated by a high carbonate content of up to 85% (Richter, 1998). Furthermore, all investigated sediment samples solely consist of coccolithophores, foraminifers, calcareous dinoflagellates, diatoms and silicoflagellates, as observed by Scanning Electron Microscopy (SEM). Because there was no surface sediment sample available for GEOFAR KF16, a surface sediment sample from the companion boxcore GEOFAR KG14 was analyzed as a modern reference sample.

Table 2.1. Sediment cores used in this study

Latitude	Longitude	Water depth	Length	Coring device	Reference
		GEOFAR KF16			
37°59.59'N	31°7.698'W	3050 m	8 m	Piston corer	Richter (1998)
		GEOFAR KG14			
37°59.59'N	31°7.698'W	3050 m	-	Boxcorer	Richter (1998)
		MD08-3179Cq			
37°50.56'N	30°17.64'W	2040 m	8.14 m	Calypso square-corer	Kissel et al. (2008)
		MD08-3180Cq			
37°59.99'N	31°8.07'W	3064 m	10.5 m	Calypso square-corer	Kissel et al. (2008)

2.2 Coccolithophore analysis

2.2.1 Quantitative coccolithophore analysis

Samples for quantitative coccolithophore analysis were prepared with a combined dilution/filtration technique following Andruleit (1996). Therefore a small amount of the freeze-dried sample (60 - 85 mg) was weighted and brought into suspension using approximately 200 ml tap water. In order to get a homogenous suspension and to disintegrate agglutinated sediment particles (e.g. fecal pellets), the solution was ultrasonicated for 15 to 30 s using a ™Bandelin Sonorex RK 106 S ultrasonic bath. Then the suspension was immediately split by a factor of 100 using a ™Fritsch Laborette 27 rotary sample divider. The resulting fraction was filtered on a polycarbonate membrane filter (™Satorius Stedim Biotech Polycarbonate Track-Etch Membrane; ⌀ = 47 mm; pore size = 0.4 µm) using a vacuum filtering device. After filtering, the membrane was stored in plastic petri dishes and dried in an oven at 40°C for 24h. After drying, a small piece of the membrane filter was cut out and mounted on an aluminum SEM stub. The sample was then sputtered with gold/palladium. At least 300 coccoliths (320 - 820; average 370) were counted in each sample using a ™CamScan 44 SEM. The coccoliths were counted on measured transects at a magnification of 5000 and identified according to the taxonomy given in Young et al. (2003). A taxonomic list and SEM pictures of selected coccolithophore species is given in the Appendix. In order to improve the accuracy of the less abundant species *C. pelagicus*, extended counts were carried out. Therefore a whole transect was scanned across the filter at a magnification of 1000 and only specimens of *C. pelagicus* were counted. Relative abundances of each species have been calculated according to:

$$R_i = \frac{C_i}{C_t} \times 100 \qquad (2.1)$$

R_i = relative abundance of species i

C_i = coccoliths of species i counted

C_t = total coccoliths counted

As the described preparation and analysis allows the determination of absolute abundances, the concentration of total coccoliths and species concentrations in the sediment were calculated according to Andruleit (1996):

$$CC_{i/t} = \frac{FA \times C_{i/t} \times SF}{IA \times SW} \qquad (2.2)$$

$CC_{i/t}$ = coccolith concentration of species i/total
FA = filter area
$C_{i/t}$ = coccoliths of species i/total counted
SF = split factor
IA = investigated filter area
SW = sample weight

Coccolith accumulation rates have been proven to be a good estimate of coccolithophore productivity (e.g. Lotoskaya et al., 1998; Kinkel et al., 2000; Baumann and Freitag, 2004; Incarbona et al., 2011). Therefore we calculated coccolith accumulation rates using sedimentation rates resulting from the applied age models (see chapters 3 - 5) and dry bulk densities from core GEOFAR KF16 (Richter, 1998), which were interpolated between two points of known densities:

$$CA = CC_t \times DBD \times SR \qquad (2.3)$$

CA = coccolith accumulation rate
CC_t = total coccolith concentration
DBD = dry bulk density
SR = sedimentation rate

The relative contribution of coccolith carbonate to the bulk sediment can be calculated if coccolith weights are known. These can be calculated using the density of calcite, species specific shape factors and species specific mean coccolith lengths (Beaufort and Heussner, 1999; Young and Ziveri, 2000). In this study coccolith carbonate was calculated using the species-specific coccolith weights given in Table 2.2. Where the coccolith weight for a species was not known, the average coccolith weight (8 pg) was used. The relative contribution of coccolith carbonate was calculated using the following equation:

$$C_{carb} = \sum \left(CC_i \times CW_i \right) \times 100 \qquad (2.4)$$

C_{carb} = coccolith carbonate

CC_i = coccolith concentration of species i

CW_i = coccolith weight of species i

Table 2.2. Coccolith weight of different coccolithophore species

Species	Coccolith weight (pg)	Reference
E. huxleyi (Type A)	2.3	Young and Ziveri (2000)
G. muellerae	8	Young and Ziveri (2000)
G. oceanica	12.3	Young and Ziveri (2000)
G. ericsonii	3.6	Young and Ziveri (2000)
C. pelagicus	143.3	Young and Ziveri (2000)
C. leptoporus (large)	164.2	Beaufort and Heussner (1999)
C. leptoporus (small)	22.6	Beaufort and Heussner (1999)
C. leptoporus (mean)	57	Young and Ziveri (2000)
F. profunda	1.7	Young and Ziveri (2000)
H. carteri	135	Young and Ziveri (2000)
O. fragilis	96.8	Young and Ziveri (2000)
R. clavigera	67.5	Young and Ziveri (2000)
R. stylifera	40.5	Young and Ziveri (2000)
S. apsteinii	540	Young and Ziveri (2000)
S. pulchra	13.5	Young and Ziveri (2000)
Syracosphaera spp.	12.1	Beaufort and Heussner (1999)
U. tenius	8.7	Young and Ziveri (2000)
U. irregularis	5.8	Young and Ziveri (2000)
U. sibogae	16.9	Young and Ziveri (2000)
U. foliosa	35	Young and Ziveri (2000)
Acanthoica spp.	0.3	Young and Ziveri (2000)
C. mediterranea	12.1	Young and Ziveri (2000)
Small coccolith	2.6	Young and Ziveri (2000)
Average coccolith	8	Honjo (1976)

2.2.2 Reliability of coccolithophore analysis

Several error sources are inherent in the above described dilution/filtration technique (for a short review see Giraudeau and Beaufort; 2007). For example it is essential to produce one layer of coccoliths, which have to be evenly distributed on the filter membrane. The use of 60 - 85 mg sample material combined with a splitting factor of 100 produced a single layer of coccoliths on the filters. If a filter was found to be unevenly covered with sediment, the sample processing was repeated. In order to avoid contamination (e.g. coccoliths from previously prepared samples), all utensils used for the preparation were rinsed with tap water after each single sample preparation. To estimate the influence of contamination on the results, a blank sample (tap water without sediment) was prepared and investigated. The blank sample yielded an error of 0.03%, indicating that the error due to contamination is negligible.

Additional errors may be induced, if the counted coccoliths are not representative for the assemblage. Therefore at least 300 individuals are commonly counted in micropaleontological studies. This number is based on calculations of Van Der Plas and Tobi (1965), who calculated that counting of 300 individuals is sufficient to reliably (95% confidence) count species whose abundance in the assemblage is 1% (also see Patterson and Fishbein, 1989). Their approach treats the assemblage as a binominal assemblage, where the 95% confidence intervals can be calculated according to:

$$\sigma_{i;95;bin} = 1.96 \times \sqrt{p_i q_i / n} \qquad (2.5)$$

$\sigma_{i;95;bin}$ = binominal 95% confidence interval of species i

p_i = proportion of species i

q_i = 1-p_i

n = total number of counted coccoliths

The 95% confidence intervals have been calculated for an abundant (*E. huxleyi*) and a less abundant (*F. profunda*) species (Figure 2.2). The average 95% confidence interval for *E. huxleyi* is ± 4.9% and for *F. profunda* ± 1.6%. These errors are negligible considering the observed changes in the abundance records (Figure 2.2). However, a more precise

evaluation of the representativeness of a selected assemblage is given by replicate measurements (Buzas, 1990), at which the 95% confidence interval is calculated according to:

$$\sigma_{i;95;clus} = 1.96 \times \sqrt{\sum n_j \left(p_j - p\right)^2 / mn^2 \left(m-1\right)} \qquad (2.6)$$

$\sigma_{i;95;clus}$ = cluster 95% confidence interval of species i

n_j = total number of counted coccoliths in sample j

$p_j = a_j/n_j$

aj = individuals of species i in sample j

$p = \sum a_j / \sum n_j$

$n = \sum n_j / m$

m = number of replicates

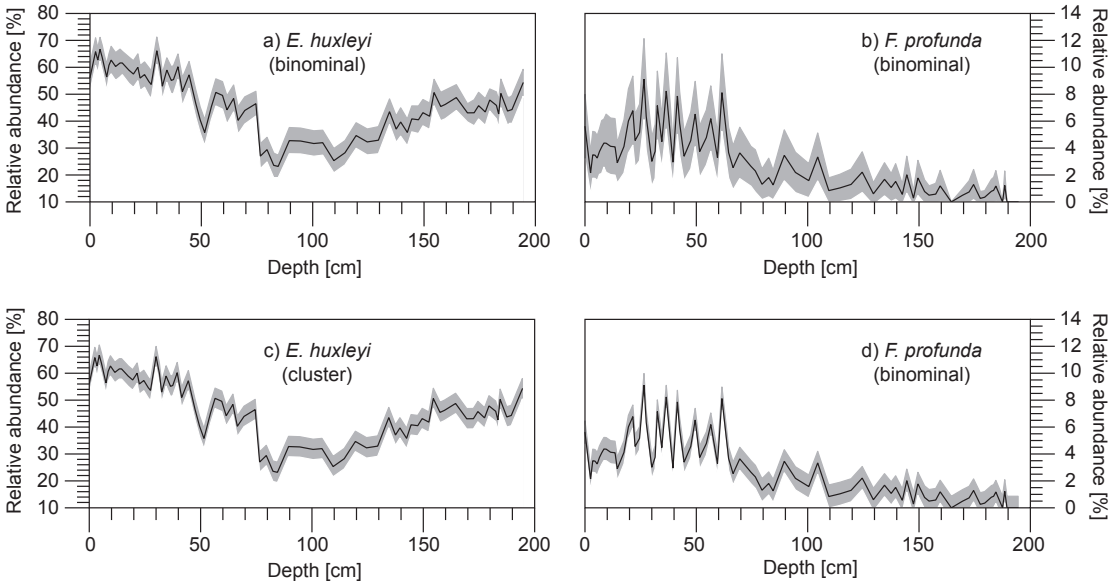

Figure 2.2. Relative abundances of a) *E. huxleyi* and b) *F. profunda* in GEOFAR KF16 with error envelopes calculated according to equation (2.5). Relative abundances of c) *E. huxleyi* and d) *F. profunda i*n GEOFAR KF16 with error envelopes calculated according to equation (2.6).

Replicate counting or replicate preparation was conducted on 17 sediment samples. Based on equation (2.6) the 95% confidence intervals of the abundant species *E. huxleyi* and of the less abundant species *F. profunda* were calculated. The calculations yielded an average 95% confidence interval of *E. huxleyi* of ± 3.8% and ± 0.86% for *F. profunda*. These values are even lower than the confidence intervals calculated assuming a binominal distribution. Therefore, the calculated errors are again negligible considering the observed abundance changes in the records (Figure 2.2). Furthermore the mean standard deviation of coccolith concentrations in the replicate samples was calculated (± 7.1 x 10^9 coccoliths/g sediment). This standard deviation was applied to the calculation of coccolith

accumulation rates, which are used to estimate coccolithophore productivity (see chapter 2.2.2; Figure 2.3). Again, the error is negligible regarding the observed fluctuations in the assemblage. In general, counting 300 coccoliths is enough to reliably trace relative and absolute abundance variations.

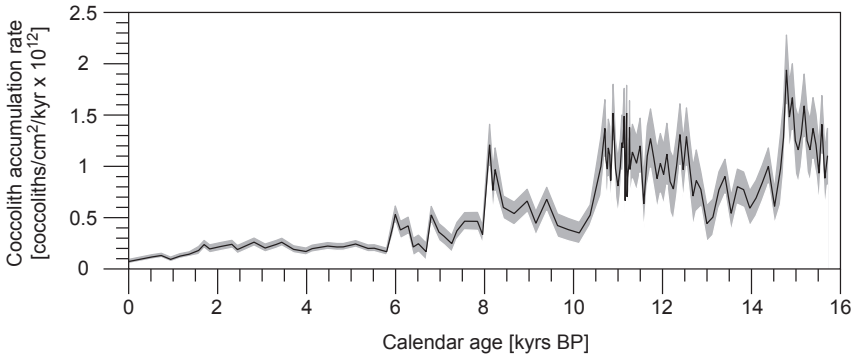

Figure 2.2. Coccolith accumulation rates in spliced sediment cores GEOFAR KF16 and MD08-3180Cq with error envelope according to the standard deviation.

2.3 Alkenone analysis

Alkenones are long-chain (C_{37} - C_{39}), primarily di- and tri-unsaturated methyl and ethyl ketones, which were first identified in sediments from the Walvis Ridge and from the Black Sea (De Leeuw et al., 1980). These compounds are synthesized by coccolithophores. Alkenones have been found to be synthesized by *E. huxleyi* and *G. oceanica*, and they are probably also synthesized by other coccolithophores of the family Noelaerhabdaceae (Volkman et al., 1980, 1995; Conte et al., 1998). According to classical membrane lipids, the composition of alkenones (unsaturation state) changes in response to temperature, in order to maintain the fluidity and rigidity of the membrane (Yamamoto et al., 2000). The dependence of the composition of alkenones on growth temperature has been shown by culture studies, water sample studies and studies of surface sediments (see review by Müller et al., 1998). Therefore the composition of alkenones can be used to estimate temperature. Brassell et al. (1986) introduced the following equation, which is based on the abundances of di-, tri and tetra-unsaturated C_{37} methyl alkenones, in order to quantify alkenone composition:

$$U_{37}^{K} = \frac{\left(C_{37:2} - C_{37:4}\right)}{\left(C_{37:2} + C_{37:3} + C_{37:4}\right)} \qquad (2.7)$$

Because the tetra-unsaturated $C_{37:4}$ compound is only present at low temperatures, Prahl and Wakeham (1987) introduced a simplified equation:

$$U_{37}^{K'} = \frac{\left(C_{37:2}\right)}{\left(C_{37:2} + C_{37:3}\right)} \qquad (2.8)$$

The resulting index is commonly converted into sea surface temperature (SST), using the calibration of Müller et al. (1998), which is based on analysis of surface sediments:

$$SST = \frac{\left(U_{37}^{K'} - 0.044\right)}{\left(0.033\right)} \qquad (2.9)$$

For this study, alkenones were analyzed at the biomarker laboratory at the Christian-Albrechts-University Kiel, following the procedure described by Etourneau (2009). For alkenone analysis 2 g of freeze-dried sediment sample were pestled, and 1 cm layer silicagel, 1 μg cholestean ($C_{27}H_{48}$) and 0.5 μg hexatriacontane ($C_{36}H_{74}$) were added as an internal standard. Furthermore modified Diatomeenerde (Isolute HM-N, extraction grade) was added to increase the sample volume to 11 ml. As a solvent dichloromethane (DCM) was used. Alkenones were extracted using a Dionex ASE 200 set to 75°C and 80 bar nitrogen gas pressure. The resulting extract was cooled down to -20°C in a freezer, and concentrated to 50 μl using a rotary evaporator bath set to 300 mbar and 20 - 22°C. The residue was dried over nitrogen and took up in 200 μl hexane. Alkenones were analyzed using multidimensional, double column gas chromatography (MDGC), using two Agilent 6890 gas chromatographs. Both chromatographs were individually equipped with an oven and a flame ionization detector (FID), and were connected via a transfer line. A more detailed description of the experimental setup and the measuring procedure can be found in Etourneau (2009). The first FID is used as a monitor detector, whereas the second FID is used as the main detector. Only a small, predefined fraction reaches the second FID. This FID has a much higher sensitivity compared to the first one, because of the reduced

memory effect and reduced contamination by coeluates. From the main detector chromatogram (Figure 2.4), the $U^{K'}_{37}$ index was calculated according to:

$$U^{K'}_{37} = \frac{Area\ C_{37:2}}{Area\ C_{37:2} + Area\ C_{37:3}} \qquad (2.10)$$

Area $C_{37:2}$ = area of $C_{37:2}$ peak in chromatogram

Area $C_{37:3}$ = area of $C_{37:3}$ peak in chromatogram

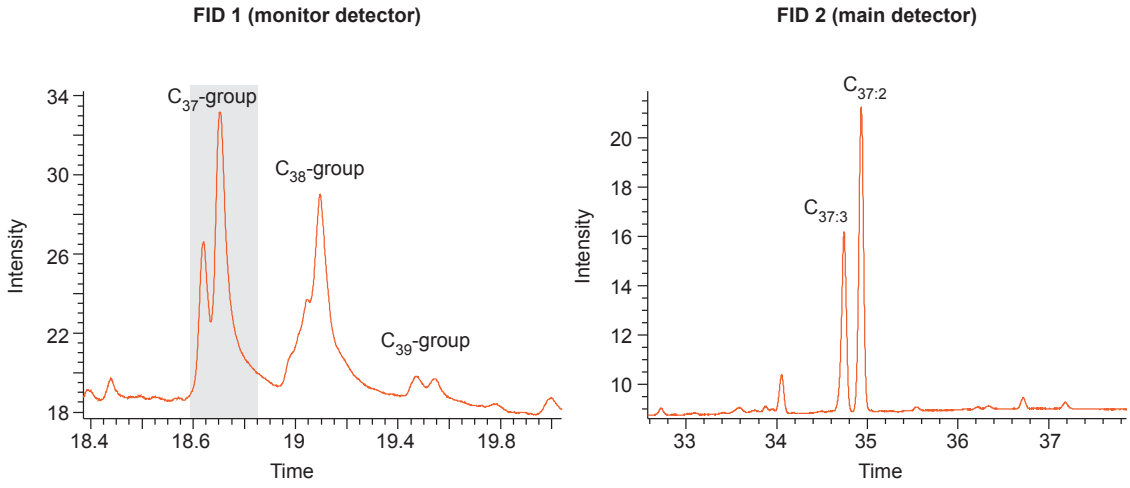

Figure 2.4. Chromatograms from the monitor detector (left) and from the main detector (right). The fraction that reaches the main detector is indicated as a grey bar in the monitor detector chromatogram. The $U^{K'}_{37}$ index was calculated from the main detector chromatogram. Chromatograms are from sample 320,25 cm (MD08-3180Cq).

The results were converted into SST using equation (2.9). Based on replicate measurements of the samples and the standard, the standard deviation of the SST estimate is ± 0.2°C. Furthermore it is possible to determine the alkenone concentrations in the sediment, when analyzing the $U^{K'}_{37}$ index. Alkenone concentrations/accumulation rates are widely used to estimate coccolithophore paleoproductivity (e.g. Hinrichs et al., 1999; Villanueva et al., 2001; Seki et al., 2004). Alkenone concentrations can be calculated according to equation (2.11), which then can be converted into accumulation rates using equation (2.12).

$$C_{37} = \frac{Area\ C_{37} \times C_{36} \times D}{IV / \left(Area\ C_{36} \times SW \right)} \qquad (2.11)$$

C_{37} = concentration of either $C_{37:2}$ or $C_{37:3}$

C_{36} = the hexatriacontane standard concentration

D = dilution of the sample for GC

IV = injected volume of extract

SW = sample weight

$$AAR = AC \times SR \times DBD \qquad (2.12)$$

AAR = alkenone accumulation rate

AC = alkenone concentration

SR = sedimentation rate

DBD = dry bulk density

2.4 X-ray fluorescence (XRF) core logging

XRF core scanning is a non-destructive method, which faithfully traces downcore changes in the relative chemical composition (major, minor and trace elements) of sediment cores (Richter, 2006). XRF scanning uses a X-ray beam to ionize atoms in a sample, which leads to an emission of element-specific fluorescence energy (e.g. Tjallingii, 2006). The intensity of the back-emitted energy is proportional to the element concentration and can be detected and measured. However, changes in the lithology of the sediment and changes in the surface roughness of the split sediment cores can influence the measurements (Richter et al., 2006). Therefore this method is considered to be semiquantitative.

XRF core scanning was conducted using the AAVATECH XRF core scanner at the Institute of Geosciences at the Christian-Albrechts-University Kiel. The measurements were carried out on sediment cores MD08-3179Cq and MD08-3180Cq with a sampling resolution of 0.5 cm. Before measuring, the core segments were scrape-cleaned and covered with a foil (SPEX CertiPrep 3525 Ultralene foil, 4 μm thick). Every core segment was measured twice, once with generator settings of 10 kV (livetime: 30 s) and once with gen-

erator settings of 50 kV (livetime: 30 s). The reliability of the measurements is given by monitoring the „deadtime“ and the χ^2 value (cf. Tjallingii, 2006). In this study, the deadtime and the χ^2 value are generally well below the critical values of 40% and 3 respectively. The downcore variability of an element is given in counts/seconds, which is obtained by normalizing the detected element intensity to the livetime.

In this study, the XRF results are given as elemental ratios, which accounts for inhomogeneities in the lithology and experimental setup. Furthermore, the ratio of selected elements can be used to refine the interpretations. For example, in this study, changes in the Ba/Ti ratio are used to monitor changes in the biogenic barium content. As barium is also contained in terrestrial material, the normalization to titanium, which is primarily contained in terrestrial material, accounts for terrestrial input. As changes in biogenic barium are widely used to monitor changes in paleoproductivity (e.g. Moreno et al., 2002; Weldeab et al., 2003), the changes in Ba/Ti have been interpreted in terms of paleoproductivity. Furthermore, in order to quantitatively estimate productivity changes, the barium counts were converted into barium concentrations using Ba concentrations measured by Richter (1998) (see chapter 3). The resulting barium concentrations were converted into new primary productivity (gC/m^2/year) using an algorithm developed by Dymond et al. (1992) and modified by Francois et al. (1995):

$$P_{new} = 1.95 \times \left(F_{Ba}\right)^{1.41} \qquad (2.13)$$

at which:

$$F_{Ba} = AR\ Ba_{bio} / 0.209 \log\left(MAR\right) - 0.213 \qquad (2.14)$$

$AR\ Ba_{bio}$ = accumulation rate of biogenic barium

MAR = mass accumulation rate

The new primary productivity was converted into primary productivity (gC/m^2/year) using an equation developed by Epply and Peterson (1979):

$$PP = 20 \times \sqrt{P_{new}} \qquad (2.15)$$

Another example is the Si/Ca ratio, which was used to monitor relative changes in the contribution of siliceous and calcareous plankton to the sediment. In order to validate this approach, we additionally conducted diatom counts, which indicate that the Si/Ca ratio can readily be used to estimate the relative contribution of siliceous plankton (diatoms) to the sediment (see chapters 3 and 4).

2.5 Age models

The age models of sediment cores GEOFAR KF16 and MD08-3180Cq were established using 15 Accelerator Mass Spectrometer (AMS) radiocarbon ages and tuning the alkenone and planktonic oxygen isotope records to the NGRIP oxygen isotope record (Andersen et al., 2007). The age model of MD08-3179Cq was established by tuning the planktonic oxygen isotope record to the LR04 stack (Lisiecki and Raymo, 2005). Furthermore, the age model of the last deglaciation and Holocene period was refined in MD08-3179Cq by tuning the Ba/Ti record measured by XRF to the well-dated Ba/Ti record of MD08-3180Cq. A detailed description of the individual age models can be found in the following chapters. The age models of GEOFAR KF16 and MD08-3180Cq are described in detail in chapter 3.3.1. The age model for MD08-3179Cq is described in chapter 4.3.1 and chapter 5.3.2.

Because only Holocene and Preboreal samples were available from core GEOFAR KF16, this core was spliced with MD08-3180Cq from the same location (Figure 2.1., Table 2.1), to get continuous coccolithophore abundance records over the Holocene and last deglacial period (see chapter 3.3.1). The cores were spliced at 11.4 kyrs BP (corresponding to 201.6 cm core depth in GEOFAR KF16 and 159.3 cm core depth in MD08-3180Cq), at which the coccolithophore abundance records before 11.4 kyrs BP are from GEOFAR KF16, whereas the coccolithophore abundance records after 11.4 kyrs BP are from MD08-3180Cq. Both cores show a very good overlap in the oxygen isotope records (Repschläger et al., submitted) and in the coccolithophore abundance records (Figure 2.5).

High-resolution C14-dating is currently conducted on the deglacial section of MD08-3180Cq (Balmer et al., in prep.). Furthermore high-resolution foraminiferal census counts are currently conducted in the same core section (Weinelt et al., in prep.). Based on pre-

liminary results, the inception of the Younger Dryas cold reversal will probably shift from 253 cm core depth to 270 cm core depth (Balmer and Weinelt, personal communication). However, as this will increase accumulation rates during the Younger Dryas and decrease them during the Bølling/Allerød, and as this change also fits to the coccolithophore census counts (Figure 2.5), it will not affect the conclusions drawn in terms of paleoproductivity and hydrographic changes (cf. chapter 3).

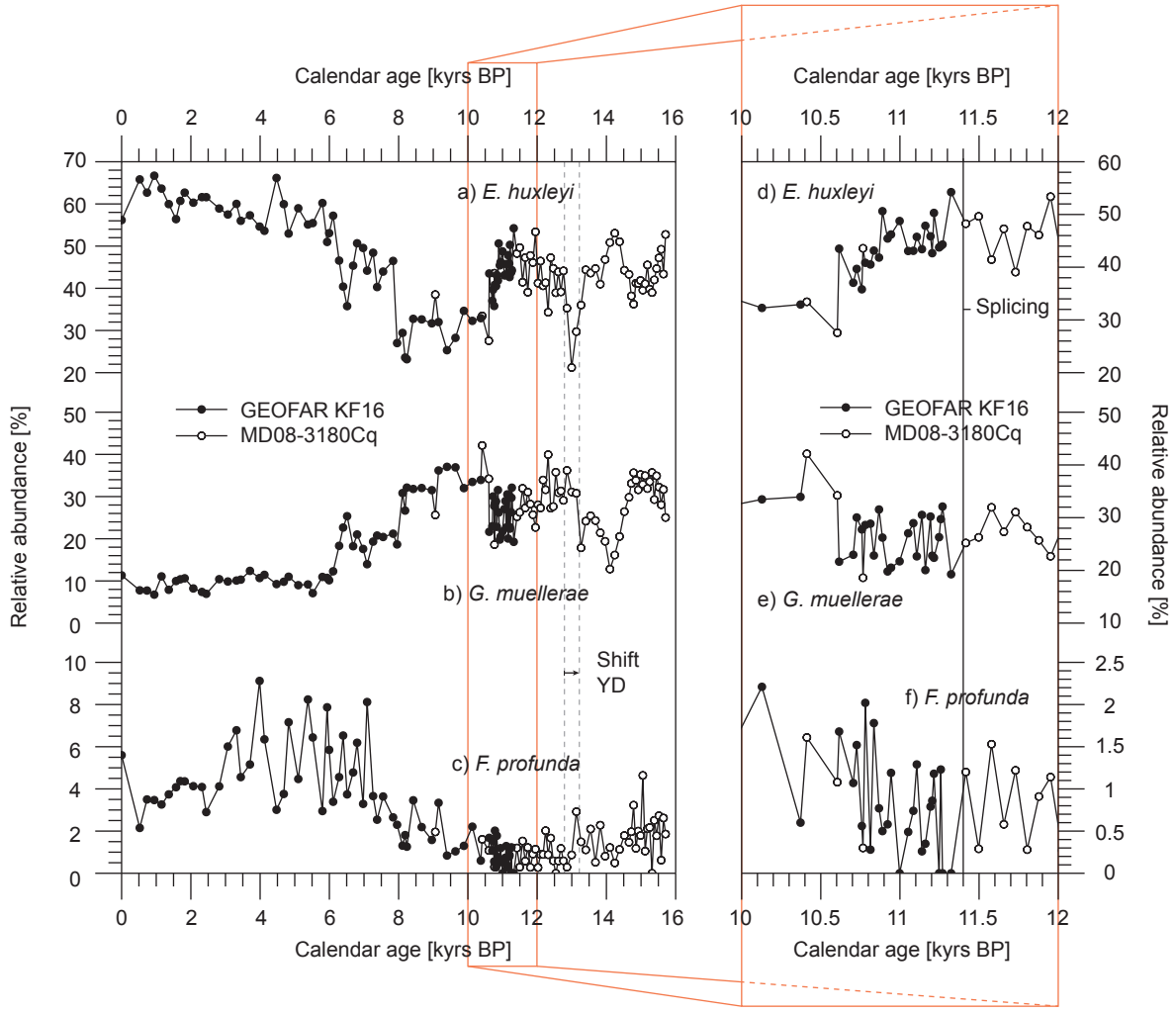

Figure 2.5. Relative abundances of coccolithophore species in sediment cores GEOFAR KF16 (filled dots) and MD08-3180Cq (open dots). The splicing is indicated with a vertical solid line. The possible shift of the Younger Dryas boundary is indicated by dashed vertical lines.

Chapter III.

Coccolithophore paleoproductivity and ecology response to deglacial and Holocene changes in the Azores Current System

(This chapter corresponds to the following manuscript published in Paleoceanography: Schwab, C., Kinkel, H., Weinelt, M., Repschläger, J., 2012. Coccolithophore paleoproductivity and ecology response to deglacial and Holocene changes in the Azores Current System. Paleoceanography 27, PA3210.)

3.1 Abstract

In order to test the sensitivity of marine primary productivity in the midlatitude open ocean North Atlantic to changes in the Atlantic Meridional Overturning Circulation (AMOC), we investigated two spliced sediment cores from a site south of the Azores Islands at the northern rim of the North Atlantic subtropical gyre. For this purpose we analyzed coccolithophore assemblages, diatom abundances, alkenones and conducted X-ray fluorescence (XRF) core scanning. During times of reduced AMOC, especially during Heinrich event 1 (H1) and the Younger Dryas, we observe a strong increase in productivity as evidenced by high coccolith accumulation rates, high alkenone concentrations/accumulation rates, high Ba/Ti-ratios, high abundances of diatoms and low abundances of *F. profunda*. The increased productivity is partly caused by a more southern position of the Azores Front (AzF), and hence by a less northward extension of the subtropical gyre, as deduced from high abundances of the temperate coccolithophore species *G. muellerae* and low abundances of subtropical species (*Oolithotus* spp., *Umbellosphaera* spp., *Umbilicosphaera* spp.). However, to explain the full range of the observed productivity increase, other factors like increased westerly winds and advection of nutrient-rich surface waters have also to be considered. Because this pattern can also be observed in other sediment cores from the midlatitude North Atlantic, we propose that during times of reduced AMOC there has been a band of strongly increased productivity across the North Atlantic at the northern rim of the contracted subtropical gyre, which partly counteracts the decreased organic carbon pump in the high northern latitudes.

3.2 Introduction

Primary productivity (PP) is an integral part of the climate system, because it affects the global carbon cycle due to the fixation of atmospheric carbon (e.g. Falkowski et al., 2000). As half of the global net PP takes place in the oceans (Field et al., 1998), changes in oceanic productivity are of high interest to the (paleo-) climate community. Therefore immense efforts have been undertaken to reconstruct past changes in productivity and to gain more insights into the sensitivity and relation of this process to climate changes (e.g.

Sarnthein et al., 1988; Kohfeld et al., 2005; Nave et al., 2007). However, regarding the North Atlantic, most paleoproductivity estimates are conducted in the high northern latitudes and/or in coastal regions (e.g. Sarnthein et al., 1988; Nave et al., 2007), where thick piles of sediments allow a detailed reconstruction of past productivity changes. Reconstructions from the open ocean are scarce, because of the notoriously low sedimentation rates in this area. However, changes in this area are crucial due to the large area covered by the open ocean.

In order to circumvent the patchy picture drawn from the sedimentary record and to gain more insights into the processes involved, this topic has also been a focus of many modeling studies (e.g. Brovkin et al., 2002; Schmittner et al., 2005). These studies suggest that during times of reduced AMOC, e.g. during Heinrich events, productivity drastically decreases in the global ocean and especially in the North Atlantic (Schmittner et al., 2005; Menviel et al., 2008; Mariotti et al., 2012). Although this result is generally corroborated by the sedimentary record, there are still mismatches between the two approaches on a regional scale (e.g. Salgueiro et al., 2010), pointing to the fact that the spatial resolution of coupled biogeochemical models is still insufficient and/or that there are processes not considered by the models (Schmittner et al., 2005; Mariotti et al., 2012).

Furthermore, PP related to the subtropical gyres is of particular interest. Although PP in these oligotrophic ecosystems is low, their large size allows for a significant contribution on a global scale (Polovina et al., 2008). They account for a quarter of global PP (Longhurst et al., 1995) and contribute up to 50% of global ocean carbon export (Emerson et al., 1997). Because of this important role in the biogeochemical cycling of carbon, which controls atmospheric CO_2 levels over time (Sarmiento and Siegenthaler, 1992), changes in their spatial extension and/or nutrient inventory are crucial to the understanding of past and future climate changes.

Because the northern boundary of the North Atlantic subtropical gyre is marked by the Azores Current System with its associated AzF (Maillard and Käse, 1989; Bashmachnikov et al., 2004), the northward extension of the gyre can be deduced from the latitudinal position of the AzF. However, results in the recent literature are contradictory concerning the past latitudinal position of the AzF and hence the past northward extension of the gyre. For example Rogerson et al. (2004) stated that in the Gulf of Cadiz the AzF did not change its position during the course of the last deglacial, whereas Schiebel et al. (2002a), based on low-resolution sediment cores from an open ocean site in the North Atlantic, recon-

structed a more southern position of the front during glacials compared to interglacials. Therefore, based on two spliced and high-resolution sedimentary records drilled near the Azores Islands, we will test, if the AzF and hence the subtropical gyre changed their position/extension during the course of the last deglacial and Holocene. Furthermore we will discuss possible reasons for the observed variability and discuss a hypothetical connection between the front dynamics in the open ocean and near the coast. At last we will test the sensitivity of PP in the open ocean North Atlantic to changes in AMOC and within the AzF, and assess its potential impact on the carbon cycle.

For this purpose we mainly analyzed coccolithophore assemblages, which are widely used to reconstruct paleoecological and paleoceanographic conditions (McIntyre and Bé, 1967; Beaufort et al., 1997; Kinkel et al., 2000; Flores et al., 2000; Giraudeau et al., 2010; Saavedra-Pellitero et al., 2011). For example relative abundances of certain coccolithophore species within coccolith assemblages have been successfully used to reconstruct frontal movements (e.g. Findlay and Giraudeau, 2002). Furthermore changes in the absolute abundances of coccolithophores have been successfully used to reconstruct past productivity changes (e.g. Stolz and Baumann, 2010). At last coccolithophores are considered to be the most important primary producers in the open ocean of tropical to temperate regions (Brand, 1994) and therefore they are ideally suited to trace past productivity and AzF dynamics at our coring site.

3.3 Recent hydrography and productivity regime

Our study area is located southwest of the Azores Islands, slightly north of the Azores Current System (Figure 3.1a). Like the Portugal Current, the Azores Current System is a branch of the northeastward flowing North Atlantic Current, the dominant surface water flow in the North Atlantic. Major components of the Azores Current System are the Azores Current and its associated AzF, which are situated between 32° and 35°N (Klein and Siedler, 1989; Maillard and Käse, 1989). Recent modeling studies suggest that the water mass transformation within the Gulf of Cadiz is responsible for the formation of the Azores Current System (e.g. Jia, 2000; Volkov and Fu, 2010, 2011). According to the β-plume theory the comparatively small outflow of Mediterranean Outflow Water (MOW) (1 Sv) forces

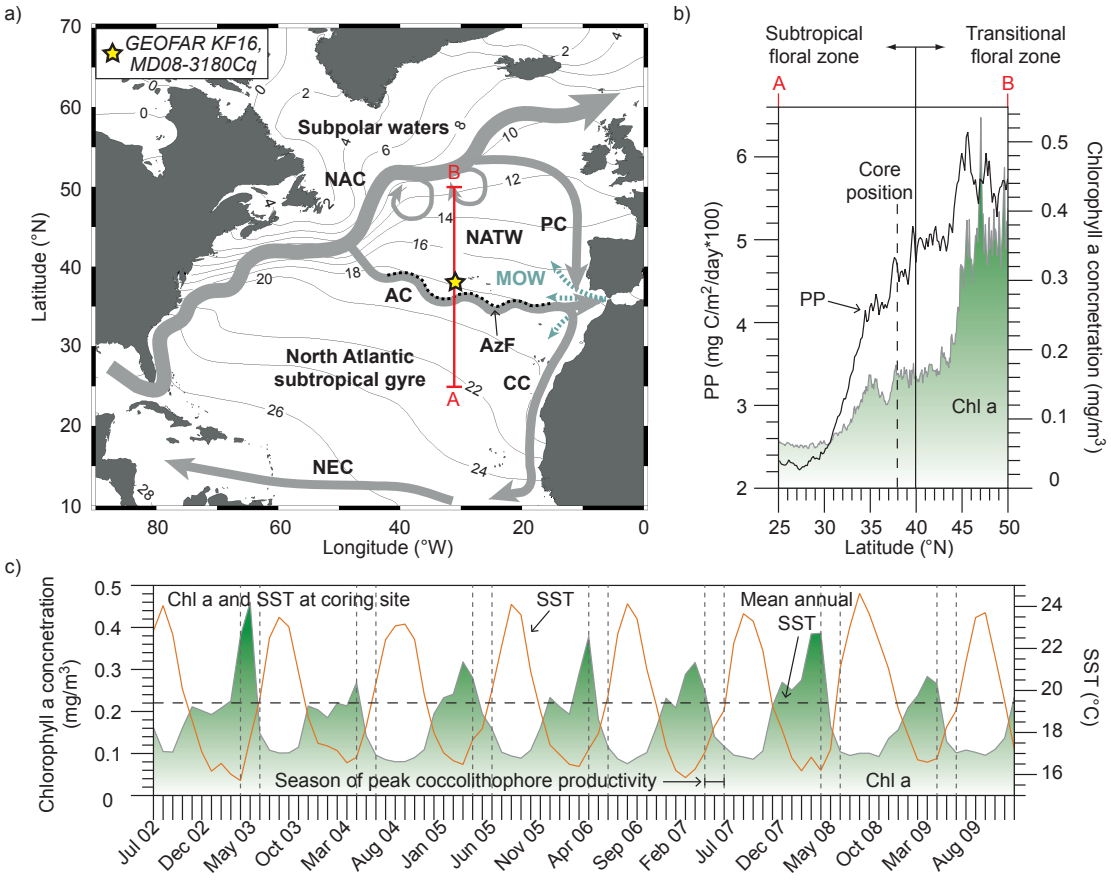

Figure 3.1. a) Schematic surface ocean circulation of the North Atlantic overlaid on contour map of spring (April – June) sea surface temperatures (SSTs) [*Locarnini et al.*, 2010]. Major surface currents (grey arrows): North Atlantic Current (NAC), Azores Current (AC), Canary Current (CC), North Equatorial Current (NEC). Black dashed lines indicate Azores Front (AzF). The position of North Atlantic Transitional Water (NATW) is bound by the NAC to the north and by the AC to the south. Yellow star marks location of studied sediment cores. Transect A-B (red line) is shown in Figure 1b. Map was generated using the ODV software by *Schlitzer* [2012]. b) Satellite based annual mean PP estimates (solid black line) and chlorophyll a concentration (green shaded area) for year 2006 (derived from MODIS and SeaWiFS satellite data availabel at http://www.science.oregonstate.edu/ocean.productivity and http://seadas.gsfc.nasa.gov) along transect A-B shown in Figure 1a. Core position is marked by vertical dashed line. Boundary between subtropical and temperate coccolithophore biographical province after McIntyre and Bé (1967) is shown as vertical sold line. c) Monthly chlorophyll a concentration (green shaded area) and SST (orange solid line) at the coring site derived from satellite data. Dashed horizontal line indicates mean SST. Dashed vertical lines delineate spring season (April – June), when peak coccolithophore productivity is expected.

the Azores Current (9-19 Sv), which partly replaces the waters lost due to the overflow. Thereby a stronger MOW results in a stronger Azores Current (Volkov et al., 2010). The Azores Current and its associated front are persistent features of the subtropical North Atlantic throughout the year and mark the northern boundary of the North Atlantic subtropical gyre (Klein and Siedler, 1989; Maillard and Käse, 1989; Bashmachnikov et al., 2004). The AzF corresponds to a region of strong dipping isotherms and is best defined as the position, where the 15°C isotherm is between 200 and 300 m water depth (Gould, 1985). It

separates southern subtropical water (Sargasso Sea mode water) with a shallow thermohaline mixed layer from colder and fresher North Atlantic Transitional Water (NATW) with a deep winter mixed layer (Käse and Siedler, 1982; Gould, 1985; Schiebel et al., 2011). Southernmost NATW is the dominant surface water at our coring site. Furthermore mesoscale activity is an important feature of the Azores Current System (e.g. Kielmann and Käse, 1987). Mature meanders pinch off the Azores Current, forming cyclonic eddies to the south and anticyclonic eddies to the north of the Azores Current (Alves et al., 2002). It is important to note that only the anticyclonic eddies, transporting a subtropical signal, can reach our coring site today (Alves et al., 2002; Pingree et al., 2002).

The different conditions on each side of the AzF result in a high north-south PP gradient in our study area (Figure 3.1b). In the subtropical region PP is low, mainly due to the paucity of nutrients resulting from strong water-column stratification and weak vertical mixing (Mouriño-Carballido and Neuer, 2008). In the region north of the AzF PP is high, because of a deep winter mixed layer (200-300 m) and associated nutrient supply (Lévy et al., 2005). Furthermore, episodic nutrient input to the south can result from eddy pumping of the cyclonic eddies, whereas the anticyclonic eddies to the north, which occasionally reach our coring site, are normally associated with downwelling and low PP (Hernández-León et al., 2007; Mouriño-Carballido and Neuer, 2008). Today peak PP takes place during early spring (March–April) (Figure 3.1c). However, it is known that peak coccolithophore productivity occurs slightly after the main PP peak (Margalef, 1978; Merico et al., 2004) and therefore maximum coccolithophore productivity should take place later in spring (April–June) at SSTs of approximately 18°C close to mean annual SST of 19.4°C (cf. Figure 3.1a and 3.1c).

The different environmental/hydrographic conditions result in a transitional and a subtropical biogeographical province, separated by the AzF. These provinces are not only very distinct e.g. in foraminiferal assemblages (Ottens, 1991; Schiebel et al., 2002a, b) but are also very well expressed in coccolithophore assemblages (McIntyre and Bé, 1967; Schiebel et al., 2011) (Figure 3.1b) and expansions/contractions of these provinces can be traced at our coring site.

3.4 Material and methods

3. 4.1 Sample material and age control

We analysed sediment cores GEOFAR KF16 and MD08-3180Cq (Table 2.1), which consist of foraminifera bearing nannofossil ooze. GEOFAR KF16 was taken during GEOFAR cruise onboard the research vessel Le Noroit (Richter, 1998). MD08-3180Cq was taken during cruise MD-168 onboard the research vessel Marion Dufresne in the framework of the AMOCINT IMAGES XVII campaign (Kissel et al., 2008). Both cores are from the same location in a small basin at the Mid Atlantic Ridge, slightly southwest of the Azores Islands (Figure 3.1a). This basin accumulates sediments at higher rates compared to the surrounding slow accumulating open ocean sites due to sediment focusing (Richter, 1998), enabling high-resolution analyses. In addition, a surface sample from companion boxcore GEOFAR KG14 was analysed.

The age models (Figure 3.2a-d) of GEOFAR KF16 and MD08-3180Cq are based on 15 Accelerator Mass Spectrometer (AMS) radiocarbon ages of mono-specific samples of planktonic foraminifera (*G. ruber* w. or *G. bulloides*) (Table 3.1), measured at Leibniz-Laboratory for Radiometric Dating and Isotope Research at Kiel University. All ages were converted into calendar ages using the Calib 6.0 software (Stuiver and Reimer, 1986) with Marine09 calibration curve (Reimer et al., 2009). Furthermore, the alkenone SST record in MD08-3180Cq and the planktonic oxygen isotope records of both cores were additionally tuned to the NGRIP oxygen isotope record (Andersen et al., 2007) (Figure 3.2a - c). To match calibrated AMS ^{14}C ages and tuned ages, additional reservoir ages were applied to the AMS ^{14}C ages of the Bølling-Allerød, Younger Dryas and 8.2 kyr event. The applied reservoir corrections are consistent with reservoir corrections in the North Atlantic during these events based on the findings of Waelbroeck et al. (2001), Kleiven et al. (2008) and Thornalley et al. (2010). Four calibrated AMS ^{14}C ages in GEOFAR KF16 measured on *G. bulloides* yielded age reversals and/or unreasonable high sedimentation rates and therefore have been discarded. As *G. bulloides* can live deeper in the water column (down to 300 m) at the coring site (Schiebel et al., 2002a), these species can be influenced by deeper, ^{14}C-depleted water masses. Furthermore the AMS ^{14}C age at 69 cm in GEOFAR KF16 is dated within the transition from high to low abundances of this species, which can

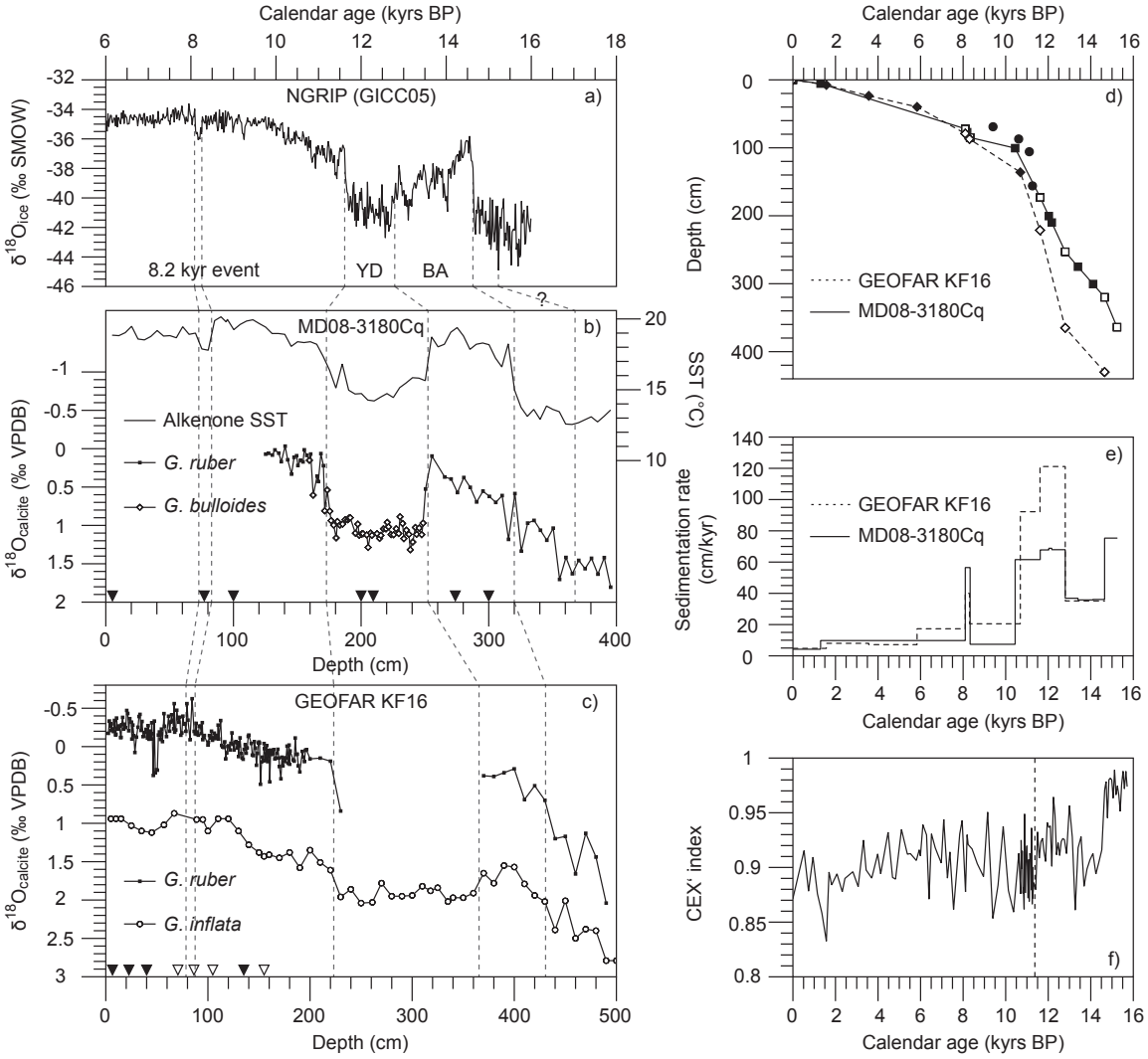

Figure 3.2. Age models and preservation index of coccolithophores of sediment cores GEOFAR KF16 and MD08-3180Cq. a) NGRIP ice core oxygen isotope record (ice) on GICC05 timescale (Andersen et al., 2007). b) Alkenone SST and planktonic oxygen isotope record of MD08-3180Cq. During the Younger Dryas *G. ruber* is absent at the coring site and therefore *G. bulloides* was measured and corrected for -0.6‰ to match *G. ruber* (Ganssen and Kroon, 2000). c) Oxygen isotope records of *G. ruber* and *G. inflata* in GEOFAR KF16 [Richter, 1998]. d) Resulting age models based on AMS ^{14}C ages (filled symbols) and tuning to NGRIP (open symbols) of GEOFAR KF16 (dashed line with diamonds) and MD08-3180Cq (solid line with squares). Filled circles are omitted AMS ^{14}C ages of GEOFAR KF16. e) Resulting sedimentation rates of GEOFAR KF16 (dashed line) and MD08-3180Cq (solid line). f) CEX' index, indicating preservation of coccoliths. Grey dashed lines indicate correlation (tuning points) of both cores to the NGRIP record. Triangles indicate measured and used (filled triangles) and omitted (unfilled triangles) AMS ^{14}C ages. Black dashed vertical line indicates splicing of cores for coccolithophore analysis as described in the text.

introduce a considerable error to AMS ^{14}C ages due to bioturbational effects (e.g. Bard et al., 1987). Based on the age models sedimentation rates range between 4 and 122 cm/kyr with maximum values during northern hemisphere cold periods (8.2 kyr event, Younger Dryas and H1) (Figure 3.2e). The constantly increasing offset between both cores in the age vs. depth profiles and sedimentation rates can be related to the well-known stretch-

Table 3.1. Age control points[a]

Depth in core (cm)	AMS ^{14}C age (yrs BP)	Error (yrs)	Calibrated age (yrs BP)	Additional reservoir age (yrs)	Tuned age (yrs BP)
			GEOFAR KF16		
7,5	2015	±30	**1572**	-	-
23,5	3660	±35	**3567**	-	-
39,75	5455	±35	**5835**	-	-
69	8715	±40	9406	-	-
79	-	-	-	-	**8100**
87	-	-	-	-	**8300**
87	9765	±45	10612	-	-
105,75	10075	±50	11111	-	-
136	9835	±55	**10689**	-	-
156	10290	±55	11260	-	-
221	-	-	-	-	**11614**
365	-	-	-	-	**12800**
430	-	-	-	-	**14650**
			MD08-3180Cq		
5,5	1755	±25	**1300**	-	-
72	-	-	-	-	**8102**
77	7935	±40	8391	201	**8190**
85	-	-	-	-	**8329**
100,5	9570	±45	**10446**	-	-
173	-	-	-	-	**11624**
200,5	11100	±60	12613	584	**12029**
210	11045	±55	12592	425	**12167**
253	-	-	-	-	**12800**
275	12560	±80	13997	600	**13397**
300,5	12780	±70	14360	250	**14110**
320	-	-	-	-	**14650**
364	-	-	-	-	**15234**

[a] Bold characters are ages used to construct the age models

ing/compaction effect of different coring devices (e.g. Skinner and McCave, 2003). Because we partly started our analysis on GEOFAR KF16 before we retrieved MD08-3180Cq, which is from the same coring site (Figure 3.1a, Table 2.1), and because the core section of GEOFAR KF16 available to us only spanned the late deglacial and Holocene section, we partly had to combine both records (e.g. Figure 3.2f) to get continuous records over the last 16 kyrs. However, a good correlation on the common time scale for both cores exists, taking into account e.g. the overlap in isotopes (cf. Figure 3.2b and 3.2c).

3.4.2 Quantification of coccoliths

For coccolithophore studies we analyzed GEOFAR KF16 from 0 to 11.4 kyrs BP with a sampling interval of 1 to 5 cm (corresponding to an average resolution of 150 yrs) and MD08-3180Cq from 11.4 to 15.7 kyrs BP with a sampling interval of 5 cm (corresponding to an average resolution of 90 yrs). Because both cores are from the same coring site (Figure 3.1a, Table 2.1), we combined them to get a continuous record with multi-centennial scale time resolution (e.g. Figure 3.2f).

Samples for coccolithophore analyses were prepared with a combined dilution/filtration technique following Andruleit (1996). For this purpose a small amount of freeze-dried sediment (0.07-0.08 g) was suspended in tab water and ultrasonicated for 15 to 30 s. The suspension was split by a factor of 100 using a rotary sample divider (™Fritsch Laborette 27) and filtered on a polycarbonate membrane filter with a pore size of 0.4 µm. After drying the filters for 24 h at 40°C a small piece of filter was cut out, mounted on a scanning electron microscope (SEM) stub and sputtered with gold/palladium. On average 375 coccoliths were counted in each sample using a CamScan 44 SEM. The coccoliths were counted on measured transects at a magnification of 5000 and identified according to the taxonomy given in Young et al. (2003). A taxonomic list of the identified species is given in the Appendix. Furthermore extended counts were carried out to improve the accuracy for the rare species *C. pelagicus*. Therefore a whole transect across the filter was additionally scanned and only specimens of *C. pelagicus* were counted. Based on the counting, relative proportions of each species to the total assemblage were calculated. Furthermore total and species coccolith concentration in a sediment sample were calculated, using equation (2.2). To estimate preservational effects on coccolithophore assem-

blages, we calculated the CEX' index following Boeckel and Baumann (2004):

$$CEX' = \frac{(\%E.\,huxleyi + \%\,small\ gephyrocapsids)}{(\%E.\,huxleyi + \%\,small\ gephyrocapsids + \%C.\,leptoporus)} \qquad (3.1)$$

For paleoproductivity estimates we calculated coccolith accumulation rates according to equation (2.3), using the sedimentation rates shown in Figure 3.2e and dry bulk densities from GEOFAR KF16 (Richter, 1998) interpolated between two points of known densities. During the Preboreal, where both cores were spliced, we used sedimentation rates from core MD08-3180Cq to calculate accumulation rates to avoid an artificial jump in accumulation rates due to the different compaction/stretching effect in both cores.

3.4.3 Alkenone measurements

Long-chain (C_{37}-C_{39}) di-, tri- and tetra-unsaturated methyl and ethyl ketones (alkenones) were measured at the biomarker laboratory at the CAU Kiel. Alkenones were extracted from 2 g of freeze-dried and grounded sediment samples using dichloromethane (DCM) as a solvent and with an Accelerator Solvent Extraction system (DionexASE 200) set to 80 bar and 75°C. Samples were then analyzed using multidimensional, double-column gas chromatography using two Agilent 6890 gas chromatographs equipped with two independent ovens and two flame ionization detectors connected via a transfer line. A detailed description of the measuring procedure can be found in Etourneau et al. (2010). SST was obtained using the $U^{K'}_{37}$ index, which is defined according to equation (2.8). The $U^{K'}_{37}$ index was converted to SST using the global core top calibration of Müller et al. (1998) (equation (2.9)). According to sample and standard replicates, the standard deviation of the SST estimate was approximately ± 0.2°C.

3.4.4 XRF core scanning

XRF measurements on core MD08-3180Cq were carried out using the AAVATECH XRF core scanner at the Insitute of Geosciences at the CAU Kiel. The core was scanned every 0.5 cm with generator settings of 10 and 50 kV. Because Barium is used as a proxy for PP (e.g. Dymond et al., 1992) we are using Ba measured by XRF scanning as a tracer

for past productivity changes. Although Ba in the sediment at the coring site is predominantly of biogenic origin (Richter, 1998), we normalized the Ba counts to Ti counts to roughly correct for Ba originating from the lithogenic fraction. However, using raw Ba counts does not alter the observed changes indicating that influence of terrigenous material is negligible. Ba measured by XRF core scanning was converted to Ba concentrations using Ba measured by XRF spectrometry (Richter, 1998). Under the above postulated assumption that terrigenous input of Ba is negligible (see also following section and chapter 3.5.2), Ba concentrations were than converted to PP using equation (2.13) (see chapter 3.5.2).

Because the coring site is far offshore the sediment is predominantly of biogenic origin. This is seen for example in the high $CaCO_3$ content which accounts for 73 wt% on average, reaching maximum values of 85 wt% during the late Holocene (Richter, 1998). The purely pelagic character of the sediment becomes also evident by the visual examination of the samples by SEM, where only coccoliths, foraminifers, calcareous dinoflagellates, diatoms and silicoflagellates are observed. Because the sediments from this open ocean site are predominantly of biogenic origin we are using the Si/Ca ratio as an indicator for the relative contribution of siliceous plankton to the sediment. To confirm this we did some control counts of diatoms under the SEM. Therefore a transect of approximately 1 cm was scanned at a magnification of 500 on filters prepared for coccolith analyses. Only intact valves were counted without identification on the species level. A possible influence of detrital Si derived from terrigenous input will be discussed in the following chapter.

3.5 Results

3.5.1 Coccolith counts

The preservation of coccoliths in the studied cores is excellent, as indicated by the presence of complete delicate species like *G. ornata*, complete coccospheres or holococcoliths observed by SEM. Furthermore the good preservation of the coccoliths can be seen in the high CEX' values (Figure 3.2f), which are always above the critical value of 0.63. Both findings indicate that the coring location was always situated above the lysocline

(Boeckel and Baumann, 2004) as also is postulated by Crowley (1983).

As the relative abundances of coccoliths from individual coccolithophore species closely parallel their concentrations in the sediment (Figure 3.3), only abundances are furthermore considered. In general the coccolith assemblage is dominated by *E. huxleyi*, *G. muellerae* and small gephyrocapsids, together comprising up to 84% of the total assemblage (Figure 3.3a-c). All other species are minor contributors to the assemblage with relative abundances of each of these species never exceeding 12%.

E. huxleyi tolerates a wide range of ecological conditions and therefore is abundant in nearly all oceanic environments (Okada and Honjo, 1973; Okada and McIntyre, 1979). Therefore it may be difficult to reconstruct past ecological changes based on abundance variations of this species and no paleoecological interpretation of this species is given in this study (Table 3.2). However, at our coring site this species shows long-term (> 500 yrs) minima during H1, beginning Younger Dryas and during the early Holocene (Figure 3.3a). After 6 kyrs BP *E. huxleyi* is the solely dominant species at our coring site with relative abundances of up to 67%. This overall evolution is interrupted by several pronounced short-term minima found at 13, 8.2 and 6.5 kyrs BP. A nearly opposite trend is found in the abundance record of the cold/temperate water species *G. muellerae*, which shows lowest abundances after 6 kyrs BP (Figure 3.3b). Regarding the North Atlantic, and aside of its occurrence in the upwelling regions off northwest Africa (Sprengel et al., 2002) and in the subpolar realm of the North Atlantic due to drifting within waters of the North Atlantic Current (e.g. Samtleben and Schroeder, 1992), this species has been reported to be restricted to the eastern North Atlantic occurring in waters with a temperature range of 12–18°C (optimum 14°C) (Giraudeau et al., 2010). As this spatial distribution and temperature range of *G. muellerae* corresponds to NATW (cf. Locarnini et al., 2010) it has been reported to occur only north of the AzF (Jordan, 1988; Schiebel et al., 2011) and can be used to reconstruct the influence of NATW at our coring site.

In our samples small gephrocapsids (≤ 2.7 µm) mainly comprise *G. ericsonii* with an occasional low contribution of *G. ornata*. Like *E. huxleyi*, this species tolerates a wide range of ecological conditions (Haidar and Thierstein, 2001), although an affinity to high productivity (Baumann et al., 2008; and references therein) as well as a slight affinity to low salinities (Boeckel et al., 2006) have been reported. Assuming that the distribution of small gephyrocapsids is governed by PP and salinity, we conclude that low saline and high

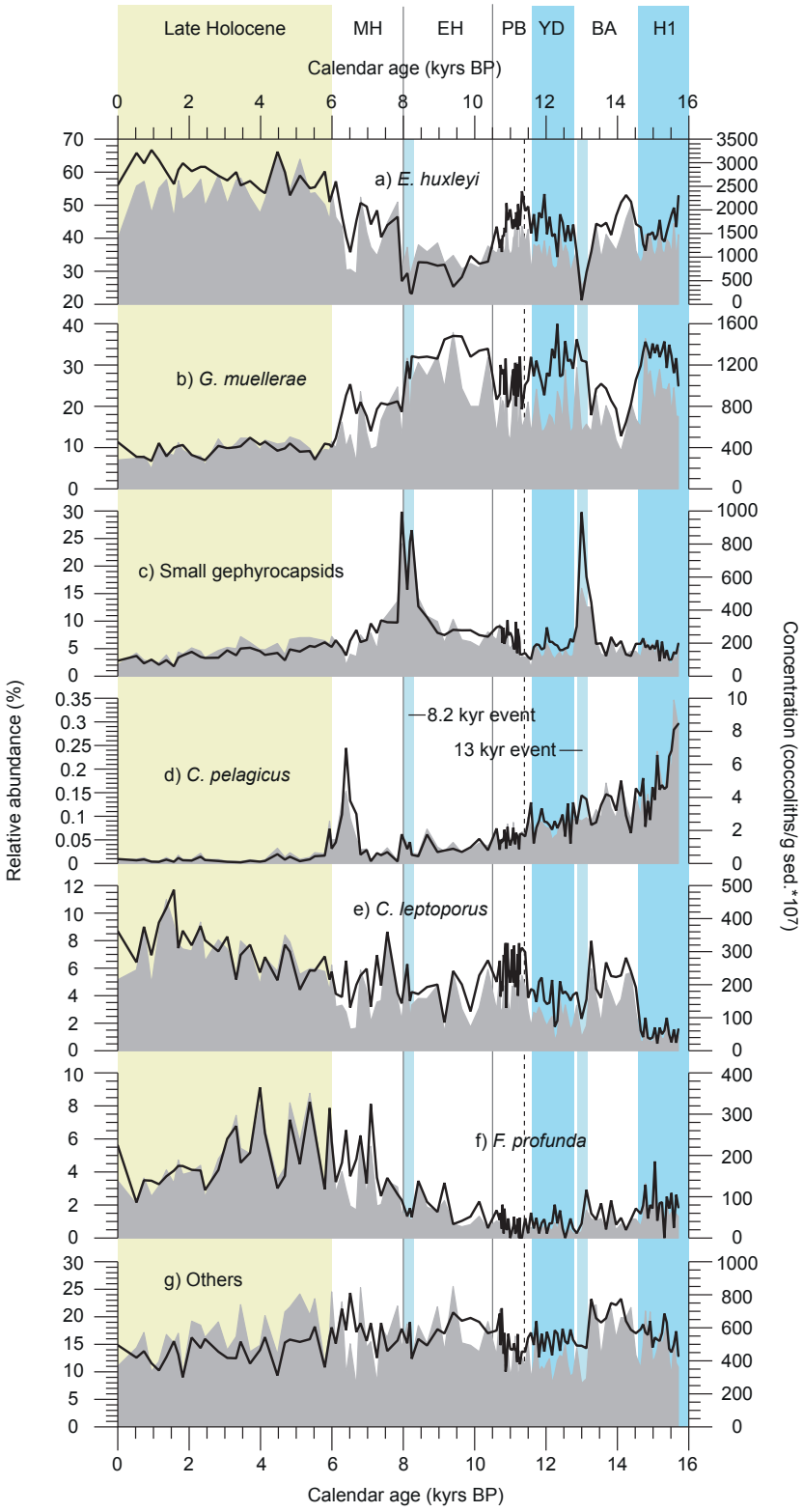

Figure 3.3. Relative abundance of coccolith species (solid lines) and their concentration in the sediment (filled lines). a) *E. huxleyi*, b) *G. muellerae*, c) small gephyrocapsids, d) *C. pelagicus*, e) *C. leptoporus*, f) *F. profunda* and g) Others (cf. Appendix). Abbreviations: mid Holocene (MH), early Holocene (EH), Preboreal (PB), Younger Dryas (YD), Bølling-Allerød (BA), Heinrich event 1 (H1). Vertical light blue bars mark the cold periods of H1 and the YD. Small vertical lighter blue bars mark the 13 and 8.2 kyr events. Vertical yellowish bar marks the stable late Holocene as discussed in the text. Vertical solid lines denote the boundaries between PB/EH and EH/MH. Dashed vertical line indicates splicing of cores for coccolithophore analysis as described in the text.

productive conditions prevailed at the coring site at 13 and 8.2 kyrs BP as deduced from pronounced peak abundances of up to 30% (Figure 3.3c).

During the deglacial the abundance of *C. pelagicus* gradually decreases and it becomes nearly absent at the coring site since the mid Holocene (Figure 3.3d). Although there are two well established morphotypes of *C. pelagicus*, a small (6-10 *µ*m) morphotype (*C. pelagicus* ssp. *pelagicus*) associated with arctic conditions and a larger (9-15 *µ*m) morphotype (*C. pelagicus* ssp. *braarudii*) associated with more temperate and nutrient-rich conditions (Ziveri et al., 2004; and references therein), we did not distinguish between the two morphotypes due to their very low abundances in the cores (< 0.35%). However, as the overall abundance of *C. pelagicus* in surface sediments closely parallels the abundance pattern of the small morphotype, with clear abundance maxima in the polar and subpolar North Atlantic (Baumann et al., 2005), we are using this species as an indicator for cool and nutrient-rich surface water masses of subpolar origin. Therefore the abundance the observed abundance variations indicate a gradual decrease in the influence of subpolar water masses during the course of the daglacial. Furthermore a distinct maximum in its abundance is evident at 6 kyrs BP. However, distinct minima e.g. in less calcified coccolithophore species like *E. huxleyi* and exceptionally high oxygen isotope values of planktonic and benthic foraminifers (Repschläger et al., in prep; Figure 3.2c), indicate an "artificial" enrichment of *C. pelagicus*, which is one of the most heavy calcified coccolithophores, due to dissolution. As all coccolithophore species used to calculate the CEX' index are affected by this dissolution (cf. chapter 3.4.2, Figure 3.3), this event cannot be detected in the CEX' index (Figure 3.2f). As this core interval is associated with the transition from reddish, oxygenated sediments to greyish, unoxidized sediments (cf. Richter, 1998), the dissolution is probably caused by digenetic processes associated with the oxygenation horizon.

Although the cosmopolitan species *C. leptoporus* has an affinity to cold and nutrient-rich conditions in the equatorial Atlantic and in the Arabian Sea (Kinkel et al., 2000; Andruleit and Rogalla, 2002), the distribution pattern of this species in the North Atlantic is patchy, with no clear ecological preferences (Ziveri et al., 2004). At the Azores, this species clearly shows minimum abundances during H1 and the Younger Dryas and a slight increase in its abundance is obvious during the last 6 kyrs with maximum abundances of up to 11% during the last 3 kyrs (Figure 3.3e).

The lower photic zone species *F. profunda* is widely used to monitor past changes in

nutricline-depth and associated changes in productivity (Molfino and McIntyre, 1990a, b; Beaufort et al., 1997; Kinkel et al., 2000). Thereby high abundances of *F. profunda* indicate a deep nutricline and low productivity. During the deglacial and early Holocene *F. profunda* occasionally disappears from the coring site and shows low abundances never exceeding 5% (Figure 3.3f). However, a pronounced increase in its abundance can be observed during the mid Holocene, resulting in maximum abundances of up to 9% during the late Holocene, indicating a deep nutricline and low productivity.

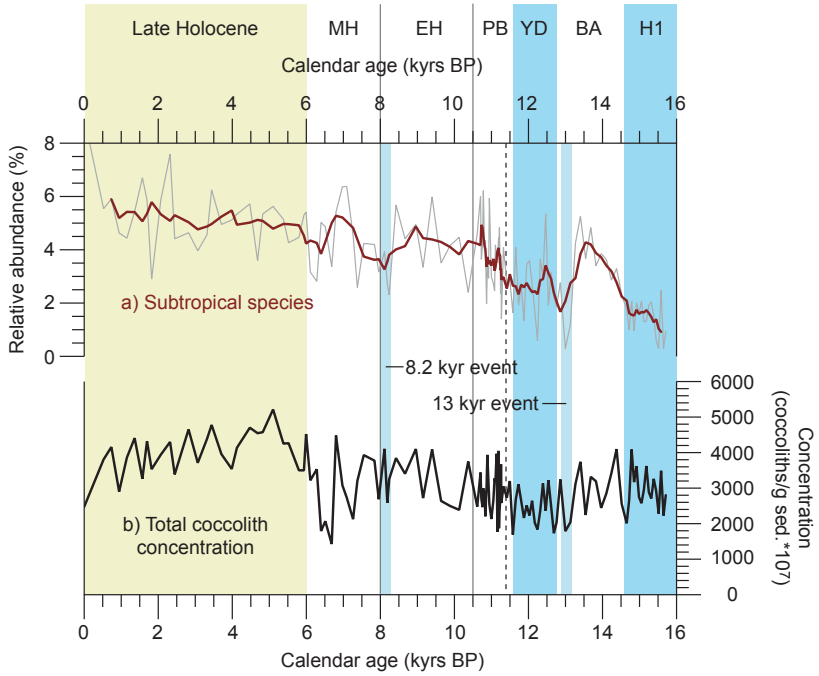

Figure 3.4. a) Abundance of subtropical species (*Oolithotus* spp., *Umbellosphaera* spp., *Umbilicosphaera* spp.) (solid grey line) and 5pt moving average (solid red line). b) Total coccolith concentration in investigated sediment samples. Abbreviations and markers as in Figure 3.3.

The species *Umbellosphaera* spp., *Umbilicosphaera* spp. and *Oolithotus* spp. are associated with warm and oligotrophic water masses (Incarbona et al., 2011; and references therein). Here we summarize these species as subtropical species and use abundance variations within this group as an indicator for the influence of subtropical waters brought by the anticyclonic eddies to our coring site. Therefore the minimum abundances observed during H1 and the Younger Dryas indicate a decreased influence of subtropical waters (Figure 3.4a). During the late Holocene maximum abundances (up to 8%) indicate a maximum influence of this water mass at the coring site. Furthermore maximum coccolith concentrations of up to 5.2 x 10^{10} coccoliths/g sediment are observed during the late Holocene (Figure 3.4b).

Table 3.2. Selected coccolithophores and inferred ecological changes

Species	Used as a proxy for:
E. huxleyi	-
G. muellerae	Influence of NATW
Small gephyrocapsids	Nutrient-rich, less saline surface water conditions
C. pelagicus	Influence of subpolar water
C. leptoporus	-
F. profunda	Nutricline-depth
Grouped subtropical species	Influence of subtropical water

3.5.2 SST and PP reconstructions

Alkenone derived SSTs were 7 and 5°C colder than today during H1 and the Younger Dryas respectively (Figure 3.5a). These changes are within the range of previously reported SST reconstructions from the midlatitude eastern North Atlantic (Bard et al., 2000; Chapman et al., 2000). After rising during the Preboreal and early Holocene, SST stabilize between 18.5 and 19.5°C after 8 kyrs BP, close to modern annual mean SST of 19.3°C at the coring site (Locarnini et al., 2010). This indicates that at least today alkenone SST reliably traces mean annual temperature. However, alkenone production probably shifted towards the summer season during extreme cold events like H1 and the Younger Dryas (Leduc et al., 2010; Schneider et al., 2010). Therefore alkenone SST might be biased towards the warm season showing higher than average SSTs at the coring site during these events. This would mute the amplitude of change during H1 and Younger Dryas, but would not affect the general SST pattern. Aside of the observed general SST pattern several

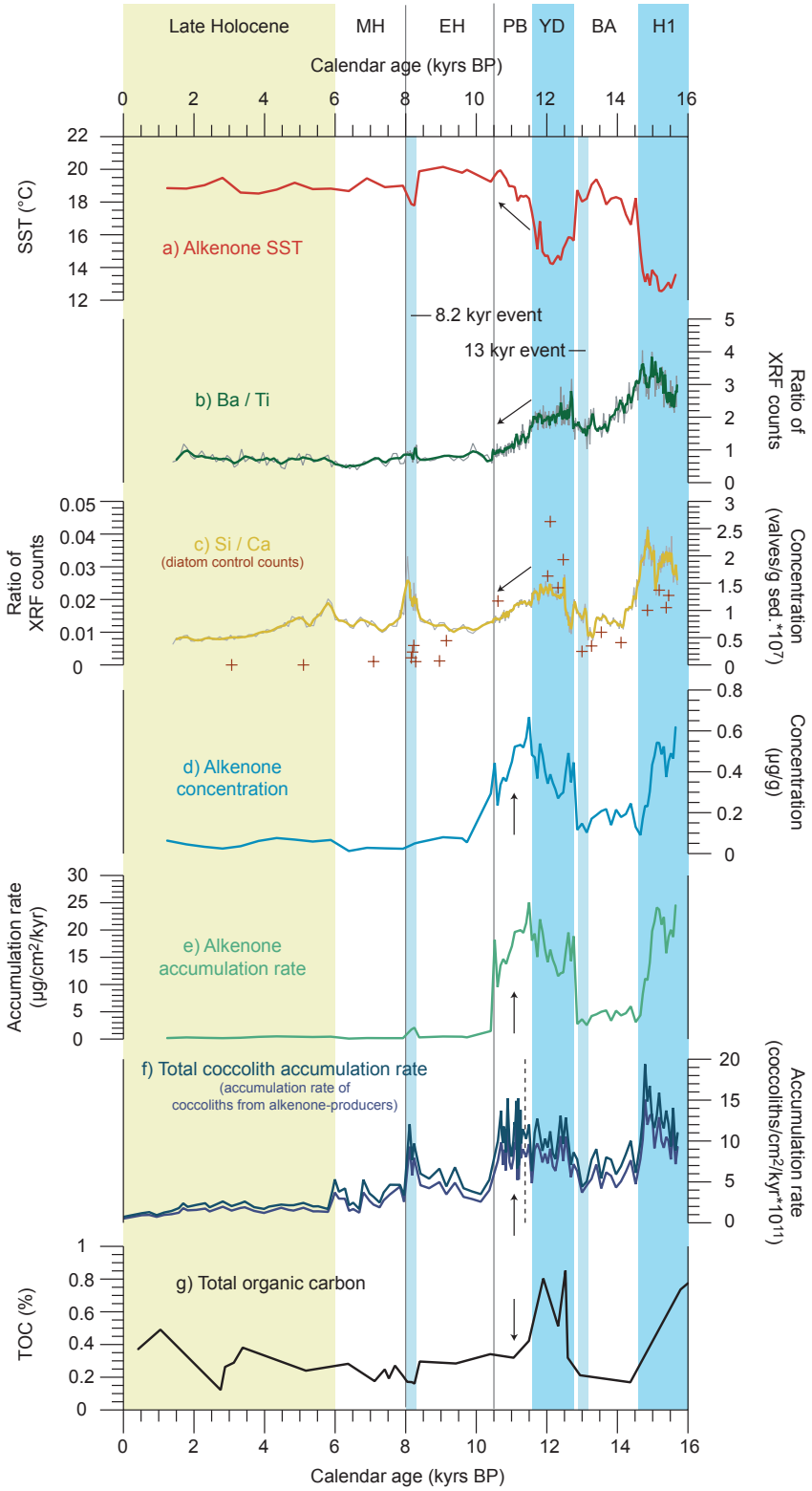

Figure 3.5. a) Alkenone derived sea surface temperatures. b) Ba/Ti ratio measured with XRF core scanner (grey solid line) and 5pt moving average (green solid line). c) Si/Ca ratio measured with XRF core scanner (grey solid line) and 5pt moving average (yellow solid line), brown crosses show diatom control counts. d) Total (C37:2 + C37:3) alkenone concentration of investigated sediment samples. e) Total (C37:2 + C37:3) alkenone accumulation rate. f) Accumulation rate of coccoliths (dark blue line) from alkenone-producing coccolithophores (*E. huxleyi* and gephyrocapsids) (purple line). Dashed vertical line indicates splicing of cores for coccolithophore analysis as described in the text. g) Percentage of total inorganic carbon in core GEOFAR KF16 (Richter, 1998). Small arrows mark direction of observed changes during the Preboreal. Abbreviations and markers as in Figure 3.3.

small-scale perturbations are evident in the SST record (Figure 3.5a). The most pronounced perturbation is at 8.2 kyrs BP, where SST abruptly decrease down from 19.9 to 17.8°C.

Based on our multi-proxy approach a generally consistent pattern emerges with high productivity during the deglacial, especially during H1 and the Younger Dryas (Figure 5b-g). For example a fourfold and twofold increase of the Ba/Ti ratio is observed during the cold H1 and Younger Dryas respectively (Figure 3.5b). Furthermore Ba/Ti ratios are decreased during the Bølling-Allerød and Preboreal but do not reach the very low values of the Holocene period. Although the use of Barium as a paleoproductivity proxy is still discussed controversially (e.g. McManus et al., 1998), the most common limitation of this proxy, which are water depth and lateral advection of refractory organic matter and/or resuspended barite from the continental shelf (Dymond et al., 1992), can be ruled out at our open ocean site at a water depth > 1000 m. Furthermore Barium has been proposed to be a good indicator for productivity at the coring site due to its close correlation to TOC and PP estimates from the nearby Canary basin (Richter, 1998). However, it has been recently supposed that a Ba peak in sediments off northwest Africa during H1 originates from Ba-enriched meltwater transported via the Azores and Canary Current (Plewa et al., 2006), therefore the Ba/Ti peak observed during H1 might have been influenced by these meltwaters. But as increased productivity is also observed in all other proxies, we conclude that Ba/Ti mainly reflects productivity, although a minor influence of meltwater cannot be ruled out.

An increased abundance of siliceous phytoplankton, mainly diatoms, during H1, Younger Dryas and the 8.2 kyr event can be deduced from the Si/Ca ratio (Figure 3.5c). However although diatom abundances are increased during H1 the exceptional Si/Ca peak during this period partly stems from increased abundances of silicoflagellates, as observed by SEM. As diatoms are opportunistic species (e.g. Abrantes et al., 2002), the increased abundances during the mentioned periods again indicate an increased productivity.

Because westerly winds were increased during H1 and the Younger Dryas (Nebout et al., 2002; Rodrigo-Gámiz et al., 2011), an increased Si input via dust during these times would hamper our interpretation of the Si/Ca record. However, based on the visual examination of the samples under the SEM we found no evidences for any detrital input. A negligible aeolian input to the midlatitude open ocean North Atlantic during Heinrich events has also been proposed by Villanueva et al. (1997) and Naafs et al. (2010) based on the

abundance of aeolian derived n-alkanes in nearby cores SU90/08 (43°20'N, 30°24'W) and U1313 (41°N, 32°34'W). Therefore fluctuations in aeolian dust input did not seem to exert a major control on Si/Ca ratio and therefore can also be ruled out to drive the observed productivity pattern.

Increased PP during H1 and the Younger Dryas can also be deduced from coccolithophore specific PP proxies (Figure 3.5d-f). Alkenone concentrations reach values up to 0.62 and 0.54 µg/g during H1 and Younger Dryas respectively, whereas maximum values during the Holocene are as low as 0.08 µg/g (Figure 3.5d). During the Bølling-Allerød PP is low, as deduced from alkenone concentrations, with maximum values of 0.25 µg/g, but not as low as during the Holocene. A similar PP pattern is observed in the accumulation rates of alkenones with maximum values of 25, 6 and 22 µg/cm^2/kyr during H1, Bølling-Allerød and Younger Dryas respectively (Figure 3.5e). During the Holocene alkenone accumulation rates reach a maximum of 2 µg/cm^2/kyr during the 8.2 kyr event. The changes in the accumulation rates of alkenones are paralleled by changes in the accumulation rates of coccoliths from alkenone-producing coccolithophores (*E. huxleyi* and gephyrocapsids) (Figure 3.5f). They show maximum values of 15, 8 and 11 * 10^{11} coccoliths/cm^2/kyr during H1, Bølling-Allerød and Younger Dryas respectively. Lowest values are found throughout the entire late Holocene with increased values at 8.2 kyrs BP. Total coccolith accumulation rates show values of 19, 10 and 13 * 10^{11} coccoliths/cm^2/kyr during H1, Bølling-Allerød and Younger Dryas respectively (Figure 3.5f). Again, lowest values are found throughout the entire late Holocene with increased values at 8.2 kyrs BP.

All coccolithophore specific PP proxies show strongly increased PP during the Preboreal, with maximum alkenone concentrations up to 0.7 µg/g, maximum alkenone accumulation rates up to 25 µg/cm^2/kyr, maximum accumulation rates of coccoliths from alkenone-producing coccolithophores up to 13 * 10^{11} coccoliths/cm^2/kyr and maximum total coccolith accumulation rates up to 15 * 10^{11} coccoliths/cm^2/kyr. This indicates that growth conditions for coccolithophores were optimal, just after the main PP peak during the Younger Dryas that favored the growth of diatoms. Furthermore slightly enhanced coccolithophore productivity seems to prevail until 6 kyrs BP based on coccolith accumulation rates, which is not supported by alkenone concentrations and accumulations. This discrepancy might stem from the fact that the onset of modern NADW production sets in during early Holocene (Alley and Clark, 1999; Chapman and Shackleton, 2000; Piotrowski et

al., 2004; McManus et al., 2004), providing oxygen-rich bottom-water to the coring site and therefore organic material (e.g. alkenones) might have been affected by preservation throughout the entire Holocene, resulting in their observed minimal concentrations. In summary, coccolithophores seem to sustain relative high productivity after the YD until 6 kyrs BP, especially during the Preboreal. That coccolithophores can sustain high productivity after the main PP peak is also observed in the seasonal succession of phytoplankton species in which diatoms occur close to peak PP early in the year, whereas peak coccolithophore productivity can prevail into the more stratified, warmer season (Margalef, 1978; Merico et al., 2004).

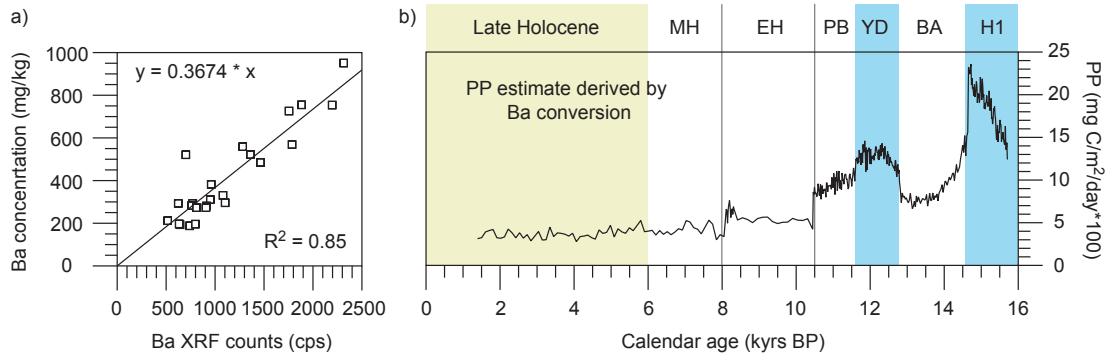

Figure 3.6. Conversion of Ba measured by XRF core scanning to PP. a) Correlation of Ba counts measured by XRF to Ba concentrations measured by XRF spectrometry (Richter, 1998). The relation y = 0.3674x is used to convert Ba counts into concentrations. b) Ba concentration converted to PP using equation (2.13). Abbreviations and markers as in Figure 3.3.

Although we can observe a general pattern with increased PP during the deglacial, especially during H1 and the Younger Dryas, in all PP proxies, which therefore seems to be very robust, the amplitude of changes in the different PP proxies are different (Figure 3.5b-g). The different amplitudes might be the result of the different sensitivities of the PP proxies to actual PP changes (cf. Sarnthein et al., 1988; Dymond et al., 1992; Nelson et al., 1995; Beaufort et al., 1997; Haidar and Thierstein, 2001) and/or of the different preservation potential of the different PP proxies (cf. Tréguer et al., 1995; Gingele et al., 1999; Rühlemann et al., 1999; Romero et al., 1999). However, despite their different sensitivities and preservation potential, all shown PP proxies reveal the same pattern with increased PP at least during H1 and the Younger Dryas, although we want to note, that the observed changes have to been viewed from a qualitative rather than from a quantitative point of view.

On the other hand, quantitative changes can be inferred from the conversion of Ba fluxes to PP (Figure 3.6). Because PP derived from Ba fluctuates close to the modern PP value of 461 mg C/m^2/day during the mid and late Holocene, the conversion seems to yield reasonable results. Maximum values of 2457, 664 and 1460 mg C/m^2/day, indicating an increase of PP by a factor of 5.3, 1.4 and 3.2 compared to modern values, are observed during H1, Younger Dryas and Bølling-Allerød respectively. Furthermore, in accordance to coccolithophore specific PP proxies, especially to coccolith accumulation rates, increased PP can be observed during the Preboreal and early Holocene compared to late Holocene values.

3.6 Discussion

3.6.1 Frontal movements and PP changes during the deglacial and early Holocene

During H1 and the Younger Dryas a higher influence of NATW and a decreased influence of subtropical water is indicated by maximum abundances of *G. muellerae* (Figure 3.3b) and minimum abundances of subtropical species (Figure 3.4a) respectively. Thus we assume that during deglacial cold periods the AzF resided at a more southern position as compared to today. For warm Bølling-Allerød both proxies indicate a significant northward movement of the AzF and hence a northward extension of the subtropical gyre. This suggests that the AzF did not only migrate on glacial/interglacial timescales, as deduced by Schiebel et al. (2002a) from low-resolution records, but also on shorter, millennial-scale timescales, and in parallel to the reorganization of the North Atlantic during the course of the last deglacial (e.g. Sarnthein et al., 2001). This result seems to contradict the findings of Rogerson et al. (2004) from the Gulf of Cadiz, who concluded no latitudinal displacement of the AzF during cold periods of the last declacial. However, recent modeling studies suggest that the water mass transformation in the Gulf of Cadiz is responsible for the formation of the Azores Current and that a stronger MOW would lead to a stronger Azores Current (e.g. Volkov and Fu, 2010). As MOW existed and was even stronger than today during cold climatic intervals (e.g. Heinrich events, Younger Dryas) (e.g. Voelker et al., 2006), the Azores Current would have still resided and a front could have developed in the

Gulf of Cadiz as observed by Rogerson et al. (2004). Therefore the connection between the Azores Current Sytem and the MOW as suggested by models could be the reason for the observed decoupling of the AzF dynamics in the open ocean and near the coast, which is also seen in the modeling studies, where the Azores Current exhibits latitudinal variability only west of 20°W (Volkov and Fu, 2010). Furthermore the modeling studies suggest that the latitudinal variability of the Azores Current is driven by the strength of the westerly winds (Volkov and Fu, 2010, 2011). Therefore, the increased westerly winds during the deglacial and early Holocene, especially during H1 and the Younger Dryas (Nebout et al., 2002; Rodrigo-Gámiz et al., 2011) could have been responsible for the observed shift of the Azores Current System in the open ocean North Atlantic.

Aside of this general trend, a slight northward shift of the AzF seems to be obvious during the Preboreal, as evidenced by minimum abundances of *G. muellerae* (Figure 3.3b). However, we argue that this minimum is caused by optimal growth conditions for coccolithophores (cf. chapter 3.5.2), in which the blooming of the opportunistic species *E. huxleyi* (Figure 3.3a), which is a much tougher competitor than *G. muellerae* (e.g. Okada and Wells, 1997), lowered the relative abundance of temperate species like *G. muellerae* (Figure 3.3b). A similar behavior of *E. huxleyi* during the Preboreal is reported by Hass et al. (2001) in a core from the northern North Atlantic (Voering Plateau), where due to a first intrusion of North Atlantic water masses the opportunistic species *E. huxleyi* recovered rapidly, whereas other species needed longer to adapt to the conditions following the Younger Dryas. Furthermore, contrary to *G. muellerae*, the abundance of subtropical species indicates a significant northward shift of the AzF during the Preboreal and early Holocene comparable to the Bølling-Allerød (Figure 4.4a). But as the abundance record of subtropical species more closely parallels the temperature record than the abundance record of *G. muellerae* (abundance subtropical species vs. alkenone SST: $R^2 = 0.47$; abundance *G. muellerae* vs. alkenone SST: $R^2 = 0.28$), these species probably are additionally affected by temperature. However, slightly lower abundances of subtropical species during the Preboreal and early Holocene indicate a (slightly) more southern position of the AzF compared to the late Holocene in accordance to the *G. muellerae* record.

Because of the high PP gradient in our region (Figure 3.1b) even small movements of the AzF and the associated climatic and productivity regimes are likely to result in substantial changes of our paleoproductivity signals. Therefore the enhanced paleoproductivity during the deglacial and early Holocene, and especially during H1 and the Younger Dryas

(Figure 3.5b – g), might be the result of the above postulated more southern position of the front. However, an increase of PP by a factors of up to 5.3 and 3.2 during H1 and the Younger Dryas respectively, as indicated by Ba derived PP changes (Figure 3.6), can not be explained by a shift of the front solely, as such high values are nowhere found in the open North Atlantic today (e.g. Behrenfeld et al., 2006; cf. Figure 3.1b). Therefore additional factors, like increased westerly winds during H1 and the Younger Dryas (Nebout et al., 2002; Rodrigo-Gámiz et al., 2011), which would raise the nutricline due to deeper winter mixing, probably enhanced PP.

Furthermore nutrients brought by subpolar water and/or by freshwater from melted icebergs might have affected PP at the coring site. Today nutrient-rich subpolar water is admixed to NATW via cold core rings pinching off the NAC (Kupferman et al., 1986) and transporting a subpolar fauna and flora to lower latitudes (The Ring Group, 1981; Beckmann et al., 1987). An increased influence of subpolar water during the deglacial and early Holocene at the coring site can be deduced from the increased abundance of the subpolar species *C. pelagicus* (Figure 3.3d). During these periods a more southern position of the NAC and its associated Subpolar Front, as proposed by Ruddiman and Glover (1975), would have allowed the cold core rings to penetrate to the coring site and to fuel PP. However, a clear deglacial sequence with H1, Bølling-Allerød and Younger Dryas is missing in the abundance record of *C. pelagicus*. There might be at least two explanations for this: the NAC gradually moved northward during the deglacial and/or complex interplay and abundance changes between the two different morphotypes of *C. pelagicus* (cf. chapter 3.5.1).

Although there are no evidences for icebergs at our coring site, an enhanced input of IRD to the North Atlantic just north of our coring site is recorded during H1 and the Younger Dryas (Bond et al., 1997; Chapman and Shackleton, 1998), indicating at least the vicinity of icebergs at our coring site. As icebergs can act as nutrient sources (*S*chwarz and Schodlok, 2009), nutrients derived by melted icebergs have been described to increase PP in the midlatitude North Atlantic, especially during H1 (e.g. Kiefer et al., 1995; Gil et al., 2009). Therefore nutrient-rich meltwaters from icebergs probably entered the coring site during H1 and the Younger Dryas and fueled productivity. This scenario is also supported by a freshening of the sea surface at the coring site during H1 and the Younger Dryas as recognized by Repschläger et al. (submitted) (cf. Figure 3.2). In summary, the increased

PP during the deglacial and early Holocene, especially during H1 and the Younger Dryas, are the result of a more southern position of the AzF, increased westerly winds, advection of subpolar waters and advection of nutrient-rich waters from melted icebergs.

Recent modeling studies indicate that a reduction in AMOC, due to a freshwater input like during Heinrich events, would lead to a reduction in global export production, most notably in the North Atlantic (Schmittner, 2005; Menviel et al., 2008). In order to support this observation, the results have been compared to paleoproductivity records from south of Iceland, the Brazilian Margin and the northwest African upwelling areas. However, no comparison between model and proxy-data has been shown for the open Atlantic, which would be crucial regarding the large area covered.

Although we cannot test the global outcome of these models, our results from the Azores are in contrast to what the modeling studies suggest for this region. During all deglacial cold events associated with a reduction in AMOC we observe a strong increase in PP. This points to regional factors and/or processes, like AzF dynamics or advection of nutrient-rich surface waters, affecting PP in the Azores region, which are not considered and/or resolved by the models (Schmittner, 2005; Mariotti et al., 2012). However, enhanced surface water productivity during deglacial cold periods associated with advection of fertile subpolar waters and amplified by nutrients derived from icebergs, has also been reported from the Bermuda Rise, offshore southwestern Iberian Margin, Gulf of Cadiz and from the western Mediterranean Sea (Lebreiro et al., 1997; Rogerson et al., 2004; Jimenez-Espejo et al., 2007; Gil et al., 2009; Penaud et al., 2011). Therefore we propose that during the mentioned cold periods there has been a band of high productivity across the midlatitude North Atlantic at the northern boundary of the contracted subtropical gyre, which also seems to penetrate into the western Mediterranean and can be associated with the advection of fresh and nutrient-rich surface waters. As biogeochemical models potentially do not take into account the transport of nutrients at the surface into the subtropics (see e.g. Mariotti et al., 2012), we propose that the implications of freshwater forced AMOC perturbations on the biological activity in the midlatitude North Atlantic might have to be reconsidered.

However, in accordance to the modeling studies, productivity was decreased in the higher latitudes of the North Atlantic (Nave et al., 2007). Decreased productivity during periods of reduced AMOC, in particular during Heinrich events, has been reported from core SU90-08 (40°3‘N, 32°W) (Nave et al., 2007), just north of our coring site. This decreased

productivity has been related to a strong water column stratification induced by the freshwater input (Nave et al., 2007). Therefore the boundary between the low productive northern areas and the southern areas, where only a diluted component of the nutrient-rich freshwater arrives and promotes productivity, is somewhere between 38° and 40°N in the open ocean North Atlantic.

Unfortunately no paleoproductivity reconstructions from more southern open ocean sites in the North Atlantic are available, and therefore the southern boundary of the high productivity band cannot be estimated. Nevertheless the band can be traced across the North Atlantic, at least from the Bermuda Rise to the Gulf of Cadiz, and within the western Mediterranean Sea, and therefore it probably occupied a large area. Furthermore, aside of an increase in PP due to a shift of the productivity regimes, the level of productivity within this band was strongly increased due to additional processes like the advection of nutrient-rich surface waters (Figure 3.6, see sections above). Because of the large areal coverage and the strongly increased level of PP, this high productivity band potentially could have counteracted the decreased productivity and resulting decreased organic carbon pump in the more northern latitudes of the North Atlantic during times of reduced AMOC.

3.6.2 Mid Holocene onset of modern hydrographic and productivity conditions

Based on coccolith assemblages and PP reconstructions a reorganization of the hydrographic and productivity regime is evident during the mid Holocene (Figures 3.3 - 3.6). Most proxies shift to full interglacial values during this period and stabilize on these values at the latest after 6 kyrs BP. For example, lowest abundances of *G. muellerae* (Figure 3.3b) are accompanied by highest abundances of subtropical species (Figure 3.4a). Based on the interpretation of these proxies given above, this indicates, that the AzF reached its modern, northernmost position after 6 kyrs BP and hence the contributions of NATW and subtropical water at the coring site were minimal and maximal respectively.

Like during the deglacial, the reorganization of the hydrographic conditions is accompanied by changes in PP. Thereby most oligotrophic conditions during the last 16 kyrs prevailed since the mid Holocene as indicated e.g. lowest coccolith accumulation rates and lowest Ba derived PP (Figure 3.5f, 3.6). The shift towards oligotrophic conditions can also be deduced based on the abundance of *F. profunda* (Figure 3.3f), at which highest abun-

dances since the mid Holocene indicate a deep nutricline and associated lowest productivity. Furthermore the establishment of the oligotrophic conditions can also be deduced from the increased concentration of coccoliths in the sediment since the mid Holocene (Figure 3.4b). As many coccolithophore species are K-selected they increase their relative contribution to the plankton assemblage under oligotrophic conditions (Baumann et al., 2005). Therefore, unlike coccolith accumulation rates (fluxes), which are high under nutrient-rich conditions, high coccolith concentrations in the sediment are found in nutrient-depleted environments (e.g. subtropical gyres) (Baumann et al., 2004). The oligotrophic conditions since the mid Holocene are a consequence of the maximum contribution of nutrient-depleted subtropical waters to the coring site (Figure 3.4a) and/or the absence of fertile water masses originating from the higher northern latitudes of the North Atlantic. The latter is indicated by the absence of *C. pelagicus* at the coring site since 6 kyrs BP (Figure 3.3d).

Beside this general shift during the mid Holocene a decrease in the abundance of *F. profunda* occurs during the last 3 kyrs (Figure 3.3f). This decrease is accompanied by maximum abundances of *C. leptoporus* (Figure 3.3e). The observed changes probably correspond to a slight shallowing of the nutricline, decreasing the abundance of the lower photic zone species and increasing the abundance of the nutrient affiliated *C. leptoporus* (see chapter 3.5.1). But the advection of nutrients associated with this process probably was insignificant resulting in low coccolith productivity (Figure 3.5f).

In general, the observed changes indicate the most northern position of the AzF and hence the maximum northward extension of the subtropical gyre in the North Atlantic since the mid Holocene. Furthermore, a general pattern emerges, with an expansion of the gyre during warm periods (Bølling-Allerød, (late) Holocene) and a contraction during cold periods (H1, Younger Dryas). Although it is hard to define a quantitative temperature/ expansion relationship based on our proxy results, one could easily hypothesize that a further increase in temperatures, as expected for the following decades (Jansen et al., 2007), would probably lead to a further expansion of the oligotrophic gyre. Indeed an expansion of the subtropical gyres, especially of the North Atlantic subtropical gyre, due to an increase of global temperatures between 1998 and 2006 has been reported (Polovina et al., 2008). Furthermore, this study indicates that the expansion of the oligotrophic gyres takes place at the expense of more productive areas. If this expansion is not compensated by increased productivity in the high latitudes due to an occupation of new habitats, such an

expansion and resulting decreased overall marine productivity would provide a positive feedback to the temperature increase due to a decreased atmospheric carbon fixation by marine organisms.

3.6.3 Short-term reorganizations caused by freshwater input

One of the most pronounced short-term events is recorded at 8.2 kyrs BP (Figures 3.3-3.6), coincident with the well-known 8.2 kyr event in the North Atlantic (Ellison et al., 2006; Kleiven et al., 2008). This event was most probably triggered by a rapid drainage of glacial Lake Agassiz into the North Atlantic via Hudson Strait (Barber et al., 1999; Teller and Leverington, 2004). In the Azores region SSTs abruptly dropped by 2°C (Figure 3.5a) and PP slightly increased (Figure 3.5, 3.6). Also the coccolith assemblage changed remarkably during this event, e.g. abundances of *E. huxleyi* show a distinct minimum (Figure 3.3a). The most profound change in the coccolith assemblage is recorded in the abundance of small gephyrocapsids (Figure 3.3c), which together with *G. muellerae* dominate the assemblage. Furthermore low abundances of subtropical species are observed (Figure 3.4a). Altogether this points to a southward shift of the AzF during the 8.2 kyr event, due to an incursion of NATW. At 8.2 kyrs BP a considerable freshening of the sea surface is recognized at the coring site (Repschläger et al., submitted; cf. Figure 3.2). This is consistent with a routing of the discharged meltwater into the subtropical realm (Condron and Winsor, 2011). Furthermore recent modeling studies show exactly the observed SST drop in the Azores region during the 8.2 kyr event, if the model is forced by a freshwater discharge through Hudson Strait and with additional icebergs (Wiersma and Jongma, 2009). As already stated, there are no evidence for icebergs in the Azores region, but ice-rafted detritus (IRD) just north of our coring site indicates at least the vicinity of icebergs, which can act as additional nutrient sources (Schwarz and Schodlok, 2009). Therefore, in addition to a latitudinal shift of the productivity regime, nutrient-rich freshwaters, probably partly originating from melted icebergs, again fueled PP at the coring site. These fresh and nutrient-rich conditions under still relatively moderate temperatures (17.8°C) seem to be optimal for the growth of small gephyrocapsids at the coring site, resulting in their observed peak abundances.

Another short-term reorganization of the hydrographic and productivity regime is re-

corded at 13 kyrs BP (Figures 3.3 - 3.5), coincident with the well-known Inter-Allerød Cold Period (Benson et al., 1997). In our records this event bears striking similarities to the 8.2 kyr event. At this time SSTs dropped by 1.4°C (Figure 3.5a) and the coccolith assemblage changed in the same manner as during the 8.2 kyr event. The most striking similarity is seen in the abundance of small gephyrocapsids (Figure 3.3c), which at 13 kyrs BP together with *G. muellerae* dominate the assemblage. The peak abundance of small gephyrocapsids might again be linked to additional nutrients and to a freshening of the sea surface as recognized by Repschläger et al. (submitted) (cf. Figure 3.2). This freshening event can be related to a meltwater discharge from St. Lawrence River (Clark et al., 2001) and/or to an export of less saline seawater from the Caribbean (Flower et al., 2004). Evidences for additional nutrients, probably brought by melting icebergs, may come from an enhanced IRD input at the onset of the Inter-Allerød Cold Period (Bond et al., 1997). However, based on the abundance of small gephyrocapsids, the 8.2 and 13 kyr events are the only two meltwater/freshwater events associated with iceberg discharge recognized in the Azores region. As there have been numerous of such events in the North Atlantic during the last 16 kyrs (e.g. Bond et al., 1997; Clark et al., 2001), this probably points to unique conditions (SST, salinity, nutrients, etc.) found during these two events in the Azores region, which favored the growth of small gephyrocapsids.

3.7 Conclusions

Our multi-proxy reconstructions from sediment cores GEOFAR KF16 and MD08-3180Cq reveal significant changes in the hydrographic and productivity conditions near the Azores Islands during the last 16 kyrs. Based on changes within coccolithophore assemblages, the temperate and subtropical biogeographical provinces, and hence the AzF, resided at a more southern latitude during the deglacial and early Holocene, especially during H1 and the Younger Dryas. Furthermore southward shifts of the AzF are recognized during the 8.2 kyr event and during the Inter-Allerød Cold Period. These results indicate, that the AzF in the open ocean North Atlantic did not only migrate on glacial/interglacial timescales, as deduced by Schiebel et al. (2002a) on low-resolution records, but also on millennial and even shorter timescales. Although, these results seem to contradict the find-

ings of Rogerson et al. (2004) from the Gulf of Cadiz, recent modeling studies suggest that the connection between the Azores Current System and the MOW might be responsible for the decoupling of the AzF dynamics in the open ocean and near the coast.

Furthermore, we observe an increased productivity during the deglacial and early Holocene, especially during H1 and the Younger Dryas. Although the observed productivity increase partly is caused by the more southern position of the AzF and the resulting shift of the productivity regimes, other factors like increased westerly winds and advection of nutrient-rich surface waters have to be considered to fully explain the observed productivity increase.

Because we observe an increased productivity during times of reduced AMOC, e.g. H1 and the Younger Dryas, our results are in contrast to what modeling studies suggest for this region. This indicates that the observed PP changes were driven by regional factors and/or processes, like AzF dynamics and advection of nutrient-rich surface waters, which are not considered/resolved by the models. However, similar increases in productivity during times of reduced AMOC, related to the advection of nutrient-rich surface waters, have been reported from other midlatitude North Atlantic sites. Therefore we propose that during times of reduced AMOC there has been a band of strongly increased productivity across the midlatitude North Atlantic, at the northern rim of the contracted subtropical gyre, which potentially could have counteracted the decreased organic carbon pump in the high northern latitudes.

Chapter IV.

Paleoenvironmental changes in the Azores region between 130 and 48 ka BP with special emphasizes on MIS 5.5

(This chapter corresponds to the following manuscript submitted to Quaternary Science Reviews: Schwab, C., Kinkel, H., Weinelt, M., Repschläger, J., 2012. Paleoenvironmental changes in the Azores region between 130 and 48 ka BP with special emphasizes on MIS 5.5. Submitted to Quaternary Science Reviews.)

4.1 Abstract

As oceanographic changes in the North Atlantic are known to modulate global climate, they are key to the understanding of past and future climate changes. Especially the mid-latitudes of the open ocean North Atlantic may be of interest, regarding the large area covered. We therefore reconstructed past changes in productivity and hydrography from a new sediment core (MD08-3179Cq) taken in the open ocean mid-latitude North Atlantic in the vicinity of the Azores Current System. Concomitant to the reorganizations of environmental conditions in the North Atlantic between 130 and 48 ka BP, changes in coccolithophore assemblages and changes in the abundance of siliceous plankton (diatoms) indicate a southward shift of the Azores Front (AzF), and hence a southward retreat of the North Atlantic subtropical gyre, as well as an increased productivity during glacial Marine Isotope Stages (MIS 4 and Termination II) and cold substages of MIS 5. Furthermore we hypothesize that the ecological changes lead to distinct evolutionary patterns of coccolithophores, resulting e.g. in a dominance of *G. ornata* between 76 and 105 ka BP. Additionally, high-resolution analysis of MIS 5.5 indicate a short reversal towards cool conditions during MIS 5.5, corresponding to a basin-wide cooling event. Full interglacial conditions are reached only late in the Azores region. The peak interglacial conditions during MIS 5.5 result in peak abundances of *E. huxleyi*, an event, which seems to be time-transgressive in the eastern North Atlantic, and which probably can be related to more severe changes (i.e. changes with higher amplitude) in the higher latitudes. An increased advection of Subantarctic Mode Water (SAMW) and/or the possibility to occupy new habitats after glacial conditions result in a distinct coccolithophore productivity peak during full interglacial conditions of MIS 5.5. As global temperature during MIS 5.5 are assumed to be similar to the expected future global climate change, MIS 5.5 serves as a possible scenario for future changes. Taking MIS 5.5 as a possible analogue for expected future climate change, our results indicate that an expected decrease in marine primary productivity, due to the expansion of the oligotrophic gyres, may be attenuated by increased coccolithophore productivity.

4.2 Introduction

Most marine sediment cores, serving as paleoclimate archives, are retrieved from coastal and shelf areas, where thick sediment layers exist. Regarding the open ocean, which covers a much larger area, high-resolution sediment cores are rare, mainly due to prevailing low sedimentation rates in these areas (Ewing et al., 1973). However, records from these parts of the oceans are urgently needed, because they are absolutely essential for a complete picture of past climatic and oceanic changes.

Here we present a study from a new core (MD08-3179Cq) taken in the midlatitude open ocean eastern North Atlantic in the vicinity of the boundary between the North Atlantic subtropical gyre and northern temperate water masses. We will focus on the time period between 130 and 48 ka BP with special emphasis on the Last Interglacial (LIG), which is known as MIS 5.5 in marine records and as the Eemian in terrestrial (European) records, and has been the subject of many paleoclimatic and paleoceanographic studies (e.g. McManus et al., 1994; Bauch et al., 1999; Shackleton et al., 2002, 2003; Oppo et al., 2006). Especially in the light of the predicted future climate change (see e.g. Jansen et al., 2007), the study of past interglacials, like MIS 5.5, is an important issue. This is because past interglacials, which are comparable to the present Holocene, ran their full course and demise, and therefore can teach us about natural climate variability during interglacials (e.g. Kukla et al., 2002; Müller and Kukla, 2004). Furthermore, as most of the Late Quaternary interglacials are characterized by different orbital parameters (cf. Laskar et al., 2004), the study and comparison of interglacials can hint on the climate sensitivity to this external forcing (insolation). Especially MIS 5.5 may be of interest, as global temperatures during this period were 1.5 to 2°C warmer than the pre-anthropogenic global average of the past 10 kyrs, and therefore MIS 5.5 could serve as a possible scenario for human induced climate change (e.g. Clark and Huybers, 2009; Kopp et al., 2009).

Besides being generally warmer, global sea-level during the LIG was several meters higher than at present due to smaller polar ice-sheets (Kopp et al., 2009; and references therein). Thereby the warmer temperatures and smaller ice-sheets can be related to a positive summer insolation anomaly in the northern hemisphere during the LIG (e.g. Rohling et al., 2007; Kopp et al., 2009). Some other factors, like the redistribution of heat by the Atlantic Meridional Overturning Circulation (AMOC), which is assumed to have strengthened

during the LIG compared to glacial modes (e.g. Adkins et al., 1997; McManus et al., 2002), have to be invoked to explain the observed climatic patterns during the LIG (Keigwin et al., 1994; Adkins et al., 1997; McManus et al., 2004). Although the climatic conditions during the LIG are reported to have been rather stable (e.g. McManus et al., 1994; Cheddadi et al., 1998; Andersen et al., 2004), there are also other studies, which show considerable internal variability during this period (e.g. Fronval and Jansen, 1996; Rohling et al., 2007; Couchoud et al., 2009). However, the causes of the observed variability are still largely unexplained (Bauch et al., 2011).

One of the most intriguing paleoclimatic archives of past changes in the North Atlantic realm are ice core records from Greenland. These paleoclimatic archives offer a high resolution on an annual scale (e.g. Svensson et al., 2011) and therefore allow detailed paleoclimatic studies. For example the well-known Dansgaard-Oeschger cycles, which start after the last glacial inception around 115 ka BP, were first identified in Greenland ice core records (Dansgaard et al., 1993; Grootes et al., 1993). Unfortunately, these ice core records have an insufficient stratigraphic length and do not encompass the entire MIS 5.5 (e.g. Andersen et al., 2004; Svensson et al., 2011). Therefore high-resolution marine records covering MIS 5.5 are needed to reconstruct past changes in the North Atlantic during this period.

In this study we will reconstruct paleoenvironmental conditions (i.e. productivity and hydrography) between 48 and 130 ka BP from a key oceanographic position in the open ocean midlatitude eastern North Atlantic (boundary between subtropical gyre and northern water masses), an area where available paleoclimate/-oceanographic data are scarce. Special emphasis will be given to the structure and variability of MIS 5.5 (LIG) in the midlatitude eastern North Atlantic, based on high-resolution records during this period.

For this purpose we analyzed coccolithophore assemblages. As an important component of the primary producers in the photic zone of the oceans, coccolithophores strongly rely on surface water conditions (e.g. light, nutrients, temperature, salinity) (Winter et al., 1994), and therefore changes within this phytoplankton community have been successfully used to reconstruct past oceanic conditions (e.g. McIntyre and Bé, 1967; Beaufort, 1997; Kinkel and al, 2000; Giraudeau et al., 2010; Saavedra-Pellitero et al., 2011). Furthermore, coccolithophores are considered to be the most important primary producers in the open oceans of tropical to temperate regions (Brand, 1994), which makes them ideally suited to trace past productivity changes at our coring site. At last, changes in coccolithophore as-

semblages have been successfully used to reconstruct environmental conditions during the LIG at more northern sites of the eastern North Atlantic (Lototskaya et al., 1998; Stolz and Baumann, 2010), and therefore: a) our study completes the picture of changes during the LIG in the eastern North Atlantic based on coccolithophores and b) the previous studies could serve as a robust basis to which our results can be compared to.

4.3 Regional hydrography and productivity regime

Core MD08-3179Cq (37.8493°N, 30.294°W) was retrieved from 2040 m water depth, slightly north of the Azores Current System (Figure 4.1). Major components of the Azores Current System are the Azores Current with its associated Azores Front (AzF), which are persistent features of the subtropical North Atlantic throughout the year and mark the northern boundary of the North Atlantic subtropical gyre (Klein and Siedler, 1989; Bashmachnikov et al., 2004). Recent modeling studies indicate that the Mediterranean Outflow Water (MOW), which enters the North Atlantic through the Street of Gibraltar, is responsible for the formation of the Azores Current (e.g. Volkov and Fu, 2010; 2011). Thereby a stronger outflow results in a more vigorous Azores Current (Volkov and Fu, 2010; 2011). As already mentioned, the Azores Current is accompanied by a distinct front, the AzF, which position is best defined as the location where the 15°C isotherm is situated between 200 and 300 m water depth (Gould, 1985). It separates warmer and saltier southern Sargasso Sea mode water from colder and fresher northern water masses (Alves et al., 2002; Schiebel et al., 2002a). Furthermore the regions to the south of the AzF are characterized by a permanent thermohaline mixed layer and a subtropical thermocline, whereas the northern regions exhibit a seasonal thermocline formation and winter convective and advective mixing (Käse and Siedler, 1982). We will refer to the southern surface waters as subtropical water and to the northern surface waters as North Atlantic Transitional Water (NATW) (e.g. Schiebel et al., 2011). Although NATW is the dominant surface water mass at the coring site, subtropical water occasionally reaches the site due to anticyclonic eddies pinching off the Azores Current (Alves et al., 2002).

Due to upwelling, oceanic frontal structures are generally associated with increased primary productivity (PP) (Le Fèvre, 1987; Pollard and Regier, 1992). However, the impact

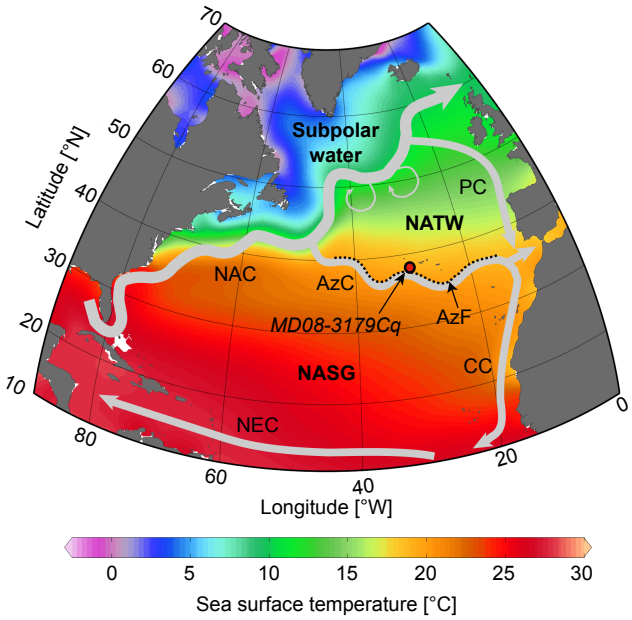

Figure 4.1. Schematic surface circulation (grey arrows) in the North Atlantic, overlain on mean annual sea surface temperature (Locarnini et al., 2009). Abbreviations: North Atlantic Current (NAC), Azores Current (AzC), Azores Front (AzF), Portugal Current (PC), Canary Current (CC), North Equatorial Current (NEC), North Atlantic Transitional Water (NATW), North Atlantic subtropical gyre (NASG). Azores Front is marked with dashed black line. Location of core MD08-3179Cq is marked with red dot.

of the frontal structure on primary productivity in the Azores region is discussed controversially in the literature. For example Fernández and Pingree (1996) observed high chlorophyll concentrations within the Azores frontal system, whereas Fasham et al. (1985) found no evidence for an increased productivity in this region. However, the different hydrographic conditions on each side of the front result in two different productivity regimes and a high primary productivity gradient in the Azores region. In the subtropical area to the south of the front PP is low, because strong water-column stratification and weak vertical mixing suppress the replenishment of nutrients (Mouriño-Carballido and Neuer, 2008). On the other hand, PP in the region to the north of the AzF is high, because a deep winter mixed layer (200 - 300 m) causes upward mixing of nutrients (Lévy et al., 2005). Additionally, PP at the coring site can be influenced by the eddy activity in the region. Thereby the anticyclonic eddies, which occasionally reach our coring site, are characterized by downwelling and low PP (Hernández-León et al., 2007), whereas the cyclonic eddies to the south of the AzF are associated with increased PP due to eddy pumping (Mouriño-Carballido and Neuer, 2008).

The different hydrographic and productivity conditions on each side of the front result in a northern transitional and a southern subtropical biogeographical province, which are

well expressed e.g. in foraminiferal (Ottens, 1991; 1992; Schiebel et al., 2002a; b) but also in coccolithophore assemblages (McIntyre and Bé, 1967; Schiebel et al., 2011). Therefore expansions/contractions of these provinces, corresponding to latitudinal displacements of the AzF, can be traced at our coring site, based on plankton abundance changes. For example, a more southern position of the AzF would result in a diminished influence of subtropical water and an increased influence of NATW at the coring site (cf. chapter 2), and therefore a more transitional plankton assemblage is expected.

4.4 Materials and methods

4.4.1 Sample material and age control

We analyzed sediment core MD08-3179Cq, which was retrieved during Marion Dufresne cruise MD-168, conducted within the framework of the AMOCINT IMAGES XVII campaign (Kissel et al., 2008). The 814 cm long core consists of nannofossil ooze with foraminiferal sand, which together with discrete laminations indicates an undisturbed sedimentation in the pelagic realm.

Throughout the entire studied core interval, coccolithophore assemblages mainly consist of gephyrocapsids and *E. huxleyi* (see chapter 4.5.1) and therefore the investigated core section belongs to the most recent nannoplankton zone NN21 of Martini (1971), with an age of less than 294 kyrs (Wei and Peleo-Alampay, 1993). The more detailed stratigraphy of core MD08-3179Cq is based on identifying Marine Isotope Stages (MIS) and substages in the planktonic foraminiferal oxygen isotope record and tuning this record to the oxygen isotope stack of Lisiecki and Raymo (2005) (Figure 4.2, Table 4.1). Although MIS 1, 2, 3 and 4 can be readily identified in the oxygen isotope record, the transition from MIS 6 to MIS 5 is not very clear, as MIS 6 is not fully reached in the core. However, oxygen isotope values down to 1.16 ‰ are typical for glacial inceptions/terminations in the record and therefore the low values at the end of the core have been placed into Termination II (TII). Further evidences that the hindmost part of MD08-3179Cq can be placed into TII are derived from coccolithophore assemblages, which indicate deglacial/glacial conditions at the end of the core (see chapters 4.5.1, 4.6.1). At last, and aside of the good correlation to

the oxygen isotope stack of Lisiecki and Raymo (2005) (R^2=0.88), the good correlation (R^2=0.83) to the planktonic oxygen isotope record from nearby sediment core SU90-08 (43.3533 °N, 30,4083 °W) further supports the age model.

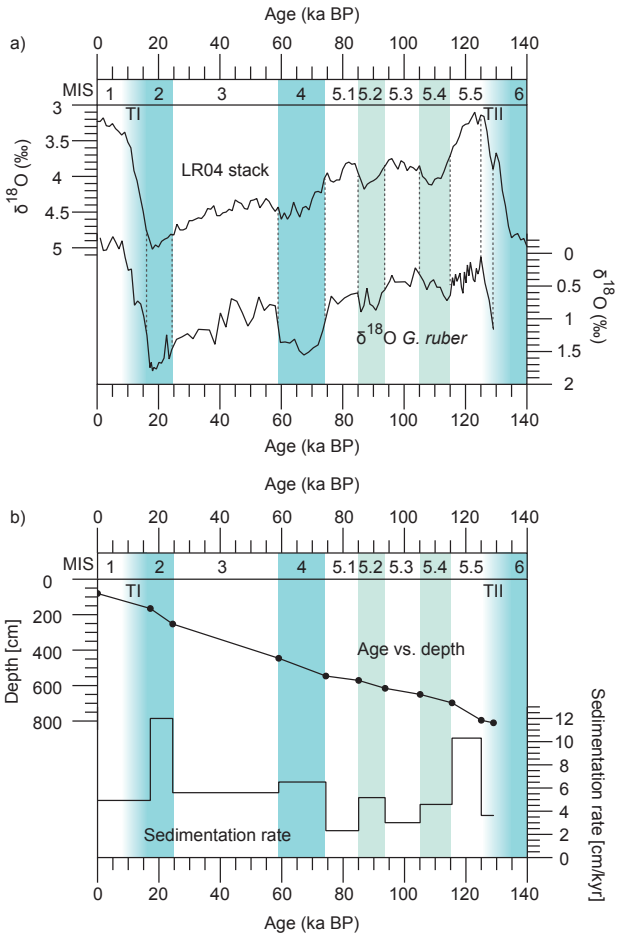

Figure 4.2. Age model of core MD08-3179Cq. Blue vertical bars indicate glacial stages. Light blue vertical bars indicate glacial substages. Shaded blue bars indicate Termination I (TI) and Termination II (TII). a) Upper record: $\delta^{18}O$ stack of Lisiecki and Raymo (2005); lower record: $\delta^{18}O$ of *G. ruber* from core MD08-3179Cq; dashed vertical lines indicate tie points used to reconstruct age model of core MD08-3179Cq. b) Upper record: resulting age vs. depth plot of MD08-3179Cq; lower record: resulting sedimentation rates in core MD08-3179Cq.

Based on the age model, resulting sedimentation rates range between 2.3 and 12 cm/kyr (Figure 4.2). Basically, increased sedimentation rates can be observed during glacial stages and substages, whereas interglacial stages and substages are characterized by low sedimentation rates. An exception to this general pattern is MIS 5.5, which is characterized by a maximum in sedimentation rates of 10.3 cm/kyr. Similar increased sedimentation rates during MIS 5.5 can also be observed in other cores from the eastern North At-

lantic (Bout-Roumazeilles et al., 1997; Shackleton et al., 2000; Calvo et al., 2001; Stolz and Baumann, 2010), therefore this feature further corroborates our age model.

Table 4.1. Age-depth assignments used for the chronology of core MD08-3179Cq

Depth (cm)	Age (ka BP)	Comment
80.5	0	First 80.5 cm due to double penetration of coring device
165	17.2	MIS 2 / MIS 2.2
253	24.5	MIS 2 / MIS 3
446	59	MIS 3 / MIS 4
546	74	MIS 4 / MIS 5
571	85	MIS 5.1 / MIS 5.2
615	94	MIS 5.2 / MIS 5.3
650	105	MIS 5.3 / MIS 5.4
697	115	MIS 5.4 / MIS 5.5
796	125	First peak MIS 5.5
810	129	MIS 5.53 / MIS 6

4.4.2 Coccolithophore analyses

For coccolithophore analyses MD08-3179Cq was sampled every 5 cm from 385 to 814 cm, corresponding to an average time resolution of 943 years. Additionally core section 690 - 814 cm was sampled every 1 cm in order to increase the resolution of the record during MIS 5.5. Therefore the time-resolution during this period corresponds to 97 years.

For an estimation of the abundances of coccolithophore species, samples were treated following Andruleit (1996). Therefore a small amount of sediment was weighed (0.06 - 0.08 g) and brought into suspension with tab water. The suspension was ultrasonicated for 15 to 20 s to disaggregate agglomerated sediment particles (e.g. fecal pellets). Then it was split by a factor of 100 using a rotary wet splitter (™Fritsch Laborette 27). After splitting, the suspension was filtered on polycarbonate filters with a pore size of 0.4 µm. The filters were dried at 40°C for 24 h. After drying, a small piece of filter was cut out and mounted on a Scanning Electron Microscopy (SEM) stub. After sputtering the sample with Au/Pd, coccoliths were counted under the SEM. Therefore a measured transect was

scanned under a magnification of 5000 and coccoliths were identified according to the taxonomy given in (Young and al, 2003). At least 300 coccoliths (average: 367, minimum: 319, maximum: 544) were counted. A taxonomic list of all identified coccolithophore species is given in the Appendix. In order to improve the accuracy of the less abundant species *C. pelagicus*, we performed extended counts (scanning a measured transect across the entire filter at a magnification of 1000). The above described preparation technique allows a qualitative and quantitative estimation of coccolithophore abundances. For a quantitative estimation of coccolithophore abundances, we calculate species and total coccolith concentrations following equation (2.2). Because coccolith accumulation rates have been shown to be a good indicator for paleoproductivity (Lototskaya et al., 1998; Stolz and Baumann, 2010), we calculated coccolith accumulation rates according to equation (2.3). To calculate accumulation rates we used sedimentation rates shown in Figure 4.2 and average dry bulk density of nearby core GEOFAR KF16 (Richter, 1998). At last, we pooled coccoliths from *Umbilcosphaera* spp., *Umbellosphaera* spp. and *Oolithotus* spp. into a subtropical group, based on their well-known ecological preferences (McIntyre and Bé, 1967; Incarbona et al., 2010).

4.4.3 XRF core scanning

XRF core scanning was performed on core MD08-3179Cq using the AAVATECH XRF core scanner at the Institute of Geosciences in Kiel. The core was scanned every 0.5 cm with generator settings of 10 and 50 kV. Because the core location is far offshore, the sediments are primarily of biogenic origin, which has also been shown for nearby cores GEOFAR KF16 (Richter, 1998) and MD08-3180Cq (Schwab et al., 2012). Furthermore the purely pelagic character of the sediment can also be deduced by the visual examination of the samples by SEM, where only coccolithophores, diatoms, silicoflagellates and calcareous dinoflagellates have been observed. Therefore we are using Si/Ca measured by XRF as a tracer for the relative contribution of siliceous plankton to the sediment. To validate this approach, diatom control counts were taken out along measured transects on filters prepared for coccolithophore analysis using SEM. Only intact valves were counted without identification on the species level.

4.5 Results

4.5.1 Coccolithophore assemblage changes between 130 and 48 ka BP

The core location is situated above the present and even above the glacial lysocline (Crowley, 1983). Therefore the preservation of coccoliths is excellent. The excellent preservation can be deduced by the presence of well-preserved coccoliths from fragile coccolithophore species like *G. ornata* and by the presence of complete coccospheres and holococcoliths. In general the observed changes in the relative abundances of coccolithophore species are paralleled by changes in their absolute abundances (Figure 4.3). The coccolithophore assemblages in the investigated interval are dominated by species of the genus *Gephyrocapsa*, together comprising up to 88% of the total assemblage and reaching maximum absolute abundances of up to 7.9 x 10^{10} coccoliths/g sediment.

In general the relative and absolute changes in the coccolithophore assemblage closely match the succession of MIS and substages. For example small gephyrocapsids (distal shield length ≦2.7 μm), which dominate coccolithophore assemblages during MIS 5 with values up to 71%, show high relative and particularly high absolute abundances during substages 5.1, 5.3 and 5.5 (Figure 4.3a). The opposite pattern is observed in the abundance of *G. muellerae* with high abundances during substages 5.2 and 5.4 as well as during Termination II (TII) and low abundances during substages 5.1, 5.3 and 5.5 (Figure 4.3b). A marked turnover within these species is observed at the MIS 5/4 boundary, where small gephyrocapsids abruptly decrease and *G. muellerae* increase to peak during MIS 4. Especially during MIS 5 the assemblage is dominated by coccolithophores of the genus *Gephyrocapsa*, together comprising up to 88% of the total assemblage. The dominance of gephyrocapsids during this period is a well-known feature of coccolithophore records, at least in the eastern basin of the North Atlantic (e.g. Weaver et al., 1999; Stolz and Baumann, 2010), which fits to our observations.

Like small gephyrocapsids, *E. huxleyi* shows peak relative and especially peak absolute abundances during substages 5.1, 5.3 and 5.5 (Figure 4.3c). After minimum abundances during early MIS 4, *E. huxleyi* becomes a more important part of the assemblage after 72 ka BP. This increase is in line with other North Atlantic coccolithophore records,

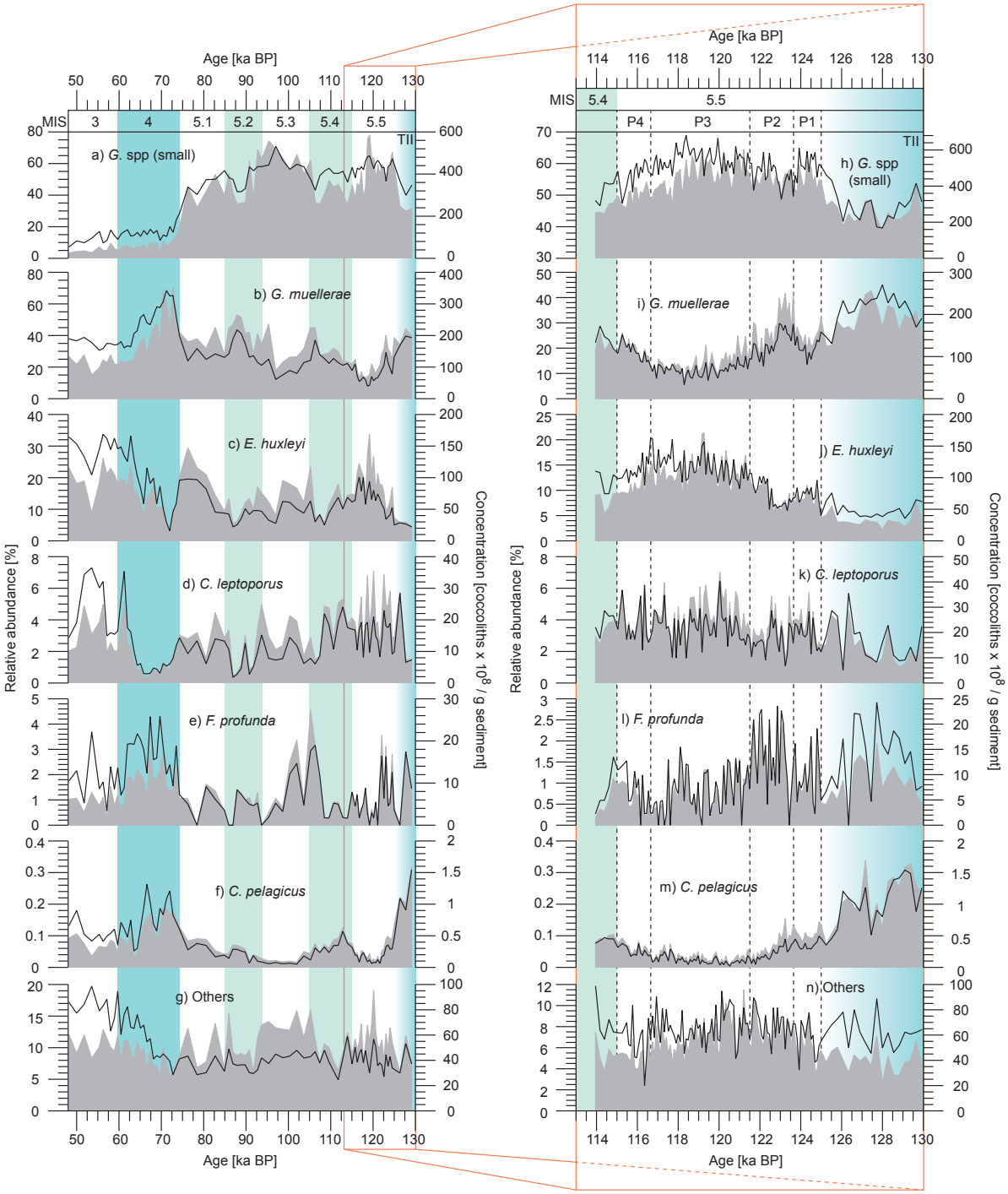

Figure 4.3. Relative (black solid lines) and absolute (grey filled areas) abundances of individual coccolithophore species. Blue vertical bar indicates glacial stage. Light blue vertical bars indicate glacial substages. Shaded blue bar indicate Termination II (TII). Left panel (low-resolution counting between 48 and 130 ka BP): a) Small gephyrocapsids; b) *G. muellerae*; c) *E. huxleyi*; d) *C. leptoporus*; e) *F. profunda*; f) *C. pelagicus*; g) Others. Right panel (high-resolution counting between 115 and 125 ka BP): h) Small gephyrocapsids; i) *G. muellerae*; j) *E. huxleyi*; k) *C. leptoporus*; l) *F. profunda*; m) *C. pelagicus*; n) Others; black dashed vertical lines indicate subdivision (P1 – P4) of MIS 5.5 as described in the text.

which document an increase of *E. huxleyi* abundances above previous values around the MIS 5/4 boundary (Thierstein et al., 1977) (see chapter 5.2.2).

Unlike in the open equatorial Atlantic, *C. leptoporus* is only a minor component of the coccolithophore assemblage during the investigated time interval (cf. Kinkel et al. 2000). However, distinct minimum abundances of this species are observed during MIS 4 (Figure 4.3d). Furthermore this species shows minimum abundances during substage 5.2 and maximum abundances during substage 5.5 and after 64 ka BP.

F. profunda is only abundant in the subtropical regions south of the AzF (e.g. Schiebel et al., 2011). Therefore this species is rare at our coring site, which is situated slightly north of the AzF (Figure 4.1). *F. profunda* hardly exceeds the critical value of 3% during the investigated period, but it shows distinct maximum abundances at the beginning of substage 5.5, at the beginning of substage 5.3 and during MIS 3 (Figure 4.3e).

Similarly, our coring site is situated at the southern distribution limit of *C. pelagicus* (Ziveri et al., 2004), and therefore this species is very rare in our record (Figure 4.3f). Based on the extended counts of *C. pelagicus* (see chapter 4.4.2) this species shows distinct maximum abundances during TII and MIS 4 and a less distinct maximum during substage 5.4 (Figure 4.3f). Although interrupted by several minima the abundance of *C. pelagicus* is slightly increasing from the beginning of substage 5.2 to the end of substage 5.1. All other species identified never exceed 3% relative abundance during MIS 5 and together comprise between 5 and 20% of the total assemblage (Figure 4.3g, Appendix).

4.5.2 Coccolith abundance changes during MIS 5.5

Based on our high resolution coccolith counting during MIS 5.5, this substage can be divided into four intervals: an early part one (P1) from 125 - 123.6 ka BP, a part two (P2) from 123.6 - 121.5 ka BP, a part three (P3) from 121.5 - 116.6 ka BP and a part four (P4) from 116.6 - 115 ka BP (Fig. 4.3h - n). Following TII, P1 is characterized by a maximum in small gephyrocapsids (Figure 4.3h), a first minimum in *G. muellerae* (Figure 4.3i) and a slight maximum in *E. huxleyi* (Figure 4.3j). *C. leptoporus* increased during late TII and still shows enhanced abundances during P1 (Figure 4.3k). Furthermore P1 is characterized by low abundances of *F. profunda* (Figure 4.3l) and *C. pelagicus* (Figure 4.3m) compared to TII. During P2 a decrease in small gephyrocapsids, an increase in *G. muellerae* and a decrease in *E. huxleyi* is observed. Furthermore minima in abundances of *C. leptoporus* and

a marked increase in the abundances of *F. profunda* are observed during P2. *C. pelagicus* shows abundances comparable to P1 at the beginning of P2 and subsequently decreases during P2. The third part of MIS 5.5 (P3) is characterized by peak abundances of small gephyrocapsids, *E. huxleyi* and *C. leptoporus*, as well as minimum abundances of *G. muellerae*, *F. profunda* and *C. pelagicus*. The last part of MIS 5.5 (P4) shows decreasing abundances of small gephyrocapsids and *E. huxleyi* whereas the abundances of *G. muellerae*, *F. profunda* and *C. pelagicus* are increasing again. In general, the observed changes in the coccolithophore assemblage during MIS 5.5 closely match the observations of Lotoskaya et al. (1998) from sediment core T90-9P (45°17.5'N, 25°41.3'W) north of our coring site.

4.5.3 Changes within the abundances of subtropical species, total coccolith concentrations and coccolith accumulation rates

Like the abundance records of the individual coccolithophore species, the abundance record of subtropical coccolithophore species (Figure 4.4a) and the total coccolith concentration (Figure 4.4b) show a strong correlation to isotopic stages and substages between 130 and 48 ka BP. Thereby high abundances of subtropical species and high total coccolith concentrations prevail during substages 5.1, 5.3 and 5.5. During subsequent MIS 4 subtropical species and coccolith concentration decrease, whereas subtropical species start to increase again after 64 ka BP. Total coccolith concentrations remain low well into the beginning of MIS 3. In general, the observed variations in coccolith concentrations between 2.1 and 9.8 x 10^{10} coccoliths/g sediment are typical for subtropical to temperate regions of the open ocean (Baumann et al., 2004). The most significant feature in the coccolith accumulation rate record is a distinct maximum during MIS 5.5 (Figure 4.4c). However, subordinate maxima during MIS 5.4, MIS 5.2 and MIS 4 are also evident in the coccolith accumulation rate record.

The detailed view on MIS 5.5 also reveals a clear correlation of the subtropical species and coccolith concentration records to the different parts of this substage. Following TII an increase in subtropical species (Figure 4.4d) and an increase in coccolith concentrations (Figure 4.4e) is evident during P1. P2 is characterized by a minimum and P3

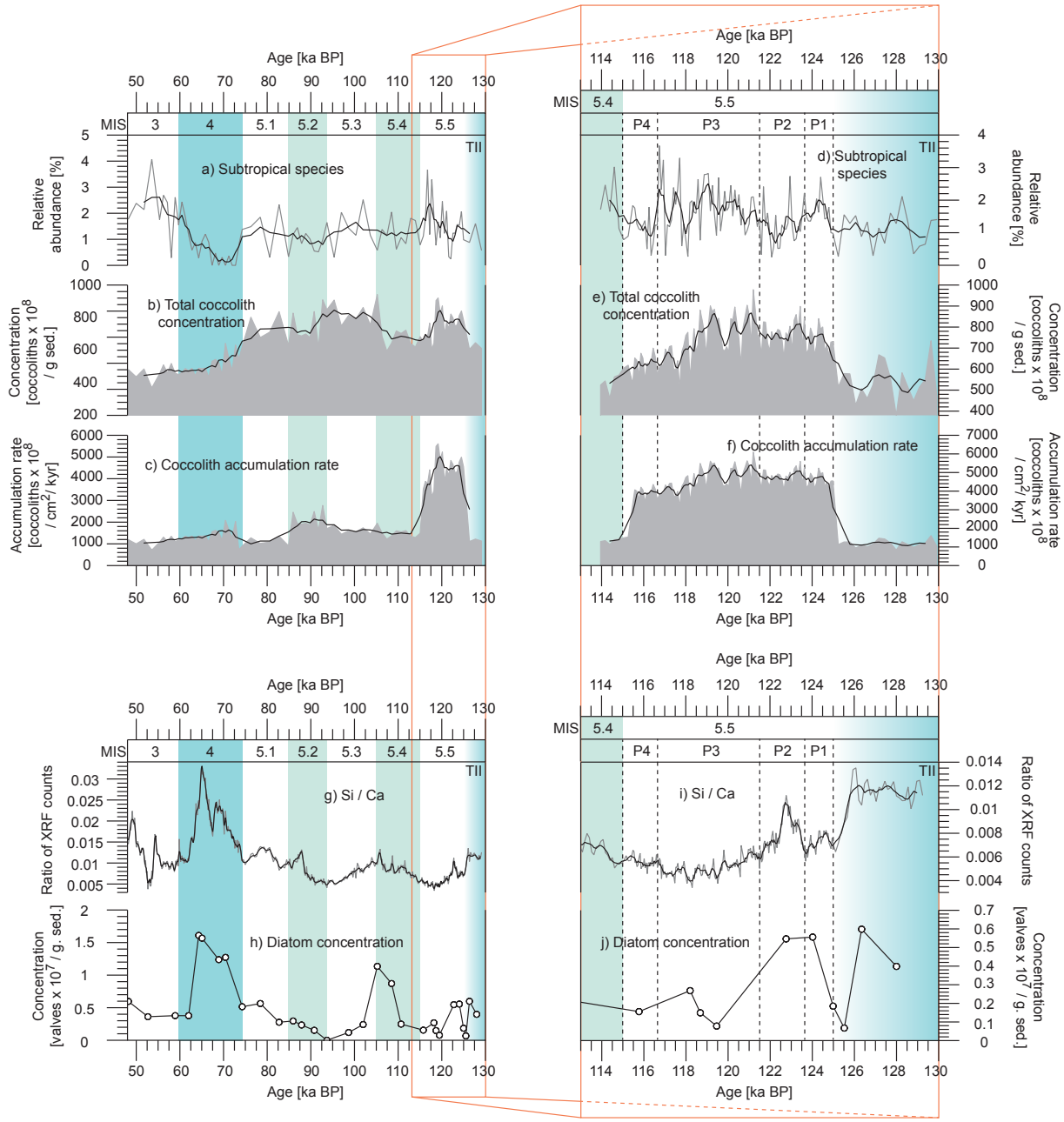

Figure 4.4. Upper left panel (low-resolution counting between 48 and 130 ka BP): a) Relative abundance of subtropical coccolithophore species (grey solid line) and 5pt moving average (black solid line); b) Total coccolith concentration in the sediment (grey filled area) and 5pt moving average (black solid line); c) Coccolith accumulation rate (grey filled area) and 5pt moving average (black solid line). Upper right panel (high-resolution counting between 115 and 125 ka BP): d) Relative abundance of subtropical coccolithophore species (grey solid line) and 5pt moving average (black solid line); e) Total coccolith concentration in the sediment (grey filled area) and 5pt moving average (black solid line); f) Coccolith accumulation rate (grey filled area) and 5pt moving average (black solid line); black dashed vertical lines indicate subdivision of MIS 5.5. Lower left panel: g) Si/Ca ratio measured by XRF; h) Diatom concentration in the sediment. Lower right panel (close-up of lower left panel between 113 and 130 ka BP): i) Si/Ca ratio measured by XRF; j) Diatom concentration in the sediment; black dashed vertical lines indicate subdivision of MIS 5.5. Blue vertical bar indicates glacial stage. Light blue vertical bars indicate glacial substages. Shaded blue bar indicates Termination II (TII).

by a maximum in these records. During P4 a minimum and subsequent slight increase in subtropical species and a decrease in coccolith concentration are observed. The observed coccolith concentrations of around 8 x 10^{10} coccoliths/g sediment are within the range of previously reported coccolith concentrations during MIS 5.5 from the eastern North Atlantic (around 6 x 10^{10} coccoliths/g sediment) (Lotoskaya et al., 1998; Stolz and Baumann, 2010). The slightly higher values may reflect the more southern core position compared to the other studies, because coccolithophores increase their abundance within the total plankton community towards the oligotrophic subtropical gyres (Baumann et al., 2005).

Although strongly increased during the entire MIS 5.5, slight variations during this period can also be observed in the coccolith accumulation rates (Figure 4.4f). However, as sedimentation rates are constant during this period, these variations are solely controlled by coccolith concentrations, and therefore may not reflect the actual changes in coccolith accumulation rates. Nevertheless, values around 5 x 10^{11} coccoliths/cm^2/kyr closely match the observations of Lotoskaya et al. (1998) from sediment core T90-9P north to our coring site.

4.5.4 Si/Ca measured by XRF (siliceous plankton abundances)

Compared to coccolithophore records, siliceous plankton (diatom) records are often affected by a diagenetic overprint, because biogenic opal (SiO_2) gets easily dissolved in seawater (e.g. Romero et al., 1999). Nevertheless, abundance records of diatoms are widely used to reconstruct past oceanic conditions (Abrantes, 2000; Romero et al., 2011). Thereby the abundance of diatoms is assumed to reliably reflect past productivity conditions, as these species prefer turbulent and nutrient-rich surface water conditions (Abrantes et al., 2002). Therefore, in supplement to our coccolithophore records, we use abundance changes of siliceous plankton (diatoms) as an indicator for past productivity changes.

In general, we observe a good correlation of diatom abundances to Si/Ca measured by XRF (Figures 4.4g, h). Therefore, the variations in the Si/Ca record will be interpreted as abundance changes of siliceous plankton (mainly diatoms). Based on our record, we observe pronounced peak abundances of siliceous plankton (diatoms) during MIS 4. A second distinct but less pronounced peak can be observed at the end of MIS 5.4. Furthermore, slight maximum abundances are evident during TII and MIS 5.2. The slight maxi-

mum abundances during MIS 5.2 prevail into MIS 5.1, where they are interrupted by two minor minima. During MIS 5.5 minimum abundances of siliceous plankton (diatoms) abundances can be observed during P1, following maximum abundances during TII (Figure 4.4i, j). Increased abundances can again be observed during P2, whereas the following P3 is characterized by a minimum with a subsequent slight increase during P4.

4.6. Discussion

4.6.1 Orbital scale response of coccolithophore assemblages to ecology changes between 48 and 130 ka BP

The succession of Marine Isotope Stages and substages is driven by insolation changes due to changes in the orbital configuration of Earth's rotation axis (e.g. Lisiecki and Raymo, 2005). The succession of MISs and substages at our coring site between 48 and 130 ka BP, as deduced from the planktonic foraminiferal oxygen isotope record (Figure 4.2), is closely paralleled by distinct changes in coccolithophore assemblages (Figure 4.3). As it is known that the individual (sub-) stages are characterized by different and distinct climatic conditions (Lehman et al., 2002; Risebrobakken et al., 2005; Penaud et al., 2008), the good correlation indicates that coccolithophores are a valuable tool to reconstruct past environmental changes at our coring site during the considered time interval.

AzF dynamics and paleoproductivity changes

A key species to reconstruct past migrations of the AzF at the coring site is *G. muellerae*. Regarding the North Atlantic, and aside its local occurrence in the upwelling regions off northwest Africa (Sprengel et al., 2002), this species exclusively lives north of the AzF, in the temperate regions of the North Atlantic, corresponding to NATW (Jordan, 1988; Giraudeau et al., 2010; Schiebel et al., 2011). Therefore *G. muellerae* can be used as an indicator for the influence of NATW at the coring site, whereby increased abundances of this species indicate a greater influence of NATW due to a more southern position of the AzF. Increased abundances of this species are observed during MIS 4, MIS 5.2, MIS 5.4 and TII (Figure 4.3b), thus we assume that the AzF resided at a more southern position during

these periods. This scenario is also supported by the abundance pattern of subtropical species, which preferentially live in the subtropical realm (McIntyre and Bé, 1967; Incarbona et al., 2010) and therefore can be used as a tracer for the influence of subtropical waters at the coring site. Hence the low abundances of these species during MIS 4, MIS 5.2, MIS 5.4 and TII indicate a diminished influence of subtropical waters at the coring site (Figure 4.4a), most probably due to a more southern position of the AzF, in accordance to the *G. muellerae* record. Furthermore, this result fits into the concept of a more southern position of the AzF during cold/glacial periods, as it has been described by Schiebel et al., (2002b) and Schwab et al. (2012). At last, further evidence for this scenario comes from the coccolith concentration record (Figure 4.4b). As many coccolithophore species are K-selected, they increase their abundances within plankton communities under oligotrophic conditions (Baumann et al., 2005), resulting in highest coccolith concentrations in sediments underneath waters of the subtropical realm (Baumann et al., 2004). Therefore the decreased coccolith concentrations during MIS 5.2, MIS 5.4 and TII indicate less subtropical conditions in accordance to high *G. muellerae* and low subtropical species abundances. The observed changes may have been a consequence of changes in the wind-field, as a close relation between the latitudinal position of the AzF and the wind regime on annual and inter-annual timescales have been described (Klein and Siedler, 1989; Volkov and Fu, 2010; 2011). Thereby periods with strengthened westerly winds result in a more southern position of the AzF. As westerly winds were increased during glacial (sub-) stages (Heusser and Oppo, 2003; Incarbona et al., 2009), the more southern positions of the AzF, as recorded in our proxy data, may have been the response to the strengthened westerly winds during these periods.

As described above, our proxy records indicate a consistent pattern, with a more southern position of the AzF during glacial (sub-) stages, and a more northern position of the AzF during interglacial (sub-) stages. This also holds true for the interglacial substage MIS 5.1, where the changes, e.g. in the abundance of *G. muellerae* (Figure 4.3b), indicate a more northern position of the AzF in comparison to adjacent cold MIS 4 and MIS 5.2. However, the absolute values, e.g. the abundance of *G. muellerae* (Figure 4.3b), are more comparable to the cold substages of MIS 5, indicating that the AzF did not migrated as far north as it did during other warm substages of MIS 5. This may be in line with other paleoclimate records of the North Atlantic region, which indicate that although relative warm, MIS 5.1 is cooler than the other warm substages of MIS, 5 and considerable climate fluc-

tuations occur during this period precursory to full glacial MIS 4 (Shackleton et al., 2000; Lehman et al., 2002; Andersen et al., 2004).

Aside from abundance changes of *G. muellerae*, which indicate a varying contribution of NATW to the coring site due to latitudinal displacements of the AzF, a varying contribution of subpolar waters to the coring site can be deduced from the abundance record of the subpolar species *C. pelagicus* (Figure 4.3f). This species preferentially lives in polar to subpolar water masses and tolerates temperatures below 0°C (McIntyre and Bé, 1967; Okada and McIntyre, 1979). Therefore it displays distinct maximum abundances in polar to subpolar regions (Baumann et al., 2005), and has been used as an indicator for the influence of subpolar water masses in this study. Today subpolar water masses, transporting a subpolar fauna and flora, are admixed to NATW via cold core rings, which pinch off the North Atlantic Current (Kupferman et al., 1986; Beckmann et al., 1987). However, today these cold core rings do not penetrate down to the latitudes of the coring site and therefore *C. pelagicus* is nearly absent in the Azores region today (Schwab et al., 2012). Increased abundances of *C. pelagicus* during TII, MIS 5.4, MIS 5.2 and MIS 4 may indicate a greater contribution of subpolar water masses during these periods, probably due to a more southern position of the North Atlantic Current and its associated subpolar front (McIntyre et al., 1972), which would have allowed the cold core rings to penetrate to the coring site. Furthermore, the relatively cold character of MIS 5.1 as explained above, is also evidenced by an increased abundance of *C. pelagicus*, indicating an increased incursion of cold subpolar water masses during this period. At last, peak abundances of this species during TII are characteristic for glacial conditions in the Azores region (Schwab et al., 2012), corroborating the validity of the isotope stratigraphy.

Past productivity changes in the Azores region have been reconstructed using abundance variations of siliceous phytoplankton (diatoms) (Figure 4.4g, h). A distinct abundance peak of diatoms can be observed during MIS 4, indicating an enhanced productivity during this period. This enhanced productivity can be related to the above postulated more southern position of the AzF and its associated climatic and productivity regimes, which would bring more nutrient-rich NATW to the coring site (cf. chapter 2). Additionally, increased westerly winds during this period (Heusser and Oppo, 2003; Incarbona et al., 2009), which would enhance winter mixing, and/or an increased advection of nutrient-rich subpolar surface waters (Kupferman et al., 1986), as evidenced by the *C. pelagicus* record, could have further fuelled productivity. In addition to this pronounced productivity peak

during MIS 4, some smaller scale productivity peaks are indicated by increased diatom abundances during TII, MIS 5.4 and MIS 5.2, which can also be related to the processes described above.

Although the above described productivity pattern can also be inferred by slight changes in coccolith accumulation rates (Figure 4.4c), a pronounced coccolithophore productivity peak is observed during MIS 5.5, which cannot be related to a more southern position of the AzF, enhanced westerly winds or advection of subpolar waters. There are at least two explanations for the observed coccolithophore productivity peak: 1) The observed coccolithophore productivity peak is related to a basin-wide coccolithophore productivity peak during MIS 5.5, which extended at least in the eastern basin of the North Atlantic (Lototskaya et al., 1998; Stolz and Baumann, 2010). This increased coccolithophore productivity has been related to the opportunity for coccolithophores to occupy new habitats under optimal conditions (warm and stratified) following glacial MIS 6 (Stolz and Baumann, 2010). 2) Additionally, a greater presence of silicate- and nitrate-rich Subantarctic Mode Water (SAMW) during MIS 5.5 in the North Atlantic probably further fueled coccolithophore productivity (Romero et al., 2011). Today SAMW partly replenishes the nutrient-loss in the North Atlantic (Sarmiento et al., 2004). These nutrient-rich thermocline waters are preferentially transported via the Brazil and North Atlantic Current into the North Atlantic (Williams et al., 2006). As the Azores Current System is an eastward branch of the North Atlantic Current (Figure 4.1), these waters potentially could enter the Azores region. Upwelling of these waters within the AzF, which resided close to the coring position during MIS 5.5, might have additionally fueled coccolithophore productivity within the AzF (cf. chapter 4.3). However, the more subtropical and nutrient-rich conditions during MIS 5.5 preferentially favored the growth of coccolithophores (Brand, 1994), and therefore this productivity peak is not observed in the abundance record of diatoms.

Abundance changes of the deep-dwelling coccolithophore species *F. profunda* are well correlated to changes in nutricline depth (Molfino and McIntyre, 1990a; 1990b), and therefore are widely used to reconstruct past productivity changes (e.g. Beaufort et al., 1997; Flores et al., 2000; Li et al., 2010). Thereby low abundances of *F. profunda* are commonly assumed to reflect high productivity, whereas high abundances would indicate low productivity. However, most paleoproductivity studies based on abundance changes of *F. profunda* are from tropical to subtropical regions, where this species is common (e.g. Okada and McIntyre, 1979; Molfino and McIntyre, 1990a, 1990b; Beaufort et al., 1997). As

our coring site is situated in the transition zone between the subtropical and temperate oceanic realm, we observe only a rare occurrence of this species (Figure 4.3e), which may hamper a robust interpretation. Nevertheless, distinct maximum abundances of *F. profunda* can be observed during TII, early MIS 5.5, MIS 5.4 and MIS 4. Applying the above-described relation, this would indicate low productivity during these periods, which is in contrast to the previously described productivity pattern. We therefore suppose that the commonly used interpretation of this species cannot be applied to our record during the investigated period, and care must be taken in the interpretation of this species in terms of productivity, as it has already been stated by Kinkel et al. (2000). Instead we propose that the nutrients that fueled surface productivity during TII, early MIS 5.5, MIS 5.4 and MIS 4 also affected the deeper layers, which thereby increased the abundances of deep dwelling species.

In general, we observe a more southern position of the AzF and increased PP during cold stages and substages, whereas a more northern position and decreased productivity are found during warm stages and substages, which is in line with previous studies of AzF dynamics (Schiebel et al., 2002b; Schwab et al., 2012). As the AzF delineates the North Atlantic subtropical gyre (Bashmachnikov et al., 2004), these results indicate a northward/southward expansion of the gyre during warm/cold climatic periods respectively. Therefore our results fuel the hypothesis that due to an expected future global temperature rise (Jansen et al., 2007) the oligotrophic subtropical gyre could enlarge its areal extend, as it has also been observed during recent decades (Polovina et al., 2008). Such an expansion of oligotrophic waters would lead to a decreased primary productivity, which is an integral part of the climate system due to the photosynthetic fixation of atmospheric carbon. Therefore a decreased North Atlantic productivity, resulting in a decreased atmospheric carbon drawdown, could provide a positive feedback to rising temperatures.

Coccolithophore dominance reversals: evolutionary adaption or ecological change?

The observed dominance of gephyrocapsids during MIS 5 is a well-known feature of coccolithophore records spanning the considered time interval (Lototskaya et al., 1998; Flores et al., 1999; 2003; Baumann and Freitag, 2004; Stolz and Baumann, 2010). This pronounced dominance ends around the MIS 5/4 boundary, at the time when *E. huxleyi* starts to increase in its abundance to become a dominant part of coccolithophore assem-

blages (Thierstein et al., 1977). This reversal, defined as the point at which *E. huxleyi* starts to increase above previous relative abundance values, has been described to be a time-transgressive event, occurring early (85 ka BP) in low latitudes and late (61 ka BP) in high latitudes (Thierstein et al., 1977; Gard, 1986; 1987), matching our observations from the midlatitudes, where this reversal starts at 72 ka BP (Figure 4.3c).

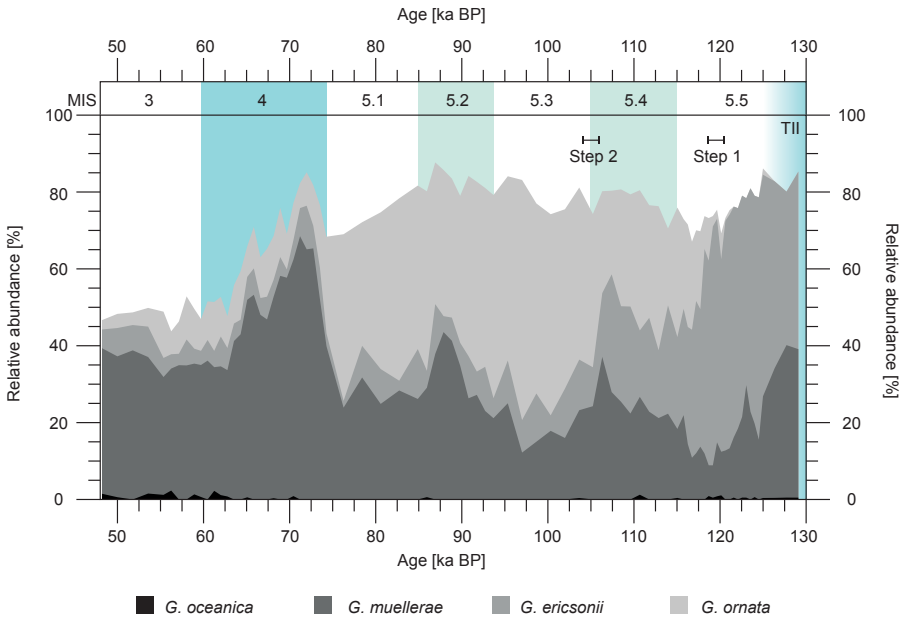

Figure 4.5. Relative abundance of identified gephyrocapsid specimens. Stepwise increase of *G. ornata* indicated by horizontal bars labeled with Step 1 and Step 2. Blue vertical bar indicates glacial stage. Light blue vertical bars indicate glacial substages. Shaded blue bar indicate Termination II (TII).

However, for simplicity, most coccolithophore studies encompassing MIS 5 only distinguish between three morphotypes of gephyrocapsids. Thereby *G. oceanica*, *G. muellerae* and grouped small gephyrocapsids are distinguished (e.g. Lototskaya et al., 1998; Flores et al., 1999; 2003; Aizawa et al., 2004; Baumann and Freitag, 2004), following the sometimes slightly modified taxonomic concept introduced by McIntyre et al. (1970). However, as there are up to 27 morphotypes of gephyrocapsids, of which 12 are smaller than 2.7 μm (Bollmann, 1997), little is known about the distribution of the different small morphotypes of gephyrocapsids during MIS 5.

Because *G. ornata* can be easily recognized by SEM without conducting detailed morphometric analysis (e.g. measurements of distal shield length and bridge angle), we distinguished between this morphotype and other small gephyrocapsids, which mainly comprise *G. ericsonii*. Based on this differentiation, we observe a successive replacement

of *G. ericsonii* by *G. ornata*, resulting in a dominance interval of the latter species between 76 and 105 ka BP (Figure 4.5). This turnover in the small gephyrocapsid assemblage takes place in two distinct steps, at which a first increase between 120 and 118 ka BP, corresponding to peak interglacial conditions (see chapter 4.6.2), is followed by a second, final increase between 106 and 104 ka BP, corresponding to the MIS 5.4/5.3 boundary. Because both steps are closely linked to distinct ecological conditions/changes, the observed dominance reversal, which are classically attributed to an evolutionary adaption (e.g. Bollmann et al., 1998), are probably triggered by ecological changes. In our case, more interglacial conditions allow *G. ornata* to conquer the habitat occupied by *G. ericsonii*. Likewise the dominance reversal at the MIS5/4 boundary between small gephyrocapsids and *E. huxleyi* (see beginning of this chapter) can also be related to ecological changes attributed to an interglacial-glacial transition. Therefore we propose that ecological changes may trigger evolutionary adaptions in Late Quaternary coccolithophore assemblage.

4.6.2 A detailed view on MIS 5.5

Although several boundary conditions such as orbital parameters and ice sheet configuration were different to the present interglacial (Shackleton et al., 2003; Laskar et al., 2004; Rohling et al., 2007; Sánchez Goñi et al., 2012), MIS 5.5 is widely used to study interglacial climate variability and serves as a potential scenario for expected global warming (Kukla et al., 2002; Bauch et al., 2012). For this purpose high-resolution records spanning the considered time period are needed. In the following, we will show and discuss the detailed structure of MIS 5.5 in the midlatitude North Atlantic based on our high-resolution coccolithophore records.

A stable MIS 5.5 in the midlatitude North Atlantic?

Based on our coccolithophore records with a temporal resolution of 97 years during MIS 5.5, pronounced multi-centennial variability can be observed during this period, indicating rather unstable conditions (Figures 4.3, 4.4). The observed variability is best expressed by a consistent subdivision of MIS 5.5 into four intervals, which span time periods from 1.4 – 4.9 kyrs, and which are characterized by distinct paleoenvironmental conditions.

Following our interpretation of the *G. muellerae* and subtropical species records (see chapter 4.6.1), the AzF migrated northward during early MIS 5.5 (P1) and reached its full interglacial position during the middle MIS 5.5 (P3). The northward migration of the front is interrupted by a southward retreat (P2), indicating a reversal to more glacial conditions, which is in line with a cooling event recorded across the entire North Atlantic during MIS 5.5 (Cortijo et al, 1994; Sánchez Goñi et al., 2005; Bauch et al., 2011; Irvalı et al., 2012). During this event, sea surface temperatures decreased by approximately 4°C in the polar and subpolar regions and deep convection in the eastern north Atlantic decreased (Maslin et al., 1998; Bauch et al., 2011; Irvalı et al., 2012) (there was no deep convection in the Labrador Sea during the entire MIS 5.5 (Hillaire-Marcel et al., 2001)). Recently it has been hypothesized that this event is analogous to the 8.2 ka BP event and probably was triggered by enhanced meltwater runoff and/or breaking of dammed proglacial lakes (Bauch et al., 2011). It has recently shown by Schwab et al. (2012) that such events, namely the 8.2 ka BP event, could penetrate to our midlatitude coring site, highlighting the sensitivity of the midlatitude (eastern) North Atlantic to high northern latitude processes. However, the analogy of this event to the 8.2 ka BP event would indicate that such cold reversals are characteristic for Interglacials and may also be found in older interglacial periods. Furthermore, the observed overall structure, with a bisection of MIS 5.5 due to a cooling event and with full interglacial conditions during the second, later part of MIS 5.5, is in line with other proxy records from the North Atlantic (Oppo et al., 2006; Vautravers et al., 2007; Bauch et al., 2011; Sánchez Goñi et al., 2012), indicating a close coupling of the AzF dynamics to North Atlantic climate variability. Thereby the strength of the westerly winds may have been responsible for the observed latitudinal variability of the AzF, as it is indicated by recent observations and modeling studies (Klein and Siedler, 1989; Volkov and Fu, 2010; 2011). Therefore the northernmost position of the AzF during peak MIS 5.5, which consistently is found between 120 and 118 ka BP (within P3), was probably caused by minimum westerly wind strength during this period.

Although we observe a distinct coccolithophore productivity peak during the entire MIS 5.5, due to optimal growth conditions and/or upwelling of nutrient-rich SAMW (see chapter 4.6.1), some smaller scale productivity changes related to the changes in the hydrographic conditions can also be observed. For example, a slight increased productivity can be observed during P2 as evidenced by slightly increased abundances of diatoms (Figure 4.4i, j). Again, this increased productivity can be related to a more southern posi-

tion of the AzF and its associated productivity regimes, as postulated above. Consistently, minimum coccolith concentrations are also found during this period and together with the increased abundances of diatoms indicate less stratified surface water conditions in the Azores region during this time. Furthermore, the nutrient supply responsible for the observed productivity increase again also affected the deeper photic zone as evidenced by maximum abundances of *F. profunda* during this time (Figure 4.3l). However, the less stratified conditions may be the consequence of slightly increased westerly winds, which would also have forced the AzF to the south during P2, and/or of the increased influence of NATW at the coring site, which is characterized by a deep winter mixed layer. Again, the observed increased productivity during P2 might additionally have been fuelled by the advection of nutrient-rich subpolar surface waters, as evidenced by slight increased abundances of *C. pelagicus* (Figure 4.3m). On the other hand, decreased productivity and more stratified conditions are found during periods when the AzF resided at a more northern position (P1 and P3).

Another issue may arise from the hypothetical connection between the Azores Current strength and the Mediterranean outflow water (MOW). Thereby model studies indicate that a strengthened MOW would lead to a stronger Azores Current (Volkov and Fu, 2010; Volkov, 2011). The volume of the water mass exchange in the Street of Gibraltar in turn is controlled by fluctuations of the sea-level, at which a higher sea-level stand results in a more vigorous water mass exchange and hence in a strengthened outflow (Rohling and Bryden, 1994; Matthiesen, 2003; Toucanne et al., 2007; Rogerson et al., 2010). As sea-level was approximately 4 to 6 m higher during MIS 5.5 compared to today (Rohling et al., 2007; Kopp et al., 2009), we suggest that the Azores Current was stronger during this period, transporting more water than the recent 9 - 19 Sv (Bryden and Stommel, 1984; Kinder and Parrilla, 1987).

In summary, we observe coupled changes in the hydrographic and productivity conditions during MIS 5.5 in the Azores region, which challenges the classical view of rather stable interglacial conditions during this period. For example, the unstable conditions are expressed by short-lived peak interglacial conditions, with a maximum duration of 4.9 kyrs (P3), which furthermore, in accordance to other marine records, are reached only late during MIS 5.5. The most pronounced instability of MIS 5.5 in the Azores region is expressed by a rapid and profound reversal towards more glacial conditions (P2), which corresponds in timing and duration to a cold reversal recorded across the entire North Atlantic, and may

have been caused by a massive freshwater discharge by glaciers or proglacial lakes. However, taking MIS 5.5 as an analog for expected future global climate change, the above hypothesized future decrease in overall productivity of the North Atlantic (see chapter 4.6.1), due to an expansion of the subtropical gyre as a result of rising global temperatures, may be attenuated by an increased production and export of SAMW as observed during MIS 5.5 (e.g. Romero et al., 2011). Therefore, the influence of SAMW on North Atlantic productivity, which is a major sink for atmospheric CO_2, and therefore provides a strong climate feedback, should be evaluated and addressed in detail in modeling studies dealing with future climate scenarios.

An early E. huxleyi peak during MIS 5.5 in the eastern North Atlantic

Following its first occurrence at approximately 294 ka BP (Wei and Peleo-Alampay, 1993), an event reported to have been time-transgressive with a slightly earlier occurrence in higher latitudes (Hine and Weaver, 1998), *E. huxleyi* evolved to become the most ubiquitous coccolithophore species in the oceans today. As described above (chapter 4.6.1), the dominance reversal from gephyrocapsid dominated to *E. huxleyi* dominated coccolithophore assemblages took place around the MIS 5/4 boundary and therefore *E. huxleyi* played only a minor role in coccolithophore assemblages during the first two-thirds of its abundance range (Thierstein et al., 1977). In accordance to this, *E. huxleyi* never exceeded 20 % of the total assemblage before MIS 4 in our record (Figure 4.3c). However, slight maximum abundances of *E. huxleyi* are observed during warm substages of MIS 5, especially during MIS 5.5, indicating that during the studied time interval this species prefers more warm and stratified surface water conditions at the coring site. This pattern is in line with other abundance records from more northern sites of the eastern North Atlantic, which at least during MIS 5.5 document optimal growth conditions for *E. huxleyi*, resulting in slight peak abundances of this species during this period (Lototskaya et al., 1998; Stolz and Baumann, 2010). Comparing this peak in the different records, we observe that it is a time-transgressive event, again occurring earlier in the higher latitudes (Figure 4.6). This would indicate that environmental conditions, favorable for the growth of *E. huxleyi*, were reached earlier in the higher latitudes, probably fitting to the concept of more severe changes in the higher latitudes than in lower latitudes during MIS 5.5, as indicated by model and proxy studies (Montoya et al., 2000; Anderson et al., 2006).

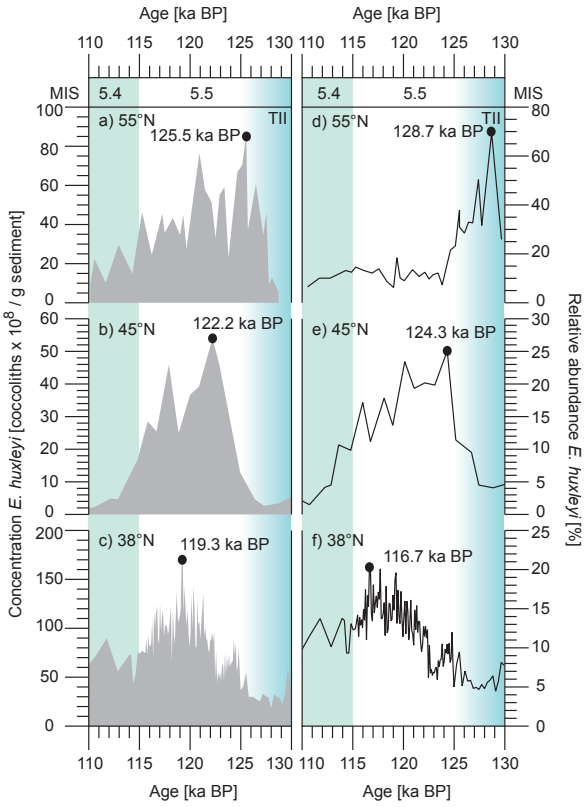

Figure 4.6. Absolute abundance (grey filled areas) of *E. huxleyi* during MIS 5.5 in: a) sediment core ODP 980 (Stolz and Baumann, 2010); b) sediment core T90-9P (Lotoskaya et al., 1998); c) sediment core MD08-3179Cq. Relative abundance (black solid lines) of *E. huxleyi* during MIS 5.5 in: d) sediment core ODP 980 (Stolz and Baumann, 2010); e) sediment core T90-9P (Lotoskaya et al., 1998); f) sediment core MD08-3179Cq. Peak abundances are labeled and marked with black dot. Light blue bar indicates MIS 5.4. Shaded blue bar indicates Termination II (TII).

4.7 Conclusions

In order to investigate regional changes in productivity and hydrography of the North Atlantic between 48 and 130 ka BP, we investigated coccolithophore assemblages in a new sediment core (MD08-3179Cq) taken in the open ocean mid-latitude North Atlantic in the vicinity of the Azores Current System, an area where existing paleoenvironmental studies are rare. Based on changes in coccolithophore assemblages, we observe southward migrations of the AzF during glacial (sub-) stages, which are furthermore accompanied by an increased productivity, as evidenced e.g. by the abundance of siliceous plankton (diatoms). These changes are most probably a result of intensified westerly winds, whereby

productivity might additionally have been fueled by an increased advection of nutrient-rich subpolar surface water masses during these periods.

Furthermore, we observe two pronounced and long-lasting reorganizations of the coccolithophore assemblage, namely the dominance interval of *G. ornata* during MIS 5 and the increase in abundances of *E. huxleyi* after MIS 5, which are closely linked to the above described paleoenvironmental changes. Therefore we hypothesize that paleoecological changes may trigger the evolutionary trends observed in Late Quaternary coccolithophore assemblages.

Based on high-resolution coccolithophore analysis during the Last Interglacial (MIS 5.5), we observe rather unstable interglacial conditions in the Azores region during this period. This instability is best expressed by the occurrence of a distinct reversal towards more glacial conditions (i.e. increased productivity, southward shift of the AzF), which is in accordance to a cooling event recorded across the entire North Atlantic. Furthermore, peak interglacial conditions are accompanied by peak abundances of *E. huxleyi*, an event that occurs earlier in the higher latitudes of the eastern North Atlantic, and which probably is related to more severe changes in the higher latitudes during MIS 5.5. At last we observe a distinct coccolithophore productivity peak during MIS 5.5, which can be related to the occupation of new habitats after glacial conditions and/or an increased advection of SAMW during this period.

Our results fuel the hypothesis that due to a future rise in global temperatures, the oligotrophic waters of the North Atlantic subtropical gyre could expand. This would lead to a decrease in primary productivity, and therefore would provide a positive feedback to the rising temperatures. However, taking MIS 5.5 as a possible analogue for expected future climate change, this scenario will probably be attenuated by an increase in coccolithophore productivity due to the occupation of new habitats and/or advection of nutrient-rich SAMW, as evidenced by a distinct coccolithophore productivity peak during MIS 5.5.

Chapter V.

Comparison of the present and last interglacial in the Azores region based on calcareous nannoplankton

(This chapter corresponds to the following manuscript to be submitted to Climate of the Past: Schwab, C., Kinkel, H., Weinelt, M., Repschläger, J., 2012. Comparison of the present and last interglacial in the Azores region based on calcareous nannoplankton. To be submitted to Climate of the Past.)

5.1 Abstract

In order to test the sensitivity of ecological changes in the Azores region to different boundary conditions, and in order to investigate natural interglacial climate variability, we analyzed and compared present and last interglacial coccolithophore assemblages in sediment cores (GEOFAR KF16, MD08-3179Cq, MD08-3180Cq) from two coring sites near the Azores Islands. Similar abundance variations of key coccolithophore species (e.g. *E. huxleyi*, *G. muellerae* and subtropical coccolithophore species) indicate a general interglacial pattern of ecological changes in the Azores region. Thereby a first climatic optimum during the early interglacials is followed by a reversal towards more glacial conditions during the early to mid interglacials. Afterward full interglacials established only late during the present and last interglacials. These changes are also reflected by latitudinal displacements of the Azores Front (AzF), at which the AzF occupied a more northern position during the early interglacials compared to the preceding glacials, followed by a southward retreat during the early to mid interglacials and a northernmost position during the late interglacials. A quantitative comparison of peak interglacial conditions reveals that the AzF most probably resided at a more northern position and that primary productivity was increased during the last interglacial. The increased coccolithophore productivity during the last interglacial resulted in an increased coccolith carbonate production, which probably prevailed in the entire eastern North Atlantic. The increased carbonate production in the eastern North Atlantic and the more northern position of the AzF, which corresponds to an expansion of the North Atlantic subtropical gyre, potentially could act as a source for atmospheric CO_2. However, as quiet similar CO_2 levels are observed during the present and last interglacial, our results indicate that the ecological changes and the resulting productivity in the eastern North Atlantic probably are insignificant on a global scale, or that the observed increased primary productivity during MIS 5.5 counteracted the combined effect of increased carbonate production and expansion of the oligotrophic gyre. In order to evaluate the impact of ecological changes in the eastern North Atlantic on global climate, further (modeling) studies are urgently needed.

5.2 Introduction

Interglacials are a recurring feature of the Late Quaternary climate record, with a recurrence rate of 100 kyrs at least during the last 400 kyrs (e.g. Imbrie et al., 1984; Raymo, 2003; Tziperman, 2003; Lisiecki and Raymo, 2005). As interglacials reflect a mean climatic state that also characterizes the present Holocene period, there is an increasing interest to study interglacial climates (e.g. Kukla et al.,1997; Maslin et al., 1998; Kukla et al., 2002; Shackleton et al., 2003; Maiorano et al., 2012), especially in the light of the predicted global climate change (Jansen et al., 2007). As the expected future climate change will be the sum of the changes induced by the natural climate variability and of the anthropogenic induced changes (e.g. due to CO_2 emissions), a deep knowledge about natural interglacial climate variability is essential in order to precisely evaluate future climate change.

Studies of natural climate variability during interglacials should focus on several issues. For example it is important to know, if there are any climatic trends (cooling/warming) associated with interglacials, especially of the present Holocene, that can be extrapolated into the future. Furthermore the occurrence of cyclic and short-term events, such as Bond-cycles and the 8.2 ka BP event during the Holocene (Bond et al., 1997; Ellison, 2006; Giraudeau et al., 2010; Kleiven et al., 2008), and their regional and global impact as well as their importance for interglacial climates should be evaluated. At last the sensitivity of interglacial climates to different boundary conditions (e.g. insolation, ice-sheet configuration, sea-level) should be tested, in order to improve future climate predictions.

All these issues can be addressed by looking into the present and past interglacials, which are well expressed in marine and terrestrial climate records (e.g. Hodell et al., 2000; Desprat et al., 2007; Urban, 2007; Wang et al., 2008). Especially past interglacials can teach us a valuable lesson about natural interglacial climate variability and interglacial climate sensitivity, as they ran their full course and demise and mostly occur under different boundary conditions (Cheddadi et al., 1998; Müller and Sánchez Goñi, 2007). For example Marine Isotope Stage (MIS) 11 is widely used as an analogue to the present Holocene, due to similar boundary conditions (i.e. insolation) (e.g. Hodell et al., 2000; Kandiano et al., 2012). Another example is MIS 5.5, which is widely used as an analogue to the expected future climate change, as it was 1.5 - 2°C warmer than the preindustrial Holocene average

(Clark and Huybers, 2009), which is within the range of the predicted future climate warming (Jansen et al., 2007).

Beside these more theoretical issues, there are some more technical problems that arise by studying past interglacials. First, the further one goes back in time, the less climate records are available (cf. Lisiecki and Raymo, 2005). This results in a sparse global coverage of climate records spanning a long time period and therefore only patchy pictures of global changes during past (interglacial) periods exist. However, a global picture of changes during past periods is needed, in order to precisely evaluate if the observed regional changes are of global importance. Furthermore, past interglacial periods are out of reach of radiocarbon dating and are not anywhere near a paleomagnetic reversal (Kiefer and Kull, 2007). Therefore the age models of past interglacials, especially in marine sediment cores, are often poorly constrained. At last, high-resolution records of past interglacial climates are needed, in order to detect short-term cyclic changes or events. In order to circumvent this problem, one needs sophisticated analytical procedures to reduce for example the sample amount, or one needs sites with high accumulation rates, which allow a high-resolution sampling.

To address these issues, the objectives of this study are the following: 1) Detecting a general structure in the evolution of interglacials in terms of paleoproductivity and paleoceanography in the Azores region. 2) Exploring the sensitivity of interglacial paleoproductivity and paleoceanography in the Azores region to different boundary conditions. 3) Detecting comparable short-term variability during different interglacials.

Therefore we investigated and compared the present (Holocene) and the last (MIS 5.5) interglacial in sediment cores retrieved from the open ocean mid-latitude North Atlantic slightly south of the Azores Islands. As climatic records from this region are sparse, mainly due to the prevailing low sedimentation rates in this area, the presented study refines the spatial resolution of existing interglacial climate records. Furthermore, the comparison is mainly based on coccolithophore assemblages, which have been shown to be good indicators for paleoproductivity and paleoceanographic conditions (e.g. Beaufort, 1997; Flores et al., 2000; Kinkel and al, 2000; Baumann and Freitag, 2004; Saavedra-Pellitero et al., 2011). Because of the small size of coccoliths (5 μm on average (e.g. Honjo, 1976)), which form the exoskeleton of coccolithophores, only a small sample size is needed for analysis, and therefore a high temporal resolution record can be obtained even if accumulation rates are low.

5.3 Regional hydrographic and productivity setting

Sediment cores GEOFAR KF16, MD08-3179Cq and MD08-3180Cq were taken slightly south of the Azores Islands, in the vicinity of the Azores Current (AzC) (Table 2.1, Figure 5.1). The AzC is an eastward branch of the North Atlantic Current, which is the most prominent surface water current in the North Atlantic, transporting tropical and subtropical heat and salinity to the higher northern latitudes (e.g. McCartney and Talley, 1984; Tomczak and Godfrey, 1994). The AzC splits off the North Atlantic Current at around 40°N 50°W and travels eastward at a mean latitude of 35°N (Klein and Siedler, 1989). Near the European margin, the AzC partly joints the Canary Current, which travels southward. Another part of the AzC flows into the Gulf of Cadiz and into the Mediterranean, replacing Mediterranean waters lost through the overflow in the Street of Gibraltar. Therefore a hypothetical connection between the AzC and the Mediterranean Overflow Waters (MOW) has been proposed, according to the β-plume theory, at which the comparatively small MOW of 1 Sv forces the formation of the AzC (Jia, 2000; Özgökmen et al., 2001; Kida et al., 2008). Due to its connections to the NAC and CC, the AzC is part of the anticyclonic circulation that characterizes the North Atlantic subtropical gyre, forming its northern boundary (e.g. Bashmachnikov et al., 2004).

Associated with the AzC is the Azores Front (AzF), which separates northern transitional water masses from southern subtropical water masses (Figure 5.1a). We will refer to the northern surface water masses as North Atlantic Transitional Waters (NATW) according to e.g. Schiebel et al. (2002b), and to the southern surface water masses as subtropical waters. As the front can be shielded by the formation of a seasonal thermocline, the location of the front is best defined where the 15°C isotherm is between 200 and 300 m waterdepth (Gould, 1985). Although upwelling within this front is indicated by modeling studies (Alves and de Verdière, 1999), the impact of the front on primary productivity is still discussed controversially in the recent literature. For example, Fernández and Pingree (1996) found an enhanced productivity (i.e. a deep chlorophyll maximum) associated with the front, whereas Fasham et al. (1985) and Schiebel et al. (2002b) found no evidences for an enhanced productivity within the front. However, the region to the north of the front is characterized by a deep winter mixed layer, which results in a surface entrainment of deep-sourced nutrients, whereas the southern subtropical region is characterized by a

strong water column stratification that permits the turbulent advection of deep-sourced nutrients (Lévy et al., 2005; Mouriño-Carballido and Neuer, 2008). Therefore a strong gradient in primary productivity is present in the study area (Figure 5.1b).

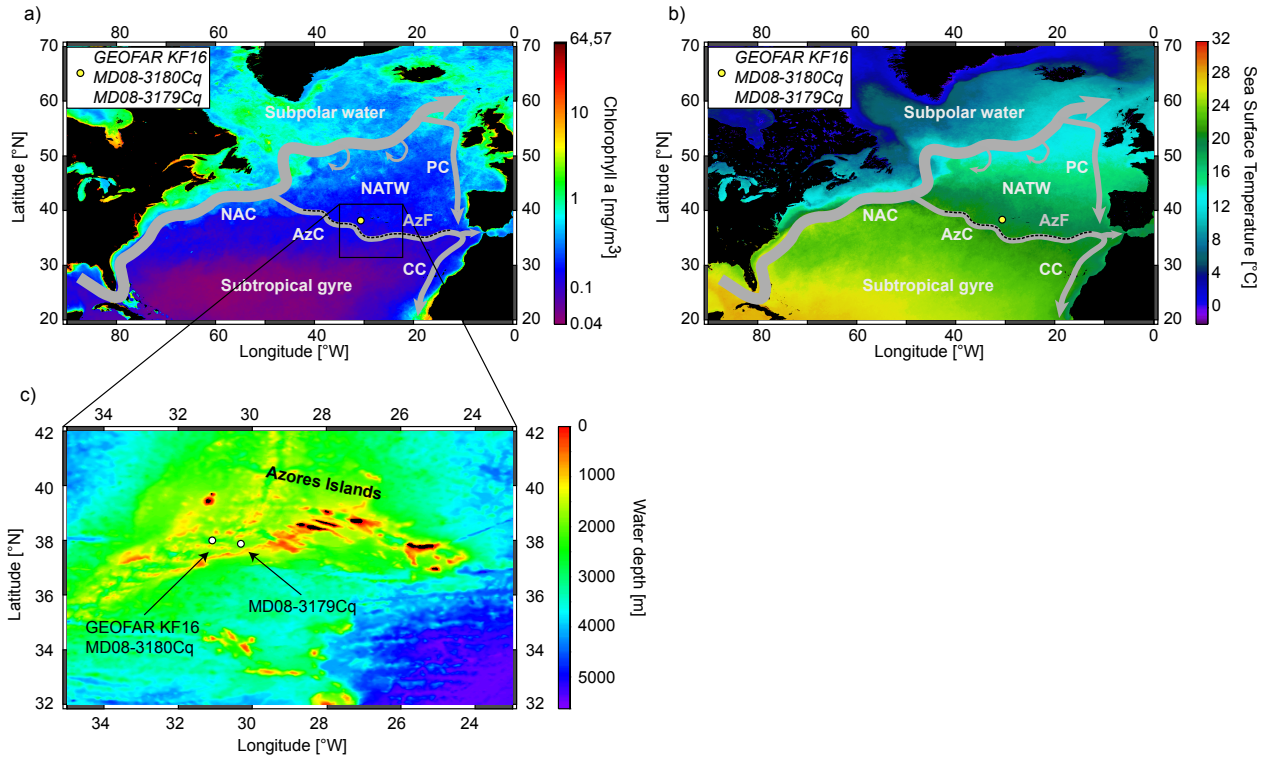

Figure 5.1: a) Map with annual mean (2006) chlorophyll a concentrations in the North Atlantic (satellite data from http://seadas.gsfc.nasa.gov). Schematic surface circulation in the North Atlantic is indicated by grey arrows. Abbreviations: North Atlantic Current (NAC), Azores Current (AC), Azores Front (AzF) indicated by black stippled line, Canary Current (CC), Portugal Current (PC), North Atlantic Transitional Water (NATW). Position of studied sediment cores is indicated by yellow dot. b) Map with annual mean (2006) sea surface temperature (satellite data from http://seadas.gsfc.nasa.gov). Schematic surface circulation in the North Atlantic is indicated by grey arrows. Abbreviations as in Figure 5.1a. Position of studied sediment cores is indicated by yellow dot. c) Bathymetric map of the area indicated by black rectangle in Figure 5.1a.

Because the AzF is a strong meandering current, it generates eddies that split off the AzC and travel southwest- and northwestward (e.g. Alves et al., 2002). Thereby anticyclonic eddies are generated to the north of the front, whereas cyclonic eddies split off to the south. Due to eddy-pumping, the cyclonic eddies result in an entrainment of nutrients in the southern subtropical regions (Mouriño-Carballido and Neuer, 2008). The anticyclonic eddies, which transport subtropical waters to the north and occasionally reach the coring sites (e.g. Alves et al., 2002), are normally associated with downwelling and low productivity. Altogether, the Azores region is characterized by strong gradients in productivity and oceanographic conditions, which is also reflected in the biogeographical distribution of or-

ganisms. For example the AzF separates the northern transitional from the southern subtropical biogeographical province of coccolithophore (McIntyre and Bé, 1967; Schiebel et al., 2011).

5.4 Material and methods

5.4.1 Sample material

Sediment core GEOFAR KF16 was retrieved during research cruise GEOFAR onboard the research vessel Le Noroit (Richter, 1998), whereas the other two cores (MD08-3179Cq, MD08-3180Cq) were taken during cruise MD-168 onboard the research vessel Marion Dufresne (Kissel et al., 2008). GEOFAR KF16 and MD08-3180Cq are nearly from the same coring site, and have been taken in a small basin at the Mid Atlantic Ridge at a water depth of approximately 3050 m (Table 2.1, Figure 5.1c). This basin acts as a sediment trap for diffusive sediment transport (Richter, 1998), resulting in high sedimentation rates and enabling high-resolution analysis (Schwab et al., 2012). On the other hand MD08-3179Cq has been taken slightly east of the two other cores and has been taken from a plateau at the Mid Atlantic Ridge at a water depth of 2040 m (Table 2.1, Figure 5.1c). All cores exhibit an undisturbed and purely pelagic character, as they consist of foraminifera bearing nannofossil ooze and show slight laminations. However, the first 80.5 cm of core MD08-3179Cq have been neglected, due to a double penetration of the coring device.

5.4.2 Age control

The age models of GEOFAR KF16 and MD08-3180Cq are based on 15 AMS ^{14}C ages and tuning the oxygen isotope and alkenone records to the NGRIP ice core record. A detailed description of the age models and of the splicing of the two cores (in order to get a continuous coccolithophore record over the last 16 kyrs) is given in Schwab et al. (2012). Likewise, the age model of MD08-3179Cq, which is based on tuning the oxygen isotope record to the oxygen isotope stack of Lisiecki and Raymo (2005), has already been de-

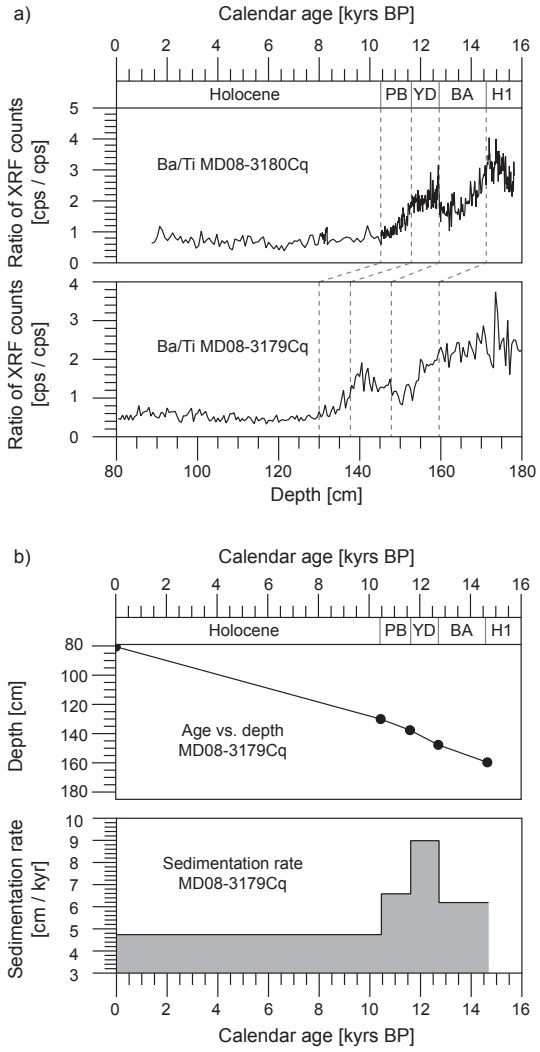

Figure 5.2: a) Ba/Ti measured by XRF in sediment core MD08-3180Cq (upper panel) and Ba/Ti measured by XRF in MD08-3179Cq. MD08-3180Cq serves as a stratigraphic reference for MD08-3179Cq. Tuning of MD08-3179Cq on MD08-3180Cq is indicated by grey stippled vertical lines. Abbreviations: Heinrich event 1 (H1), Bølling/Allerød (BA), Younger Dryas (YD), Preboreal (PB). b) Resulting age vs. depth plot (upper panel) and resulting sedimentation rates (lower panel) in MD08-3179Cq. Abbreviations as in Figure 5.2a.

scribed (Schwab et al., submitted). Additionally, an age model for Termination I and the Holocene section in core MD08-3179Cq has been constructed for this study. Therefore the Ba/Ti record measured by XRF in MD08-3179Cq has been correlated to the Ba/Ti record of MD08-3180Cq, which is well dated as described above and shows the clear deglacial sequence of Heinrich event 1, Bølling/Allerød, Younger Dryas and Preboreal (Figure 5.2, Table 5.1). The resulting sedimentation rates show maximum values of 9 cm/kyr during the Younger Dryas and a subordinate maximum during the Preboreal, whereas the Bølling/Allerød and Holocene are characterized by low sedimentation rates. This pattern of changes in sedimentation rates can also be observed in MD08-3180Cq (Schwab et al.,

2012), which therefore corroborates the applied deglacial and Holocene age model of MD08-3179Cq.

Table 5.1: Age points of MD08-3179Cq derived by tuning to MD08-3180Cq

Depth [cm]	Age [kyrs BP]	Comment
85.5	0	First 80.5 cm due to double penetration of coring device
130	10.46	End Preboreal
137.7	11.61	End Younger Dryas
147.7	12.73	Beginning Younger Dryas
159.7	14.67	Beginning Bølling/Allerød

5.4.3 Coccolithophore and diatom analysis

Coccolithophore assemblages during Termination I and the Holocene in sediment cores GEOFAR KF16 and MD08-3180Cq, as well as coccolithophore assemblages during MIS 5 to MIS 3 in sediment core MD08-3179Cq have already been investigated (Schwab et al., 2012; submitted). For this study we additionally investigated coccolithophore assemblages during Termination I and the Holocene in sediment core MD08-3179Cq. Therefore the core section 85 - 185 cm has been sampled in 5 cm intervals corresponding to an average temporal resolution of 1000 years during the Holocene and 700 years during the deglacial. For coccolithophore analysis we applied the same analytical methods as in Schwab et al. (2012), following the method described by Andruleit (1996). Therefore 0.06 - 0.07g freeze-dried bulk sediment was weight and brought into suspension in tab water. The suspension was then wet-split by a factor of 100 and filtered onto polycarbonate filters with a pore size of 0.4 μm. After drying, a small piece of filter was mounted on a Scanning Electron Microscopy (SEM) stub and sputtered with Au/Pd. The samples were then analyzed by SEM with a magnification of 5000, whereby 340 - 430 coccoliths (average: 372 coccoliths) were counted along measured transects and identified according to the taxonomy given in Young et al. (2003). A taxonomic list of the identified species is given in the Appendix. In order to improve the record of the rare species *C. pelagicus*, extended counts

(counting only *C. pelagicus* across the whole filter at a magnification of 1000) were carried out. The previously published coccolith concentrations in the three sediment cores (Schwab et al., 2012; submitted) were converted into weight% coccolith carbonate according to equation (2.4), using species-specific coccolith weights given in Table 2.2.

5.5 Results and discussion

5.5.1 Can Holocene and MIS 5.5 coccolithophore assemblages be compared?

Looking at the abundances of the individual coccolithophore species reveals significant differences between the present and last interglacial coccolithophore assemblages (Figure 5.3). During the Holocene the assemblages are dominated by *E. huxleyi* (Figure 5.3a), whereas the assemblages during MIS 5.5 are dominated by small gephyrocapsids (*G. ericsonii* and *G. ornata*) (Figure 5.3b). This difference is related to the evolutionary

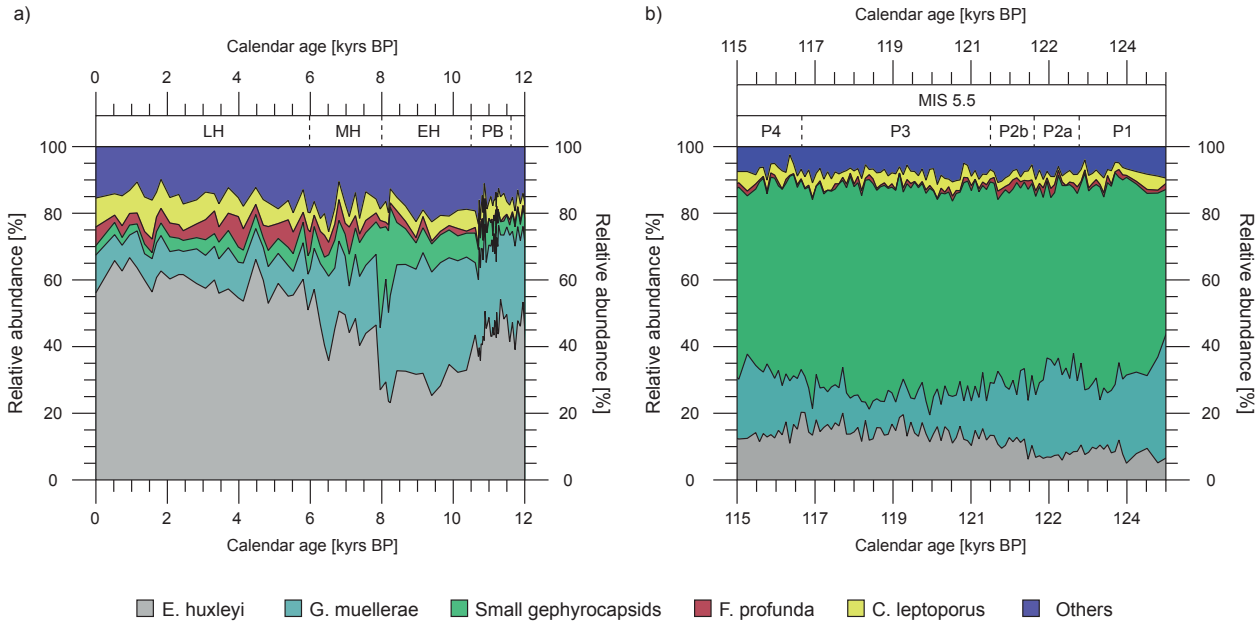

Figure 5.3: a) Contribution of individual coccolithophore species to the present interglacial assemblage. Contibution of other, minor abundant coccolithophore species (Others) to the total assemblage is given in the Appendix. Abbreviations: Preboreal (PB), early Holocene (EH), Mid Holocene (MH), late Holocene (LH). b) Contribution of individual coccolithophore species to the last interglacial assemblage. Contibution of other, minor abundant coccolithophore species (Others) to the total assemblage is given in the Appendix. P1 to P4 corresponds to the subdivision of MIS 5.5 as explained in the text.

development of coccolithophores, which results in distinct acme zones of certain coccolithophore species during particular Late Quaternary time periods (e.g. Thierstein et al., 1977; Bollmann et al., 1998; Hine and Weaver, 1998). For example the observed dominance of *E. huxleyi* during the Holocene is a well-known feature of global coccolithophore records, reflecting its evolutionary trend (e.g. Thierstein et al., 1977). This species first occurred around 294 ka BP (MIS 8) (Wei and Peleo-Alampay, 1993), an event, which is seen to be time-transgressive in the eastern North Atlantic, with progressively younger ages from north to south (Hine and Weaver, 1998). During the first two-thirds of its abundance range (including MIS 5.5), *E. huxleyi* played only a minor role in coccolithophore assemblages (Thierstein et al., 1977), as it can also be observed in our records (Figure 3b). Around 76 ka BP *E. huxleyi* started to become the dominant coccolithophore species in global coccolithophore assemblages, an event, which again is seen to be time transgressive in the North Atlantic, with progressively younger ages from south to north (Thierstein et al., 1977). This increase in *E. huxleyi* abundance is also seen at our coring site, taking place around 72 ka BP (Schwab et al., submitted), resulting in the observed dominance of this species during the Holocene (Figure 5.3a).

Contrary to the Holocene, coccolithophore assemblages during MIS 5.5 are dominated by small gephyrocapsids at the coring site (Figure 5.3b). The dominance of small to medium sized gephyrocapsids during MIS 5 is a well-known feature of Late Quaternary coccolithophore records (Flores et al., 1997; Kinkel and al, 2000; Lototskaya et al., 1998; López-Otálvaro et al., 2008), which can again be related to the evolutionary succession of Late Quaternary coccolithophore dominance intervals (e.g. Hine and Weaver, 1998). Therefore, coccolithophore assemblages during the Holocene and MIS 5.5 cannot directly be compared, and the observed marked difference between these two interglacial coccolithophore assemblages is primarily not related to any changes in the environmental conditions at the coring site.

However, the evolutionary turnovers in Late Quaternary coccolithophore assemblages are most pronounced in coccolithophore species of the family Noelaerhabdaceae, which includes the genera *Gephyrocapsa*, *Pseudoemiliania*, *Emiliania* and *Reticulofenestra* (e.g. Hine and Weaver, 1998), whereas other coccolithophore species seem to be relatively unaffected by evolutionary trends during this time period. Therefore these species can probably be used for a quantitative comparison of the Holocene and MIS 5.5. In particular only the abundance records of *E. huxleyi* and small gephyrocapsids seem to be

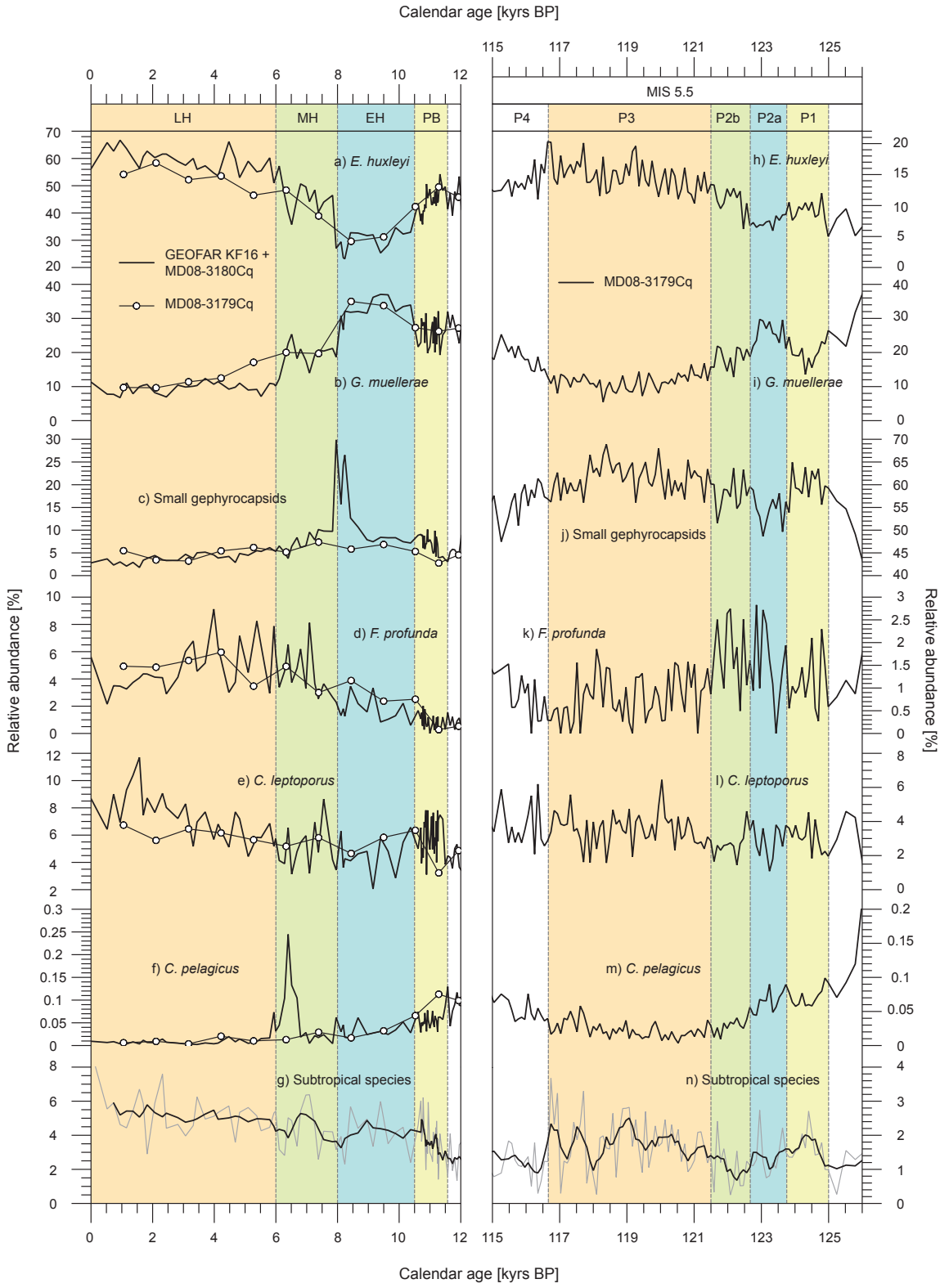

Figure 5.4: Left panel: Abundances of a) *E. huxleyi*, b) *G. muellerae*, c) small gephyrocapsids, d) *F. profunda*, e) *C. leptoporus*, f) *C. pelagicus* and g) subtropical coccolithophore species during the present interglacial. Abbreviations as in Figure 5.3a. Right panel: Abundances of h) *E. huxleyi*, i) *G. muellerae*, j) small gephyrocapsids, k) *F. profunda*, l) *C. leptoporus*, m) *C. pelagicus* and n) subtropical coccolithophore species during the last interglacial. Colored vertical bars indicate comparable periods between the present and last interglacial. P1 to P4 corresponds to the subdivision of MIS 5.5 as explained in the text.

affected by an evolutionary turnover during the considered time intervals. Thereby the dominance of small gephyrocapsids during MIS 5.5 is replaced by a dominance of *E. huxleyi* during the Holocene. As *E. huxleyi* and small gephyrocapsids show nearly the same ecological preferences (warm, stratified, oligotrophic) during MIS 5 at the coring site (Schwab et al., submitted), the dominance reversal between these two species probably took place in one distinct ecological niche, leaving all other coccolithophore species unaffected. In summary, Holocene and MIS 5.5 coccolithophore assemblages can be quantitatively compared at the coring site, except of the abundances of *E. huxleyi* and small gephyrocapsids, which are affected by an evolutionary turnover during the considered time interval.

Another drawback to the comparison of Holocene and MIS 5.5 coccolithophore assemblages may be the slightly different geographical position of the cores (Figure 5.1c). Although sediment cores GEOFAR KF16 and MD08-3179Cq are close to each other, floral and faunal assemblages can be assumed to be very diverse on a small spatial scale in the region of the Azores Current System with its associated oceanic front (cf. Ottens, 1991; 1992; Schiebel et al., 2011). Therefore we counted the Holocene section of MD08-3179Cq with a low resolution and compared the results to the Holocene section of GEOFAR KF16 (Figure 5.4). Aside of the good correlation of the Holocene records from the two different cores, two small offsets are observed at around 8 and 6.5 ka BP in the small gephyrocapsids and *C. pelagicus* record respectively (Figures 5.4c, f). The offset between the Holocene small gephyrocapsids records around 8 ka BP is most probably an artifact of the low-resolution sampling of MD08-3179Cq. As MD08-3179Cq has been sampled with a resolution of 5 cm during the Holocene, corresponding to a time-resolution of approximately 1000 yrs, the sample resolution is to low to detect the short-term event around 8 ka BP with a duration of approximately 600 yrs. Similarly, the offset in the *C. pelagicus* records around 6.5 ka BP may be the result of the under-sampling of MD08-3179Cq together with an offset due to the coarse Holocene age model of MD08-3179Cq (Figure 5.2). Another explanation may be that dissolution, which caused the drastic increase of the heavily calcified *C. pelagicus* in GEOFAR KF16 (Schwab et al., 2012), took place only in the deep basin where GEOFAR KF16 has been retrieved (Table 2.1, Figure 5.1). However, beside the two small discrepancies due to low-resolution sampling and dissolution, a very good correlation of the two different Holocene records exist in terms of absolute values and observed trends (Figure 5.4). Therefore we conclude that coccolithophore assemblages are not af-

fected by the different geographical position of the cores, and the two interglacial periods from the different cores can be compared.

5.5.2 A general structure of interglacials in the Azores region

Although a quantitative comparison of coccolithophore assemblages can be hindered by evolutionary processes as described above, the individual trends in the coccolithophore records still contain valuable information about ecological changes. In the following we will investigate and compare ecological changes during the Holocene and MIS 5.5 based on abundance changes of certain coccolithophore species.

A generally consistent pattern of interglacial changes is observed during the Holocene and MIS 5.5 based on abundance changes of individual coccolithophore species (Figure 5.4). This can be deduced for example from similar interglacial abundance changes of *E. huxleyi* (Figure 5.4a, h). *E. huxleyi* is a cosmopolitan species occurring in nearly every oceanic realm and tolerating temperatures between 1 and 30°C (McIntyre and Bé, 1970; Okada and Honjo, 1973; Okada and McIntyre, 1979). Because of its broad ecological tolerance, it is difficult to deduce any ecological changes based on its abundance variations. However, high abundances of *E. huxleyi* are observed during warm and stratified periods during the last 130 ka BP at the coring site (Schwab et al., 2012; submitted). Therefore the observed peak abundances of this species during the early interglacials (PB during the Holocene and P1 during MIS 5.5) indicate a first amelioration of climate following the glacial terminations. This is followed by a reversal towards glacial conditions during the early/mid interglacials (EH during the Holocene and P2a during MIS 5.5) as evidenced by minimum abundances of *E. huxleyi* (Figure 5.4a, h). After a transitional phase (MH during the Holocene and P2b during MIS 5.5) maximum abundances of *E. huxleyi* are observed during the late interglacials (LH during Holocene and P3 during MIS 5.5), indicating that peak interglacial conditions (warm, stratified) are reached only late during both interglacials.

A similar picture of climatic changes in the Azores region can be drawn from abundance variations of *G. muellerae* (Figure 5.4b, i). This species prefers cold-water conditions (Samtleben, 1980; Samtleben and Bickert, 1990; Samtleben et al., 1995) and therefore is used as an indicator for cold-water temperatures (e.g. Di Stefano and Incarbona, 2004; Weaver and Pujol, 1988). Minimum abundances of *G. muellerae* are observed dur-

ing the early interglacials, followed by a maximum during the early to mid interglacials and minimum abundances during the late interglacials (Figure 5.4b, i). In accordance to the abundance records of *E. huxleyi* this indicates a first climatic optimum during the early interglacials, followed by a reversal towards glacial conditions. Based on minimum abundances of *G. muellerae*, warmest sea surface temperatures are observed during the late interglacials. Furthermore, in the midlatitude North Atlantic, this species only occurs north of the AzF within NATW (cf. Figure 5.1a) (Jordan, 1988; Giraudeau et al., 2010; Schiebel et al., 2011) and can be used as an indicator for the influence of NATW at the coring site, which is related to latitudinal displacements of the AzF (Schwab et al., 2012). Based on the abundance records of *G. muellerae*, a southward retreat of the AzF is recognized during the early to mid interglacials, which is followed by the northernmost position of the AzF during the late interglacials. The observed changes in the latitudinal position of the AzF are in line with the well-known AzF dynamics, at which warm interglacial periods are characterized by a more northern position of the AzF, whereas cold glacial periods are characterized by a southward retreat (Schiebel et al., 2002a; Schwab et al., 2012).

Although the consistent subdivision of the interglacials into three to four distinct periods can be observed in the abundance records of small gephyrocapsids (Figure 5.4c, j), especially during MIS 5.5, we observe opposite trends in the abundance records of these species during the Holocene and MIS 5.5. For example, the late and very early periods of the present interglacial are characterized by minimum abundances of these species, whereas maximum abundances of small gephyrocapsids are observed during the same periods of the last interglacial. This difference indicates different ecological preferences of small gephyrocapsids during the present and last interglacial. During MIS 5 maximum abundances of small gephyrocapsids are observed during substages 5.5, 5.3 and 5.1, indicating an affinity to warm and stratified conditions (Schwab et al., submitted). On the other hand, during the last deglaciation and Holocene increased abundances of small gephyrocapsids in the Azores region are observed during periods of cold, nutrient-rich and fresh sea surface water conditions (Schwab et al., 2012). Especially the fresh and nutrient-rich conditions during the 8.2 kyr event resulted in maximum abundances of these species at the coring site (Figure 5.4c) (Schwab et al., 2012). The shift in the ecological preferences is most probably related to the dominance reversal at the MIS 5/4, at which *E. huxleyi* replaced small gephyrocapsids (Schwab et al., submitted), forcing these species to occupy a new ecological niche. These findings shed new light on the temperature equation

based on the abundance of different *Gephyrocapsa* morphotypes proposed by Bollmann et al. (2002). As small gephyrocapsids altered their ecological preferences, which are assumed to be constant over time when applying the equation, temperature estimates might be biased at least during MIS 5.

Difficulties in dividing the interglacials, especially the present one, into three to four periods arise, when looking at the abundances of *F. profunda* (Figure 5.4d, k). This species dwells in the lower photic zone (150 - 200 m water depth) and is abundant in tropical to subtropical regions (e.g. Andruleit and Rogalla, 2002; Okada and McIntyre, 1979). *F. profunda* is only abundant south of the AzF (Schiebel et al., 2011), and therefore our coring site is situated at the northern distribution limit of this species, resulting in its observed low abundances. The low abundances of this species, which hardly exceed 3% of the total assemblage during most of the investigated periods, hampers a robust interpretation and most probably results in the observed difficulties. However, increased abundances of *F. profunda* are observed during the late period of the present interglacial (Figure 5.4d), whereas minimum abundances are observed during the late period of the last interglacial (Figure 5.4k). This species is widely used to monitor changes in nutricline depth (Molfino and McIntyre, 1990a; 1990b) and associated surface water productivity changes (Ahagon and al, 1993; Beaufort, 1997; Flores et al., 2000; Kinkel and al, 2000; Li et al., 2010), at which minimum abundances indicate a shallow nutricline and associated enhanced surface productivity and vice versa. Therefore the lower abundances of *F. profunda* during the late period of MIS 5.5 indicate an increased productivity compared to the late Holocene. This discrepancy in the productivity conditions during the two interglacials will be discussed more thoroughly in the next section. However, in accordance to the previously described subdivision of the interglacials, an abundance peak of *F. profunda* is observed during the early to mid MIS 5.5 (Figure 5.4k). In contrast to the widely used interpretation of this species, the observed increased abundances during the early to mid MIS 5.5 occur during a period of enhanced productivity (Schwab et al., submitted). This discrepancy indicates that the nutrients that fueled surface water productivity had a deep source and therefore reached the lower photic zone, whereas the surface dwelling coccolithophores are outcompeted by more opportunistic plankton species (e.g. diatoms) during this time (Schwab et al., submitted).

A consistent subdivision of both interglacials can again be observed in the abundances of *C. leptoporus* (Figure 5.4e, l). Although *C. leptoporus* is a cosmopolitan species,

occurring at nearly all latitudes (McIntyre and Bé, 1967), this species has been shown to be abundant during periods of warm and oligotrophic surface water conditions at the coring site (Schwab et al., 2012; submitted). Therefore, in accordance to the previously inferred ecological conditions at the coring site, the observed minimum abundances of *C. leptoporus* during the early to mid interglacials (early and mid Holocene, and P2a and P2b during MIS 5.5) indicate a reversal towards more glacial conditions, which are characterized by cold temperatures and an increased surface water productivity. Maximum abundances of *C. leptoporus* during the late interglacials again indicate that full interglacial conditions are reached only late in the Azores region.

A consistent pattern of interglacial changes can be observed in the abundance records of *C. pelagicus* (Figure 5.4f, m). This species is known to tolerate very low temperatures (< 0°C) and to live preferentially in the polar to subpolar regions, where it can dominate the coccolithophore assemblages (e.g. Okada and McIntyre, 1979; Baumann and Matthiessen, 1992; Samtleben et al., 1995). Although there are different morphotypes of this species, all with distinct ecological preferences (e.g. Parente et al., 2004), the low abundances at the coring site permit a statistically robust differentiation. However, as the overall abundance pattern of *C. pelagicus* shows clear abundance maxima in the polar to subpolar regions (Baumann et al., 2005), we use this species as a proxy for the influence of subpolar waters at the coring site (cf. Schwab et al., 2012). Based on the gradually decreasing abundances of *C. pelagicus* during the early and mid interglacials (Figure 5.4f, m), a gradually decreasing influence of subpolar waters at the coring site can be deduced. The decreasing influence of subpolar waters might reflect the decreasing influence of cold core rings, which pinch off the North Atlantic Current and potentially can transport subpolar waters to the coring site (e.g. Kupferman et al., 1986; Beckmann et al., 1987). The decreasing influence of the cold core rings may in turn reflect the gradual northward retreat of the North Atlantic Current and its associated subpolar front (cf. Schwab et al., 2012). Minimum abundances of *C. pelagicus* are consistently found during the late interglacials, indicating a minimum influence of subpolar waters during this period (Figure 5.4f, m).

A consistent pattern of interglacial changes can also be deduced based on abundance variations of grouped subtropical species (*Umbellosphaera* spp., *Umbilicosphaera* spp., *Oolithotus* spp.) (Figure 5.4g, n). These K-strategic species are adapted to warm and especially oligotrophic conditions, and therefore preferentially live in the subtropical realm of the oceans (e.g. Incarbona et al., 2010, and references therein). These species can be

used to trace the influence of subtropical water, which occasionally reaches the coring site due to the advection within anticyclonic eddies (cf. chapter 5.3). Thereby minimum abundances of subtropical species indicate a diminished influence of subtropical waters at the coring site due to a diminished influence of anticyclonic eddies, which is most probably caused by a more southern position of the AzF (cf. Schwab et al., 2012). Consistent with the abundance variations of *G. muellerae* and the inferred changes in the latitudinal position of the AzF, slight peak abundances of subtropical species during the early interglacials indicate a more northern position of the AzF (Figure 5.4g, n). A southward retreat of the AzF is recognized during the mid interglacials, based on minimum abundances of subtropical species. After these reversals, full interglacial conditions, characterized by the northernmost position of the AzF, are consistently reached during the late interglacials based on maximum abundances of subtropical species (Figure 5.4g, n).

In summary, based on abundance variations of individual coccolithophore species, a consistent pattern of ecological changes in the Azores region is observed during the present and the last interglacial. Thereby a first amelioration of climatic conditions and a northward displacement of the AzF are observed during the early interglacials, following the glacial terminations. After this first interglacial peak, a reversal towards more glacial conditions is observed during the early to mid interglacials, which is characterized by a southward retreat of the AzF. Finally, full interglacial conditions, characterized by the northernmost position of the AzF, are observed during the late interglacials. That full interglacial conditions established late during the present and last interglacial in the Azores region is in line with other results from more northern North Atlantic sites (Bauch et al., 2011; Baumann and Matthiessen, 1992; Oppo et al., 2006; Sánchez Goñi et al., 2012; Solignac et al., 2008; 2004; Vautravers et al., 2007), indicating that this is probably a basin-wide phenomena. Overlain on these changes, a varying contribution of subpolar waters, probably due to latitudinal displacements of the North Atlantic Current and its associated subpolar front, is observed. Thereby the influence of subpolar waters gradually decrease following the glacial terminations culminating in a nearly absence of these waters during the late interglacials.

Although the succession of a first interglacial peak followed by a reversal towards glacial conditions and followed by full interglacial conditions during the late interglacials can be observed during the present as well as during the last interglacial, the timing and duration of the individual periods seem to be different during the two interglacials (Figure

5.4). This might be due to the less well-constrained age model of the last interglacial, where only the flanks of MIS 5.5 have been tuned (cf. chapter 5.4.2). However, the timing and duration of the reversal towards more glacial conditions during MIS 5.5 (P2a) is comparable to previously published results from the North Atlantic (Bauch et al., 2011; Irvalı et al., 2012; Stolz and Baumann, 2010). This period probably has been triggered by an increased input of freshwater to the North Atlantic due to melting ice sheets, as evidenced by an accelerated sea level increase (Rohling et al., 2007) and a freshwater anomaly in the North Atlantic (Irvalı et al., 2012). Similarly a still increased input of freshwater due to melting ice sheets can be observed during the early to mid present interglacial (e.g. Fairbanks, 1989). In a final step the melting ice sheets caused a collapse of ice-dammed proglacial lakes, which than delivered an immense amount of freshwater to the North Atlantic, causing an abrupt and wide-spread cooling like during the 8.2 kyr event (e.g. Ellison et al., 2006; Kleiven et al., 2008). The same scenario can be observed during MIS 5.5, where a short-lived salinity decrease and increase in ice rafted detritus is observed at the end of the interglacial cooling period (Bauch et al., 2011; Irvalı et al., 2012). That such short-term interglacial cooling events, caused by an immense and rapid input of freshwater to the North Atlantic due to the collapse of ice-dammed proglacial lakes, are probably characteristic for interglacials has recently been proposed by Bauch et al. (2011). Although the 8.2 kyr event is well-expressed at the coring site (Schwab et al., 2012), an additional further cooling is missing at the end of the last interglacial cooling period (Figure 5.4). This probably indicates that the final outburst of proglacial lakes into the northern North Atlantic during MIS 5.5 was not as severe as during the Holocene, and therefore is not well-expressed at our subtropical coring site.

Altogether, we propose the following scenario of causes and consequences that may have led to the observed similar pattern of changes during the present and last interglacial in the North Atlantic, and that probably can also be applied to older interglacials: An early maximum in Northern Hemisphere summer insolation during both interglacials (cf. Laskar et al., 2004) resulted in an early interglacial peak, characterized by warm conditions and a more northern position of the AzF in the midlatitude North Atlantic (e.g. Figure 5.4b, i). Due to the delayed response of ice sheets to solar forcing, melting of ice sheets continued after the maximum in insolation (e.g. Fairbanks, 1989; Rohling et al., 2007), delivering freshwater to the North Atlantic and causing a reversal towards more glacial conditions. This melting culminated in a collapse of ice-dammed proglacial lakes, which then abruptly delivered

an immense amount of freshwater to the North Atlantic and therefore caused for example a widespread cooling (Barber et al., 1999; Kleiven et al., 2008; Bauch et al., 2011). After the freshwater forcing ceased, full interglacial conditions in the North Atlantic established during the late interglacials. This scenario is in line with a previously proposed scenario for observed changes during the present and last interglacial period in the more northern latitudes of the North Atlantic (Baumann and Matthiessen, 1992; Solignac et al., 2004; 2008; Sánchez Goñi et al., 2012). Therefore our results extend these findings to the open ocean subtropical realm of the North Atlantic, an area where existing high-resolution records are rare.

5.5.3 A quantitative comparison of peak interglacial conditions during the present and last interglacial in the Azores region

As already mentioned, it is important to know about the interglacial climate sensitivity to different boundary conditions, in order to improve future climate predictions (cf. chapter 5.2). During the last interglacial several boundary conditions were different compared to the present one. For example, insolation forcing in the high northern latitudes was increased during this time (Laskar et al., 2004). Furthermore global temperatures were 1.5 - 2°C warmer (e.g. Clark and Huybers, 2009), the Greenland ice shield was smaller (e.g. Carlson and Winsor, 2012) and global sea-level was about 6 m higher than today (e.g. Kopp et al., 2009). In the following we will quantitatively compare the present and last interglacial, in order to test if the different boundary conditions during these periods have an impact on the ecological conditions in the Azores region.

Assuming that evolutionary processes of coccolithophores do not affect coccolith concentrations in the sediment, we carried out a quantitative comparison of the last and present interglacial. However, this proxy can be affected by carbonate dissolution, which would also hamper a quantitative comparison. As the coring sites are situated above the present and even above the glacial lysocline in the eastern North Atlantic (e.g. Crowley, 1983), dissolution most probably can be neglected during the investigated periods at the coring site. Furthermore, the excellent preservation of coccoliths in the sediment at the coring sites is indicated by high CEX‘ values and the presence of well-preserved fragile coccoliths of e.g. *G. ornata* and holococcoliths (Schwab et al., 2012; submitted). Therefore we conclude that dissolution does not exert a major control on the observed coccolith con-

centrations in the sediment. Looking at the coccolith concentration records during the peak interglacials reveal a nearly doubling of coccolith concentrations during peak MIS 5.5 compared to the late Holocene (Figure 5.5a). This doubling might have two explanations: 1) As most coccolithophores are K-selected, they increase their abundance within plankton communities under oligotrophic conditions, resulting in maximum coccolith concentrations in the subtropical gyre realm (e.g. Baumann et al., 2004). Therefore the increased concentrations during peak MIS 5.5 may reflect more oligotrophic conditions compared to the Holocene. This is probably a consequence of a more northern position of the AzF, corresponding to an expansion of the North Atlantic subtropical gyre (cf. chapter 5.3), which would result in an increased advection of oligotrophic subtropical waters to the coring site. A more northern position of the AzF and therefore an expanded North Atlantic subtropical gyre during MIS 5.5 has been reported by Schwab et al. (submitted). 2) The increased coccolith concentrations may be the result of increased coccolithophore productivity during MIS 5.5. Increased coccolithophore productivity during MIS 5.5 in the eastern North Atlantic has been reported by Lototskaya et al. (1998), Stolz and Baumann (2010) and Schwab et al. (submitted). Thereby the increased coccolithophore productivity has been related to optimal grow conditions (warm and stratified) and to the opportunity to occupy new habitats after the preceding glacial period (e.g. Stolz and Baumann, 2010). However, as the Holocene at the coring site is also characterized by more warm and stratified conditions after the preceding glacial period (Schwab et al., 2012), this factor alone can probably not explain the observed difference between the present and last interglacial coccolith concentrations. Therefore, additional nutrients probably further increased coccolithophore productivity during MIS 5.5. An increased production and advection of nutrient-rich Subantarctic Mode Water (SAMW) into the North Atlantic during MIS 5.5, which resulted in an increased productivity in the North Atlantic, has been proposed by Romero et al. (2011). Therefore, the upwelling of these waters within the AzF and their advection to the coring site during MIS 5.5, probably further enhanced coccolithophore productivity (Schwab et al., submitted).

If coccolithophore productivity was increased during peak MIS 5.5 compared to the late Holocene, can be deduced from coccolith fluxes, which are more directly related to coccolithophore productivity. As coccolith fluxes during peak MIS 5.5 were twice as high as during the late Holocene (Figure 5.5b), the observed increased coccolith concentrations

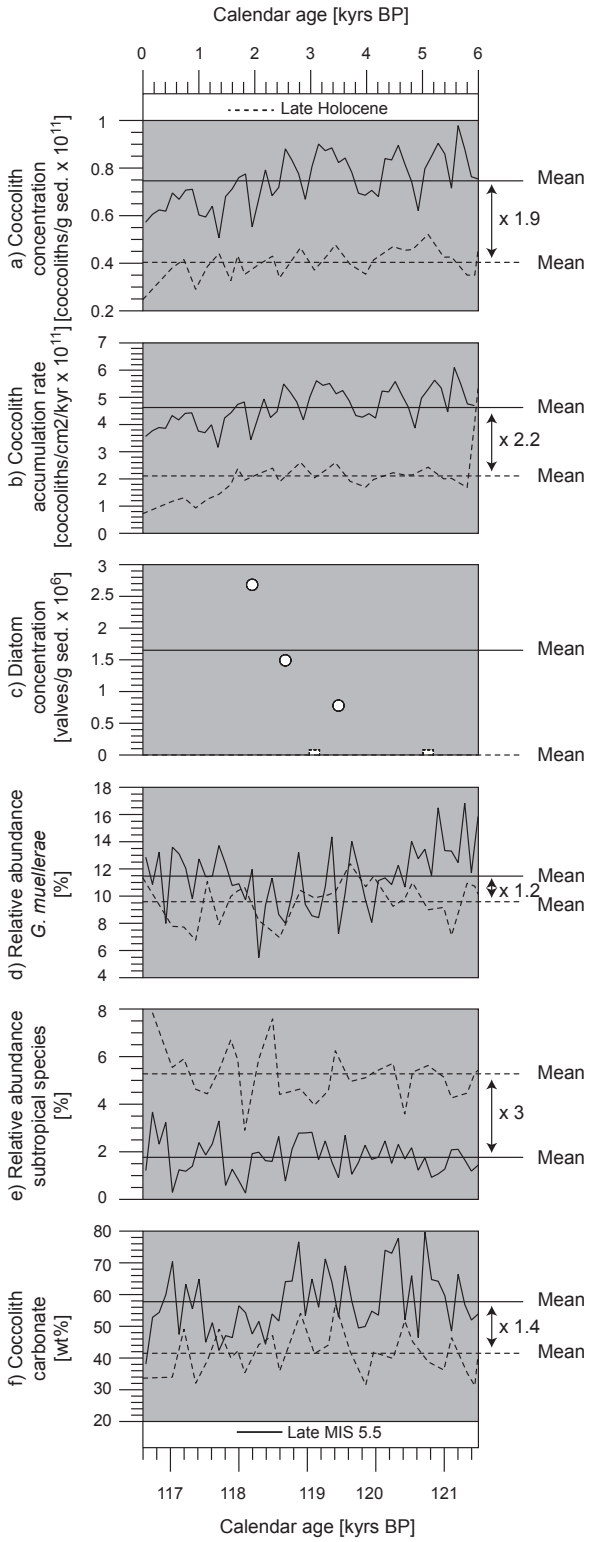

Figure 5.5: a) Coccolith concentrations during the late Holocene (black solid line) and during late MIS 5.5 (P3) (black stippled line). b) Coccolith accumulation rates during the late Holocene (black solid line) and during late MIS 5.5 (P3) (black stippled line). c) Diatom concentrations during the late Holocene (dots) and during late MIS 5.5 (P3) (squares). d) Relative abundance of *G. muellerae* during the late Holocene (black solid line) and during late MIS 5.5 (P3) (black stippled line). e) Relative abundance of grouped subtropical coccolithophore species during the late Holocene (black solid line) and during late MIS 5.5 (P3) (black stippled line). f) Coccolith carbonate content in the sediment during the late Holocene (black solid line) and during late MIS 5.5 (P3) (black stippled line). Horizontal lines indicate mean values during the late Holocene (black solid lines) and during the late MIS 5.5 (black stippled line). Difference between the two mean values is given as a factor.

are at least partly caused by an increased coccolithophore productivity. Furthermore, not only coccolithophore productivity was increased during peak MIS 5.5 but also diatom productivity (Figure 5.5c). Diatoms are known to be opportunistic species, occurring under nutrient-rich conditions (e.g. Abrantes et al., 2002). Therefore the observed increased diatom concentrations indicate an increased surface nutrient inventory (probably due to an increased production and advection of SAMW) and most probably an enhanced overall productivity during peak MIS 5.5 compared to the late Holocene.

Assuming a positive correlation between temperature and the position of the AzF, at which increased temperatures are associated with a more northern position of the AzF (Schwab et al., 2012), the increased global temperatures during MIS 5.5 (e.g. Clark and Huybers, 2009) imply a more northern position of the AzF during the last interglacial compared to the present one. In order to deduce differences in the latitudinal position of the AzF during both interglacials we are investigating the abundances of key coccolithophore species (*G. muellerae* and grouped subtropical species), which can be used to trace latitudinal displacements of the AzF (cf. chapter 5.5.2). As already mentioned, care must be taken in comparing the abundance records of coccolithophore species, as evolutionary processes resulted in different coccolithophore assemblages during the present and last interglacial (chapter 5.5.1). However, as the differences in coccolithophore assemblages is most pronounced in the abundances of *E. huxleyi* and small gephyrocapsids, due to a dominance reversal within the same ecological niche, other coccolithophore species are probably unaffected and may well be compared (see chapter 5.5.1). Assuming that other coccolithophore species are unaffected by evolutionary processes, a same or slightly more southern position of the AzF during peak MIS 5.5 compared to the late Holocene can be deduced, based on the abundance records of *G. muellerae* and subtropical species (Figure 5.5d, e). This is in contrast to what can be expected due to higher global temperatures during MIS 5.5. However, the increased abundances of *G. muellerae* and the decreased abundances of subtropical species may result from the increased surface nutrient inventory during MIS 5.5. An affinity of *G. muellerae* to nutrient-rich conditions has been proposed by Sprengel et al. (2002). Therefore the nearly similar abundances of this species during late MIS 5.5 and late Holocene, due to the increased nutrient availability during the last interglacial, probably indicate a more northern position of the AzF during MIS 5.5 in accordance to what would be expected. Similarly, the low abundances of subtropical species during peak MIS 5.5 may be the result of the increased surface nutrient availability. As the-

se species are adapted to oligotrophic conditions (e.g. Incarbona et al., 2010, and references therein), the additional nutrients during MIS 5.5 (due to an increased production and advection of SAMW) are less favorable for these species. Therefore subtropical species may have been outcompeted by the more r-selected coccolithophore species of the family Noelaerhabdaceae (e.g. *E. huxleyi* and gephyrocapsids) during MIS 5.5, resulting in the observed low abundances.

In summary, we propose that the AzF most probably resided at a more northern position during the last interglacial compared to its present position. Furthermore an increased productivity, as evidenced by increased coccolithophore and diatom productivities, is observed during the last interglacial in the Azores region. This increased productivity is most probably related to an increased production and advection of nutrient-rich SAMW into the North Atlantic during MIS 5.5 (Romero et al., 2011).

Furthermore, the increased coccolithophore productivity resulted in an increased coccolith carbonate content of the sediment during peak MIS 5.5 compared to the late Holocene (Figure 5.5f). Increased coccolithophore productivity during MIS 5.5 has also been reported from more northern latitudes of the eastern North Atlantic (Lototskaya et al., 1998; Stolz and Baumann, 2010). Therefore these results probably indicate an enhanced carbonate production in the entire eastern North Atlantic during MIS 5.5. As calcification of coccolithophores releases CO_2 (e.g. Buitenhuis et al., 1999; Van der Wal et al., 1995), the proposed enhanced coccolithophore carbonate production in the eastern North Atlantic potentially acted as an atmospheric CO_2 source during MIS 5.5. A similar impact on atmospheric CO_2 levels can be expected from the more northern position of the AzF and the associated expansion of the subtropical gyre during MIS 5.5. This is because an expansion of the oligotrophic waters of the North Atlantic subtropical gyre would decrease overall marine primary productivity (Polovina et al., 2008), which is a sink for atmospheric CO_2 (e.g. Falkowski, 2000). However, similar or only slightly increased atmospheric CO_2 levels are observed during MIS 5.5 compared to the Holocene (e.g. Petit et al., 1999; Rundgren et al., 2005). This indicates that the observed changes in the eastern North Atlantic probably were insignificant for global atmospheric CO_2 levels or that the observed increased primary productivity during MIS 5.5 (due to an increased production and advection of SAMW) counteracted the combined effects of the increased carbonate production and expanded oligotrophic subtropical gyre. Therefore modeling experiments are urgently need-

ed, in order to evaluate the impact of ecological changes in the eastern North Atlantic on global climate.

5.6 Conclusions

Holocene and MIS 5.5 coccolithophore assemblages are markedly different, due to the evolutionary adaption of certain coccolithophore species during the Late Quaternary. This hampers a quantitative comparison of individual coccolithophore species abundances. However, the evolutionary processes probably only affected abundances of *E. huxleyi* and small gephyrocapsids during the investigated time periods at the coring site, as evidenced by a dominance reversal within the same ecological niche. Nevertheless, abundance variations within individual coccolithophore species still contain valuable information about past ecological changes. Comparing the individual abundance changes of key coccolithophore species at the coring site indicates a general pattern of ecological changes in the Azores region that can be observed during both interglacials. A first interglacial peak, characterized by warm, stratified conditions and a more northern position of the AzF, is observed during the early interglacials, as evidenced by abundance changes of *E. huxleyi*, *G. muellerae* and subtropical coccolithophore species. This first amelioration of climate is followed by a reversal towards more glacial conditions, which in turn is followed by peak interglacial conditions during the late interglacials. The observed similar pattern of interglacial changes may be the consequence of an early interglacial peak in Northern Hemisphere summer insolation, resulting in the observed early interglacial peak conditions. The delayed response of ice-sheets and the associated input of freshwater to the North Atlantic then caused a reversal towards the more glacial conditions during the early to mid interglacials. After the freshwater forcing ceased, full interglacial conditions are established during the late interglacials. The melting of the ice sheets during the early to mid interglacials culminated in a collapse of ice-dammed proglacial lakes, leading to an abrupt and immense input of freshwater to the North Atlantic and resulting in a wide-spread cooling. Although this event is well-expressed at the coring site during the Holocene (8.2 kyr event), an additional further cooling is missing in our records at the end of the last interglacial cooling period, indicating that this event probably was weaker than during the Holocene.

In order to test the sensitivity of ecological changes in the Azores region to the different boundary conditions during the last and present interglacial, we quantitatively compared different proxies between the present and last interglacial period. This comparison indicates that the AzF most probably resided at a more northern position and that primary productivity was increased during MIS 5.5 compared to the Holocene. The increased primary productivity probably resulted from an increased production and advection of SAMW into the North Atlantic during MIS 5.5. The increased coccolithophore productivity during MIS 5.5 resulted in an increased coccolith carbonate production, which probably can be traced into the more northern latitudes of the eastern North Atlantic. The increased carbonate production in the eastern North Atlantic as well as the expansion of the subtropical gyre could potentially act as a source for atmospheric CO_2. However, as atmospheric CO_2 levels are more or less similar during MIS 5.5 and the Holocene, the observed changes in the eastern North Atlantic were probably insignificant on a global scale. Another explanation would be that the observed increased primary productivity during MIS 5.5 counteracted the combined effect of the increased carbonate production and the expanding oligotrophic subtropical gyre. Therefore further (modeling) studies are need, in order to evaluate the impact of ecological changes in the eastern North Atlantic on global climate.

Chapter VI.

Conclusions

6.1 General conclusions

The presented study provides high-resolution reconstructions of past changes in productivity and hydrography from the transitional zone between the temperate and subtropical regions of the open ocean North Atlantic (Azores Island region). Changes in productivity and hydrography have been deduced based on quantitative coccolithophore assemblage analysis, alkenone analysis, XRF measurements and diatom counts. Considerable changes in the paleoecological conditions in the Azores region are found during the Holocene, last deglacial and between 130 and 48 ka BP. In general, the observed changes are synchronous with the well-known environmental changes in the more northern latitudes of the North Atlantic Ocean, indicating that the investigated low latitude sites are strongly influenced by high latitude processes. Furthermore as the described changes can convincingly be deduced from changes in coccolithophore assemblages, the presented study further strengthens the potential of coccolithophores in paleoceanographic studies.

6.2 Holocene and last deglacial

Based on changes in coccolithophore assemblages, the AzF resided at a more southern latitude during the deglacial and early Holocene, especially during H1 and the Younger Dryas. This corroborates and refines the results of Schiebel et al. (2002a), who postulated that the AzF occupied a more southern position during glacial periods. As the AzF delineates the northern boundary of the North Atlantic subtropical gyre, the more southern position of the AzF also corresponds to a less northward extension of the gyre. Furthermore, the last deglacial and early Holocene, and particularly H1 and the Younger Dryas, are characterized by an increased productivity at the coring site. This can be deduced based on increased coccolith accumulation rates, increased diatom abundances, high Ba/Ti ratios and increased alkenone concentrations/accumulation rates. Especially the increased productivity during H1 and the Younger Dryas might be related to the advection of northern-sourced, fresh and nutrient-rich surface waters to the coring site. Similar increased productivities during H1 and the Younger Dryas have also been reported from more eastern and more western sites of the midlatitude North Atlantic (Lebreiro et al.,

1997; Rogerson et al., 2004; Gil et al., 2009; Penaud et al., 2011) and from the western Mediterranean Sea (Jimenez-Espejo et al., 2007). As Heinrich event 1 and the Younger Dryas are associated with a reduced AMOC (e.g. McManus et al., 2004; Carlson et al., 2007; Barker et al., 2009), the observed increased productivity is in contrast to model predictions in this region (Schmittner, 2005; Menviel et al., 2008; Mariotti et al., 2012). However, this might be related to the low spatial resolution of models and/or to processes (e.g. advection of nutrient-rich surface waters) not considered by the models (Mariotti et al., 2012). In general, during times of reduced AMOC, a band of strongly increased productivity can be found at the northern rim of the contracted North Atlantic subtropical gyre, which potentially could have counteracted the decreased organic carbon pump in the high northern latitudes of the North Atlantic (Nave et al., 2007).

Regarding the Holocene, a major reorganization of the productivity and hydrographic conditions in the Azores region is found during the mid-Holocene. The early Holocene is characterized by an increased productivity and a more southern position of the AzF, whereas lowest productivity and the northernmost position of the AzF are found during the late Holocene. This mid-Holocene reorganization of the productivity and hydrographic conditions in the Azores region is in line with a global reorganization of environmental conditions (Steig, 1999).

6.3 Changes between 130 and 48 ka BP

The coccolithophore assemblage records indicate a more southern position of the AzF during cold periods (Termination II, MIS 5.4, MIS 5.2 and MIS 4), whereas warm periods (MIS 5.5, MIS 5.3, MIS 5.1 and MIS 3) are characterized by a more northern position of the AzF. Again, the cold periods, which are also characterized by a weak AMOC (e.g. Evans et al., 2007), are accompanied by an increased productivity at the coring site, as indicated by increased coccolith accumulation rates and increased diatom abundances. However, the last interglacial period (MIS 5.5) is an exception to the general productivity pattern. During this warm period, a strongly increased coccolithophore productivity is found, which is in line with results from more northern latitudes of the eastern North Atlantic (Lototskaya et al., 1998; Stolz and Baumann, 2010). This coccolithophore productivity

peak can be related to the opportunity for coccolithophores to occupy new habitats after glacial conditions (Stolz and Baumann, 2010) and/or to the advection of nutrient-rich Subantarctic Mode Water (SAMW) and it's upwelling within the AzF (Romero et al., 2011).

In general, the results indicate that the AzF resides at a more northern position during warm periods, whereas it occupies a more southern position during cold periods. This in turn indicates that the North Atlantic subtropical gyre expands during warm periods and contracts during cold periods. Taking this relation, a global warming as it can be expected for the near future (Jansen et al., 2007), probably will lead to an expansion of the North Atlantic subtropical gyre. An expansion of the North Atlantic subtropical gyre and an associated decrease in primary productivity in the North Atlantic has already been observed during the last decade (Polovina et al., 2008). However, as global climate during MIS 5.5 was approximately 1.5 - 2°C warmer than the pre-anthropogenic global average of the past 10 kyrs, MIS 5.5 could serve as a future scenario for human induced climate change (e.g. Clark and Huybers, 2009; Kopp et al., 2009). Therefore the presented results indicate that an expected decrease in the organic carbon pump due to an expansion of the subtropical gyre could probably be mitigated by an increased coccolithophore productivity, which probably increases due to the occupation of new habitats and/or by an increased advection of SAMW.

6.4 Short-term variability

The well-known 8.2 kyr event, which was triggered by a freshwater-outburst of glacial lake Agassiz (e.g. Barber et al., 1999; Ellison et al., 2006), is recorded at the investigated midlatitude site. During this event productivity increased and the AzF resided at a more southern position. The increased productivity was probably triggered by nutrients brought by icebergs. These results corroborate modeling results, which indicate that a substantial fraction of the delivered freshwater enters the subtropical realm (Condron and Winsor, 2011). A similar short-term event, probably corresponding to the Inter-Allerød Cold Period is recognized at the Allerød/Younger Dryas boundary.

During early MIS 5.5 a short reversal towards more glacial conditions (increased productivity, more southern position of AzF) is found. The timing of this event corresponds

to the well-established Inter-Eemian Cooling Period, which is primarily recognized in records from more northern latitudes of the Atlantic Ocean (e.g. Cortijo et al., 1994; Stolz and Baumann, 2010; Bauch et al. 2011). At the end of the Inter-Eemian Cooling event a pronounced freshwater peak and a peak in ice-rafted detritus is recorded in the high northern latitudes, indicating analogies to the 8.2 kyr event (Bauch et al., 2011; Irvalı et al., 2012; Nicholl et al., 2012). Such short reversal towards glacial conditions due to a final drainage of glacial lakes may be a recurrent feature of Late Quaternary interglacials.

6.5 A general structure of interglacial climate

The comparison of the Holocene and last interglacial period reveals a general structure of changes in the Azores region. Both interglacials are characterized by a first early amelioration of climatic conditions, characterized by a decrease in productivity and northward shift of the AzF in the Azores region. This is followed by a reversal towards more glacial conditions (increase in productivity and southward shift of the AzF). The full interglacial conditions, characterized by minimum productivity and northernmost position of the AzF, are reached during the late interglacials. The sequence of changes may be caused by a similar chain of causes proposed for observed Holocene changes in the northern North Atlantic (Baumann and Matthiessen, 1992). A first insolation maximum during the early interglacials led to an amelioration of climate. Then, the delayed response of northern ice-shields to the insolation forcing caused an increased input of freshwater, resulting in a reversal towards more glacial conditions. The accelerated melting of the northern ice-shields culminated in a final collapse of the ice-shield and a drainage of proglacial lakes (e.g. lake Agassiz). Although this final drainage event is recognized during the Holocene, an additional, final cooling event is missing during the Inter-Eemian cooling period in the Azores region. This probably indicates that this event was not as severe as during the Holocene and therefore is not recognized in the midlatitudes, and/or the routing of the discharged meltwater was different during this time. Finally, as the freshwater forcing ceased, full interglacial conditions could establish during the late interglacials in the Azores region.

Chapter VII.

Outlook and perspectives

7.1 Morphometry and morphotype analysis

A fourth manuscript dealing with the ecological preferences of *C. leptoporus* and its morphotypes will be prepared. Although clear ecological preferences of this species have been established on a local scale (Kinkel et al., 2000; Andruleit and Rogalla, 2002), its patchy distribution pattern in the North Atlantic indicates no relation to specific environmental parameters (Ziveri et al., 2004). However, in the working area, the abundance pattern of this species shows the clear succession of deglacial events (Figure 7.1), indicating a close relationship to changes in the environmental conditions. As reconstructions of several

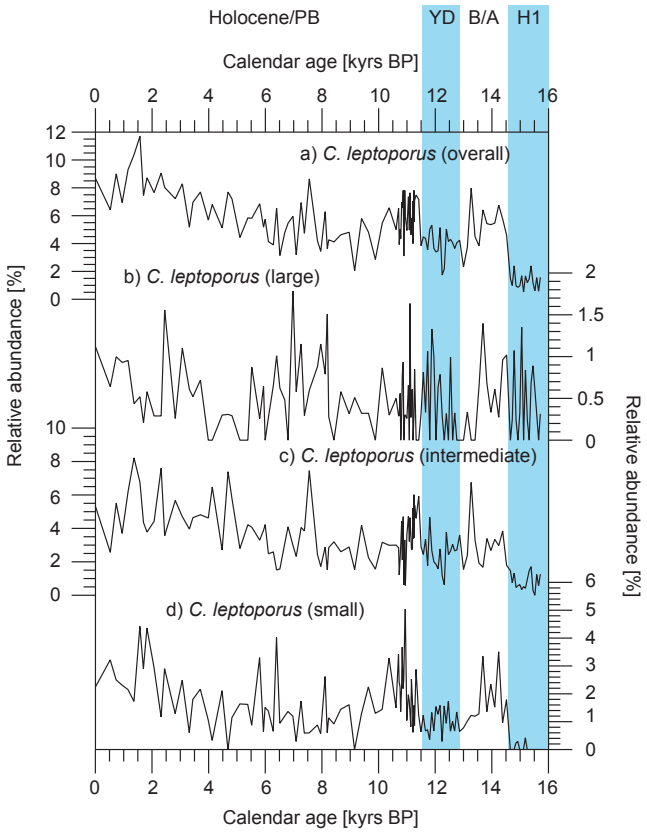

Figure 7.1. a) Abundance of all *C. leptoporus* morphotypes together. Abundances of the b) small, c) intermediate and d) small morphotype of *C. leptoporus*. Blue vertical bars mark the Heinrich event 1 and the Younger Dryas. Overall abundances and abundances of the different morphotypes show a clear response to the deglacial environmental changes at the coring site (cf. chapter 3).

environmental parameters (temperature, salinity, nutrients) are available or will be available soon, a canonical correspondence analysis (CCA) (see e.g. Boeckel et al., 2004) will help to disentangle the main factors that drive *C. leptoporus* abundances in the working area. Furthermore, the ecological preferences of the different morphotypes of *C. lepto-*

porus are still unclear (Renaud and Klaas, 2001; Renaud et al., 2002). Therefore the different morphotypes (large, intermediate, small) were counted separately. Again, a PCA conducted with the abundances of the different morphotypes will help to understand their different ecological demands.

Traditionally, *E. huxleyi* is analyzed to gain insights into the effect of rising atmospheric CO_2 on the calcification of coccolithophores (e.g. Riebesell et al., 2000; Beaufort et al., 2011; Lohbeck et al., 2012). However, as *C. leptoporus* is a cosmopolitan species, occurring in nearly every oceanic realm, and as it produces more carbonate than *E. huxleyi* (Young and Ziveri, 2000), it probably also plays an important role in the oceanic carbon cycle. Therefore, the above described analysis will be supplemented by morphometric analysis currently conducted with SYRACO and light microscopy (Claußen, in prep.). This will additionally give insights into effect of the deglacial increase in atmospheric CO_2 on the calcification of *C. leptoporus*.

Morphotype and morphometric analysis have also been conducted on *E. huxleyi*. The preliminary results indicate that *E. huxleyi* decreases in size during the course of the last deglacial. This contradicts the findings of Beaufort et al. (2011). However, the sample resolution is very low (only 12 samples during the last deglacial and Holocene period), and therefore a higher resolution is needed, which probably can be accomplished in the near future.

7.2 High-resolution analysis of the 8.2 kyr event

The high sedimentation rates during the 8.2 kyr event (see chapter 3.4.1) allow high-resolution sampling. High-resolution coccolithophore analyses have been conducted during this period (Figure 7.2). These results indicate, that the 8.2 kyr event was probably a two-step event, corroborating results from more northern latitudes of the North Atlantic Ocean (Kleiven et al., 2008; Bamberg et al., 2010). However, as only coccolithophore and XRF analysis were conducted with a high temporal resolution, other high-resolution measurements (e.g. AMS ^{14}C, planktonic and benthic oxygen and carbon isotopes, alkenones) are needed in order to fully deduce the environmental changes (productivity, temperature, salinity) in the Azores region during this period.

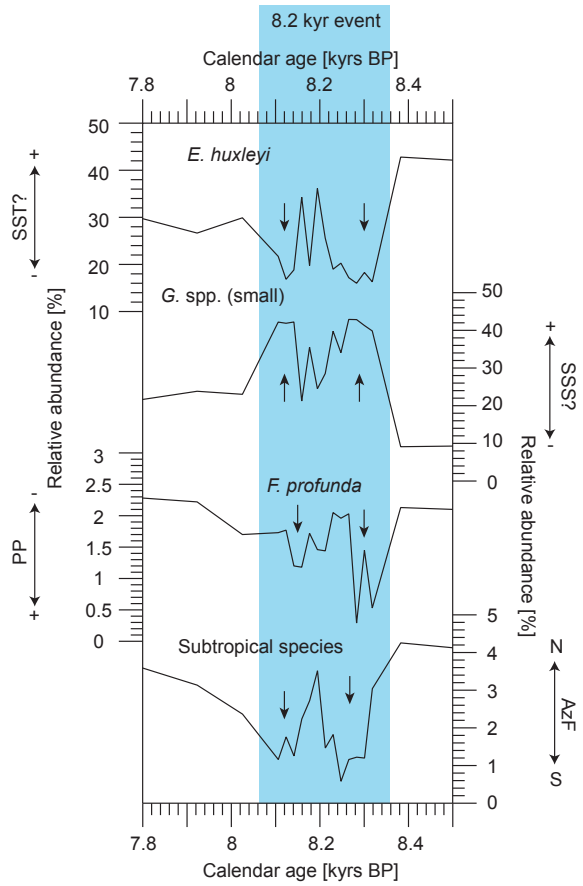

Figure 7.2. High-resolution coccolithophore analysis during 8.2 kyr event (blue vertical bar). Direction of inferred ecological changes indicated by arrows.

7.3 Other sediment cores

Another sediment core (MD08-3181Cq) from the same location as GEOFAR KF16 and MD08-3180 probably contains an expanded MIS 3 section. However, the age model of this core is yet not well constrained and therefore has not been analyzed in high resolution. Nevertheless, this core probably provides the opportunity to sample MIS 3 with a high temporal resolution, which would allow comparing the results with the famous „Shackleton Sites“ at the Iberian Margin.

At last, the analyses of coccolithophores and other primary productivity related proxies on sediment cores from more southern latitudes of the open ocean North Atlantic would yield more detailed insights into changes of the subtropical gyre geometry and productivity. This in turn could lead to a more quantitative estimation of productivity changes in the mid- to low-latitude North Atlantic, which would help to draw more quantitative conclusions in terms of ocean carbon cycle changes.

References

Abrantes, F., 2000. 200 000 yr diatom records from Atlantic upwelling sites reveal maximum productivity during LGM and a shift in phytoplankton community structure at 185 000 yr. Earth and Planetary Science Letters 176, 7–16.

Abrantes, F., Meggers, H., Nave, S., Bollman, J., Palma, S., Sprengel, C., Henderiks, J., Spies, A., Salgueiro, E., Moita, T., 2002. Fluxes of micro-organisms along a productivity gradient in the Canary Islands region (29 N): implications for paleoreconstructions. Deep Sea Research Part II: Topical Studies in Oceanography 49, 3599–3629.

Adkins, J., Boyle, E., Keigwin, L., Cortijo, E., 1997. Variability of the North Atlantic thermohaline circulation during the last interglacial period. Nature 390, 154–156.

Ahagon, N., Tanaka, Y., Ujjie, H., 1993. Florisphaera profunda, a possible nannoplankton indicator of late Quaternary changes in sea-water turbidity at the northwestern margin of the Pacific. Marine Micropalaeontology 22, 255- 273.

Aizawa, C., Oba, T., Okada, H., 2004. Late Quaternary paleoceanography deduced from coccolith assemblages in a piston core recovered off the central Japan coast. Marine Micropaleontology 52, 277–297.

Alley, R.B., Clark, P.U., 1999. The deglaciation of the northern hemisphere: a global perspective. Annual Review of Earth and Planetary Sciences 27, 149–182.

Alves, M.L.G.R., de Verdière, A.C., 1999. Instability dynamics of a subtropical jet and applications to the Azores Front Current System: eddy-driven mean flow. Journal of Physical Oceanography 29, 837–864.

Alves, M., Gaillard, F., Sparrow, M., Knoll, M., Giraud, S., 2002. Circulation patterns and transport of the Azores Front-Current system. Deep-Sea Research Part II 49, 3983–4002.

Andersen, C., Koç, N., Moros, M., 2004. A highly unstable Holocene climate in the subpolar North Atlantic: evidence from diatoms. Quaternary Science Reviews 23, 2155–2166.

Andersen, K.K., NGRIP members, 2004. High-resolution record of Northern Hemisphere climate extending into the last interglacial period. Nature 431, 147–151.

Andersen, K. K, NGRIP members, 2007. Greenland Ice Core Chronology 2005 (GICC05) and 20 year means of oxygen isotope data from ice core NGRIP. doi:10.1594/PANGAEA.586838.

Anderson, P., Bermike, O., Bigelow, N., Brigham-Grette, J., Duvall, M., Edwards, M., Frechette, B., Funder, S., Johnsen, S., Knies, J., 2006. Last Interglacial Arctic warmth confirms polar amplification of climate change. Quaternary Science Reviews 25, 13–14.

Andruleit, H., 1996. A filtration technique for quantitative studies of coccoliths. Micropaleontology 42, 403–406.

Andruleit, H., Rogalla, U., 2002. Coccolithophores in surface sediments of the Arabian Sea in relation to environmental gradients in surface waters. Marine Geology 186, 505–526.

Archer, D., Winguth, A., Chicago, I., Lea, D., Mahowald, N., 2000. What caused the glacial/interglacial atmospheric pCO_2 cycles? Reviews of Geophysics 38, 159–189.

Bamberg, A., Rosenthal, Y., Paul, A., Heslop, D., Mulitza, S., Rühlemann, C., Schulz, M., 2010. Reduced North Atlantic Central Water formation in response to early Holocene ice-sheet melting. Geophysical Research Letters 37, L17705.

Barber, D., Dyke, A., Hillaire-Marcel, C., Jennings, A., Andrews, J., Kerwin, M., Bilodeau, G., McNeely, R., Southon, J., Morehead, M., Gagnon, J., 1999. Forcing of the cold event of 8,200 years ago by catastrophic drainage of Laurentide lakes. Nature 400, 344–348.

Bard, E., Arnold, M., Duprat, J., Moyes, J., Duplessy, J., 1987. Reconstruction of the last deglaciation: deconvolved records of $\delta^{18}O$ profiles, micropaleontological variations and accelerator mass spectrometric ^{14}C dating. Climate Dynamics 1, 101–112.

Bard, E., Rostek, F., Turon, J., Gendreau, S., 2000. Hydrological impact of Heinrich events in the subtropical northeast Atlantic. Science 289, 1321.

Bard, E., Rickaby, R.E.M., 2009. Migration of the subtropical front as a modulator of glacial climate. Nature 460, 380–383.

Barker, S., Diz, P., Vautravers, M.J., Pike, J., Knorr, G., Hall, I.R., Broecker, W.S., 2009. Interhemispheric Atlantic seesaw response during the last deglaciation. Nature 457, 1097–1102.

Bashmachnikov, I., Laffon, V., Martins, A., 2004. Sea surface temperature distribution in the Azores region. Part II: space time variability and underlying mechanisms. Arquipélago—Life and Earth Sciences 21A, 19-32.

Bauch, H., Erlenkeuser, H., Fahl, K., Spielhagen, R., Weinelt, M., Andruleit, H., Henrich, R., 1999. Evidence for a steeper Eemian than Holocene sea surface temperature gradient between Arctic and sub-Arctic regions. Palaeogeography Palaeoclimatology Palaeoecology 145, 95–117.

Bauch, H.A., Kandiano, E.S., Helmke, J., Andersen, N., Rosell-Melé, A., Erlenkeuser, H., 2011. Climatic bisection of the last interglacial warm period in the Polar North Atlantic. Quaternary Science Reviews 30, 1813–1818.

Bauch, H.A., Kandiano, E.S., Helmke, J.P., 2012. Contrasting ocean changes between the subpolar and polar North Atlantic during the past 135 ka. Geophysical Research Letters 39.

Baumann, K., Matthiessen, J., 1992. Variations in surface water mass conditions in the Norwegian Sea: evidence from Holocene coccolith and dinoflagellate cyst assemblages. Marine Micropaleontology 20, 129–146.

Baumann, K.-H., Čepek, M., Kinkel, H., 1999. Coccolithophores as Indicators of Ocean Water Masses, Surface Water Temperature, and Paleoproductivity - Examples from the South Atlantic. In: Fischer, G., Wefer, G. (Eds.), Use of proxies in paleoceanography, Springer, Berlin, pp. 117-144.

Baumann, K., Freitag, T., 2004. Pleistocene fluctuations in the northern Benguela Current system as revealed by coccolith assemblages. Marine Micropaleontology 52, 195–215.

Baumann, K.-H., Boeckel, B., Frenz, M., 2004. Coccolith contribution to South Atlantic carbonate sedimentation. In: Thierstein, H.R., Young, J.R. (Eds.), From Molecular Processes to global Impact. Springer, Berlin, Germany, pp. 367-403.

Baumann, K.H., al, E., 2005. The significance of extant coccolithophores as indicators of ocean water ... Paläontologische Zeitschrift 1–20.

Baumann, K.H., Boeckel, B., Čepek, M., 2008. Spatial distribution of living coccolithophores along an east-west transect in the subtropical South Atlantic. Journal of Nannoplankton Research 30, 9-21.

Beal, L., De Ruijter, W., Biastoch, A., 2011. On the role of the Agulhas system in ocean circulation and climate. Nature 472, 429-436.

Beaufort, L., 1997. Insolation Cycles as a Major Control of Equatorial Indian Ocean Primary Production. Science 278, 1451–1454.

Beaufort, L., Heussner, S., 1999. Coccolithophorids on the continental slope of the Bay of Biscay–production, transport and contribution to mass fluxes. Deep-Sea Research Part II 46, 2147–2174.

Beaufort, L., Probert, I., Buchet, N., 2007. Effects of acidification and primary production on coccolith weight: Implications for carbonate transfer from the surface to the deep ocean. Geochemistry Geophysics Geosystems 8.

Beaufort, L., Probert, I., de Garidel-Thoron, T., Bendif, E.M., Ruiz-Pino, D., Metzl, N., Goyet, C., Buchet, N., Coupel, P., Grelaud, M., Rost, B., Rickaby, R.E.M., de Vargas, C., 2011. Sensitivity of coccolithophores to carbonate chemistry and ocean acidification. Nature 476, 80–83.

Beckmann, W., Auras, A., Hemleben, C., 1987. Cyclonic Cold-Core Eddy in the Eastern North-Atlantic. 3. Zooplankton. Marine Ecology Progress Series 39, 165–173.

Behrenfeld, M., Falkowski, P., 1997. Photosynthetic rates derived from satellite-based chlorophyll concentration. Limnology and oceanography 42, 1–20.

Behrenfeld, M.J., O'Malley, R.T., Siegel, D.A., McClain, C.R., Sarmiento, J.L., Feldman, G.C., Milligan, A.J., Falkowski, P.G., Letelier, R.M., Boss, E.S., 2006. Climate-driven trends in contemporary ocean productivity. Nature 444, 752–755.

Benson, L., Burdett, J., Lund, S., Kashgarian, M., Mensing, S., 1997. Nearly synchronous climate change in the Northern Hemisphere during the last glacial termination. Nature 388, 263–265.

Berger, A., 1988. Milankovitch Theory and climate. Reviews of Geophysics 26, 624–657.

Billard, C., Inouye, I., 2004. What is new in coccolithophore biology? In: Thierstein, H.R., Young, J.R. (Eds.), From Molecular Processes to global Impact. Springer, Berlin, Germany, pp. 1-30.

Bintanja, R., van de Wal, R.S.W., Oerlemans, J., 2005. Modelled atmospheric temperatures and global sea levels over the past million years. Nature 437, 125–128.

Boeckel, B., Baumann, K., 2004. Distribution of coccoliths in surface sediments of the south-eastern South Atlantic Ocean: ecology, preservation and carbonate contribution. Marine Micropaleontology 51, 301–320.

Boeckel, B., Baumann, K., 2008. Vertical and lateral variations in coccolithophore community structure across the subtropical frontal zone in the South Atlantic Ocean. Marine Micropaleontology 67, 255-273.

Boeckel, B., Baumann, K., Henrich, R., Kinkel, H., 2006. Coccolith distribution patterns in South Atlantic and Southern Ocean surface sediments in relation to environmental gradients. Deep-Sea Research Part I 53, 1073–1099.

Bollmann, J., 1997. Morphology and biogeography of Gephyrocapsa coccoliths in Holocene sediments. Marine Micropaleontology 29, 319-350.

Bollmann, J., Baumann, K., Thierstein, H., 1998. Global dominance of *Gephyrocapsa* coccoliths in the late Pleistocene: Selective dissolution, evolution, or global environmental change? Paleoceanography 13, 517-529.

Bollmann, J., Henderiks, J., Brabec, B., 2002. Global calibration of *Gephyrocapsa* coccolith abundance in Holocene sediments for paleotemperature assessment. Paleoceanography 17.

Bollmann, J., Herrle, J., 2007. Morphological variation of *Emiliania huxleyi* and sea surface salinity. Earth and Planetary Science Letters 255, 273–288.

Bollmann, J., Herrle, J.O., Cortés, M.Y., Fielding, S.R., 2009. The effect of sea water salinity on the morphology of *Emiliania huxleyi* in plankton and sediment samples. Earth and Planetary Science Letters 284, 320–328.

Bond, G., Kromer, B., Beer, J., Muscheler, R., Evans, M., Showers, W., Hoffmann, S., Lotti-Bond, R., Hajdas, I., Bonani, G., 2001. Persistent solar influence on North Atlantic climate during the Holocene. Science 294, 2130.

Bond, G., Showers, W., Cheseby, M., Lotti, R., Almasi, P., deMenocal, P., Priore, P., Cullen, H., Hajdas, I., Bonani, G., 1997. A pervasive millennial-scale cycle in North Atlantic Holocene and glacial climates. Science 278, 1257.

Bout-Roumazeilles, V., Debrabant, P., Labeyrie, L., Chamley, H., Cortijo, E., 1997. Latitudinal control of astronomical forcing parameters on the high-resolution clay mineral distribution in the 45 degrees-60 degrees N range in the North Atlantic Ocean during the past 300,000 years. Paleoceanography 12, 671–686.

Bown, P.R. 1994. Calcareous Nannofossil Biostratigraphy, Kluwer Academic Publishers.

Bown, P., Lees, J.A., Young, J. R., 2004. Calcareous nannoplankton evolution and diversity through time. In: Thierstein, H.R., Young, J.R. (Eds.), From Molecular Processes to global Impact. Springer, Berlin, Germany, pp. 455-480.

Brand, L.E., 1984. The salinity tolerance of forty-six marine phytoplankton isolates. Estuarine, Coastal and Shelf Science 18, 543–556.

Brand, L. E., 1994. Physiological ecology of marine coccolithophores. In: Winter, A., Siesser , W. (Eds.), Coccolithophores, Cambridge University Press, Cambridge, pp. 39-50.

Brassell, S., Eglinton, G., Marlowe, I., Pflaumann, U., Sarnthein, M., 1986. Molecular stratigraphy: a new tool for climatic assessment. Nature 320, 129-133.

Broecker, W., 1982a. Glacial to interglacial changes in ocean chemistry. Progress in Oceanography 11, 151–197.

Broecker, W.S., 1982b. Ocean chemistry during glacial time. Geochimica et Cosmochimica Acta 46, 1689–1705.

Broecker, W.S., Denton, G.H., 1989. The role of ocean-atmosphere reorganizations in glacial cycles. Geochimica et Cosmochimica Acta 53, 2465–2501.

Broecker, W., Bond, G., Klas, M., Clark, E., McManus, J., 1992. Origin of the northern Atlantic's Heinrich events. Climate Dynamics 6, 265–273.

Broecker, W., Clark, E., 2009. Ratio of coccolith $CaCO_3$ to foraminifera $CaCO_3$ in late Holocene deep sea sediments. Paleoceanography 24, PA3205.

Broerse, A., Ziveri, P., van Hinte, J., Honjo, S., 2000a. Coccolithophore export production, species composition, and coccolith-$CaCO_3$ fluxes in the NE Atlantic (34°N 21°W and 48°N 21°W). Deep Sea Research Part II: Topical Studies in Oceanography 47, 1877-1905.

Broerse, A., Brummer, G., Hinte, J., 2000b. Coccolithophore export production in response to monsoonal upwelling off Somalia (northwestern Indian Ocean). Deep Sea Research Part II: Topical Studies in Oceanography 47, 2179–2205.

Brovkin, V., Bendtsen, J., Claussen, M., Ganopolski, A., Kubatzki, C., Petoukhov, V., Andreev, A., 2002. Carbon cycle, vegetation, and climate dynamics in the Holocene: Experiments with the CLIMBER-2 model. Global Biogeochemical Cycles 16.

Brown, C., Yoder, J., 1994. Coccolithophorid blooms in the global ocean. Journal of Geophysical Research 99, 7467–7482.

Brownlee, C., Taylor, A., 2004. Calcification in coccolithophores: A cellular perspective. In: Thierstein, H.R., Young, J.R. (Eds.), From Molecular Processes to global Impact. Springer, Berlin, Germany, pp. 31-50.

Bryden, H.L., Stommel, H.M., 1984. Limiting processes that determine basic features of the circulation in the Mediterranean Sea. Oceanologica Acta 7, 289-296.

Buitenhuis, E.T., De Baar, H.J.W., Veldhuis, M.J.W., 1999. Photosynthesis and calcification by *Emiliania huxleyi* (Prymnesiophyceae) as a function of inorganic carbon species. Journal of Phycology 35, 949–959.

Burkill, P.H., Archer, S.D., Robinson, C., Nightingale, P.D., Groom, S.B., Tarran, G.A., Zubkov, M.V., 2002. Dimethyl sulphide biogeochemistry within a coccolithophore bloom (DISCO): an overview. Deep-Sea Research Part II 49, 2863–2885.

Cachão, M., Moita, M.T., 2000. *Coccolithus pelagicus*, a productivity proxy related to moderate fronts off Western Iberia. Marine Micropaleontology 29, 131-155.

Calvo, E., Villanueva, J., Grimalt, J., Boelaert, A., Labeyrie, L., 2001. New insights into the glacial latitudinal temperature gradients in the North Atlantic. Results from UK'37 sea surface temperatures and terrigenous inputs. Earth and Planetary Science Letters 188, 509–519.

Carlson, A.E., Clark, P.U., Haley, B.A., Klinkhammer, G.P., Simmons, K., Brook, E.J., Meissner, K.J., 2007. Geochemical proxies of North American freshwater routing during the Younger Dryas cold event. Proceedings of the National Academy of Sciences 104, 6556–6561.

Carlson, A.E., Winsor, K., 2012. Northern Hemisphere ice-sheet responses to past climate warming. Nature Geoscience 5, 607–613.

Chapman, M., Shackleton, N., 1998. Millennial-scale fluctuations in North Atlantic heat flux during the last 150,000 years. Earth and Planetary Science Letters 159, 57–70.

Chapman, M., Shackleton, N., Duplessy, J., 2000. Sea surface temperature variability during the last glacial-interglacial cycle: assessing the magnitude and pattern of climate change in the North Atlantic. Palaeogeography Palaeoclimatology Palaeoecology 157, 1–25.

Cheddadi, R., Mamakowa, K., Guiot, J., De Beaulieu, J.L., Reille, M., Andrieu, V., Granoszewski, W., Peyron, O., 1998. Was the climate of the Eemian stable? A quantitative climate reconstruction from seven European pollen records. Palaeogeography Palaeoclimatology Palaeoecology 143, 73–85.

Chiyonobu, S., Mori, Y., Oda, M., 2012. Reconstruction of paleoceanographic conditions in the northwestern Pacific Ocean over the last 500kyr based on calcareous nannofossil and planktic foraminiferal assemblages. Marine Micropaleontology 96-97, 29–37.

Clark, P.U., 2001. Freshwater Forcing of Abrupt Climate Change During the Last Glaciation. Science 293, 283–287.

Clark, P.U., Huybers, P., 2009. Interglacial and future sea level. Nature 462, 856.

Colmenero-Hidalgo, E., Flores, J.-A., Sierro, F., 2002. Biometry of *Emiliania huxleyi* and its biostratigraphic significance in the Eastern North Atlantic Ocean and Western Mediterranean Sea in the last 20.000 years. Marine Micropaleontology 46, 247–263.

Condron, A., Winsor, P., 2011. A subtropical fate awaited freshwater discharged from glacial Lake Agassiz. Geophysical Research Letters 38, L03705.

Conte, M.H., Thompson, A., Lesley, D., Harris, R.P., 1998. Genetic and physiological influences on the alkenone/alkenoate versus growth temperature relationship in *Emiliania huxleyi* and *Gephyrocapsa oceanica*. Geochimica et Cosmochimica Acta 62, 51–68.

Cortés, M.Y., Bollmann, J., Thierstein, H.R., 2001. Coccolithophore ecology at the HOT station ALOHA, Hawaii. Deep-Sea Research Part II 48, 1957–1981.

Cortijo, E., al, E., 1994. Eemian cooling in the Norwegian Sea and North Atlantic ocean preceding continental ice-sheet growth. Nature 372, 446-449.

Couchoud, I., Genty, D., Hoffmann, D., Drysdale, R., Blamart, D., 2009. Millennial-scale climate variability during the Last Interglacial recorded in a speleothem from south-western France. Quaternary Science Reviews 28, 3263–3274.

Cros, L., Kleijne, A., Zeltner, A., Billard, C., Young, J.R., 2000. New examples of holococcolith–heterococcolith combination coccospheres and their implications for coccolithophorid biology. Marine Micropaleontology 39, 1–34.

Crowley, T.J., 1983. Calcium-carbonate preservation patterns in the central North Atlantic during the last 150,000 years. Marine Geology 51, 1–14.

Dansgaard, W., Johnsen, S.J., Clausen, H.B., Dahl-Jensen, D., Gundestrup, N.S., Hammer, C.U., Hvidberg, C.S., Steffensen, J.P., Sveinbjörnsdóttir, A.E., Jouzel, J., Bond, G., 1993. Evidence for General Instability of Past Climate From a 250-Kyr Ice-Core Record. Nature 364, 218–220.

de Leeuw, J.W., van der Meer, F.W., Rijpstra, W.I.C., Schenck, P.A., 1979. On the occurrence and structural identification of long-chain unsaturated ketones and hydrocarbons in recent and subrecent sediments. In: Douglas, A.G., Maxwell, J.R. (Eds.), Advances in Organic Geochemistry 1979. Pergamon Press, New York, pp. 211–217.

De Vargas, C., Aubry, M.-P., Probert, I., Young, J., 2007. Origin and Evolution of Coccolithophores: From Coastal Hunters to Oceanic Farmers. In: Falkowski, P., Knoll, A. (Eds.), Evolution of Primary Producers in the Sea, Elsevier, pp. 251-286.

Desprat, S., Sánchez Goñi, M. F., Naughton, F., Turon, J.-L., Malaizé, B., Cortijo, E., Peypouquet, J.-P., 2007. Climate Variability of the Last Five Isotopic Interglacials: Direct Land-Sea-Ice Correlation from the Multiproxy Analysis of North-Western Iberian Margin Deep-Sea Cores. In: Sirocko, F., Claussen, M., Sánchez Goñi, M. F., Litt, T. (Eds.), The Climate of Past Interglacials. Elsevier, Amsterdam, The Netherlands, pp. 375-386.

Di Stefano, E., Incarbona, A., 2004. High-resolution palaeoenvironmental reconstruction of ODP Hole 963D (Sicily Channel) during the last deglaciation based on calcareous nannofossils. Marine Micropaleontology 52, 241–254.

Dokken, T.M., Jansen, E., 1999. Rapid changes in the mechanism of ocean convection during the last glacial period. Nature 401, 458–461.

Dymond, J., Suess, E., Lyle, M., 1992. Barium in deep-sea sediment: a geochemical proxy for paleoproductivity. Paleoceanography 7, 163-181.

Edvardsen, B., Eikrem, W., Green, J.C., Andersen, R.A., Moon-van der Staay, S.Y., Medlin, L.K., 2000. Phylogenetic reconstructions of the Haptophyta inferred from 18S ribosomal DNA sequences and available morphological data. Phycologia 39, 19–35.

Ellison, C.R.W., 2006. Surface and Deep Ocean Interactions During the Cold Climate Event 8200 Years Ago. Science 312, 1929–1932.

Emerson, S., Quay, P., Karl, D., Winn, C., Tupas, L., Landry, M., 1997. Experimental determination of the organic carbon flux from open-ocean surface waters. Nature 389, 951–954.

EPICA members, 2004. Eight glacial cycles from an Antarctic ice core. Nature 429, 623–628.

Eppley, R., Peterson, B.J., 1979. Particulate organic matter flux and planktonic new production in the deep ocean. Nature 282, 677- 680.

Escartín, J., Cannat, M., Pouliquen, G., Rabain, A., Lin, J., 2001. Crustal thickness of V-shaped ridges south of the Azores; interaction of the Mid-Atlantic Ridge (36°-39°N) and the Azores hot spot. Journal of Geophysical Research 106, 21719-21735.

Etourneau, J., 2009. Pliocene-Pleistocene variability of upwelling activity, productivity and nutrient cycle in the Benguela Upwelling System and the Eastern Equatorial Pacific. Ph.D. Thesis, Institut für Geowissenschaften, Kiel, Germany.

Etourneau, J., Schneider, R., Blanz, T., Martinez, P., 2010. Intensification of the Walker and Hadley atmospheric circulations during the Pliocene–Pleistocene climate transition. Earth and Planetary Science Letters 297, 103–110.

Evans, H.K., Hall, I.R., Bianchi, G.G., Oppo, D.W., 2007. Intermediate water links to Deep Western Boundary Current variability in the subtropical NW Atlantic during marine isotope stages 5 and 4. Paleoceanography 22, PA3209.

Ewing, M., Carpenter, G., Windisch, C., Ewing, J., 1973. Sediment Distribution in the Oceans: The Atlantic. Geological Society of America Bulletin 84, 71–88.

Fairbanks, R., 1989. A 17, 000-year glacio-eustatic sea level record: influence of glacial melting rates on the Younger Dryas event and deep-ocean circulation. Nature 342, 637–642.

Falkowski, P., 2000. The Global Carbon Cycle: A Test of Our Knowledge of Earth as a System. Science 290, 291–296.

Fasham, M., Platt, T., Irwin, B., Jones, K., 1985. Factors affecting the spatial pattern of the deep chlorophyll maximum in the region of the Azores Front. Progress in Oceanography 14, 129–165.

Fernández, E., Pingree, R., 1996. Coupling between physical and biological fields in the North Atlantic subtropical front southeast of the Azores. Deep-Sea Research Part I 43, 1369–1393.

Field, C.B., 1998. Primary Production of the Biosphere: Integrating Terrestrial and Oceanic Components. Science 281, 237–240.

Fincham, M., Winter, A., 1989. Paleoceanographic Interpretations of Coccoliths and Oxygen-Isotopes From the Sediment Surface of the Southwest Indian-Ocean. Marine Micropaleontology 13, 325–351.

Findlay, C., Giraudeau, J., 2002. Movement of oceanic fronts south of Australia during the last 10 ka: interpretation of calcareous nannoplankton in surface sediments from the Southern Ocean. Marine Micropaleontology 46, 431–444.

Flores, J., Sierro, F., Francés, G., Vázquez, A., Zamarreno, I., 1997. The last 100,000 years in the western Mediterranean: sea surface water and frontal dynamics as revealed by coccolithophores. Marine Micropaleontology 29, 351–366.

Flores, J., Bárcena, M., Sierro, F., 2000. Ocean-surface and wind dynamics in the Atlantic Ocean off Northwest Africa during the last 140 000 years. Palaeogeography Palaeoclimatology Palaeoecology 161, 459–478.

Flores, J.-A., Marino, M., Sierro, F.J., Hodell, D.A., Charles, C.D., 2003. Calcareous plankton dissolution pattern and coccolithophore assemblages during the last 600 kyr at ODP Site 1089 (Cape Basin, South Atlantic): paleoceanographic implications. Palaeogeography Palaeoclimatology Palaeoecology 196, 409–426.

Flores, J.-A., Colmenero-Hidalgo, E., Mejía-Molina, A.E., Baumann, K.-H., Henderiks, J., Larsson, K., Prabhu, C.N., Sierro, F.J., Rodrigues, T., 2010. Distribution of large Emiliania huxleyi in the Central and Northeast Atlantic as a tracer of surface ocean dynamics during the last 25,000years. Marine Micropaleontology 76, 53–66.

Flower, B.P., Hastings, D.W., Hill, H.W., Quinn, T.M., 2004. Phasing of deglacial warming and Laurentide Ice Sheet meltwater in the Gulf of Mexico. Geology 32, 597.

Francois, R., Honjo, S., Manganini, S., Ravizza, G., 1995. Biogenic Barium Fluxes to the Deep-Sea - Implications for Paleoproductivity Reconstruction. Global Biogeochemical Cycles 9, 289–303.

Frenz, M., 2005. Quantification of Foraminifer and Coccolith Carbonate in South Atlantic Surface Sediments by Means of Carbonate Grain-Size Distributions. Journal of Sedimentary Research 75, 464–475.

Fronval, T., Jansen, E., 1996. Rapid changes in ocean circulation and heat flux In the Nordic seas during the last interglacial period. Nature 383, 806–810.

Ganeshram, R.S., Pedersen, T.F., Calvert, S.E., Murray, J.W., 1995. Large changes in oceanic nutrient inventories from glacial to interglacial periods. Nature 376, 755–758.

Gard, G., 1986. Calcareous Nannofossil Biostratigraphy of Late Quaternary Arctic Sediments. Boreas 15, 217-229.

Gard, G., 1989. Variations in coccolith assemblages during the Last Glacial Cycle in the High and Mid-Latitude Atlantic and Indian Ocean. In. Crux, J.A., van Heck, S.E. (Eds.), Nannofossils and their applications. Ellis Horwood, Chichester, United Kingdom, pp. 108-121.

Geisen, M., Billard, C., Broerse, A., Cros, L., Probert, I., Young, J., 2002. Life-cycle associations involving pairs of holococcolithophorid species: intraspecific variation or cryptic speciation? European Journal of Phycology 37, 531–550.

German, C.R., Parson, L.M., Team, H.S., Bougault, H., Coller, D., Critchley, M., Dapoigny, A., Day, C., Eardley, D., Fearn, A., 1996. Hydrothermal exploration near the Azores Triple Junction: tectonic control of venting at slow-spreading ridges? Earth and Planetary Science Letters 138, 93–104.

Gil, I.M., Keigwin, L.D., Abrantes, F.G., 2009. Deglacial diatom productivity and surface ocean properties over the Bermuda Rise, northeast Sargasso Sea. Paleoceanography 24.

Gingele, F. X., Zabel, M., Kasten, S., Bonn, W.J., Nürnberg, C.C., 1999. Biogenic barium as a proxy for paleoproductivity: methods and limitations of application. In: Fischer, G., Wefer, G. (Eds.), Use of proxies in paleoceanography. Springer, Berlin, pp. 345-364.

Giraudeau, J., Monteiro, P., Nikodemus, K., 1993. Distribution and malformation of living coccolithophores in the northern Benguela upwelling system off Namibia. Marine Micropaleontology 22, 93–110.

Giraudeau, J., Cremer, M., Manthé, S., Labeyrie, L., Bond, G., 2000. Coccolith evidence for instabilities in surface circulation south of Iceland during Holocene times. Earth and Planetary Science Letters 179, 257–268.

Giraudeau, J., Jennings, A., Andrews, J., 2004. Timing and mechanisms of surface and intermediate water circulation changes in the Nordic Seas over the last 10,000 cal years: a view from the North Iceland shelf. Quaternary Science Reviews 23, 2127–2139.

Giraudeau, J., Beaufort, L., 2007. Coccolithophores: from extant populations to fossil assemblages. In: Hilaire-Marcel, C. and de Vernal, A. (Eds.), Developments in marine geology, Proxies in late Cenozoic paleoceanography, Elsevier, Amsterdam 409–439.

Giraudeau, J., Grelaud, M., Solignac, S., Andrews, J.T., Moros, M., Jansen, E., 2010. Millennial-scale variability in Atlantic water advection to the Nordic Seas derived from Holocene coccolith concentration records. Quaternary Science Reviews 29, 1276–1287.

Gould, W., 1985. Physical oceanography of the Azores Front. Progress in Oceanography 14, 167–190.

Grootes, P.M., Stuiver, M., White, J., Johnsen, S., Jouzel, J., 1993. Comparison of oxygen isotope records from the GISP2 and GRIP Greenland ice cores, Nature 366, 552-554.

Grootes, P.M., Stuiver, M., 1997. Oxygen 18/16 variability in Greenland snow and ice with 10^{-3} to 10^{5}-year time resolution, Journal of Geophysical Research 102, 26455-26470.

Hagino, K., Okada, H., Matsuoka, H., 2005. Coccolithophore assemblages and morphotypes of *Emiliania huxleyi* in the boundary zone between the cold Oyashio and warm Kuroshio currents off the coast of Japan. Marine Micropaleontology 55, 19–47.

Haidar, A., Thierstein, H., 2001. Coccolithophore dynamics off Bermuda (N. Atlantic). Deep Sea Research Part II: Topical Studies in Oceanography 48, 1925–1956.

Harris, R., 1994. Zooplankton grazing on the coccolithophore *Emiliania huxleyi* and its role in inorganic carbon flux. Marine Biology 119, 431–439.

Hass, H. C., Andruleit, H., Baumann, A., Baumann, K.-H., Kohly, A., Jensen, S., Matthiessen, J., Samtleben, C., Schäfer, P., Schröder-Ritzrau, A., Thiede, J., 2001. The Potential of Synoptic Plankton Analyses for Paleoclimatic Investigations: Five Plankton Groups from the Holocene Nordic Seas. In: Schäfer, P., Ritzrau, W., Schlüter, M., Thiede, J. (Eds.), The Northern North Atlantic: A Changing Environment. Springer, Berlin, pp. 291-318.

Hays, J.D., Imbrie, J., Shackleton, N.J., 1976. Variations in the Earth's orbit: pacemaker of the ice ages. Science 194, 1121-1132.

Heinrich, H., 1988. Origin and Consequences of Cyclic Ice Rafting in the Northeast Atlantic-Ocean During the Past 130,000 Years. Quaternary Research 29, 142–152.

Henriksen, K., Young, J.R., Bown, P.R., Stipp, S., 2004. Coccolith biomineralisation studied with atomic force microscopy. Palaeontology 47, 725–743.

Hernández-León, S., Gómez, M., Arístegui, J., 2007. Mesozooplankton in the Canary Current System: The coastal-ocean transition zone. Progress in Oceanography 74, 397–421.

Heusser, L., Oppo, D., 2003. Millennial- and orbital-scale climate variability in southeastern United States and in the subtropical Atlantic during Marine Isotope Stage 5: evidence from pollen and isotopes in ODP Site 1059. Earth and Planetary Science Letters 214, 483–490.

Hillaire-Marcel, C., de Vernal, A., Bilodeau, G., Weaver, A., 2001. Absence of deep-water formation in the Labrador Sea during the last interglacial period. Nature 410, 1073–1077.

Hine, N., Weaver, P.P.E., 1998. Quaternary. In: Bown, P.R. (Ed.), Calcareous Nannofossil Biostratigraphy, Kluwer Academic Publishers, pp. 266-384.

Hinrichs, K.-U., Schneider, R.R., Müller, P.J., Rullkötter, J., 1999. A biomarker perspective on paleoproductivity variations in two Late Quaternary sediment sections from the Southeast Atlantic Ocean. Organic Geochemistry 30, 341–366.

Hodell, D.A., Charles, C.D., Ninnemann, U.S., 2000. Comparison of interglacial stages in the South Atlantic sector of the southern ocean for the past 450 kyr: implifications for Marine Isotope Stage (MIS) 11. Global and Planetary Change 24, 7–26.

Holligan, P.M., Fernández, E., Aiken, J., Balch, W.M., Boyd, P., Burkill, P.H., Finch, M., Groom, S.B., Malin, G., Muller, K., 1993. A biogeochemical study of the coccolithophore, *Emiliania huxleyi*, in the North Atlantic. Global Biogeochemical. Cycles 7, 879–900.

Honjo, S., 1976. Coccoliths: Production, Transportation and Sedimentation. Marine Micropaleontology 1, 65-79.

Houdan, A., Billard, C., Marie, D., Not, F., Sáez, A.G., Young, J.R., Probert, I., 2004. Flow cytometric analysis of relative ploidy levels in holococcolithophore-heterococcolithophore (Haptophyta) life cycles. Systematics and Biodiversity 1, 453–465.

Howard, W.R., 1997. Palaeoclimatology: A warm future in the past. Nature 388, 418–419.

Imbrie, J., Hays, J. D., Martinson, D. G., McIntyre, A., Mix, A. C., Morley, J. J., Pisias, N. G., Prell, W. L., Shackleton, N. J., 1984. The orbital theory of Pleistocene climate: Support from a revised chronology of the marine $\delta^{18}O$ record. In: Berger, A.I., Imbrie, J., Hays, J., Kukla, G., Saltzman, B. (Eds.), Milankovitch and Climate: Part I. Reidel, Netherlands, pp. 269-305.

Incarbona, A., Di Stefano, E., Sprovieri, R., Bonomo, S., 2009. Millennial-scale paleoenvironmental changes in the central Mediterranean during the last interglacial: Comparison with European and North Atlantic records. Geobios 43, 111-122.

Incarbona, A., Martrat, B., Di Stefano, E., Grimalt, J.O., Pelosi, N., Patti, B., Tranchida, G., 2010. Primary productivity variability on the Atlantic Iberian Margin over the last 70,000 years: Evidence from coccolithophores and fossil organic compounds. Paleoceanography 25.

Incarbona, A., Ziveri, P., Sabatino, N., Manta, D.S., Sprovieri, M., 2011. Conflicting coccolithophore and geochemical evidence for productivity levels in the Eastern Mediterranean sapropel S1. Marine Micropaleontology 81, 131–143.

Irvalı, N., Ninnemann, U.S., Galaasen, E.V., Rosenthal, Y., Kroon, D., Oppo, D.W., Kleiven, H.F., Darling, K.F., Kissel, C., 2012. Rapid switches in subpolar North Atlantic hydrography and climate during the Last Interglacial (MIS 5e). Paleoceanography 27.

Jansen, E., Overpeck, J., Briffa, K.R., Duplessy, J., Joos, F., Masson-Delmotte, V., Olago, D., Otto-Bliesner, B., Peltier, W.R., Rahmstorf, S., Ramesh, R., Raynaud, D., Rind, D., Solomina, O., Villalba, R., Zhang, D., 2007. Palaeoclimate. In: Solomon, S., Qin, D., Manning, M., Chen, Z., Marquis, M., Ayert, K.B., Tignor, M., Miller, H.L. (Eds), The Physical Science Basis. Contribution of Working Group I to the

Fourth Assessment Report of the Intergovernmental Panel on Climate Change. Cambridge University Press, Cambridge, United Kingdom.

Jia, Y., 2000. Formation of an Azores Current due to Mediterranean overflow in a modeling study of the North Atlantic. Journal of Physical Oceanography 30, 2342–2358.

Jimenez-Espejo, F.J., Martinez-Ruiz, F., Sakamoto, T., Iijima, K., Gallego-Torres, D., Harada, N., 2007. Paleoenvironmental changes in the western Mediterranean since the last glacial maximum: High resolution multiproxy record from the Algero–Balearic basin. Palaeogeography Palaeoclimatology Palaeoecology 246, 292–306.

Jordan, R. W., 1988. Coccolithophorid communities in the North East Atlantic. Ph.D. Thesis, University of Surrey, Guildford.

Jouzel, J., Masson-Delmotte, V., Cattani, O., Dreyfus, G., Falourd, S., Hoffmann, G., Minster, B., Nouet, J., Barnola, J.M., Chappellaz, J., Fischer, H., Gallet, J.C., Johnsen, S., Leuenberger, M., Loulergue, L., Luethi, D., Oerter, H., Parrenin, F., Raisbeck, G., Raynaud, D., Schilt, A., Schwander, J., Selmo, E., Souchez, R., Spahni, R., Stauffer, B., Steffensen, J.P., Stenni, B., Stocker, T.F., Tison, J.L., Werner, M., Wolff, E.W., 2007. Orbital and Millennial Antarctic Climate Variability over the Past 800,000 Years. Science 317, 793–796.

Kandiano, E.S., Bauch, H.A., 2007. Phase relationship and surface water mass change in the Northeast Atlantic during Marine Isotope Stage 11 (MIS 11). Quaternary Research 68, 445–455.

Kandiano, E.S., Bauch, H.A., Fahl, K., Helmke, J.P., Röhl, U., Pérez-Folgado, M., Cacho, I., 2012. The meridional temperature gradient in the eastern North Atlantic during MIS 11 and its link to the ocean–atmosphere system. Palaeogeography Palaeoclimatology Palaeoecology 333-334, 24–39.

Käse, R., 1982. Meandering of the subtropical front south-east of the Azores. Nature 300, 245-246.

Keigwin, L., Curry, W., Lehman, S., Johnsen, S., 1994. The role of the deep ocean in North Atlantic climate change between 70 and 130 kyr ago. Nature 371, 323–326.

Kida, S., Price, J., Yang, J., 2008. The upper-oceanic response to overflows: A mechanism for the Azores Current. Journal of Physical Oceanography 38, 880–895.

Kiefer, T., Abrantes, F., Sarnthein, M., Weinelt, M., Labeyrie, L., 1995. Prominent productivity spikes in the subtropical North Atlantic parallel Heinrich meltwater events. In: Book of abstracts of the V International Conference on Paleoceanography, Canada, 85 pp..

Kiefer, T., Kull, C., 2007. Climate of Past Interglacials - a PAGES Perspective. In: Sirocko, F., Claussen, M., Sánchez Goñi, M. F., Litt, T. (Eds.), The Climate of Past Interglacials. Elsevier, Amsterdam, The Netherlands, Preface.

Kielmann, J., Käse, R., 1987. Numerical modeling of meander and eddy formation in the Azores Current frontal zone. Journal of Physical Oceanography 17, 529–541.

Kinder, T.H., Parrilla, G., 1987. Yes, Some of the Mediterranean Outflow Does Come From Great Depth. Journal of Geophysical Research 92, 2901–2906.

Kinkel, H., al, E., 2000. Coccolithophores in the equatorial Atlantic Ocean: response to seasonal and Late Quaternary surface water variability. Marine Micropaleontology 39, 87-112.

Kissel, C., Kleiven, H., Morin, X., Scientific Shipboard Party, 2008. MD168-AMOCINT/XVII IMAGES cruise report. In: Les rapports de campagne à la mer, IPEV, ref:OCE/2008/02.

Klein, B., Siedler, G., 1989. On the origin of the Azores Current. Journal of Geophysical Research 94, 6159–6168.

Kleiven, H.F., Kissel, C., Laj, C., Ninnemann, U.S., Richter, T.O., Cortijo, E., 2008. Reduced North Atlantic Deep Water Coeval with the Glacial Lake Agassiz Freshwater Outburst. Science 319, 60–64.

Knappertsbusch, M., Cortes, M., Thierstein, H., 1997. Morphologic variability of the coccolithophorid *Calcidiscus leptoporus* in the plankton, surface sediments and from the Early Pleistocene. Marine Micropaleontology 30, 293–317.

Kohfeld, K.E., 2005. Role of Marine Biology in Glacial-Interglacial CO_2 Cycles. Science 308, 74–78.

Kopp, R.E., Simons, F.J., Mitrovica, J.X., Maloof, A.C., Oppenheimer, M., 2009. Probabilistic assessment of sea level during the last interglacial stage. Nature 462, 863–867.

Kristiansen, S., Thingstad, T.F., van der Wal, P., Farbrot, T., Skjoldal, E.F., 1994. An Emiliania huxleyi dominated subsurface bloom in Samnangerfjorden, western Norway. Importance of hydrography and nutrients. Sarsia 79, 357–368.

Kukla, G.J., Bender, M.L., de Beaulieu, J.-L., Bond, G., Broecker, W.S., Cleveringa, P., Gavin, J.E., Herbert, T.D., Imbrie, J., Jouzel, J., Keigwin, L.D., Knudsen, K.L., McManus, J.F., Merkt, J., Muhs, D.R., Müller, H., Poore, R.Z., Porter, S.C., Seret, G., Shackleton, N.J., Turner, C., Tzedakis, P.C., Winograd, I.J., 2002. Last Interglacial Climates. Quaternary Research 58, 2–13.

Kupferman, S., Becker, G., Simmons, W., 1986. An intense cold core eddy in the North-East Atlantic. Nature 319, 474-477.

Kutzbach, J.E., Gallimore, R.G., Guetter, P.J., 1991. Sensitivity experiments on the effect of orbitally-caused insolation changes on the interglacial climate of high northern latitudes. Quaternary International 10–12, 223–229.

Lambeck, K., Esat, T., Potter, E., 2002. Links between climate and sea levels for the past three million years. Nature 419, 199–206.

Laskar, J., Robutel, P., Joutel, F., Gastineau, M., Correia, A.C.M., Levrard, B., 2004. A long-term numerical solution for the insolation quantities of the Earth. A&A 428, 261–285.

Lea, D.W., 2003. Synchroneity of Tropical and High-Latitude Atlantic Temperatures over the Last Glacial Termination. Science 301, 1361–1364.

Lebreiro, S., Moreno, J., Abrantes, F., Pflaumann, U., 1997. Productivity and paleoceanographic implications on the Tore Seamount (Iberian Margin) during the last 225 kyr: Foraminiferal evidence. Paleoceanography 12, 718–727.

Leduc, G., Schneider, R., Kim, J.-H., Lohmann, G., 2010. Holocene and Eemian sea surface temperature trends as revealed by alkenone and Mg/Ca paleothermometry. Quaternary Science Reviews 29, 989–1004.

Le Fèvre, J., 1987. Aspects of the Biology of Frontal Systems. In: Blaxter, J.H.S., Southward, A.J. (Eds.), Advances in Marine Biology 23, Academic Press, pp. 163–299.

Lehman, S.J., Sachs, J.P., Crotwell, A.M., Keigwin, L.D., Boyle, E.A., 2002. Relation of subtropical Atlantic temperature, high-latitude ice rafting, deep water formation, and European climate 130,000-60,000 years ago. Quaternary Science Reviews 21, 1917–1924.

Levasseur, M., Michaud, S., Egge, J., Cantin, G., Nejstgaard, J.C., Sanders, R., Fernández, E., Solberg, P.T., Heimdal, B., Gosselin, M., 1996. Production of DMSP and DMS during a mesocosm study of an *Emiliania huxleyi* bloom: influence of bacteria and *Calanus finmarchicus* grazing. Marine Biology 126, 609–618.

Lévy, M., Lehahn, Y., André, J., Mémery, L., Loisel, H., Heifetz, E., 2005. Production regimes in the northeast Atlantic: A study based on Sea-viewing Wide Field-of-view Sensor (SeaWiFS) chlorophyll and ocean general circulation model mixed layer depth. Journal of Geophysical Research 110, 1998–2006.

Li, T., Zhao, J., Sun, R., Chang, F., Sun, H., 2010. The variation of upper ocean structure and paleoproductivity in the Kuroshio source region during the last 200 kyr. Marine Micropaleontology 75, 50–61.

Lisiecki, L., Raymo, M., 2005. A Plio-Pleistocene stack of 57 globally distributed benthic $\delta^{18}O$ records. Paleoceanography 20, 522–533.

Locarnini, R. A., Mishonov, A.V., Antonov, J.I., Boyer, T.P., Garcia, H.E., 2010. In: Levitus, S. (Ed.), World Ocean Atlas 2009, Volume 1: Temperature. NOAA Atlas NESDIS 68, U.S. Government Printing Office, Washington, D.C.

Lohbeck, K.T., Riebesell, U., Reusch, T.B.H., 2012. Adaptive evolution of a key phytoplankton species to ocean acidification. Nature Geoscience 5, 346–351.

Longhurst, A., Sathyendranath, S., Platt, T., Caverhill, C., 1995. An estimate of global primary production in the ocean from satellite radiometer data. Journal of Plankton Research 17, 1245.

Lopes dos Santos, R.A., Prange, M., Castañeda, I.S., Schefuß, E., Mulitza, S., Schulz, M., Niedermeyer, E.M., Damsté, J.S.S., Schouten, S., 2010. Glacial–interglacial variability in Atlantic meridional overturning circulation and thermocline adjustments in the tropical North Atlantic. Earth and Planetary Science Letters 300, 407–414.

López-Otálvaro, G., Flores, J., Sierro, F., Cacho, I., Grimalt, J., Michel, E., Cortijo, E., Labeyrie, L., Desbois, G., Urai, J., 2008. Late Pleistocene palaeoproductivity patterns during the last climatic cycle in the Guyana Basin as revealed by calcareous nannoplankton. eEarth Discussions 3, 11–40.

Lototskaya, A., Ziveri, P., Ganssen, G., van Hinte, J., 1998. Calcareous nannofloral response to Termination II at 45°N, 25°W (northeast Atlantic). Marine Micropaleontology 34, 47–70.

Loutre, M.F., 2003. Clues from MIS 11 to predict the future climate – a modelling point of view. Earth and Planetary Science Letters 212, 213–224.

Lüthi, D., Le Floch, M., Bereiter, B., Blunier, T., Barnola, J.-M., Siegenthaler, U., Raynaud, D., Jouzel, J., Fischer, H., Kawamura, K., Stocker, T.F., 2008. High-resolution carbon dioxide concentration record 650,000–800,000 years before present. Nature 453, 379–382.

Maillard, C., Käse, R., 1989. The near-surface flow in the subtropical gyre south of the Azores. Journal of Geophysical Research 94, 16133.

Maiorano, P., Tarantino, F., Marino, M., De Lange, G.J., 2012. Paleoenvironmental conditions at Core KC01B (Ionian Sea) through MIS 13-9: Evidence from calcareous nannofossil assemblages. Quaternary International, in press.

Margalef, R., 1978. Life-Forms of Phytoplankton as Survival Alternatives in an Unstable Environment. Oceanologica Acta 1, 493–509.

Mariotti, V., Bopp, L., Tagliabue, A., Kageyama, M., Swingedouw, D., 2012. Marine productivity response to Heinrich events: a model-data comparison. Climate of the Past Discussions 8, 557–594.

Martini, E., 1971. Standard Tertiary and Quaternary calcareous nannoplankton zonation. In: Farinacci, A. (Ed.), Proceedings of the Second Planktonic Conference Roma 1970. Edizioni Tecnoscienza, Rome, pp. 739-785.

Martins, C.S., 2002. Surface circulation in the eastern North Atlantic, from drifters and altimetry. Journal of Geophysical Research 107, 1–28.

Maslin, M.A., Shackleton, N.J., Pflaumann, U., 1995. Surface water temperature, salinity, and density changes in the northeast Atlantic during the last 45,000 years: Heinrich events, deep water formation, and climatic rebounds. Paleoceanography 10, 527–544.

Maslin, M., Sarnthein, M., Knaack, J.-J., Grootes, P., Tzedakis, C., 1998. Intra-interglacial cold events: an Eemian-Holocene comparison. Geological Society, London, Special Publications 131, 91–99.

Maslin, M.A., Ridgwell, A.J., 2005. Mid-Pleistocene revolution and the “eccentricity myth.” Geological Society, London, Special Publications 247, 19–34.

Matthiesen, S., 2003. A hydraulic box model study of the Mediterranean response to postglacial sea-level rise. Paleoceanography 18.

McCartney, M.S., Talley, L.D., 1984. Warm-to-cold water conversion in the northern North Atlantic Ocean. Journal of Physical Oceanography 14, 922–935.

McElroy, M.B., 1983. Marine biological controls on atmospheric CO_2 and climate. Nature 302, 328-329.

McIntyre, A., Bé, A., 1967. Modern coccolithophoridae of the atlantic ocean--I. Placoliths and cyrtoliths. Deep Sea Research and Oceanographic Abstracts 14, 561–564.

McIntyre, A., Bé, A., Roche, M.B., 1970. Modern Pacific Coccolithophorida: a paleontological thermometer. Transactions New York Academy of Sciences, Ser. II, 720-731.

McIntyre, A., Ruddiman, W.F., 1972. Northeast Atlantic post-Eemian paleooceanography: a predictive analog of the future. Quaternary Research 2, 350–354.

McManus, J., Bond, G., Broecker, W., Johnsen, S., Labeyrie, L., Higgins, S., 1994. High-resolution climate records from the North Atlantic during the last interglacial. Nature 371, 326–329.

McManus, J., Berelson, W., Klinkhammer, G., Johnson, K., Coale, K., Anderson, R., Kumar, N., Burdige, D., Hammond, D., Brumsack, H., McCorkle, D., Rushdi, A., 1998. Geochemistry of barium in marine sediments: Implications for its use as a paleoproxy. Geochimica et Cosmochimica Acta 62, 3453–3473.

McManus, J.F., Oppo, D.W., Keigwin, L.D., Cullen, J.L., Bond, G.C., 2002. Thermohaline Circulation and Prolonged Interglacial Warmth in the North Atlantic. Quaternary Research 58, 17–21.

McManus, J., Oppo, D., Cullen, J., Healey, S., 2003. Marine Isotope Stage 11 (MIS 11): Analog for Holocene and future climate? Geophysical Monograph Series 137, 69–85.

McManus, J.F., Francois, R., Gherardi, J.-M., Keigwin, L.D., Brown-Leger, S., 2004. Collapse and rapid resumption of Atlantic meridional circulation linked to deglacial climate changes. Nature 428, 834–837.

Menviel, L., Timmermann, A., Mouchet, A., Timm, O., 2008. Meridional reorganizations of marine and terrestrial productivity during Heinrich events. Paleoceanography 23.

Merico, A., Tyrrell, T., Lessard, E.J., Oguz, T., Stabeno, P.J., Zeeman, S.I., Whitledge, T.E., 2004. Modelling phytoplankton succession on the Bering Sea shelf: role of climate influences and trophic interactions in generating *Emiliania huxleyi* blooms 1997–2000. Deep Sea Research Part I: Oceanographic Research Papers 51, 1803–1826.

Mix, A.C., Le, J., Shackleton, N.J., 1995. Benthic foraminiferal stable isotope stratigraphy of site 846: 0-1.8 Ma. Proceedings of the Ocean Drilling Program 138, 839-854.

Molfino, B., McIntyre, A., 1990a. Nutricline Variation in the Equatorial Atlantic Coincident with the Younger Dryas. Paleoceanography 5.

Molfino, B., McIntyre, A., 1990b. Precessional Forcing of Nutricline Dynamics in the Equatorial Atlantic. Science 249, 766–769.

Monterey, G., Levitus, S., 1997. Seasonal variability of mixed layer depth for the world ocean. NOAA Atlas NESDIS 14, U.S. Government Printing Office, Washington ,D.C., 96 pp..

Montoya, M., Storch, von, H., Crowley, T.J., 2000. Climate simulation for 125 kyr BP with a coupled ocean-atmosphere general circulation model. Journal of Climate 13, 1057–1072.

Moreno, E., Thouveny, N., Delanghe, D., 2002. Climatic and oceanographic changes in the Northeast Atlantic reflected by magnetic properties of sediments deposited on the Portuguese Margin during the last 340 ka. Earth and Planetary Science Letters 202, 465-480.

Mouriño, B., Fernandez, E., Etienne, H., Hernandez, F., Giraud, S., 2003. Significance of cyclonic SubTropical Oceanic Rings of Magnitude (STORM) eddies for the carbon budget of the euphotic layer in the subtropical northeast Atlantic. Journal of Geophysical Research 108.

Mouriño-Carballido, B., Neuer, S., 2008. Eddy Pumping in the North atlantic subtropical gyre. Oceanography 21, 52.

Mudelsee, M., Stattegger, K., 1997. Exploring the structure of the mid-Pleistocene revolution with advanced methods of time-series analysis. Geologische Rundschau 86, 499–511.

Muller, R.A., MacDonald, G.J., 1995. Glacial cycles and orbital inclination. Nature 377, 107–108.

Müller, P., Kirst, G., Ruhland, G., Storch, von, I., Rosell-Melé, A., 1998. Calibration of the alkenone paleotemperature index U37K′ based on core-tops from the eastern South Atlantic and the global ocean (60° N-60° S). Geochimica et Cosmochimica Acta 62, 1757–1772.

Müller, U.C., Kukla, G.J., 2004. North Atlantic Current and European environments during the declining stage of the last interglacial. Geology 32, 1009.

M□ller, U. C., S□nchez Go□i, M. F., 2007. Vegetation Dynamics in Southern Germany During Marine Isotope Stage 5 (~130 to 70 kyr Ago), In: Sirocko, F., Claussen, M., S□nchez Go□i, M. F., Litt, T. (Eds.), The Climate of Past Interglacials. Elsevier, Amsterdam, The Netherlands, pp. 375-386.

Naafs, B.D.A., Hefter, J., Acton, G., Haug, G.H., Martínez-Garcia, A., Pancost, R., Stein, R., 2010. Strengthening of North American dust sources during the late Pliocene (2.7Ma). Earth and Planetary Science Letters 317-318, 1–12.

Nave, S., Labeyrie, L., Gheradi, J., Caillon, N., Cortijo, E., Kissel, C., Abrantes, F., 2007. Primary productivity response to Heinrich events in the North Atlantic Ocean and Norwegian Sea. Paleoceanography 22.

Nebout, N., Turon, J., Zahn, R., Capotondi, L., 2002. Enhanced aridity and atmospheric high-pressure stability over the western Mediterranean during the North Atlantic cold events of the past 50 ky. Geology 30, 863-866.

Nelson, D., Treguer, P., Brezinzki, M., Leynaert, A., Queguiner, B., 1995. Production and Dissolution of Biogenic Silica in the Ocean - Revised Global Estimates, Comparison with Regional Data and Relationship to Biogenic Sedimentation. Global Biogeochemical Cycles 9, 359–372.

Okada, H., Honjo, S., 1973. The distribution of oceanic coccolithophorids in the Pacific. Deep Sea Research 20, 355-374.

Okada, H., McIntyre, A., 1979. Seasonal distribution of modern coccolithophores in the western North Atlantic Ocean. Marine Biology 54, 319–328.

Okada, H., Wells, P., 1997. Late Quaternary nannofossil indicators of climate change in two deep-sea cores associated with the Leeuwin Current off Western Australia. Palaeogeography Palaeoclimatology Palaeoecology 131, 413–432.

Onken, R., 1993. The Azores Countercurrent. Journal of Physical Oceanography 23, 1638–1646.

Oppo, D.W., McManus, J.F., Cullen, J.L., 2006. Evolution and demise of the Last Interglacial warmth in the subpolar North Atlantic. Quaternary Science Reviews 25, 3268–3277.

Oschlies, A., 2001. NAO-induced long-term changes in nutrient supply to the surface waters of the North Atlantic. Geophysical Research Letters 28, 1751–1754.

Ottens, J., 1991. Planktic foraminifera as North Atlantic water mass indicators. Oceanologica Acta 14, 123–140.

Ottens, J., 1992. April and August northeast Atlantic surface water masses reflected in planktic foraminifera. Netherlands Journal of Sea Research 28, 261–283.

Özgökmen, T., Chassignet, E., Rooth, C., 2001. On the connection between the Mediterranean outflow and the Azores Current. Journal of Physical Oceanography 31, 461–480.

Paasche, E., Brubak, S., Skattebøl, S., Young, J.R., Green, J.C., 1996. Growth and calcification in the coccolithophorid *Emiliania huxleyi* (Haptophyceae) at low salinities. Phycologia 35, 394–403.

Parente, A., Cachao, M., Baumann, K.-H., Abreu, L. de, Ferreira, J., 2004. Morphometry of *Coccolithus pelagicus* s.l. (Coccolithophore, Haptophyta) from offshore Portugal, during the last 200 kyr. Micropaleontology 50, 107-120.

Patterson, R.T., Fishbein, E., 1989. Re-examination of the statistical methods used to determine the number of point counts needed for micropaleontological quantitative research. Journal of Paleontology 63, 245-248.

Peeters, F.J.C., Acheson, R., Brummer, G.J.A., De Ruijter, W.P.M., Schneider, R.R., Ganssen, G.M., Ufkes, E., Kroon, D., 2004. Vigorous exchange between the Indian and Atlantic oceans at the end of the past five glacial periods. Nature 430, 661–665.

Penaud, A., Eynaud, F., Turon, J.L., Zaragosi, S., Marret, F., Bourillet, J.F., 2008. Interglacial variability (MIS 5 and MIS 7) and dinoflagellate cyst assemblages in the Bay of Biscay (North Atlantic). Marine Micropaleontology 68, 136–155.

Penaud, A., Eynaud, F., Voelker, A., Marret, F., Turon, J.L., Rossignol, L., Blamart, D., Mulder, T., 2011. Hydrological processes affecting the subtropical NE Atlantic (34–38° N) over the last 30 ka: evidence from phyto- and zooplankton assemblages. Biogeosciences Discussions 8, 2281–2327.

Petit, J.R., Jouzel, J., Raynaud, D., Barkov, N.I., Barnola, J.M., Basile, I., Bender, M., Chappellaz, J., Davis, M., Delaygue, G., Delmotte, M., Kotlyakov, V.M., Legrand, M., Lipenkov, V.Y., Lorius, C., Pepin, L., Ritz, C., Saltzman, E., Stievenard, M., 1999. Climate and atmospheric history of the past 420,000 years from the Vostok ice core, Antarctica. Nature 399, 429–436.

Pingree, R., Kuo, Y., Garcia-Soto, C., 2002. Can the Subtropical North Atlantic permanent thermocline be observed from space? Journal of the Marine Biological Association of the UK 82, 709–728.

Pingree, R.D., 1997. The Eastern Subtropical Gyre (North Atlantic): Flow Rings Recirculations Structure and Subduction. Journal of the Marine Biological Association of the UK 77, 573-624.

Piotrowski, A.M., Goldstein, S.L., Hemming, S.R., Fairbanks, R.G., 2004. Intensification and variability of ocean thermohaline circulation through the last deglaciation. Earth and Planetary Science Letters 225, 205–220.

Plewa, K., Meggers, H., Kasten, S., 2006. Barium in sediments off northwest Africa: A tracer for paleoproductivity or meltwater events? Paleoceanography 21.

Pollard, R.T., Regier, L.A., 1992. Vorticity and vertical circulation at an ocean front. Journal of Physical Oceanography 22, 609–625.

Polovina, J.J., Howell, E.A., Abecassis, M., 2008. Ocean's least productive waters are expanding. Geophysical Research Letters 35, L03618.

Prahl, F., Wakeham, S., 1987. Calibration of unsaturation patterns in long-chain ketone compositions for palaeotemperature assessment. Nature 330, 367–369.

Rahmstorf, S., 2003. The current climate. Nature 421, 699.

Rasmussen, T.L., Thomsen, E., Troelstra, S.R., Kuijpers, A., Prins, M.A., 2003. Millennial-scale glacial variability versus Holocene stability: changes in planktic and benthic foraminifera faunas and ocean circulation in the North Atlantic during the last 60 000 years. Marine Micropaleontology 42. 143-176.

Rasmussen, T.L., Thomsen, E., 2004. The role of the North Atlantic Drift in the millennial timescale glacial climate fluctuations. Palaeogeography Palaeoclimatology Palaeoecology 210, 101–116.

Raymo, M.E., 2003. The 41 kyr world: Milankovitch's other unsolved mystery. Paleoceanography 18, 1011.

Reimer, P.J., al, E., 2009. INTCAL09 and MARINE09 radiocarbon age calibration curves, 0–50,000 years cal BP. Radiocarbon 51, 1111–1150.

Renaud, S., Klaas, C., 2001. Seasonal variations in the morphology of the coccolithophore Calcidiscus leptoporus off Bermuda (N. Atlantic). Journal of Plankton Research 23, 779.

Renaud, S., Ziveri, P., Broerse, A., 2002. Geographical and seasonal differences in morphology and dynamics of the coccolithophore Calcidiscus leptoporus. Marine Micropaleontology 46, 363–385.

Repschläger, J., M. Weinelt, H. Kinkel, N. Andersen, T. Blanz, C. Schwab (2012). Response of the subtropical North Atlantic surface hydrography to deglacial and Holocene changes of AMOC. Submitted to Paleoceanography.

Richter, T. 1998. Sedimentary fluxes at the Mid-Atlantic Ridge - sediment sources, accumulation rates, and geochemical characterization. PhD thesis, Christian Albrechts University Kiel, Germany.

Richter, T.O., Van der Gaast, S., Koster, B., Vaars, A., Gieles, R., De Stiger, H., De Haas, H., van Weering, T.C.E., 2006. The Avaatech XRF core scanner: technical description and applications to NE Atlantic sediments. In: Rothwell, R.G. (Ed.), New Techniques in Sediment Core Analysis, 267, Geological Society, London, pp. 39-50.

Riebesell, U., Zondervan, I., Rost, B., Tortell, P., Zeebe, R., Morel, F., 2000. Reduced calcification of marine plankton in response to increased atmospheric CO_2. Nature 407, 364–367.

Risebrobakken, B., Dokken, T., Jansen, E., 2005. Extent and variability of the meridional Atlantic circulation in the eastern Nordic seas during marine isotope stage 5 and its influence on the inception of the last glacial. Geophysical Monograph - American Geophysical Union 158, 323.

Rodrigo-Gámiz, M., Martínez-Ruiz, F., Jiménez-Espejo, F.J., Gallego-Torres, D., Nieto-Moreno, V., Romero, O., Ariztegui, D., 2011. Impact of climate variability in the western Mediterranean during the last 20,000 years: oceanic and atmospheric responses. Quaternary Science Reviews 1–17.

Rogerson, M., Colmenero-Hidalgo, E., Levine, R.C., Rohling, E.J., Voelker, A.H.L., Bigg, G.R., Schönfeld, J., Cacho, I., Sierro, F.J., Löwemark, L., Reguera, M.I., de Abreu, L., Garrick, K., 2010. Enhanced Mediterranean-Atlantic exchange during Atlantic freshening phases. Geochemistry Geophysics Geosystems 11, Q08013.

Rogerson, M., Rohling, E., Weaver, P., Murray, J., 2004. The azores front since the last glacial maximum. Earth and Planetary Science Letters 222, 779–789.

Rohling, E., 1994. Review and New Aspects Concerning the Formation of Eastern Mediterranean Sapropels. Marine Geology 122, 1–28.

Rohling, E.J., Grant, K., Hemleben, C., Siddall, M., Hoogakker, B.A.A., Bolshaw, M., Kucera, M., 2007. High rates of sea-level rise during the last interglacial period. Nature Geoscience 1, 38–42.

Romero, O. E., Lange, C.B., Fischer, G., Treppke, U.F., Wefer, G., 1999. Variability in export production documented by downward fluxes and species composition or marine planktic diatoms: observations from the tropical and equatorial Atlantic. In: Fischer, G., Wefer, G. (Eds.), Use of proxies in paleoceanography. Springer, Berlin, pp. 365-392.

Romero, O.E., Swann, G.E.A., Hodell, D.A., Helmke, P., Rey, D., Rubio, B., 2011. A highly productive Subarctic Atlantic during the Last Interglacial and the role of diatoms. Geology 39, 1015-1018.

Rosell-Melé. A., Weinelt, M., Sarnthein, M., Koç, N., Jansen, E., 1998. Variability of the Arctic front during the last climatic cycle: application of a novel molecular proxy. Terra Nova 10, 86-89.

Rowson, J.D., Leadbeater, B.S.C., Green, J.C., 1986. Calcium carbonate deposition in the motile (Crystallolithus) phase of *Coccolithus pelagicus* (Prymnesiophyceae). British Phycological Journal 21, 359–370.

Ruddiman, W.F., McIntyre, A., 1973. Time-transgressive deglacial retreat of polar waters from the North Atlantic. Quaternary Research 3, 117–130.

Ruddiman, W., Glover, L., 1975. Subpolar North-Atlantic Circulation at 9300 Yr Bp - Faunal Evidence. Quaternary Research 5, 361–389.

Rundgren, M., Björck, S., Hammarlund, D., 2005. Last interglacial atmospheric CO_2 changes from stomatal index data and their relation to climate variations. Global and Planetary Change 49, 47–62.

Rühlemann, C., Müller, P.J., Schneider, R.R., 1999. Organic carbon and carbonate as paleoproductivity proxies: examples from high and low productivity areas of the tropical Atlantic. In: Fischer, G., Wefer, G. (Eds.), Use of proxies in paleoceanography. Springer, Berlin, pp. 315-344.

Saavedra-Pellitero, M., Flores, J.A., Lamy, F., Sierro, F.J., Cortina, A., 2011. Coccolithophore estimates of paleotemperature and paleoproductivity changes in the southeast Pacific over the past ~27 kyr. Paleoceanography 26, PA1201.

Salgueiro, E., Voelker, A.H.L., de Abreu, L., Abrantes, F., Meggers, H., Wefer, G., 2010. Temperature and productivity changes off the western Iberian margin during the last 150 ky. Quaternary Science Reviews 29, 680–695.

Samtleben, C., 1980. Die Evolution der Coccolithophoriden-Gattung *Gephyrocapsa* nach Befunden im Atlantik. Paläontologische Zeitschrift 54, 91–127.

Samtleben, C., Bickert, T., 1990. Coccoliths in sediment traps from the Norwegian Sea. Marine Micropaleontology 16, 39–64.

Samtleben, C., Schröder, A., 1992. Living coccolithophore communities in the Norwegian-Greenland Sea and their record in sediments. Marine Micropaleontology 19, 333–354.

Samtleben, C., Schäfer, P., Andruleit, H., Baumann, A., Baumann, K., Kohly, A., Matthiessen, J., Schröder-Ritzrau, A., 1995. Plankton in the Norwegian-Greenland Sea: from living communities to sediment assemblages—an actualistic approach. Geologische Rundschau 84, 108–136.

Sarmiento, J.L., Toggweiler, J.R., 1984. A new model for the role of the oceans in determining atmospheric pCO_2. Nature 308, 621–624.

Sarmiento, J., Siegenthaler, U., 1992. New production and the global carbon cycle. In: Falkowski, P.G., Woodhead, A,D. (Eds.), Primary productivity and biogeochemical cycles in the sea. Plenum Press, New York, 317–333.

Sarmiento, J.L., Hughes, T.M.C., Stouffer, R.J., Manabe, S., 1998. Simulated response of the ocean carbon cycle to anthropogenic climate warming. Nature 393, 245–249.

Sarmiento, J., Gruber, N., Brezinzki, M., Dunne, J., 2004. High-latitude controls of thermocline nutrients and low latitude biological productivity. Nature 427, 56–60.

Sarnthein, M., Winn, K., Duplessy, J.C., Fontugne, M.R., 1988. Global variations of surface ocean productivity in low and mid latitudes: influence on CO_2 reservoirs of the deep ocean and atmosphere during the last 21,000 years. Paleoceanography 3, 361–399.

Sarnthein, M., Winn, K., Jung, S., Duplessy, J.C., Labeyrie, L., Erlenkeuser, H., Ganssen, G., 1994. Changes in East Atlantic Deep-Water Circulation Over the Last 30,000 Years - 8 Time Slice Reconstructions. Paleoceanography 9, 209–267.

Sarnthein, M., Stattegger, K., Dreger, D., 2001. Fundamental modes and abrupt changes in North Atlantic circulation and climate over the last 60 ky—concepts, reconstruction and numerical modeling. In: Schäfer, P., Ritzrau, W., Schlüter, M., Thiede, J. (Eds.), The Northern North Atlantic: A Changing Environment. Springer, Berlin, pp. 365-410.

Sánchez Goñi, M.F., Loutre, M.F., Crucifix, M., Peyron, O., Santos, L., Duprat, J., Malaizé, B., Turon, J.L., Peypouquet, J.P., 2005. Increasing vegetation and climate gradient in Western Europe over the Last Glacial Inception (122–110 ka): data-model comparison. Earth and Planetary Science Letters 231, 111–130.

Sánchez Goñi, M.F., Bakker, P., Desprat, S., Carlson, A.E., Van Meerbeeck, C.J., Peyron, O., Naughton, F., Fletcher, W.J., Eynaud, F., Rossignol, L., Renssen, H., 2012. European climate optimum and enhanced Greenland melt during the Last Interglacial. Geology 40, 627–630.

Schiebel, R., Schmuker, B., Alves, M., Hemleben, C., 2002. Tracking the Recent and late Pleistocene Azores front by the distribution of planktic foraminifers. Journal of Marine Systems 37, 213–227.

Schiebel, R., Waniek, J., Zeltner, A., Alves, M., 2002. Impact of the Azores Front on the distribution of planktic foraminifers, shelled gastropods, and coccolithophorids. Deep-Sea Research Part II 49, 4035–4050.

Schiebel, R., Brupbacher, U., Schmidtko, S., Nausch, G., Waniek, J.J., Thierstein, H.-R., 2011. Spring coccolithophore production and dispersion in the temperate eastern North Atlantic Ocean. Journal of Geophysical Research 116.

Schmidt, M.W., Vautravers, M.J., Spero, H.J., 2006. Rapid subtropical North Atlantic salinity oscillations across Dansgaard–Oeschger cycles. Nature 443, 561–564.

Schmidt, M.W., Spero, H.J., 2011. Meridional shifts in the marine ITCZ and the tropical hydrologic cycle over the last three glacial cycles. Paleoceanography 26, PA1206.

Schmittner, A., 2005. Decline of the marine ecosystem caused by a reduction in the Atlantic overturning circulation. Nature 434, 628–633.

Schmitz, W.J., McCartney, M.S., 1993. On the north Atlantic circulation. Reviews of Geophys 31, 29–49.

Schneider, B., Leduc, G., Park, W., 2010. Disentangling seasonal signals in Holocene climate trends by satellite-model-proxy integration. Paleoceanography 25.

Schulz, M., 2002. On the 1470-year pacing of Dansgaard-Oeschger warm events. Paleoceanography 17, 1014.

Schwab, C., Kinkel, H., Weinelt, M., Repschläger, J., 2012. Coccolithophore paleoproductivity and ecology response to deglacial and Holocene changes in the Azores Current System. Paleoceanography 27, PA3210.

Schwab, C., Kinkel, H., Weinelt, M., Repschläger, J., 2013. Schwab, C., Kinkel, H., Weinelt, M., Repschläger, J., 2012. Paleoenvironmental changes in the Azores region between 130 and 48 ka BP with special emphasizes on MIS 5.5. Submitted to Quaternary Science Reviews.

Schwarz, J.N., Schodlok, M.P., 2009. Impact of drifting icebergs on surface phytoplankton biomass in the Southern Ocean: Ocean colour remote sensing and in situ iceberg tracking. Deep Sea Research Part I: Oceanographic Research Papers 56, 1727–1741.

Searle, R., 1980. Tectonic pattern of the Azores spreading centre and triple junction. Earth and Planetary Science Letters 51, 415–434.

Seidov, D., Maslin, M., 1999. North Atlantic deep water circulation collapse during Heinrich events. Geology 27, 23–26.

Seki, O., 2004. Reconstruction of paleoproductivity in the Sea of Okhotsk over the last 30 kyr. Paleoceanography 19, PA1016.

Shackleton, N., Hall, M., Vincent, E., 2000. Phase relationships between millennial-scale events 64,000-24,000 years ago. Paleoceanography 15, 565–569.

Shackleton, N.J., Chapman, M., Sánchez-Goñi, M.F., Pailler, D., Lancelot, Y., 2002. The Classic Marine Isotope Substage 5e. Quaternary Research 58, 14–16.

Shackleton, N., Sánchez-Goņi, M., Pailler, D., Lancelot, Y., 2003. Marine isotope substage 5e and the Eemian Interglacial. Global and Planetary Change 36, 151–155.

Siegenthaler, U., Sarmiento, J.L., 1993. Atmospheric carbon dioxide and the ocean. Nature 365, 119–125.

Sigman, D.M., Boyle, E.A., 2000. Glacial/interglacial variations in atmospheric carbon dioxide. Nature 407, 859-869.

Skinner, L., 2003. Analysis and modelling of gravity- and piston coring based on soil mechanics. Marine Geology 199, 181–204.

Solignac, S., de Vernal, A., Hillaire-Marcel, C., 2004. Holocene sea-surface conditions in the North Atlantic—Contrasted trends and regimes in the western and eastern sectors (Labrador Sea vs. Iceland Basin). Quaternary Science Reviews 23, 319–334.

Solignac, S., Grelaud, M., de Vernal, A., Giraudeau, J., Moros, M., McCave, I.N., Hoogakker, B., 2008. Reorganization of the upper ocean circulation in the mid-Holocene in the northeastern Atlantic. Canadian Journal of Earth Sciences 45, 1417–1433.

Sorrosa, J.M., Satoh, M., Shiraiwa, Y., 2005. Low Temperature Stimulates Cell Enlargement and Intracellular Calcification of Coccolithophorids. Marine Biotechnology 7, 128–133.

Sprengel, C., Baumann, K., Henderiks, J., Henrich, R., Neuer, S., 2002. Modern coccolithophore and carbonate sedimentation along a productivity gradient in the Canary Islands region: seasonal export production and surface accumulation rates. Deep-Sea Research Part II 49, 3577–3598.

Mudelsee, M., Stattegger, K., 1997. Exploring the structure of the mid-Pleistocene revolution with advanced methods of time-series analysis. Geologische Rundschau 86, 499-511.

Steig, E., 1999. Mid-Holocene climate change. Science 286, 1485-1487.

Stolz, K., 2009. Shifts in North Atlantic surface water regimes during the last interglacial-glacial cycle (late Quaternary) investigated by coccolithophore-based ecological and chemical proxies. Ph.D. Thesis, University of Bremen, Germany.

Stolz, K., Baumann, K.-H., 2010. Changes in palaeoceanography and palaeoecology during Marine Isotope Stage (MIS) 5 in the eastern North Atlantic (ODP Site 980) deduced from calcareous nannoplankton observations. Palaeogeography Palaeoclimatology Palaeoecology 292, 295–305.

Stramma, L., Siedler, G., 1988. Seasonal changes in the North Atlantic subtropical gyre. Journal of Geophysical Research 93, 8111–8118.

Stuiver, M., Reimer, P.J., 1986. A computer program for radiocarbon age calibration. Radiocarbon 28, 1022-1030.

Svensson, A., Bigler, M., Kettner, E., Dahl-Jensen, D., Johnsen, S., Kipfstuhl, S., Nielsen, M., Steffensen, J.P., 2011. Annual layering in the NGRIP ice core during the Eemian. Climate of the Past 7, 1427–1437.

Sy, A., 1988. Investigation of large-scale circulation patterns in the central North Atlantic: the North Atlantic Current, the Azores Current, and the Mediterranean Water plume in the area of the Mid-Atlantic Ridge. Deep Sea Research 1–31.

Tyrrell, T., Holligan, P.M., Mobley, C.D., 1999. Optical impacts of oceanic coccolithophore blooms. Journal of Geophysical Research 104, 3223-3241.

Tanaka, Y., Tada, R., 2000. 27. Data Report: Calcareous Nannofossil Assemblages of the last 27 ky in Hole 1017E, Santa Lucia Slope, off Point Conception. Proceedings of the Ocean Drilling Program 167.

Taylor, A.R., Russell, M.A., Harper, G.M., Collins, T.F.T., Brownlee, C., 2007. Dynamics of formation and secretion of heterococcoliths by *Coccolithus pelagicus* ssp. *braarudii*. European Journal of Phycology 42, 125–136.

Teller, J.T., Leverington, D.W., 2004. Glacial Lake Agassiz: A 5000 yr history of change and its relationship to the $\delta^{18}O$ record of Greenland. Geological Society of America Bulletin 116, 729.

The Ring Group, 1981. Gulf Stream cold-core rings- Their physics, chemistry, and biology. Science 212, 1091-1100.

Thierstein, H., Geitzenauer, K., Molfino, B., Shackleton, N., 1977. Global synchroneity of late Quaternary coccolith datum levels Validation by oxygen isotopes. Geology 5, 400.

Thomas, E., Booth, L., Maslin, M., Shackleton, N., 1995. Northeastern Atlantic Benthic Foraminifera During the Last 45,000 Years - Changes in Productivity Seen From the Bottom Up. Paleoceanography 10, 545–562.

Thornalley, D.J., Elderfield, H., 2009. Freshwater input and abrupt deglacial climate change in the North Atlantic. in press 1–48.

Tjallingii, R., 2006. Application and quality of X-Ray Fluorescence core scanning in reconstructing late Pleistocene NW African continental margin sedimentation patterns and paleoclimate variations. Ph.D. Thesis, University of Bremen, Germany.

Tomczak, M., Godfrey, J. S., 1994. Regional Oceanography: An Introduction. Pergamon, Great Britain, 422 pp..

Toucanne, S., Mulder, T., Schönfeld, J., Hanquiez, V., Gonthier, E., Duprat, J., Cremer, M., Zaragosi, S., 2007. Contourites of the Gulf of Cadiz: A high-resolution record of the paleocirculation of the Mediter-

ranean outflow water during the last 50,000 years. Palaeogeography Palaeoclimatology Palaeoecology 246, 354–366.
Treguer, P., Nelson, D.M., Van Bennekom, A.J., DeMaster, D.J., Leynaert, A., Queguiner, B., 1995. The silica balance in the world ocean: a reestimate. Science 268, 375.
Turner, J.T., 2002. Zooplankton fecal pellets, marine snow and sinking phytoplankton blooms. Aquatic Microbial Ecology 27, 57–102.
Tzedakis, P.C., Raynaud, D., McManus, J.F., Berger, A., Brovkin, V., Kiefer, T., 2009. Interglacial diversity. Nature Geoscience 2, 751–755.
Tzedakis, P.C., Wolff, E.W., Skinner, L.C., Brovkin, V., Hodell, D.A., McManus, J.F., Raynaud, D., 2012. Can we predict the duration of an interglacial? Climate of the Past 8, 1473-1485.
Tziperman, E., 2003. On the mid-Pleistocene transition to 100-kyr glacial cycles and the asymmetry between glaciation and deglaciation times. Paleoceanography 18, 1001.
Urban, B., 2007. Interglacial Pollen Records from Schöningen, Germany, In: Sirocko, F., Claussen, M., Sánchez Goñi, M. F., Litt, T. (Eds.), The Climate of Past Interglacials. Elsevier, Amsterdam, The Netherlands, pp. 417-444.
Van der Plas, L., Tobi, A., 1965. A Chart for Judging Reliability of Point Counting Results. American Journal of Science 263, 87–90.
Van der Wal, P., Kempers, R.S., Veldhuis, M., 1995. Production and downward flux of organic matter and calcite in a North Sea bloom of the coccolithophore *Emiliania huxleyi*. Marine Ecology Progress Series 126, 247–265.
Vautravers, M.J., Bianchi, G., Shackleton, N.J., 2007. Subtropical NW Atlantic Surface Water Variability During the Last Interglacial. In: Sirocko, F., Claussen, M., Sánchez Goñi, M.F., Litt, T. (Eds.), The Climate Of Past Interglacials. Elsevier, Amsterdam, pp. 289-304.
Villanueva, J., Calvo, E., Pelejero, C., Grimalt, J., Boelaert, A., Labeyrie, L., 2001. A Latitudinal Productivity Band in the Central North Atlantic Over the Last 270 kyr: An Alkenone Perspective. Paleoceanography 16.
Villanueva, J., Grimalt, J., Cortijo, E., Vidal, L., Labeyrie, L., 1997. A biomarker approach to the organic matter deposited in the North Atlantic during the last climatic cycle. Geochimica et Cosmochimica Acta 61, 4633–4646.
Villanueva, J., Grimalt, J., Labeyrie, L., Cortijo, E., Vidal, L., Louis-Turon, J., 1998. Precessional Forcing of Productivity in the North Atlantic Ocean. Paleoceanography 13.
Voelker, A., Lebreiro, S., Schönfeld, J., Cacho, I., Erlenkeuser, H., Abrantes, F., 2006. Mediterranean outflow strengthening during northern hemisphere coolings: A salt source for the glacial Atlantic? Earth and Planetary Science Letters 245, 39–55.
Voelker, A.H.L., 2002. Global distribution of centennial-scale records for Marine Isotope Stage (MIS) 3: a database. Quaternary Science Reviews 21, 1185–1212.
Volkman, J., Barrerr, S., Blackburn, S., Sikes, E., 1995. Alkenones in Gephyrocapsa oceanica: Implications for studies of paleoclimate. Geochimica et Cosmochimica Acta 59, 513–520.
Volkman, J., Eglinton, G., Corner, E., Forsberg, T., 1980. Long-chain alkenes and alkenones in the marine coccolithophorid Emiliania huxleyi. Phytochemistry 19, 2619–2622.
Volkov, D.L., Fu, L.-L., 2010. On the Reasons for the Formation and Variability of the Azores Current. Journal of Physical Oceanography 40, 2197–2220.
Volkov, D., 2011. Interannual Variability of the Azores Current Strength and Eddy Energy in Relation to Atmospheric Forcing. Journal of Geophysical Research 116.
Waelbroeck, C., Duplessy, J., Michel, E., Labeyrie, L., Paillard, D., Duprat, J., 2001. The timing of the last deglaciation in North Atlantic climate records. Nature 412, 724-727.
Walin, G., 1985. The thermohaline circulation and the control of ice ages. Palaeogeography Palaeoclimatology Palaeoecology 50, 323–332.
Wang, Y., Cheng, H., Edwards, R.L., Kong, X., Shao, X., Chen, S., Wu, J., Jiang, X., Wang, X., An, Z., 2008. Millennial- and orbital-scale changes in the East Asian monsoon over the past 224,000 years. Nature 451, 1090–1093.
Weaver, P., Chapman, M., Eglinton, G., Zhao, M., Rutledge, D., Read, G., 1999. Combined coccolith, foraminiferal, and biomarker reconstruction of paleoceanographic conditions over the past 120 kyr in the northern North Atlantic (59 degrees N, 23 degrees W). Paleoceanography 14, 336–349.
Weaver, P., Pujol, C., 1988. History of the last deglaciation in the Alboran Sea(Western Mediterranean) and adjacent North Atlantic as revealed by coccolith floras. Palaeogeography Palaeoclimatology Palaeoecology 64, 35–42.

Wei, W., Peleo-Alampay, A., 1993. Updated Cenozoic Nannofossil Magnetobiochronology. In: Young, J. (Ed.), Newsletter of International Nannoplankton Association (INA) 1993, pp. 15-17.

Weinelt, M., Rosell-Melé, A., Pflaumann, U., Sarnthein, M., Kiefer, T., 2003. Zur Rolle der Produktivität im Nordostatlantik bei abrupten Klimaänderungen in den letzten 80 000 Jahren. Zeitschrift der Deutschen Gesellschaft für Geowissenschaften 154, 47–66.

Weldeab, S., Siebel, W., Wehausen, R., Emeis, K.C., Schmiedl, G., Hemleben, C., 2003. Late Pleistocene sedimentation in the Western Mediterranean Sea: implications for productivity changes and climatic conditions in the catchment areas. Palaeogeography Palaeoclimatology Palaeoecology 190, 121–137.

Westbroek, P., al, E., 1993. A model system approach to biological climate forcing. The example of *Emiliania huxleyi*. Global and Planetary Change 8, 27-46.

Wiersma, A.P., Jongma, J.I., 2009. A role for icebergs in the 8.2 ka climate event. Climate Dynamics 35, 535–549.

Williams, R.G., Roussenov, V., Follows, M.J., 2006. Nutrient streams and their induction into the mixed layer. Global Biogeochemical Cycles 20.

Winter, A., Reiss, Z., Luz, B., 1979. Distribution of living coccolithophore assemblages in the Gulf of Elat ('Aqaba). Marine Micropaleontology 4, 197–223.

Winter, A., Jordan, R.W., Roth, P.H., 1994. Biogeography of living coccolithophores in ocean waters. In: Winter, A., Siesser, W.G. (Eds.), Coccolithophores. Cambridge University Press, Cambridge, pp. 161-178.

Wolfe, G.V., Steinke, M., 1996. Grazing-activated production of dimethyl sulfide (DMS) by two clones of *Emiliania huxleyi*. Limnology and oceanography 1151–1160.

Yamamoto, M., Shiraiwa, Y., Inouye, I., 2000. Physiological responses of lipids in Emiliania huxleyi and Gephyrocapsa oceanica (Haptophyceae) to growth status and their implications for alkenone paleothermometry. Organic Geochemistry 31, 799–811.

Young, J., Westbroek, P., 1991. Genotypic variation in the coccolithophorid species *Emiliania huxleyi*. Marine Micropaleontology 18, 5–23.

Young, J.R., Didymus, J.M., Brown, P.R., Prins, B., Mann, S., 1992. Crystal assembly and phylogenetic evolution in heterococcoliths. Nature 356, 516–518.

Young, J., 1994. Function of coccoliths. In: Winter, A., Siesser, W.G. (Eds.), Coccolithophores. Cambridge University Press, Cambridge, pp. 63-82.

Young, J., Ziveri, P., 2000. Calculation of coccolith volume and it use in calibration of carbonate flux estimates. Deep Sea Research Part II: Topical Studies in Oceanography 47, 1679–1700.

Young, J., Geisen, M., Cros, L., Kleijne, A., Sprengel, C., Probert, I., Østergaard, J., 2003. A guide to extant coccolithophore taxonomy. Journal of Nannoplankton Research Special Issue 1.

Zahn, R., Schönfeld, J., Kudrass, H.R., Park, M.H., Erlenkeuser, H., Grootes, P., 1997. Thermohaline instability in the North Atlantic during meltwater events: Stable isotope and ice-rafted detritus records from core SO75-26KL, Portuguese margin. Paleoceanography 12, 696–710.

Ziveri, P., Thunell, R.C., Rio, D., 1995. Export production of coccolithophores in an upwelling region: results from San Pedro Basin, Southern California Borderlands. Marine Micropaleontology 24, 335–358.

Ziveri, P., Thunell, R., 2000. Coccolithophore export production in Guaymas Basin, Gulf of California: response to climate forcing. Deep Sea Research Part II: Topical Studies in Oceanography 47, 2073–2100.

Ziveri, P., Baumann, K.-H., Boeckel, B., Bollmann, J., Young., J., 2004. Biogeography of selected Holocene coccoliths in the Atlantic Ocean. In: Thierstein, H.R., Young, J.R. (Eds.), From Molecular Processes to global Impact. Springer, Berlin, Germany, pp. 403-429.

Ziveri, P., de Bernardi, B., Baumann, K.-H., Stoll, H.M., Mortyn, P.G., 2007. Sinking of coccolith carbonate and potential contribution to organic carbon ballasting in the deep ocean. Deep Sea Research Part II: Topical Studies in Oceanography 54, 659–675.

Zondervan, I., Zeebe, R., Rost, B., Riebesell, U., 2001. Decreasing marine biogenic calcification: A negative feedback on rising atmospheric pCO_2. Global Biogeochemical Cycles 15, 507–516.

Appendix

Taxonomic list of identified species

Acanthoica spp.

Algirosphaera robusta (Lohmann, 1902) Norris, 1984

Alisphaera spp.

Alisphaera unicornis Okada & McIntyre, 1977

Alveosphaera spp.

Calcidiscus leptoporus small type

Calcidiscus leptoporus (Murray & Blackman, 1898) Loeblich & Tappan, 1978

Calcidiscus quadriperforatus (Kamptner, 1937) Geisen et al., 2002

Calciopappus caudatus Gaarder & Ramsfjell, 1954

Calciosolenia brasiliensis (Lohmann, 1919) Young in Young et al., 2003

Calciosolenia murrayi Gran, 1912

Ceratolithus cristatus Kamptner, 1950

Coccolithus pelagicus (Wallich, 1877) Schiller, 1930

Coronosphaera mediterranea (Lohmann 1902) Gaarder, in Gaarder & Heimdal, 1977

Coronosphaera spp.

Cyrtosphaera lecaliae Kleijne, 1992

Discosphaera tubifera (Murray & Blackman 1898) Ostenfeld, 1900

Emiliania huxleyi (Lohmann, 1902) Hay & Mohler in Hay et al., 1967

Florisphaera profunda Okada and Honjo, 1973

Gephyrocapsa ericsonii McIntyre & Bé, 1967

Gephyrocapsa muellerae Bréhéret, 1978

Gephyrocapsa oceanica Kamptner, 1943

Gephyrocapsa ornata Heimdal, 1973

Gephyrocapsa protohuxleyi McIntyre, 1970

Gladiolithus flabellatus (Halldal & Markali 1955) Jordan & Chamberlain, 1993

Hayaster perplexus (Bramlette & Riedel, 1954) Bukry, 1973

Helicosphaera carteri (Wallich, 1877) Kamptner, 1954

Helicosphaera hyalina Gaarder, 1970

Helicosphaera pavimentum Okada & McIntyre, 1977

Michaelsarsia elegans Gran 1912 emend. Manton et al., 1984

Oolithotus antillarum (Cohen, 1964) Reinhardt in Cohen & Reinhardt, 1968

Oolithotus fragilis (Lohmann, 1912) Martini & Müller, 1972

Ophiaster formosus Gran 1912 emend Manton & Oates, 1983

Pontosphaera syracusana Lohmann, 1902

Pontosphaera discopora Schiller, 1925

Pontosphaera spp.

Retculofenestra spp.

Rhabdosphaera clavigera Murray & Blackman, 1898

Scyphosphaera apsteinii Lohmann, 1902

Syracosphaera molischii Schiller, 1925

Syracosphaera ossa (Lecal 1966) Loeblich & Tappan,1968

Syracoshaera pulchra Lohmann, 1902

Syracosphaera spp.

Tetralithoides spp.

Umbellosphaera irregularis Paasche *in* Markali & Paasche, 1955

Umbellosphaera tenuis (Kamptner, 1937) Paasche in Markali & Paasche, 1955

Umbilicosphaera anulus (Lecal, 1967) Young & Geisen n. comb.

Umbilicosphaera foliosa (Kamptner 1963, ex Kleijne 1993) Geisen in Sáez et al., 2003

Umbilicosphaera hulburtiana Gaarder, 1970

Umbilicosphaera sibogae (Weber-van Bosse 1901) Gaarder, 1970

SEM pictures of coccoliths

a)

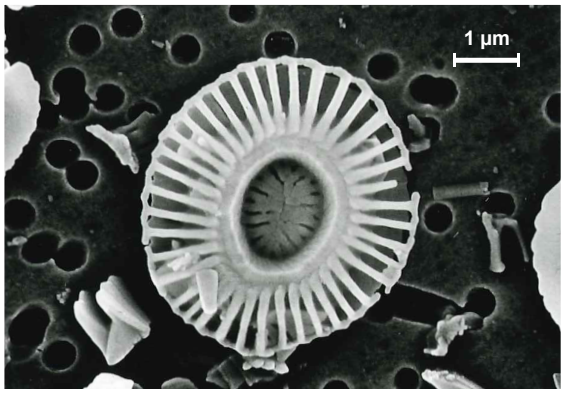

b)

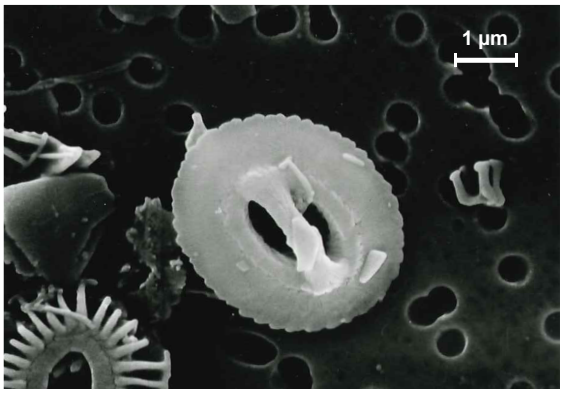

c)

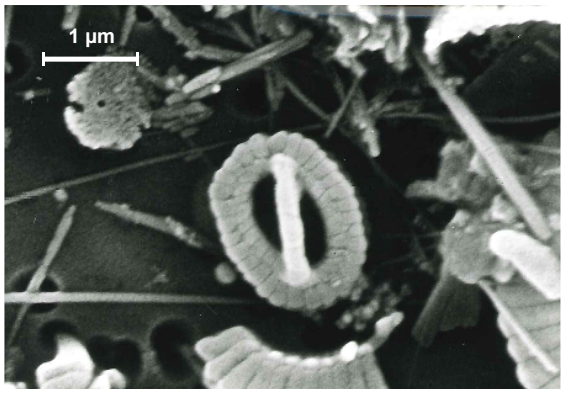

d)

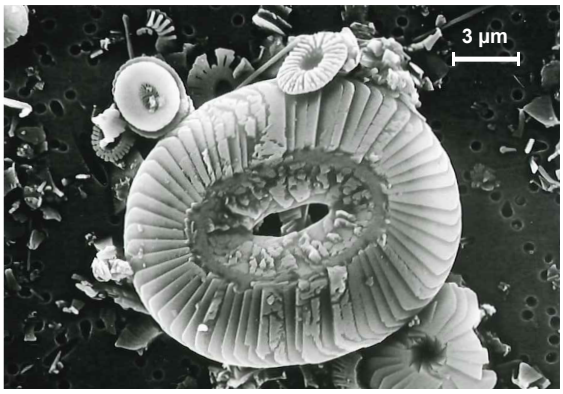

e)

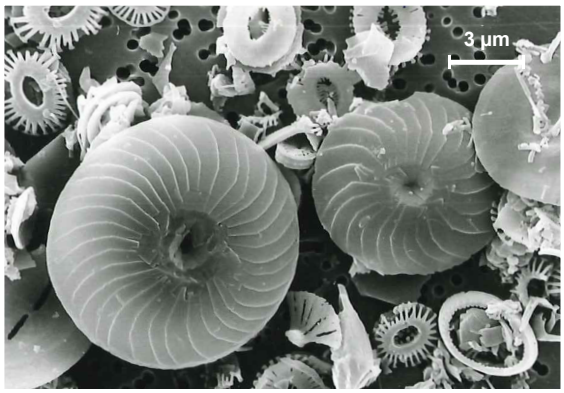

f)

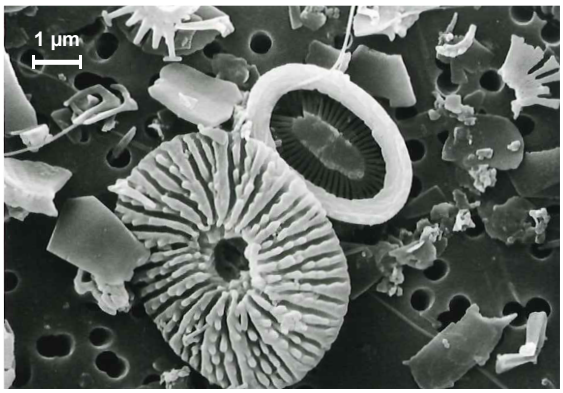

g)

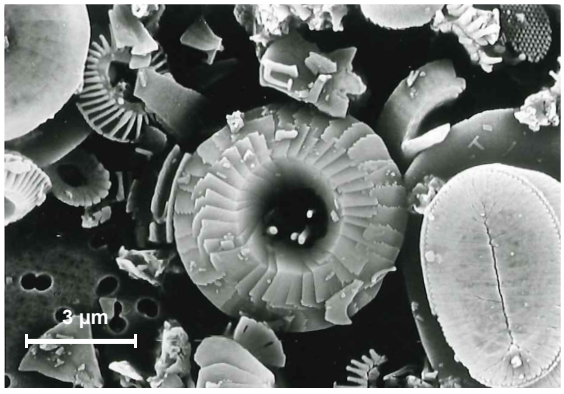

h)

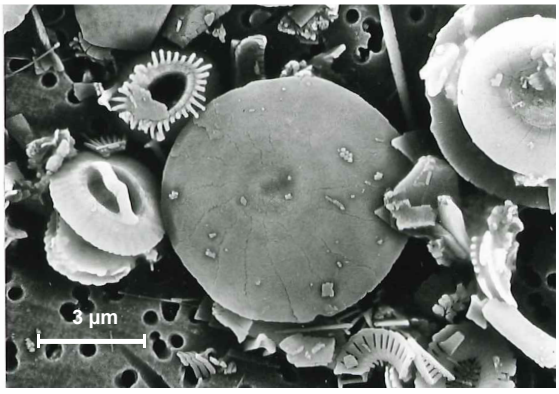

SEM pictures of coccoliths from important coccolithophore species (previouse page). a) coccolith from *E. huxleyi* (sample: GEOFAR KF16 94.5 cm, magnification: 14000), b) coccolith from *G. mullerae* (sample: MD08-3180Cq 50.25 cm, magnification: 13500), c) coccolith from *G. ericsonii* (sample: MD08-3180Cq 79.25 cm, magnification: 20000), d) coccolith from *C. pelagicus* (sample: MD08-3180Cq 290.25 cm, magnification: 5000), e) coccoliths from *C. leptoporus* (left: large morphotype, right: intermediate morphotype) (sample: GEOFAR KF16 8.5 cm, magnification: 5500), f) in the center of this picture: coccolith from *Umbellosphaera tenius*, to the left: coccolith from *F. profunda*, to the upper right: coccolith from *C. mediterranea* (sample: GEOFAR KF16 30 cm; magnification: 10500), g) coccolith from *Umbilicosphaera foliosa* (sample: GEOFAR KF16 39.5 cm, magnification: 8000), h) coccolith from *O. fragilis* (sample: GEOFAR KF16 39.5 cm, magnification: 8000).

Records of less abundant species in GEOFAR KF16 and MD08-3180Cq

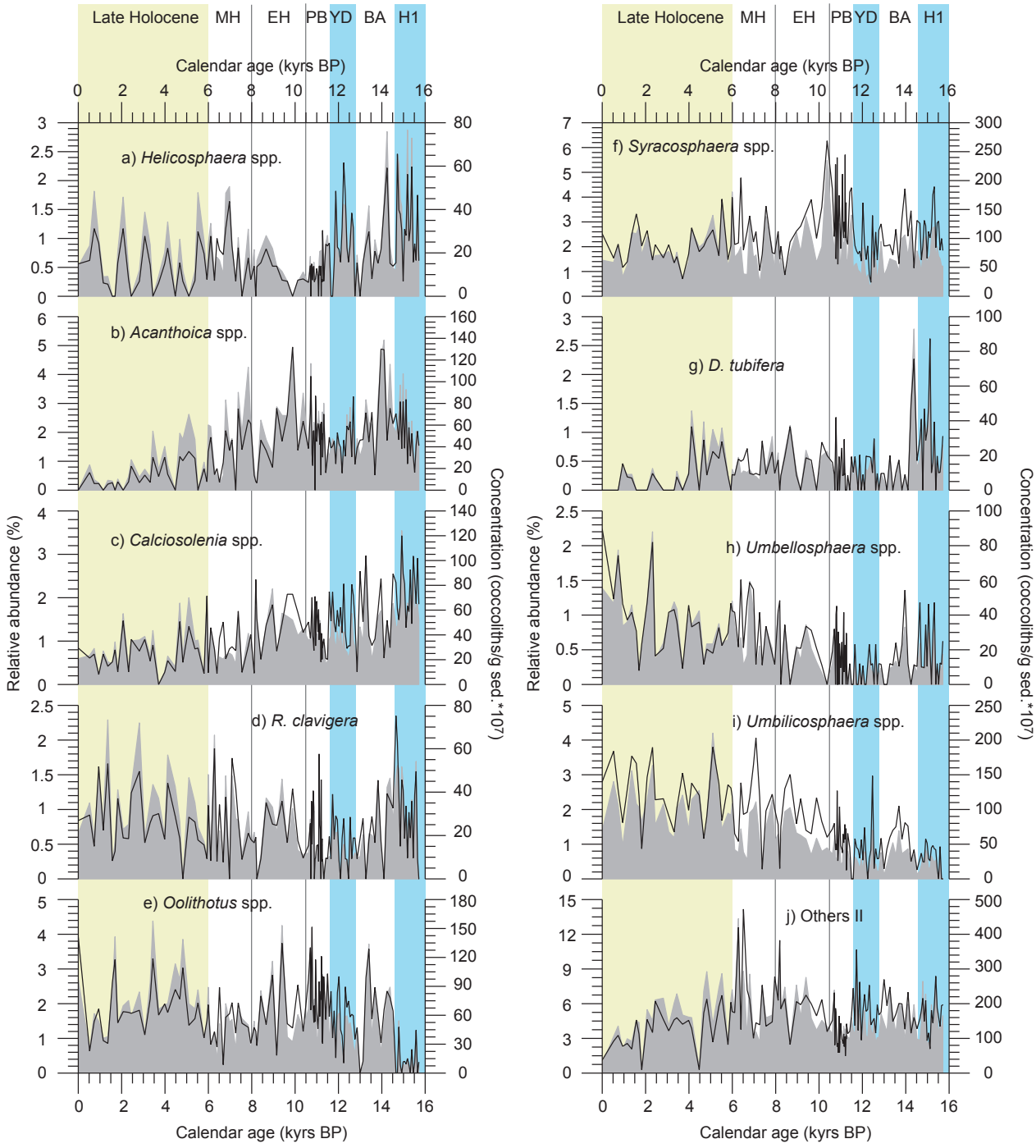

Relative (solid lines) and absolute (grey areas) abundances of coccolithophore species that contribute to the group Others from Figure 3.3. Only coccoliths from species that contribute significantly are shown. All other species identified but not shown only occur sporadically in abundances < 1% and are grouped under the term Others II. a) *Helicosphaera* spp., b) *Acanthoica* spp., c) *Calciosolenia* spp., d) *Rhabdosphaera clavigera*, e) *Oolithotus* spp., f) *Syracosphaera* spp., g) *Discosphaera tubifera*, h) *Umbellosphaera* spp., i) *Umbilicosphaera* spp., j) Others II. Abbreviations and markers used are the same as in Figure 3.3.

Records of less abundant species in MD08-3179 (low resolution)

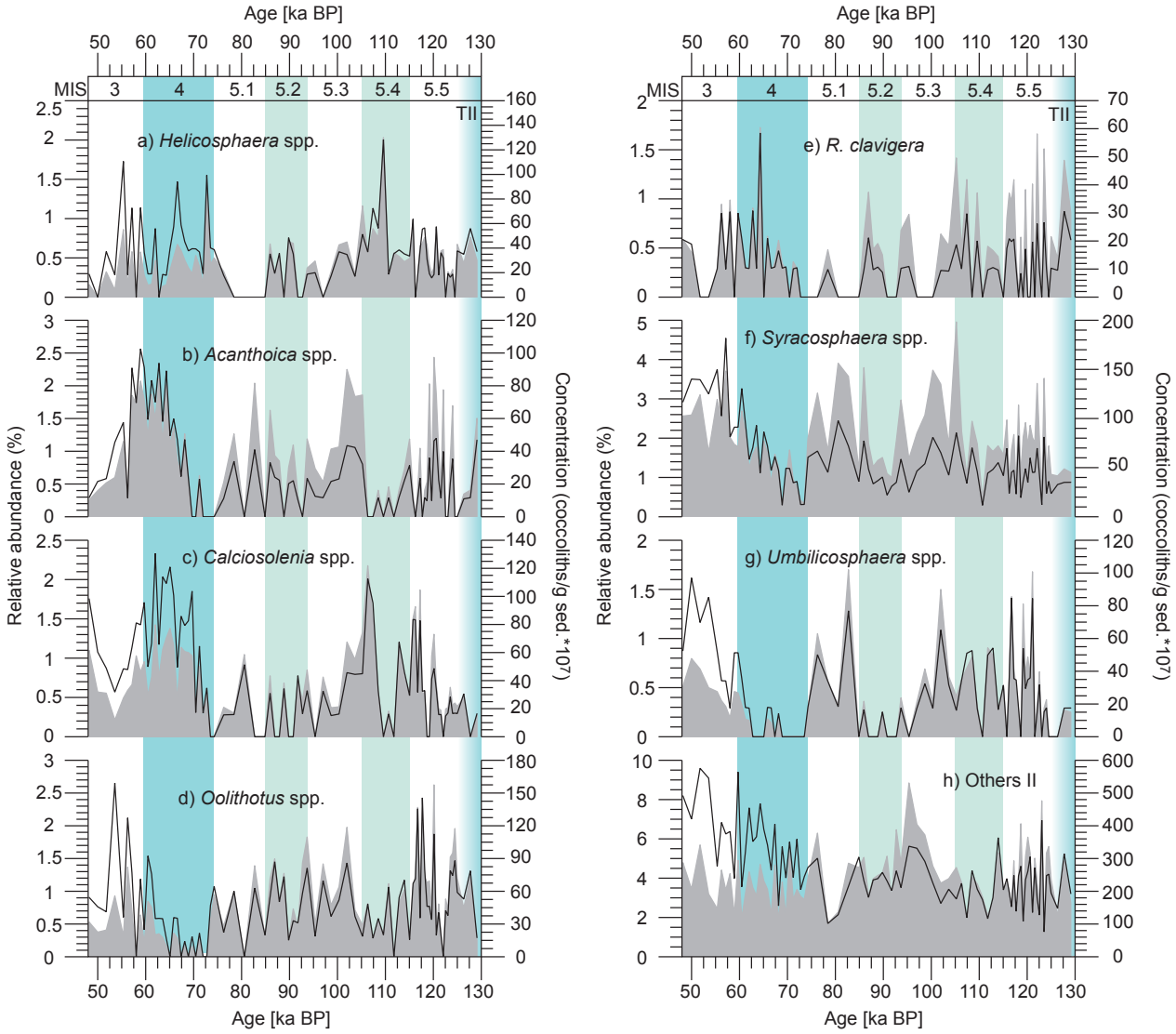

Relative (solid lines) and absolute (grey areas) abundances of coccolithophore species that contribute to the group Others from Figure 4.3. Only coccoliths from species that contribute significantly are shown. All other species identified but not shown only occur sporadically in abundances < 1% and are grouped under the term Others II. a) *Helicosphaera* spp., b) *Acanthoica* spp., c) *Calciosolenia* spp., d) *Oolithotus* spp., e) *R. clavigera*, f) *Syracosphaera* spp., g) *Umbilicosphaera* spp., h) Others II. Abbreviations and markers used are the same as in Figure 4.3.

Records of less abundant species in MD08-3179Cq (high resolution)

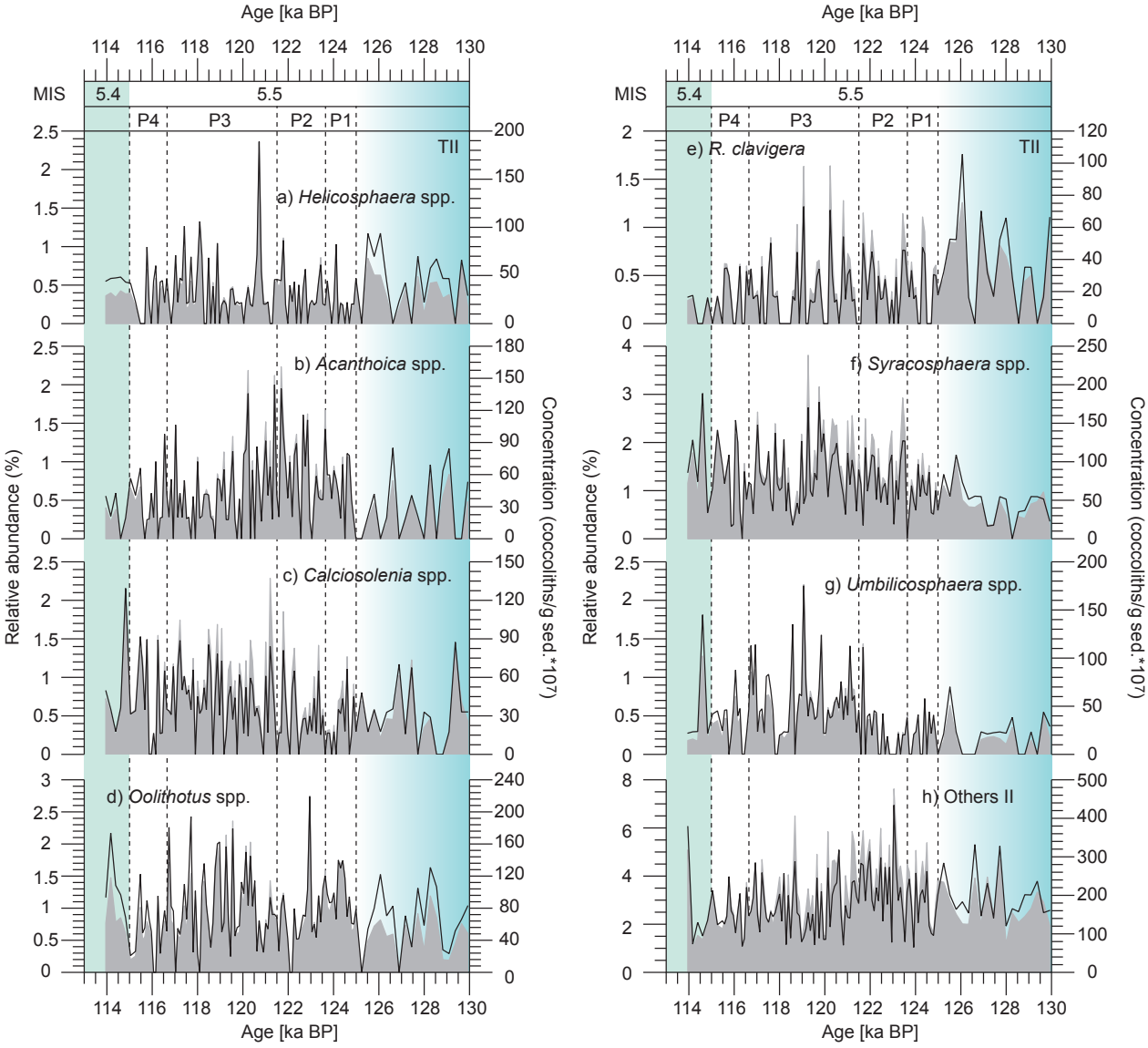

Relative (solid lines) and absolute (grey areas) abundances of coccolithophore species that contribute to the group Others from Figure 4.3. Only coccoliths from species that contribute significantly are shown. All other species identified but not shown only occur sporadically in abundances < 1% and are grouped under the term Others II. a) *Helicosphaera* spp., b) *Acanthoica* spp., c) *Calciosolenia* spp., d) *Oolithotus* spp., e) *R. clavigera*, f) *Syracosphaera* spp., g) *Umbilicosphaera* spp., h) Others II. Abbreviations and markers used are the same as in Figure 4.3.

Records of less abundant species in MD08-3179Cq (Holocene)

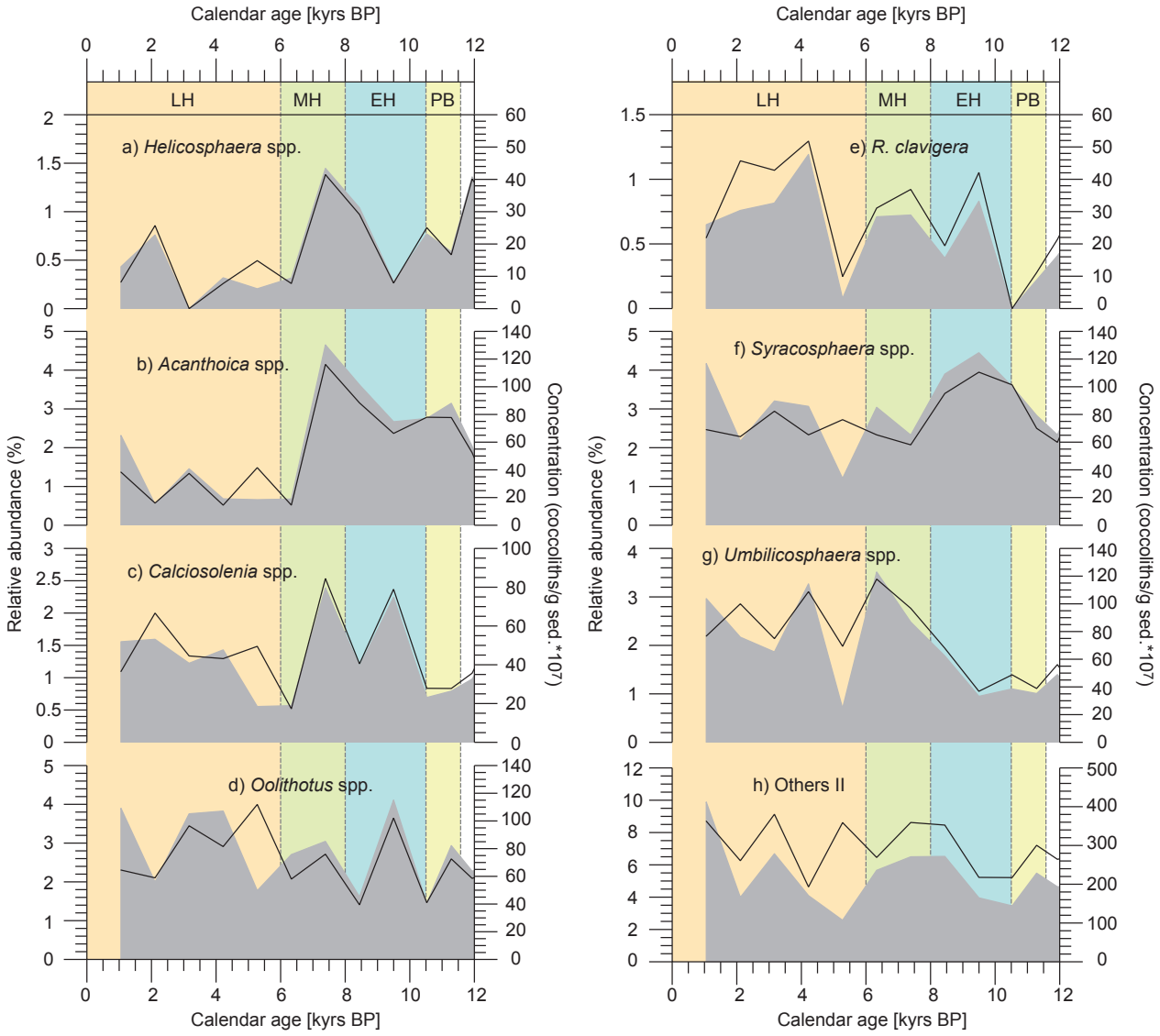

Relative (solid lines) and absolute (grey areas) abundances of less abundant coccolithophore species in the Holocene section of MD08-3179Cq. Only coccoliths from species that contribute significantly are shown. All other species identified but not shown only occur sporadically in abundances < 1% and are grouped under the term Others II. a) *Helicosphaera* spp., b) *Acanthoica* spp., c) *Calciosolenia* spp., d) *Oolithotus* spp., e) *R. clavigera*, f) *Syracosphaera* spp., g) *Umbilicosphaera* spp., h) Others II. Abbreviations and markers used are the same as in Figure 5.4.

Coccolithophore abundance data from GEOFAR KF16

Depth [cm]	*E. huxleyi*	*G. muellerae*	*G.* spp. (small)	*C. pelagicus*	*C. leptoporus*	*F. profunda*	Others	Concentration [coccoliths/g sed. x 10^{10}]
0	56.2	11.3	2.8	0.009	8.7	5.6	15.4	2.48
2.5	65.8	7.8	3.7	0.007	6.4	2.2	14.1	3.81
3.5	62.7	7.7	2.3	0.009	9	3.5	14.8	4.16
4.5	66.7	6.8	3	0.004	6.9	3.5	13.1	2.9
5.5	63.6	11.1	2.1	0.003	9.3	3.3	10.6	3.86
6.5	60	7.9	2.9	0.008	10.4	3.7	15.1	4.41
7.5	56.4	10	1.8	0.004	11.7	4.1	16	3.26
8.5	60.7	10.4	3.4	0.012	7.5	4.4	13.6	4.32
9.5	62.7	10.6	3.8	0.007	8.7	4.4	9.8	3.53
11.5	60.3	8.2	4.4	0.006	7.7	4.1	15.3	3.94
13.5	61.6	7.4	3.5	0.014	9.1	4.1	14.3	4.3
14.5	61.6	6.9	3.3	0.007	8	2.9	17.3	3.39
17.5	58.9	10.4	3.4	0.005	7.2	4.1	16	4.65
19.5	57.5	9.9	4.7	0.004	8.3	6	13.6	3.71
21.5	60	10.1	3.8	0.003	5.2	6.8	14.1	4.39
22.5	56	10.3	5	0.002	7	4.6	17.1	4.78
24.5	57.3	12.4	5.2	0.006	7.7	5.2	12.2	3.96
26.5	54.6	10.7	4.6	0.004	5.7	9.1	15.3	3.54
27.5	53.6	11.4	3.9	0.005	6.8	6.4	17.9	4.14
30	66.2	9.2	4.2	0.02	5.1	3	12.3	4.7
31.5	60	9.8	2.9	0.008	7.7	3.8	15.8	4.55
32.5	53	11	4.9	0.014	7.2	7.2	16.7	4.57
34.5	59	9	4.5	0.005	4.4	4.5	18.6	5.21
36.5	55.1	9.2	5.5	0.009	5.8	8.2	16.2	4.25
37.5	55.5	7.1	5.3	0.015	5.8	6.4	19.9	4.26
39.5	60.2	10.9	6.2	0.017	6.9	3	12.8	3.5
41.5	51	10.7	5.5	0.073	5.2	7.9	19.6	3.5
42.5	53.1	10.2	5.3	0.031	5.7	5.9	19.8	4.52
44.5	57.2	12.3	6.5	0.045	4.1	3.4	16.5	3.22
47.5	46.6	18.3	5.1	0.104	3.9	4.6	21.4	3.53
49.5	40.4	22.7	3.8	0.245	6.5	6.5	19.9	1.79
51.5	35.8	25.3	6.4	0.133	3.1	3.7	25.6	2.07
54.5	45.4	18.2	8.4	0.105	4.8	4.8	18.3	1.43
56.5	50.7	21	6.2	0.019	5.5	6.2	10.4	4.48
59.5	49.6	17.6	6.6	0.029	6	3.3	16.9	3.08
61.5	44.2	14	9.6	0.005	3.2	8.1	20.9	2.74
64.5	48.4	19.3	7.8	0.022	6.9	3.7	13.9	2.13
66.5	40.3	20.8	10.1	0.018	4.7	2.5	21.6	3.2
69.5	44	20.4	9.8	0.024	8.6	3.6	13.6	3.93
74.5	46.5	21.2	9.7	0.004	4.2	2.7	15.7	3.77

Depth [cm]	*E. huxleyi*	*G. muellerae*	*G.* spp. (small)	*C. pelagicus*	*C. leptoporus*	*F. profunda*	Others	Concentration [coccoliths/g sed. x 10^{10}]
76.5	27	18.7	29.9	0.062	3.4	2.3	18.6	2.69
79.5	29.4	30.8	15.7	0.03	6.3	1.3	16.5	4.11
82.5	23.6	26.7	24.5	0.045	3.6	1.8	19.8	2.58
84.5	23.2	32.1	26.5	0.018	4.3	1.3	12.6	3.25
89.5	32.8	31.8	12.7	0.015	4.1	3.5	15.1	3.85
94.5	32.6	32	10.7	0.061	4.6	2.2	17.8	3.4
100.5	31.7	31.5	7.9	0.024	4.8	1.6	22.5	4.1
104.5	32	36.2	7.5	0.027	2.1	3.3	18.9	2.72
109.5	25.3	37.1	8.4	0.031	5.8	0.8	22.6	4.09
114.5	28.3	36.9	8.3	0.024	4.8	1	20.7	2.64
119.5	34.7	32	8.3	0.034	2.9	1.3	20.8	2.5
124.5	32.3	33.5	7.5	0.052	5.5	2.2	18.9	2.39
129.5	32.9	33.9	7.2	0.028	6.6	0.6	18.8	3.75
134.5	43.5	21.7	8.9	0.074	5	1.7	19.1	2.48
137.5	37	23	9.1	0.029	6.5	1.1	23.3	3.44
139.5	39.7	30	8.8	0.05	3.9	1.5	16.1	2.7
142.5	35.8	27.8	9	0.043	5	0.6	21.8	2.46
144.5	40.8	28.6	6	0.052	4.3	2	18.2	2.99
147.5	40.5	28.9	8.8	0.047	7	0.3	14.5	2.83
149.5	43.1	22.8	5.9	0.072	6.6	1.8	19.7	2.21
152.5	41.8	31.5	7	0.049	7.8	0.8	11.1	3.04
154.5	50.6	26.2	7.1	0.031	3.1	0.5	12.5	3.94
157.5	45.4	19.8	10.2	0.077	7.8	0.6	16.1	3.09
159.5	46.2	20.5	7.4	0.057	5.9	1.2	18.7	2.55
164.5	48.8	21.7	7.9	0.038	4.9	0	16.7	2.13
169.5	43.1	27	7.1	0.053	7.4	0.5	14.8	2.66
172.5	43.1	29	5.4	0.076	5	0.7	16.7	3.28
174.5	45.8	22.7	4.9	0.05	7.6	1.3	17.7	3.15
177.5	43.4	30.5	5.2	0.041	4.6	0.3	16	3.97
179.5	47.9	20.1	9.9	0.065	5.8	0.4	15.8	1.77
182.5	45.9	30.2	4.2		5.2	0.8	13.6	4.05
183.5	42.7	22.8	8.6		7	0.9	18	1.87
184.5	50.3	22.4	8.3	0.055	4	1.2	13.7	2.36
187.5	43.7	26.3	7	0.03	7.8	0	15.1	2.74
188.5	44	29.7	6.1		5.5	1.2	13.5	3.67
189.5	44.3	32.1	4	0.062	7.1	0	12.5	2.58
194.5	54.2	19.3	4	0.063	7.5	0	15	3.05

Coccolithophore abundance data from MD08-3180Cq

Depth [cm]	*E. huxleyi*	*G. muellerae*	*G.* spp. (small)	*C. pelagicus*	*C. leptoporus*	*F. profunda*	Others	Concentration [coccoliths/g sed. x 10^{10}]
90.25	38.5	25.6	10.08	0.03	4.9	1.96	18.9	3.05
100.25	33.4	42.1	4.14	0.035	6.6	1.61	12.1	3.51
110.25	27.6	34.2	8.94	0.023	5.5	1.08	22.7	3.5
120.25	43.6	18.6	6.85	0.09	4.4	0.3	26.2	1.61
160.25	48.2	25.2	4.2	0.057	7.2	1.2	13.9	2.73
165.25	49.6	26.3	3.5	0.087	3.8	0.3	16.4	3.2
170.25	41.4	32	3.1	0.129	4.5	1.5	17.4	1.69
175.25	47.3	27.3	5.3	0.043	4.4	0.6	15.1	2.67
180.25	39.1	31.1	5.8	0.076	3.5	1.2	19.2	3.11
185.25	47.8	28.2	5.7	0.09	5	0.3	12.9	2.64
190.25	46.1	25.7	4.9	0.117	5.3	0.9	17	2.16
195.25	53.4	22.7	5.1	0.089	3.6	1.1	14	2.52
200.25	41.2	28.1	8.9	0.087	3.4	0.3	18	2.23
205.25	46.5	27.3	6.2	0.081	3.5	0.9	15.5	2.64
210.25	40.6	33.9	6.2	0.072	5.1	0.9	13.2	2.02
215.25	41.3	31.6	5.8	0.09	1.7	2	17.5	1.84
220.25	34.3	39.9	5.6	0.075	2.2	0.9	17	2.36
225.25	47.3	27.2	4.7	0.087	5	1.7	14	3.13
230.25	44.7	27.6	4.8	0.104	4.2	0.6	18	2.36
235.25	38.9	35.8	5	0.057	4.3	0	15.9	3.22
240.25	43.9	30.9	5.2	0.127	4.1	0.6	15.2	2.49
245.25	39.1	31.3	6.8	0.042	3.6	1.2	18	1.73
250.25	44.1	29.1	6.2	0.129	4.1	0.6	15.8	2.04
255.25	35.3	36.2	9.1	0.084	4.2	0.3	14.8	3.24
260.25	21.2	31.1	29.8	0.144	2.3	0.9	14.6	1.79
265.25	29.7	30.8	18.1	0.136	3.7	2.9	14.7	2.04
270.25	36	17.8	13.4	0.082	8	1.5	23.2	3.11
275.25	44.4	24.2	5.9	0.087	4.5	1.1	19.8	3.74
280.25	43.6	25.4	6	0.124	3.8	2.1	19	2.24
285.25	44.7	24.3	3.7	0.147	6.4	0.5	20.3	3.32
290.25	41	21.4	7.1	0.142	5.4	2.3	22.7	3.19
295.25	46.8	19.4	5.4	0.112	5.4	0.8	22.1	2.44
300.25	50.9	12.8	6.4	0.175	5.5	1.2	23	2.85
305.25	53.1	16.1	3.9	0.102	6.8	0.5	19.5	3.43
310.25	51.1	20.5	3.7	0.064	5.8	1.1	17.7	4.1
315.25	44.3	26.4	5.9	0.159	4.6	1.8	16.8	2.56
320.25	43.3	29.8	5.9	0.143	1.5	1.5	17.9	2.01
325.25	38.2	33.1	6.9	0.181	1	2	18.6	2.66
330.25	36.2	35.7	5.2	0.078	2.4	3.2	17.2	4.09
335.25	41.2	33.8	5.7	0.132	1	1.2	17	3.17

Depth [cm]	*E. huxleyi*	*G. muellerae*	*G.* spp. (small)	*C. pelagicus*	*C. leptoporus*	*F. profunda*	Others	Concentration [coccoliths/g sed. x 10^{10}]
340.25	41.2	31.6	4.9	0.092	0.9	2	19.3	3.62
345.25	41.9	35.2	5.6	0.162	1	1.8	14.3	2.75
350.25	39.6	32.9	4.9	0.135	1.7	4.6	16.2	2.57
355.25	41.1	34.9	6.6	0.23	0.5	1.1	15.6	2.95
360.25	45.5	31.9	2.7	0.156	1.7	2.1	15.9	3.62
365.25	39.8	33.5	6.3	0.166	1.2	2.2	16.8	2.89
370.25	39	35.7	3.2	0.158	1.5	0	20.4	2.71
375.25	42	29.3	4.8	0.162	2.4	2.5	18.8	3.26
380.25	44.7	34.9	3	0.227	1.2	1.8	14.2	2.92
385.25	47.2	32.3	3	0.239	0.6	2.7	14	2.28
390.25	49.3	28.1	4.3	0.283	1.6	0.6	15.8	3.49
395.25	43.4	31.7	4.1		0.6	2.6	17.3	2.23
399.75	52.8	25	5.9	0.296	1.6	1.9	12.8	2.8

Coccolithophore abundance data from MD08-3179Cq

Depth [cm]	*E. huxleyi*	*G. muellerae*	*G.* spp. (small)	*C. pelagicus*	*C. leptoporus*	*F. profunda*	Others	Concentration [coccoliths/g sed. x 10^{10}]
85.5	54.1	9.7	5.5	0.006	6.7	4.9	19.1	4.73
90.5	58.4	9.6	3.4	0.009	5.6	4.9	18.1	2.66
95.5	52.2	11.4	3.2	0.004	6.4	5.4	21.4	3.05
100.5	53.6	12.5	5.4	0.02	6.2	6	16.3	3.68
105.5	46.5	17.1	6.2	0.01	5.7	3.5	21	1.24
110.5	48.4	20	5.2	0.013	5.2	4.9	16.3	3.65
115.5	38.9	19.7	7.4	0.029	5.8	3	25.2	3.14
120.5	29.6	35	5.8	0.017	4.7	3.9	21	3.21
125.5	31.2	33.8	6.8	0.032	5.8	2.4	20	3.16
130.5	42.3	27.3	5.3	0.066	6.3	2.5	16.2	2.77
135.5	49.5	26.2	2.8	0.113	3.2	0.3	17.9	3.17
140.5	45.8	27.2	4.5	0.099	4.9	0.5	17	3.05
145.5	45.1	27	4.6	0.151	4.2	1.6	17.3	2.98
150.5	44.1	25.4	4.8	0.131	4.2	1.4	20	2.8
160.5	40.2	29.7	4.7	0.188	3.5	2.9	18.8	2.64
165.5	39.5	33	4.4	0.222	2.7	1.6	18.6	3.74
170.5	39	34	3.8	0.303	2.6	2.6	17.7	3.44
175.5	42.1	29.8	4.5	0.352	1.1	5.3	16.8	2.28

Depth [cm]	*E. huxleyi*	*G. muellerae*	*G.* spp. (small)	*C. pelagicus*	*C. leptoporus*	*F. profunda*	Others	Concentration [coccoliths/g sed. x 10^{10}]
180.5	45.5	29.6	8.2	0.409	1.6	3.4	11.3	2.41
185.5	40.8	24.3	7.5	0.439	1.7	5.2	20.1	2.79
385.5	32.9	37.9	7.3	0.132	2.9	1.8	17.1	3.51
395.5	30.7	36.6	11.1	0.18	3.8	2.2	15.4	2.95
405.5	26.6	38.8	9.9	0.105	6.9	0.9	16.8	3.56
415.5	20.9	35.5	12.8	0.083	7.3	3.7	19.7	2.11
425.5	28.9	30.7	17	0.105	6	1.4	15.9	3.19
430.5	33.7	31.7	9.7	0.082	6.4	1.7	16.7	3.87
435.5	32.4	34.9	11.4	0.098	3	0.6	17.6	3.26
440.5	28.9	34.9	18	0.108	3.2	2.3	12.6	3.98
445.5	32.5	34	14.2	0.121	3.1	1.4	14.7	3.23
450.5	29.1	34.3	12	0.07	3.3	2.3	18.9	3.13
455.5	29.8	36.1	15.4	0.142	5.3	1.2	12.1	3.3
460.5	26.9	32.2	17	0.122	7.1	1.5	15.2	3.59
465.5	25.1	33.5	18.1	0.096	3.5	3.2	16.5	3.42
470.5	33.2	32.9	14.1	0.15	3.2	3.2	13.3	3.6
475.5	25.9	41.2	14.5	0.052	2	3.2	13.1	3.05
480.5	20.5	43	16.4	0.06	1.1	3.6	15.3	3.62
485.5	16.9	51.4	13.9	0.123	1.2	3.4	13.1	3.57
490.5	11.7	53.3	17.7	0.188	0.6	3	13.5	3.62
495.5	23.1	48	15	0.263	0.6	2.1	10.9	2.93
500.5	18.2	46.8	18.4	0.205	0.6	4.3	11.5	4.15
505.5	19.9	52.4	15.8	0.137	0.9	2.6	8.3	4.29
510.5	11.7	58.2	17.7	0.115	0.9	2.7	8.7	4.07
515.5	17.3	57.7	11.4	0.187	0.6	4.3	8.5	3.11
520.5	10.2	61.5	14.8	0.166	1.2	3.1	9	5.52
525.5	5.9	68.5	13.8	0.216	1.1	2	8.5	4.35
530.5	3.2	65.1	20.1	0.242	1.2	2.4	7.8	3.43
535.5	9.2	65.3	16.5	0.166	1.6	1.6	5.6	5.39
540.5	11.7	52.2	24.5	0	2.4	3.1	6.1	4.29
545.5	19.2	39.9	28.5	0.121	2.9	1.2	8.2	5.28
550.5	19.6	23.9	45.1	0.055	1.9	0.8	8.6	7.53
555.5	19.4	31.7	40.4	0.076	2.7	0	5.7	5.97
560.5	16.4	24.9	49.8	0.069	1.2	1.5	6.1	6.39
565.5	9.1	28.4	50	0.033	2.8	1	8.7	7.96
570.5	8.8	26.1	55.5	0.039	2.7	0.6	6.3	5.37
575.5	8.5	28.5	51.1	0.028	2.1	0	9.8	7.85
580.5	4.4	37.9	49.8	0.057	0.4	0	7.4	6.19
585.5	5.1	43.6	42.2	0.057	0.6	1.4	7	6.09
590.5	7	41.3	42.2	0.052	0.9	1.2	7.3	6.25

Depth [cm]	*E. huxleyi*	*G. muellerae*	*G.* spp. (small)	*C. pelagicus*	*C. leptoporus*	*F. profunda*	Others	Concentration [coccoliths/g sed. x 10^{10}]
595.5	10.1	34.8	44.2	0.048	2.5	1	7.4	5.97
600.5	8.4	26.3	57.9	0.013	0.6	0.8	6	7.96
605.5	9.6	27.2	55.4	0.038	1	0.8	6	5.16
610.5	9.6	23	58	0.02	1.9	0.9	6.6	8.87
615.5	9.3	21.2	58.1	0.017	3	0	8.4	8.1
620.5	6.5	25	59.1	0.012	1.6	0.3	7.5	8.85
625.5	5.5	12.2	70.9	0.015	1.5	0.9	9	6.87
630.5	12.5	15	62	0.011	1.5	0.5	8.5	7.67
635.5	12.2	17.9	56.4	0.013	2.9	2	8.6	7.38
640.5	10.1	16	59.5	0.01	2.4	2.4	9.6	8.28
645.5	8.8	22.8	57.9	0.036	1.2	0.8	8.5	6.94
650.5	12.6	24.3	50	0.023	1.6	2.9	8.6	9.27
655.5	6	37.1	43.1	0.062	1.2	3.2	9.3	6.06
660.5	8.3	27.9	52.4	0.047	1.7	2	7.7	4.93
665.5	5	25.4	55.3	0.065	4.4	0.3	9.5	5.54
670.5	8.9	22.4	57	0.047	3.7	0.3	7.7	6.48
675.5	11.4	25.5	53.8	0.069	2.1	0.9	6.2	6.28
680.5	13.7	22.8	53.7	0.07	3.9	0.8	5	6.54
685.5	10.1	21.2	55.1	0.114	4.8	0.3	8.4	5.51
690.5	13.8	22.3	48.2	0.076	3.5	0.3	11.8	5.24
691.5	13.5	28.7	46.6	0.084	2.8	0.6	7.7	5.44
692.5	9.3	24.6	54	0.094	4.6	0.6	6.8	4.61
693.5	9.3	23.3	53.5	0.09	4.2	0.9	8.7	5.63
694.5	13.1	19.8	53.6	0.091	4.3	1.6	7.5	5.72
695.5	12.3	17.9	57.6	0.063	3.4	1.3	7.4	6.04
696.5	12.5	25.3	47.5	0.076	5.9	1.4	7.3	6.18
697.5	14.2	20.2	52.9	0.067	2.8	1.5	8.3	5.3
698.5	11.5	21.8	56.2	0.052	3.7	0.6	6.1	6.53
699.5	13.9	18.4	58.1	0.035	2.8	0.6	6.2	6.42
700.5	12.9	21.9	51	0.039	3.4	0.7	10.1	5.66
701.5	13.6	19.1	58.1	0.041	2.8	1.3	5.1	6.76
702.5	12.6	17.9	60.1	0.038	3.5	0.9	5	6.52
703.5	14.9	18	55.3	0.076	4.4	1.1	6.2	5.5
704.5	13.5	14.8	58.9	0.047	5.5	0	7.3	6.28
705.5	17.4	14.4	57.1	0.037	2.1	1.2	7.8	6.23
706.5	11	18.7	61.4	0.055	6.2	0.3	2.3	6.3
707.5	16.7	14.6	60.3	0.044	3	0.3	5.1	7
708.5	15.2	15.2	57.3	0.036	2.6	0.8	8.9	6.61
709.5	20.3	12.8	56.9	0.04	2.9	0.3	6.8	5.73
710.5	20.2	10.9	56.2	0.017	3.4	0.3	9	6.06

Depth [cm]	*E. huxleyi*	*G. muellerae*	*G.* spp. (small)	*C. pelagicus*	*C. leptoporus*	*F. profunda*	Others	Concentration [coccoliths/g sed. x 10^{10}]
711.5	14.3	13.2	60.3	0.021	4.6	0.5	7.1	6.24
712.5	13.4	8	62.7	0.033	4.5	0.6	10.8	6.19
713.5	18.1	13.6	56.5	0.018	3.8	0	8	6.95
714.5	14.5	13.1	61.6	0.04	3.8	0.6	6.4	6.69
715.5	15.8	12.1	58	0.038	3.8	0.6	9.7	7.07
716.5	16.6	9.8	60.4	0.05	5.6	0	7.6	7.11
717.5	15.2	12.7	58.7	0.038	3.4	0.3	9.7	6.03
718.5	17.1	11.4	58.7	0.02	3.6	1.6	7.6	5.94
719.5	16.2	11.5	61.2	0.058	3	0	8	6.4
720.5	20.1	13.7	56.1	0.047	1.6	0.9	7.6	5.07
721.5	13.7	12.4	61.5	0.03	4.1	1.1	7.2	6.8
722.5	13.8	10.8	66.6	0.012	1.6	0.9	6.3	7.13
723.5	14.4	10.9	62.7	0.028	4	0.8	7.2	7.6
724.5	15.8	9.7	63.7	0.022	2.4	1.9	6.5	7.75
725.5	11.6	12	61.8	0.032	3.7	1.5	9.4	5.53
726.5	17.9	5.5	66.6	0.018	4.1	0.6	5.3	6.71
727.5	11.9	9.3	68.9	0.02	1.6	1.5	6.8	7.92
728.5	12.3	11.3	65.2	0.009	3	1.4	6.8	6.84
729.5	15.7	8.7	62.5	0.025	4.7	0.6	7.8	7.18
730.5	15.6	8	64.3	0.018	3.8	0.5	7.8	8.81
731.5	13.4	10.1	64.9	0.026	4.1	0.7	6.8	8.33
732.5	13.7	13.2	60.6	0.021	3.5	0.3	8.7	7.75
733.5	16.8	9.4	61.7	0.037	3.3	1	7.8	6.69
734.5	14.8	8.6	63.5	0.01	4.7	0.2	8.2	8.06
735.5	18.7	8.4	64.9	0.024	1.9	0	6.1	9.01
736.5	19.6	10.7	56.1	0.016	4	1.2	8.4	8.73
737.5	13.1	14.4	61.4	0.016	4.4	1.2	5.5	8.85
738.5	17.4	7.2	63	0.01	3.7	1.3	7.4	8.23
739.5	14.1	10.2	65	0.013	3	0.2	7.5	8.42
740.5	13.1	14	60.5	0.012	3.1	0.5	8.8	7.82
741.5	17.2	12.1	59.7	0.028	3.8	0.6	6.6	6.94
742.5	13.9	9.8	62.3	0.035	2.9	1	10.1	6.86
743.5	11.4	8.1	68	0.022	4.9	0.8	6.8	7.06
744.5	13.9	11.1	61.6	0.007	6.4	0.3	6.7	6.8
745.5	16	11.3	56.8	0.016	4.2	0.3	11.4	8.4
746.5	11.8	10.8	63.4	0.008	3.9	1.4	8.7	8.34
747.5	16	12.3	57.6	0.02	4.1	0.5	9.5	8.96
748.5	14.8	10.7	60.9	0.011	2.3	1.6	9.7	8.16
749.5	11	14	58.6	0.004	4.3	1.5	10.6	7.44
750.5	12.7	12.8	60.5	0.015	3	0.9	10.1	6.21

Depth [cm]	*E. huxleyi*	*G. muellerae*	*G.* spp. (small)	*C. pelagicus*	*C. leptoporus*	*F. profunda*	Others	Concentration [coccoliths/g sed. x 10^{10}]
751.5	16.1	13.5	56.7	0.015	3.2	0.5	10	7.97
752.5	12.2	11.5	65.5	0.019	4.3	1.6	4.9	8.5
753.5	11.8	16.5	61.4	0.022	3.7	1	5.6	9.04
754.5	10.3	13.3	63.1	0.013	2.8	1.5	9	8.59
755.5	14.9	13.3	62	0.025	2.7	0	7.1	7.15
756.5	12.3	12.5	61.7	0.02	2.8	0.9	9.8	9.78
757.5	15.4	16.8	56.1	0.012	2.4	1	8.3	8.8
758.5	12	11.7	63.4	0.037	3.1	1.4	8.4	7.64
759.5	13.4	15.8	60.2	0.029	2.9	0.9	6.8	7.54
760.5	13.3	15.7	60.1	0.012	1.7	1.7	7.5	6.64
761.5	10.7	21.9	51.5	0.026	2.6	2.5	10.8	8.25
762.5	9.5	21.3	54.9	0.009	2.3	1.6	10.4	8.23
763.5	10.4	17.7	59	0.033	2.6	1	9.3	7.24
764.5	12.7	14.5	58.8	0.025	2.6	2.6	8.8	6.88
765.5	11.5	18.5	57.4	0.034	2.7	2.7	7.2	7.77
766.5	12.8	12.8	63.6	0.032	2.6	1.4	6.8	7.46
767.5	11.3	21.6	54.7	0.041	1.4	1.9	9.1	7.63
768.5	12.3	21.1	55.9	0.029	2.7	0.5	7.5	7.89
769.5	6.2	17.7	63.3	0.025	3	2.5	7.3	7.83
770.5	10.4	21	57.6	0.038	4.6	1.1	5.3	7.48
771.5	6.8	18.8	59.5	0.056	3.5	1.6	9.7	6.5
772.5	7.3	21.9	58.8	0.046	4.1	0.9	7	7.72
773.5	6.5	23.5	54.8	0.044	2.6	2.8	9.8	7.57
774.5	6.9	29.7	53	0.068	2	1	7.3	8.04
775.5	6.8	29.3	48.6	0.066	3.6	2.7	8.9	6.86
776.5	7.3	27	51.8	0.066	2.4	2.4	9	8.33
777.5	7.5	29.1	54.7	0.09	1.1	1.6	5.9	8.6
778.5	5.9	25.6	56.8	0.049	1.8	1.1	8.8	7.82
779.5	8.4	25.2	54.7	0.056	3.8	0	7.8	8.98
780.5	7.6	22.8	58.1	0.071	3.5	0.8	7.1	6.94
781.5	8.5	29.5	49.6	0.078	2.5	1.4	8.4	8.45
782.5	8.6	21.2	56.2	0.089	3.8	1.9	8.2	6.74
783.5	10.5	24.6	53.9	0.078	3.6	0.6	6.7	6.94
784.5	7.6	19.4	64.9	0.064	3.1	1	3.9	7.95
785.5	8.3	19.1	59.3	0.058	3.8	0.9	8.5	7.67
786.5	9.8	19	59	0.061	3	1	8.1	6.66
787.5	9.3	21.3	58	0.077	2.9	1.5	6.9	7.15
788.5	10.5	13.6	63.9	0.058	3.1	0.8	8	8.4
789.5	9.2	18.4	57.2	0.06	4.5	1.2	9.4	7.9
790.5	10.6	15.6	63.1	0.058	1.8	2.1	6.7	8

Depth [cm]	*E. huxleyi*	*G. muellerae*	*G.* spp. (small)	*C. pelagicus*	*C. leptoporus*	*F. profunda*	Others	Concentration [coccoliths/g sed. x 10^{10}]
791.5	8.1	18.7	61.2	0.067	4.1	0.6	7.2	6.86
792.5	8.5	20.1	63.5	0.075	2.9	0.3	4.6	7.15
793.5	12	23.2	55.6	0.08	2	2.3	4.8	6.65
794.5	7.8	22.5	59.8	0.099	2.3	1.5	6	7.29
795.5	5	26.5	59.3	0.092	2	0.6	6.5	7.31
796.5	7.9	24.5	56.4	0.071	2.9	0.8	7.4	5.15
797.5	9.5	21.8	54.7	0.092	4.6	1.2	8.1	5.79
798.5	5.1	31.8	49.1	0.12	4.2	0.9	8.8	5.77
799.5	7	38.8	41.6	0.241	0.8	2.1	9.5	4.29
800.5	5.7	33.7	48.6	0.218	5.7	0	6.1	5.07
801.5	5.9	34.6	44	0.204	3.1	2.7	9.5	4.61
802.5	4.8	39.6	42.1	0.178	3.2	2.6	7.5	5.26
803.5	5	37.1	47.6	0.253	1.8	1.9	6.3	6.68
804.5	4.7	39.2	48.5	0.102	1.6	0.6	5.3	6.53
805.5	5.3	39.7	39.9	0.181	1.3	2.9	10.7	5.57
806.5	4.8	45	39.6	0.16	2.6	1.9	5.9	3.8
807.5	5.6	37.9	43.5	0.233	3.7	1.7	7.4	5.83
808.5	5.9	41.7	42.6	0.277	1.8	2.2	5.5	5.15
809.5	6.4	35.8	47.8	0.283	1.4	2.1	6.2	4.49
810.5	4.5	38.6	46.2	0.308	1.5	1.5	7.4	5.14
811.5	5.8	34.2	48.4	0.297	2.3	1.7	7.3	5.51
812.5	8.1	28.3	53.7	0.177	1.4	0.8	7.5	7.35
813.5	7.8	31.8	48	0.251	3.6	0.9	7.6	4.71

Diatom abundance data

Depth [cm]	Concentration [valves/g sed. x 10^7]
GEOFAR KF16	
19.5	0
34.5	0
61.5	0.06
100.5	0.07
104.5	0.44
134.5	1.17
MD08-3180Cq	
75.25	0.13
77.25	0.24
79.25	0.36
82.25	0.06
200.25	1.63
205.25	2.63
220.25	1.42
230.25	1.93
260.25	0.25
270.25	0.35
280.25	0.6
300.25	0.41
335.25	1
360.25	1.37
375.25	1.05
380.5	1.27

Depth [cm]	Concentration [valves/g sed. x 10^7]
MD08-3179Cq	
385.5	0.6
410.5	0.36
445.5	0.38
465.5	0.38
480.5	1.61
485.5	1.57
510.5	1.24
520.5	1.27
545.5	0.51
555.5	0.56
565.5	0.28
575.5	0.3
585.5	0.23
600.5	0.15
615.5	0
630.5	0.12
640.5	0.24
650.5	1.13
665.5	0.87
675.5	0.25
700.5	0.16
725.5	0.27
730.5	0.15
738.5	0.08
772.5	0.55
785.5	0.56
795.5	0.18
797.5	0.07
800.5	0.6
806.5	0.4

Alkenone analysis from MD08-3180Cq

Depth [cm]	SST [°C]	Concentration [ng/g]
5.25	18.85	63
10.25	18.82	45
15.25	19.03	33
20.25	19.48	24
25.25	18.58	36
30.25	18.52	62
35.25	18.76	76
40.25	19.18	68
45.25	18.79	59
50.25	18.82	66
55.25	18.67	12
60.25	19.45	28
65.25	18.91	26
70.25	19	24
75.25	17.88	42
80.25	17.79	49
85.25	19.88	55
90.25	20.15	80
94.25	19.79	75
95.25	19.97	55
100.25	19.24	293
105.25	19.61	443
110.25	19.85	235
115.25	19.94	336
120.25	19.67	372
125.25	19.42	354
130.25	18.97	405
135.25	18.97	449
140.25	18.91	523
145.25	18.06	527
150.25	18.39	532
155.25	18.33	519
160.25	18.39	567
165.25	18.21	667
170.25	17.36	482
175.25	16.39	471
180.25	15.12	368
185.25	16.82	538
190.25	14.97	483
195.25	14.7	400

Depth [cm]	SST [°C]	Concentration [ng/g]
200.25	14.73	342
205.25	14.27	388
210.25	14.21	346
215.25	14.48	314
220.25	14.73	270
225.25	14.45	288
230.25	15.15	299
235.25	15.48	403
240.25	15.85	492
245.25	15.82	349
250.25	15.64	446
255.25	18.73	116
260.25	18.03	147
265.25	18.21	103
270.25	19.06	170
275.25	19.39	188
280.25	18.79	208
285.25	17.85	217
290.25	18.21	139
295.25	18.3	215
300.25	18.18	179
305.25	17.24	194
310.25	16.61	245
315.25	18.24	130
320.25	14.97	90
325.25	13.76	172
330.25	13.12	233
335.25	13.61	231
340.25	12.91	304
345.25	13.85	434
350.25	13.61	478
355.25	13.45	543
360.25	12.58	541
365.25	12.55	485
370.25	12.67	524
375.25	12.88	374
380.25	13.09	451
385.25	12.73	490
390.25	13.12	465
395.25	13.55	618

Curriculum Vitae

Personal data

Name: Christian Schwab
Address: Friedenskamp 21
24119 Kronshagen

Academic education

2000	Abitur at Europa Gymnasium Wörth am Rhein
10/2001-10/2008	Diploma in Geology/Paleontology at the Institute of Geosciences at Kiel University, thesis title: „Millennial-scale climate cycles in the eastern equatorial Atlantic“, supervised by Prof. Dr. M. Sarnthein
01/2009-03/2013	PhD student at the Institute of Geosciences at Kiel University, thesis title: „Late Quaternary changes in paleoproductivity and hydrography in the Azores region deduced from coccolithophore assemblages“, supervised by Prof. Dr. R. Schneider and PD Dr. M. Weinelt

Presentations/Publications

Poster presentations

Schwab, C., Kinkel, H., Weinelt, M., Repschläger, J., (2009). Holocene and deglacial changes in coccolithophore assemblages and their hydrographic implications south of the Azores Islands. Poster presentation at the 2nd EuroMARC conference (France).

Schwab, C., Kinkel, H., Weinelt, M., Repschläger, J., (2010). Interglacial surface water variability in the subtropical North Atlantic as revealed by coccoliths. Poster presentation at ICP 10 in San Diego (USA).

Schwab, C., Kinkel, H., Weinelt, M., Repschläger, J., (2011). Comparison of interglacial coccolithophore assemblages from the central subtropical North Atlantic and their relation to hydrographic and productivity changes. Poster presentation at the final EuroMARC conference (Portugal).

Schwab, C., Kinkel, H., Weinelt, M., Repschläger, J., (2012). Productivity response to deglacial and Holocene freshwater perturbations in the midlatitude North Atlantic as revealed by coccolithophores. Poster presentation at the Geologische Vereinigung (GV) meeting in Hamburg (Germany).

Schwab, C., Kinkel, H., Weinelt, M., Repschläger, J., (2012). Late Quaternary changes in paleoproductivity and paleoceanography in the Azores region based on coccolithophore assemblages. Poster presentation at the AGU 2012 in San Francisco (USA).

Oral presentations

Schwab, C., Kinkel, H., Weinelt, M., Repschläger, J., Blanz, T., (2010). A high resolution coccolithophore record of interglacial surface water variability from the Mid Atlantic Ridge. Talk at the EGU in Vienna (Austria).

Schwab, C., Kinkel, H., Weinelt, M., Repschläger, J., (2011). Comparison of interglacial coccolithophore assemblages from the central subtropical North Atlantic and their relation to hydrographic and productivity changes. Talk at the final EuroMARC conference (Portugal).

Publications (articles in peer-reviewed journals)

Schwab, C., Kinkel, H., Weinelt, M., Repschläger, J., (2012). Coccolithophore paleoproductivity and ecology response to deglacial and Holocene changes in the Azores Current System. Paleoceanography 27, PA3210.

Schwab, C., Kinkel, H., Weinelt, M., Repschläger, J., (2012). Paleoenvironmental changes in the Azores region between 48 and 130 ka BP with special emphasizes on MIS 5.5. Submitted to Quaternary Science Reviews.

Schwab, C., Kinkel, H., Weinelt, M., Repschläger, J., (2012), Comparison of Eemian and Holocene coccolithophore assemblages from the Azores Islands. Manuscript to be submitted to Climate of the Past.